Engineering And Architecture Science

Editors

Assoc. Dr. Halil İbrahim KURT

Assoc. Prof.Gülden SANDAL ERZURUMLU

Engineering and Architectural Sciences

LIVRE DE LYON

2022

Engineering and Architecture Science

Editors

Assoc. Dr. Halil İbrahim KURT

Assoc. Prof.Gülden SANDAL ERZURUMLU

LIVRE DE LYON

Lyon 2022

Engineering and Architecture Science

Editors

Assoc. Dr. Halil İbrahim KURT

Assoc. Prof.Gülden SANDAL ERZURUMLU

LIVRE DE LYON

Lyon 2022

Editors •. Assoc. Prof. Dr. Halil İbrahim Kurt
• Orcid: 0000-0002-5992-8853

Assoc. Prof. Dr. Gülden Sandal Erzurumlu
• Orcid: 0000-0001-9664-2902

Cover Design • Point Design

Book Layout • Mirajul Kayal

First Published • March 2022, Lyon

ISBN: 978-2-38236-260-0

Cover image credit pixabay.com

Publisher • Livre de Lyon

Address • 37 rue marietton, 69009, Lyon France

website • http://www.livredelyon.com

e-mail • livredelyon@gmail.com

Contents

PREFACE

Although Engineering and Architecture are two separate disciplines, positive results emerge only when they act together.

As the needs on a global scale increase, the need for the mentioned branches becomes more evident.

As Charles Eames stated, "Recognizing the need is the primary condition of design." Evaluating the researches and the results together in line with the needs will make the problem or solution be evaluated from different perspectives and the emergence of new ideas.

This book offers researchers a different, interdisciplinary perspective on engineering and architecture.

This book, "Advances In Engineering and Architecture Sciences", provides an academic forum for academics and researchers working in the fields of Engineering and Architecture. Studies of academicians and researchers working in different fields are evaluated in the book.I would like to thank the authors who supported the book with their studies and information, and IVPE Publishing House for bringing the studies together and presenting them.

Assoc. Dr. Halil İbrahim KURT
Assoc. Prof.Dr. Gülden SANDAL ERZURUMLU

CHAPTER I

PROGRESSIVE GENERATIVE ADVERSARIAL NETWORK-PROGAN

Erkan DUMAN
Department of Computer Engineering, Firat University,
Elazig, Turkey, erkanduman@firat.edu.tr
ORCID: 0000-0003-2439-7244

1. Introduction

The insufficient dataset is a very common situation in machine learning applications. It is impossible to find a dataset with the required number of samples in some critical applications. For example, in a biomedical image processing application, the creation of samples in the dataset is possible thanks to high-cost imaging devices. Another up-to-date example that comes to mind is that the lung CT images of patients, especially at the beginning of the COVID 19 pandemic, are not enough to train a model. On the other hand, in multi-class applications, the available datasets are generally imbalanced. Models trained with imbalanced datasets are sensitive to detecting the major classes examples, but often fail to capture others that belong to minor ones. The privacy of patient information, in other words, the law on personal data protection, is another obstacle that must be overcome. Another negative case that artificial intelligence researchers must overcome is that unlabeled information in the dataset requires expert knowledge.

The difficulties highlighted above can be solved by generating synthetic samples to augment datasets. Classical data augmentation processes based on geometric transformations have been proven to partially improve model training. With operations such as horizontal flipping,

rotation with random angle, crop, zoom-in, it is possible to increase the number of samples in the dataset and thus improve the model fitting. By generating synthetic color lesion images with geometric data augmentation techniques, (Bisla, Choromanska, Berman, Stein, & Polsky, 2019) and (Vasconcelos & Vasconcelos, 2017) developed models that could provide more accurate melanoma predictions.

Generative Adversarial Networks (GANs), a cutting-edge approach created by Ian Goodfellow in 2014 (Goodfellow et al., 2014), is a more successful way of generating synthetic datasets nowadays. Before the GANs, generate data approaches were also used. None of the prior methods, however, had proven as realistic as GANs. The accuracy of the results obtained using GANs was previously thought to be impossible in machine learning applications.

GANs generate synthetic data using two competing models instead of just only one model. The word "*adversarial*" in the GANs title emphasizes that these two models compete with each other. There is a two-player system dynamic, like the game of chess and Go. One model loses as much as the other model gains. In theory, the established game should be continued up to a point called the Nash equilibrium. The game comes to such a point that; both players are hesitant to make moves. Although not possible in practice, the goal is to train both models until they reach this point.

"Network", which is the last word of the title, is due to the design of the models as artificial neural networks, as you can guess. A simple feed-forward neural network or a recent CNN architecture could be used as the network model.

Figure 1 summarizes the key components of the GANs architecture and their interactions. To begin, a real dataset should be provided to be imitated, as well as the Generator and the Discriminator, the two competing models. Using a random number vector (z), the Generator block aims to generate realistic samples from latent space. It may, for example, be requested to create a fake image using this random number input, which is represented by the z notation.

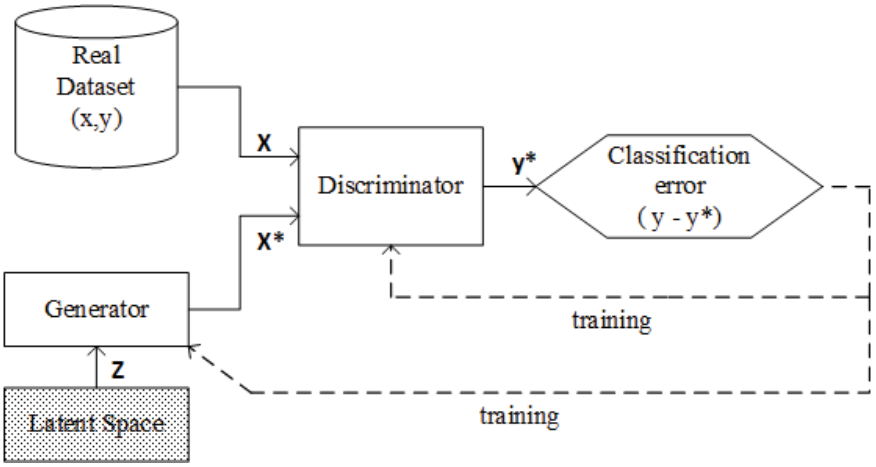

Figure 1: The subnetworks of a GAN and their interactions.

A discriminator block, on the other hand, seeks to correctly distinguish between fake and real images applied to its input. This analyzing task, which is simply due to the unrealistic fake instances generated by the generator block at the beginning, will get more challenging as the training goes.

The discriminator is a model that aims to distinguish between real and synthetic samples. It generates an accurate score about which images are fake. The Discriminator model's parameters are updated depending on the accuracy of this prediction. Fake samples from the Generator model are utilized to fool the discriminator block. The trainable parameters of the Generator model are adjusted depending on how much it can fool the Discriminator.

In Table 1, the steps of the training algorithm of GANs are given. The trainable parameters of the Discriminator are updated to maximize classification accuracy (maximizing the probability of correct prediction: x as real and x* as fake). The Generator model is similarly trained to maximize the probability that the Discriminator misclassifies x* as real.

Table 1: Training algorithm of GANs.

Training steps of Discriminator	• Take a random real sample x from the real dataset • Get a random numbers vector z from latent space and, using this vector, generate a synthetic sample x^* • The discriminator model tries to distinguish between x and x^* • Compute the prediction error and update the Discriminator's weights by backpropagation this error value.
Training steps of Generator	• Get a random numbers vector z from latent space and, using this vector, generate a synthetic sample x^* • Try to fool the Discriminator model by using x^* • Compute the prediction error and update the Generator's weights by backpropagation this error value.

In summary, GANs are a cutting-edge deep learning technique that uses a competitive dynamic between two neural networks named Generator and Discriminator to synthesize realistic data samples. GANs have numerous applications in a variety of fields, including biomedical and fashion.

2. The Structure of Progressive GAN-ProGAN

The Progressive GAN (ProGAN) approach is a state-of-art technique for high-resolution imaging. The generator and discriminator start the training process with the lowest resolution of 4x4 and grow by a factor of two with each iteration. For example, to create realistic images with a resolution of 128x128 pixels, a total of 6 GAN models must be trained

successively. The first model learns to create 4x4 images before passing on the learned weight values to the second model, which creates 8x8 images. The 8x8 model begins the training process using weight values transferred from the 4x4 model, completes its own training phase, and then sends its knowledge to the 16x16 model.

Starting with the lowest resolution and gradually raising it with each model upgrade; a shorter and more stable training procedure generates more varied and high-quality outputs.

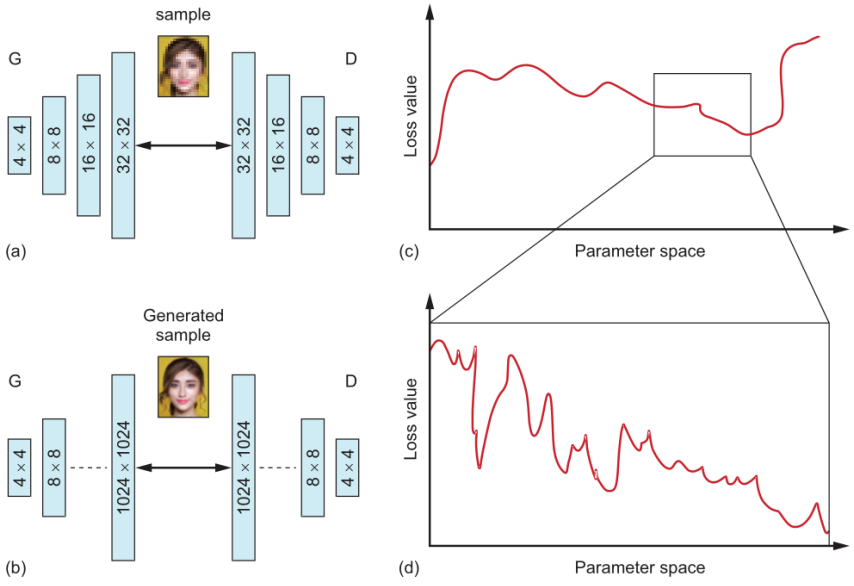

Figure 2: The growing Generator and Discriminator in the training of ProGAN. Source: adapted from (Langr & Bok, 2019).

Figure 2 demonstrates what the higher resolution means in plots (c) and (d). To begin, determine the region with the global minimum by looking at the loss function from the farthest point. Zooming in on this region continues a deep search training. The resolution and quality of the outputs are being improved as the zoom-in tilts. (a) and (c) diagrams show the differences in output quality between 32x32 and 1024x1024 models.

In the ProGAN technique, a highly abrupt transition between models might cause a shock and result in the loss of previously obtained

knowledge. In 2017, (Karras, Aila, Laine, & Lehtinen, 2017) created a ProGAN technique to overcome this challenge. Instead, the PGGAN authors fade in those layers smoothly, as seen in Figure 3, to give the system time to adjust to the higher resolution.

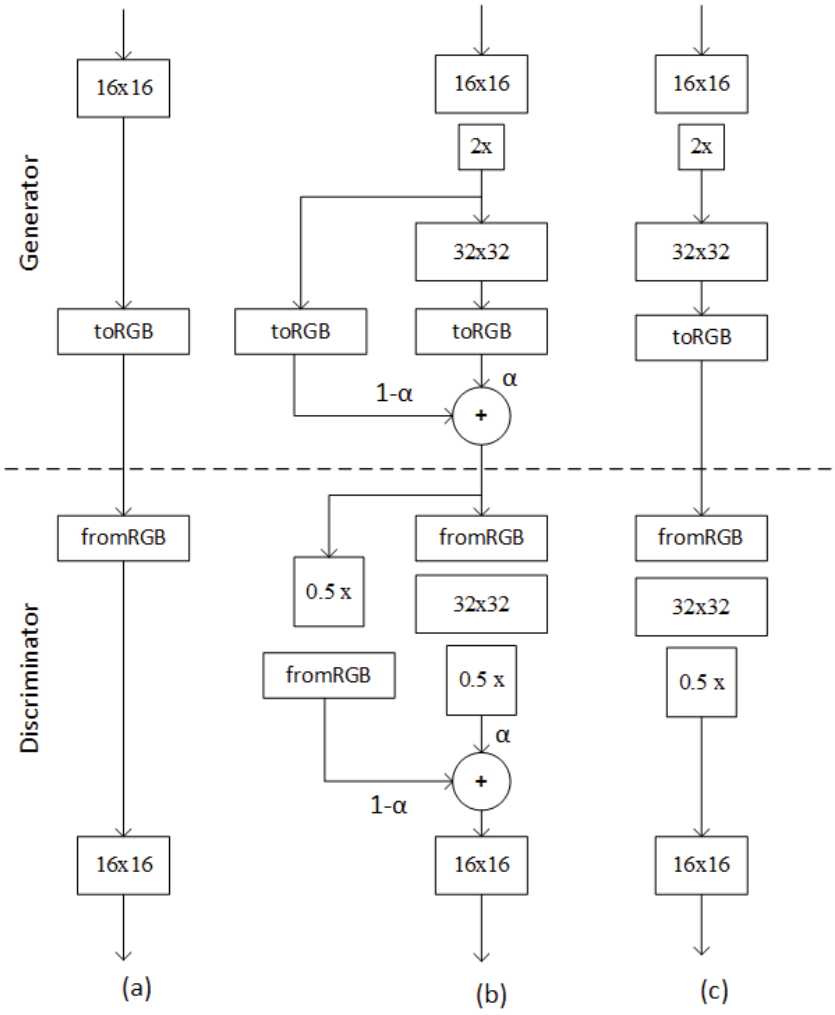

Figure 3: During training, the transformation from 16x16 to 32x32.

Figure 3 shows how the fade-in method increases the resolution of synthetic images. 16x16 models with finished training and 32x32 models

with ongoing training are presented in sections (a) and (c), respectively. The alpha parameter is used to implement the transition in section (b). In shock, a sudden switch from the 16x16 to the 32x32 model would cause the model to produce incorrect results. Instead, there is a smooth transition. The 16x16 model's knowledge is transferred to the 32x32 model. From 0 to 1, the alpha parameter is increased. The knowledge obtained from the prior resolution's training is retained in this manner. If the 32x32 model is to be trained with 4000K images, for example, the alpha parameter can be guaranteed to approach 1 during the first 800k of these images. After teaching the model the first 800K images, the 32x32 model that has recovered from the shock will be shown the remaining 3200K images. While the information from the 1-alpha path is initially prioritized, it loses its effect with time, leaving just the data from the alpha path to stand alone.

The upper portion of Figure 3 depicts the Generator model's resolution growth process, while the lower part depicts the Discriminator block's resolution decrease process. To avoid misunderstanding, some of the blocks drawn here may require explanation. The 2x block, for example, denotes the *UpSampling()* function, whereas the 0.5x block indicates the *Average_Pooling()* function. The *toRGB* block represents the process of creating an image from a 4-dimensional tensor, whereas the *fromRGB* block represents the process of converting an image to a 4-dimensional vector.

The following are some of the most significant improvements identified in the ProGAN study proposed by Karras et al. in 2017. Mini-batch standard deviation, equalized learning rate, pixel-wise feature normalization, and improved loss function called Wasserstein-GAN.

The ***mini-batch standard deviation*** of the Generator's samples was first taken into account. This procedure's purpose is to generate synthetic images that are diverse enough to cover all classes, not just a few. A low value implies that the samples in the Generator's batch come from the same or adjacent space region, even though the fact that simply a simple statistical value is computed. The Discriminator may interpret these images as fraudulent in this case. It ensures that the real-world dataset's diversity is captured.

The ***equalized learning rate*** choice is the second enhancement. Each layer's weight values are normalized in this process. Each layer's normalization is done with a separate c coefficient. As a result, the weights can make large jumps in the layers where significant changes are required. It allows you to get to the global optimum in less time.

The features that are trying to be learned during the training have been shown to cause a gradient explosion, especially at the beginning. ***Pixel-wise feature normalization*** is used to avoid this issue. The color values in the identical pixels of the images in the batch are normalized at the output of each layer.

Finally, a new comparison technique called ***Wasserstein-GAN*** was used to apply the loss function during the training. The earth-mover distance technique is used to calculate the difference between the probability distribution functions produced by the Generator and those produced by the real dataset.

3. Example Applications and Their Results

The performance of the ProGAN technique in practice can be questioned in light of the theoretical knowledge presented in the preceding sections. Sample application problems and the results obtained with ProGAN are provided below for this purpose. 1280x1024 high-resolution synthetic mammography images performed by (Korkinof et al., 2018) are provided in the first sample application we chose.

The mammography images created by (Korkinof et al., 2018) are remarkably realistic, as shown in Figure 4. This instance is significant in terms of demonstrating the ProGAN technique's generalization capacity and its ability to be utilized in a variety of fields. Figure 4 shows the comparison of randomly selected samples from ProGAN-generated synthetic images with ones from the dataset that are closest to these samples.

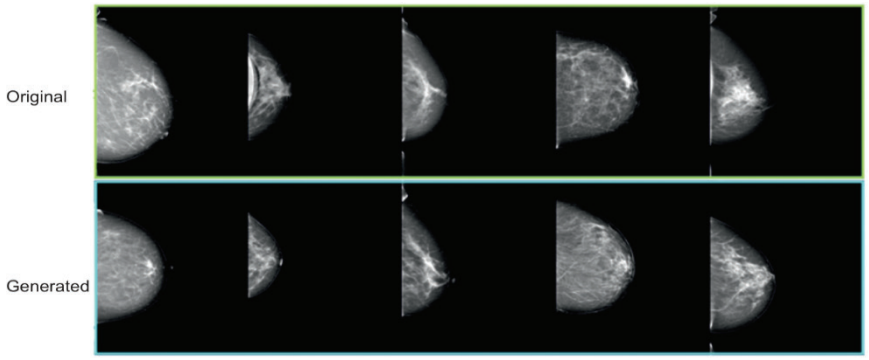

Figure 4: The obtained results by Dimitrios Korkinof et al., 2018,

In 2018, synthetic lesion images are generated using GAN, and the performance of the classifier they utilized improved by more than 10% (Frid-Adar, Klang, Amitai, Goldberger, & Greenspan, 2018). The established GAN architecture and the loss function demonstrating the achieved improvement are shown in Figure 5 and 6.

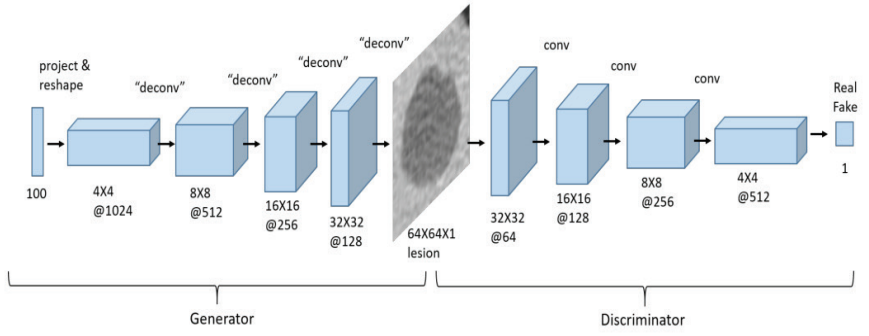

Figure 5: The developed model by Frid-Adar, Klang, Amitai, Goldberger, & Greenspan, 2018.

Figure 7 shows the results of a similar application (Pollastri, Bolelli, Paredes, & Grana, 2020). DCGAN and LAPGAN were used to create synthetic lesion images, and the segmentation outputs of these images are shown.

Figure 8 displays computed tomography (CT) images of the lungs generated by (Zhang et al., 2021) using Dense GAN. They diversified

the dataset by utilizing GAN-generated synthetic CT images to classify lung images with better accuracy using a deep learning classifier.

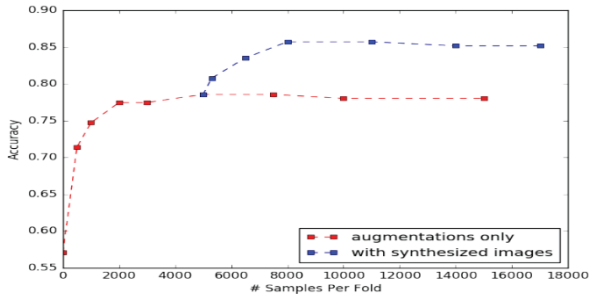

Figure 6: The obtained imporoved accuracy results by Frid-Adar, Klang, Amitai, Goldberger, & Greenspan, 2018.

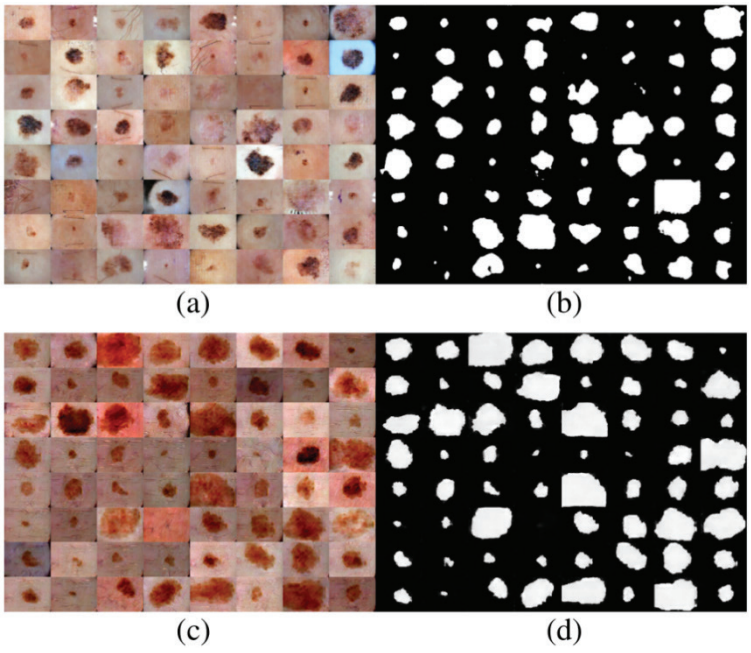

Figure 7: The obtained results by Pollastri et al. in 2020.

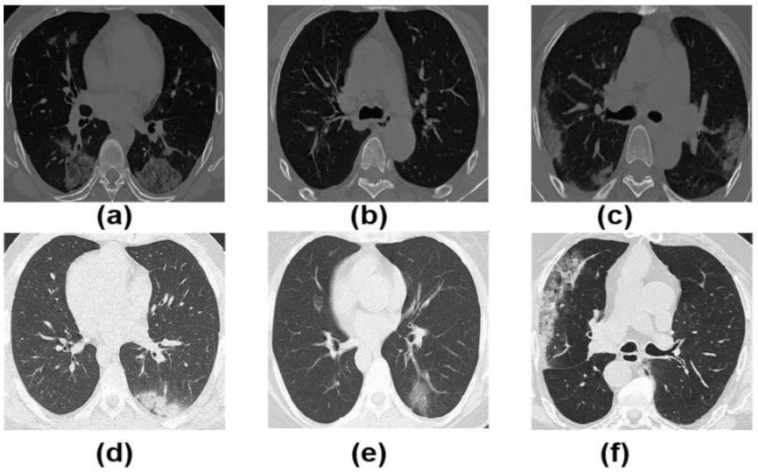

Figure 8: The obtained results by Zhang et al., in 2021.

4. Conclusion

ProGAN, the most up-to-date technique for generating large synthetic images, is explained in this article, together with practical applications and sample results. ProGAN improved the training process faster and more stable, according to the researchers. Furthermore, the model output images have been demonstrated to be more advanced in terms of diversity and resolution.

When a dataset is augmented with ProGAN, it begins with a 4x4 resolution and doubles in size with each iteration. Despite the fact that the number of models to be trained appears to be the log2 equivalent of the desired resolution, producing high-quality images with a single model takes a longer time.

It has been demonstrated with particular instances that ProGAN can boost performance in biomedical applications. Breast cancer diagnosis from mammography images, skin disease diagnosis from lesion images, and COVID-19 diagnosis from lung ct images may all be achieved with high success rates.

Although ProGAN can produce extremely successful synthetic images, some fundamental issues must be addressed. The first issue that comes to mind is that the greater the resolution value, the more mem-

ory, and processing power is needed to train the models. Although ready-made models trained for typical challenges such as creating a human face are publically available, adaption and fine-tuning to unique problems may involve considerable costs.

ProGAN works by sequentially training several models based on the resolution of the target images. Due to the hardware restrictions at hand, the batch size during training is lowered as we progress towards models with high resolution. When training the 128x128 model, for example, batch-size=16 for 64x64 images may need to be reduced to 8. This is a fundamental challenge that must be tackled adaptively based on the hardware capacity available.

References

Bisla, D., Choromanska, A., Berman, R. S., Stein, J. A., & Polsky, D. (2019). Towards automated melanoma detection with deep learning: Data purification and augmentation. 2019 IEEE/CVF Conference on Computer Vision and Pattern Recognition Workshops (CVPRW). IEEE.

Frid-Adar, M., Klang, E., Amitai, M., Goldberger, J., & Greenspan, H. (2018). Synthetic data augmentation using GAN for improved liver lesion classification. 2018 IEEE 15th International Symposium on Biomedical Imaging (ISBI 2018). IEEE.

Goodfellow, I. J., Pouget-Abadie, J., Mirza, M., Xu, B., Warde-Farley, D., Ozair, S., … Bengio, Y. (2014). Generative Adversarial Networks. Retrieved from http://arxiv.org/abs/1406.2661

Karras, T., Aila, T., Laine, S., & Lehtinen, J. (2017). Progressive growing of GANs for improved quality, stability, and variation. Retrieved from http://arxiv.org/abs/1710.10196

Korkinof, D., Rijken, T., O'Neill, M., Yearsley, J., Harvey, H., & Glocker, B. (2018). High-resolution mammogram synthesis using progressive generative adversarial networks. Retrieved from http://arxiv.org/abs/1807.03401

Langr, J., & Bok, V. (2019). *GANs in Action*. New York, NY: Manning Publications.

Pollastri, F., Bolelli, F., Paredes, R., & Grana, C. (2020). Augmenting data with GANs to segment melanoma skin lesions. *Multimedia Tools and Applications*, *79*(21–22), 15575–15592. doi:10.1007/s11042-019-7717-y

Vasconcelos, C. N., & Vasconcelos, B. N. (2017). Convolutional neural network committees for melanoma classification with classical and expert knowledge based image transforms data augmentation. Retrieved from http://arxiv.org/abs/1702.07025

Zhang, J., Yu, L., Chen, D., Pan, W., Shi, C., Niu, Y., … Cheng, Y. (2021). Dense GAN and multi-layer attention based lesion segmentation method for COVID-19 CT images. *Biomedical Signal Processing and Control*, *69*(102901), 102901. doi:10.1016/j.bspc.2021.102901

CHAPTER II

CELLULAR NETWORK TECHNOLOGY AND COMMUNİCATİON SYSTEM

Fatih TOPALOĞLU
(Asst. Prof Dr.), Department of Computer Engineering,
Malatya Turgut Özal University, e-mail:fatih.topaloglu@ozal.edu.tr
ORCID: 0000-0002-2089-5214

1. Introduction

Acellular network is a type of ground-based wireless network over cells where each cell contains a fixed location transceiver known as a base station. In this technology, service is given to each cell by a base station. This cellular structure provides radio coverage in wider geographic areas. Cellular networks offer users advanced features over alternative solutions such as high capacity, low battery power usage, better coverage and less interference from other signals. As seen in Figure 1, the same frequencies can be reused in the cellular network example and in two separate cells that do not share frequency in that cellular network, thus increasing the total capacity.

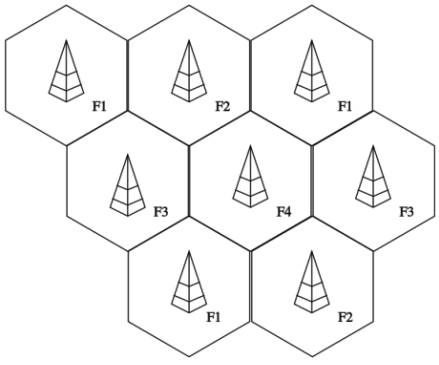

Figure 1. Frequency Reuse Factor

The concept of cellular network was introduced in order to use the frequency spectrum efficiently. Cellular networks form the basis of wireless and mobile communications. The area to be covered by the cellular network is usually divided into cells that are considered hexagonal. The cell shape is considered hexagonal because by placing cells next to each other, it can cover the entire area without overlapping and its shape is very close to a circle. If the cells were contiguous circles, there would be spaces between the circles; If it were in the form of adjacent squares, the distance from the center of the square to the edges and the distance to the corners would be different. For these reasons, the cells were assumed to be hexagonal. Each cell, which is thought of as a hexagon, has a base station at its center.

Switching between cells ensures that the existing communication is not interrupted while the user is changing cells. The mobile device, which realizes that it will switch a cell, sends a switch request message to the base station of the other cell. Meanwhile, the service is still given by the base station of the old cell. The management unit of this base station sends the pass request to the base station to which the user is currently connected, after some controls. After the two base stations negotiate between them, it sends a change base station signal to the mobile device. In this case, the mobile device connects to the new base station and the call or data communication continues from that station. When the connection is completed, the resources that the mobile device was using on its old station are made available to other users.

Cellular network technology supports a hierarchical structure formed by the base transceiver station, mobile switching center, location registers, and public switched telephone network. The base transceiver station allows cellular devices to communicate directly with mobile phones. The unit acts as a base station for routing calls to the destination host controller. The base station controller coordinates with the mobile switching center to interface with the fixed line-based public switched telephone network, visitor location recording and home location recording to route calls to different base center controllers. Cellular networks retain information to track the location of their subscribers' mobile devices. In turn, cellular devices are also equipped with details of suitable channels for signals from cellular network systems.

2. Cellular Network Technology

Bell Laboratories came up with the idea of reusing frequency in small geographic cells in 1947, thus giving birth to the cellular concept for the first time. The first widespread cellular radio system, the Advanced Mobile Phone System (AMPS), was defined entirely by Bell Labs. Bell Labs applied for frequencies around the 800 MHz band to the Federal Communications Commission (FCC) in 1958, but the FCC decided that this band would be more appropriate for public use. A patent application was filed with the FCC for AMPS in 1970. In 1979, the World Administrative Radio Conference reserved the 862-960 MHz band for mobile systems. After that, in 1981, the FCC allocated 40 MHz to "celluar land -mobile phone service" within the 800-900 MHz band.

What is meant by the concept of cell is to divide a geographical region into small cells, as seen in Figure 2. Generally, hexagonal shapes are used for cells, but these shapes can change as a result of obstacles such as buildings and hills. Cells are collected in clusters and these clusters are repeated. The number of cells in a cluster affects both capacity and interference. While it is advantageous to have a small number of cells for capacity, the number of cells should be high to prevent interference. Smaller cell size also increases capacity. Cell size is kept small by operating base stations and mobile units at low power.

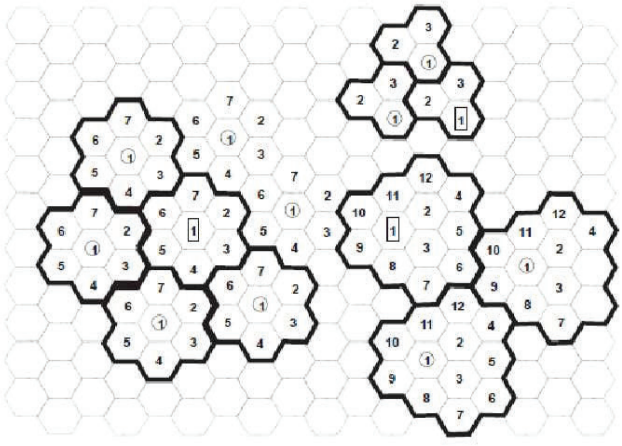

Figure 2. Cell and Cluster Structure

As stated earlier, although cells are generally considered to be hexagonal, they can take almost any shape. Although a circular shape is used in a flat desert, there may be overlap at some points and this interference is tried to be prevented by adjusting the power level. In urban areas, "urban canyon effect" and "urban waveguide effect" degrade cells to a large extent and complicate cell management.

Obtaining the highest capacity can be achieved by repeating the frequency the most. When the distance between base stations is adjusted in mobile phone systems, the same frequency is not used until the signal strength level does not fall below the noise threshold. In conventional systems, interference is caused only by background noise. In cellular systems, on the other hand, interference originates from the same frequencies used in different clusters, and this is considerably larger than the background noise.

2.1 Base Station

The base station is the cornerstone of the GSM infrastructure. It is responsible for providing the connection between the main switchboards and the user. It broadcasts on a two-way mobile network system. Unlike an antenna in a radio system, the base station consists of two antennas that both receive and transmit signals. Today, base stations use directional antennas that have the ability to broadcast in different directions at different strengths. Communication in GSM, CDMA, 3G and 4G networks is not possible without base stations.

Base stations create a coverage area called a cell with the signal they emit. These cells can be in different shapes, but mostly hexagonal cells are used in the GSM industry. These cells are preferred hexagonal according to the attenuation form of the signal emitted from the panels of the antennas in the base station. As shown in Figure 3, the base stations are located in the center of this hexagon or at each of its three corners. In other words, three antennas from three corners will signal inwards, and in this way a cell is formed. Hexagonal cells are the cell type that allows for the best coverage.

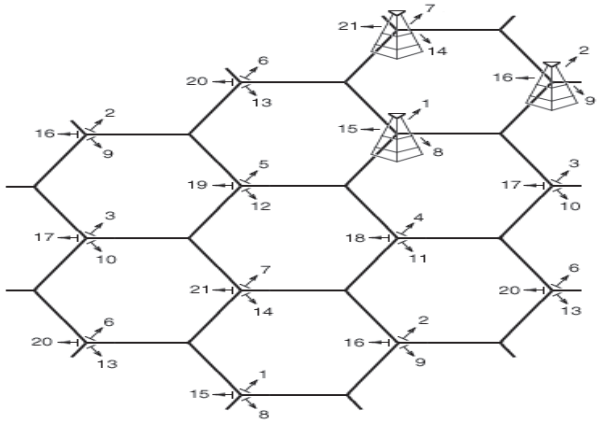

Figure 3. Base Station Oriented Antenna Diagram

When the base station cells are shown on a map, structures similar to honeycombs in the beehive appear. Mobile devices usually connect with the base station in the center of the cell, that is, closest to it. Because they aim to receive signals with the least loss and distortion. Omni-directional antennas have a round cell. Omnidirectional antennas are not used much. Because when they form cells next to each other, the out-of-coverage spaces between the round rings become too much.

Communication with mobile devices, operators use different frequencies reserved for them. They use different frequencies in and within each cell for uninterrupted communication, eliminating signal interference with other base stations that could disrupt communication. These frequencies are limited by the number of mobile devices to be communicated with. Each mobile device transmits its own frequency channel. For this reason, different channel frequencies are tried to be used in each cell. Since the frequencies that can be used are limited, each cell is set to use a different channel frequency from the cells adjacent to it. In this way, the same frequencies can be used in many stations and they do not affect each other. In order not to interfere with the frequencies, the output powers of the base stations are separated in such a way that they do not affect the cells of other base stations around.

Base stations, like mobile devices, have a coverage area. A typical cell site offers between nine and 21 miles of geographic coverage. The base

station is responsible for monitoring the level of signals when a call is made from a mobile device. When the user moves away from the geographic coverage area of the base station, the signal level may decrease. This causes one base station to request a transfer to another base station that receives the strongest signals without notifying the control to the user. In addition, we can list other factors that determine the coverage area as communication frequency, transmission power, data exchange rate for mobile devices, transmitter length, antenna height, versatility of the antennas used, the geographical region where it is installed, obstacles and weather conditions.

2.2. Multiple Access Techniques

Multiple access methods in wireless networks provide the opportunity to transmit and receive information to many users at the same time with limited bandwidth. Commonly known multiple access methods are FDMA, TDMA, CDMA as shown in Figure 4. WCDMA access technique is a broadband version of CDMA access technique. OFDMA and SC-FDMA are radio access techniques used for fourth generation communication systems.

FDMA (Frequency Division Multiple Access) technique, the bandwidth is divided into channels. Channels are allocated only when users request. FDMA allocates a single channel for each user at a time. Each channel allocated in FDMA has a different frequency band. This technique allows limited access. Because the frequency band used by one user cannot be used by another user. The FDMA technique is mostly used in analog systems.

TDMA (Time Division Multiple Access) technology allows a certain number of users to access a single frequency channel in different time zones. Users allow their transmission in their own time zone. GSM technology, which is the second generation cellular communication system, uses both TDMA and FDMA techniques.

CDMA (Code Division Multiple Access) technology, all users use the entire frequency band. Each user is assigned a set of codes to encode the information and distinguish it from other users. The bandwidth of

the code flag is much larger than the bandwidth of the information flag. In this way, the coding process spreads information over a wide spectrum.

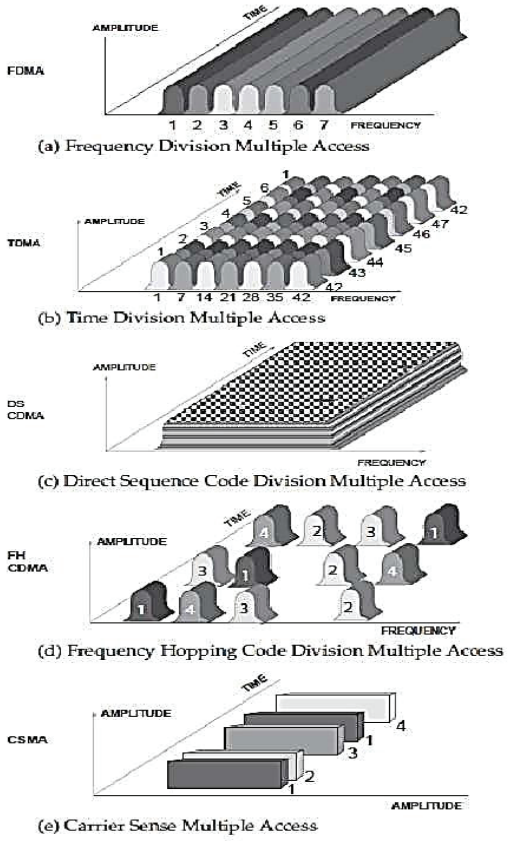

Figure 4. Multiple Access Methods

WCDMA (Wideband Code Division Multiple Access) technology is actually a derivative of CDMA technology. CDMA and WCDMA technology use the same principle. CDMA uses the 1.25 MHz frequency band, while WCDMA uses the 5 MHz frequency band. The 5 MHz frequency spectrum provides greater capacity and greater data rate.

OFDMA (Orthogonal Division Multiple Access) is a multi-user adaptation of OFDM (Orthogonal Frequency Division Multiplexing)

digital modulation technique. OFDMA uses FDMA, TDMA and CDMA with the advantages of OFDM. Basically, OFDM divides the bandwidth into N vertical subchannels and sends the data with these subchannels. It is similar to the OFDM technique and the FDM technique. OFDM technique uses the same rule as FDM technique, this rule is to transfer various messages from a single radio channel.

2.3. UMTS Technology

UMTS (Universal Mobile Technology System) is a variant of 3g (3rd generation) mobile phone technology. Also called 3GSM. It is a combination of 3G technology and GSM. It offers services such as text, audio, video and multimedia transmission in packets and at speeds higher than 2 megabits per second to portable computer and telephone users from anywhere in the world. With UMTS, you can transfer voice and data simultaneously, and the transfer rate is many times faster than Edge and almost equivalent to ADSL. However, 3G connection consumes more energy than Edge.

The UMTS network architecture basically consists of three subsystems as shown in Figure 5, namely the Radio Access Network (UTRAN), the Core Network (CN) and the user terminal (UE). UTRAN and CN are connected to each other by an interface called 'Iu'. The 'Iu' interface can be circuit switched (CS) or packet switched (PS). We can list the elements of the network units as follows: UTRAN: It consists of Node-B and RNC. Node-B is equivalent to BSC in GSM, CN : equivalent to GSM.

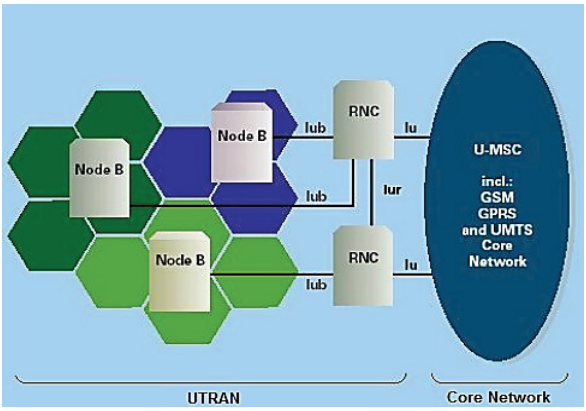

Figure 5. UMTS Terrestrial Radio Access Network

The base station of the cellular communication system of the UMTS standard. The main function of NodeB is to convert the received signal into a broadband radio signal transmitted to the phone. The base station does not make decisions about the allocation of resources, changing the speed to the subscriber, it only acts as a bridge between the controller and the subscriber's equipment and is completely dependent.

2.4. LTE Technology

LTE is the fourth generation cellular network technology that enables mobile devices on a cellular network to access data networks. Studies on LTE have aimed to develop a new radio access technology using only a packet switched network structure (Dalhman at al., 2013). This radio access technology uses IPv4 and IPv6 address structure and is completely IP based. LTE provides high data rate, low interference, more user support and low latency rates in data transfer thanks to OFDM and high-level modulation techniques it uses (Ersoy, 2017). In LTE, resource assignment is performed by creating resource blocks with 180KHz bandwidth created by OFDM technique in eNodeBs known as base stations.

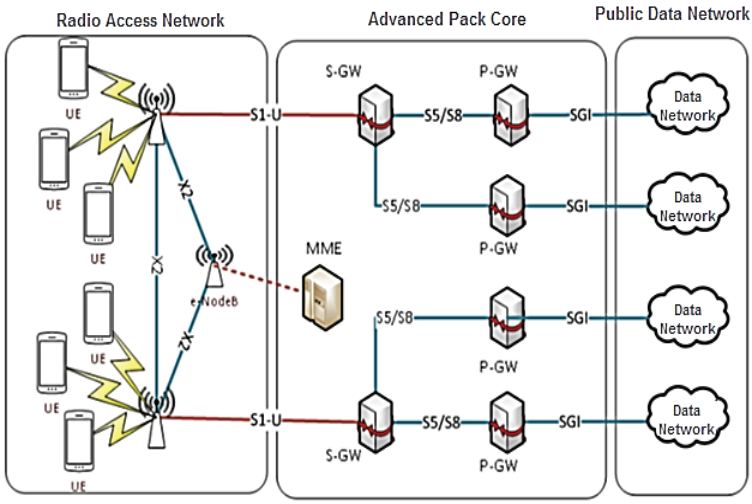

Figure 6. LTE Architecture

The network core of the LTE architecture shown in Figure 6, EPC is created using the packet switching structure. P-GW is the unit that provides operator connections, internet access, data exchange with external devices, QoS management and IP address assignment over the SGI interface (Stefania at al., 2009). S-GW are router devices that forward data between P-GW and base stations in Turkey and abroad using the S5/S8 interface (Stefania at al., 2009).

The eNodeBs in the RAN shown in Figure 6 perform data transfer operations between mobile devices called user equipment (UE) and S-GW over the S1/U interface, responsible for radio functions in one or more cells, and multiple UEs. They are smart base stations that have the ability to share load if there is a connection (Cox, 2012).

3. Cellular Communication System

Cellular communication systems; It is a method that has emerged to increase efficiency and the number of users. Cellular communication is based on the principle of placing a smaller and narrower but more than one base station (cells) in the area where the service will be distributed, instead of placing one and powerful base station. The first wireless communication experience started with the wireless telegraph developed by Marconi in 1897 (Bondyopadhyay, 1998). Electronic and semiconductor technologies, which have developed rapidly in recent years, have brought important developments in communication. Telegraph, telephone and internet communications, which started with wired transmission, have left their place to wireless communication in many areas with the developing technological possibilities. Due to the fact that mobile calls provide significant advantages to users, especially with the use of wireless and mobile calls, it has spread rapidly and studies have increased in the direction of improving sound quality, bandwidth, coverage area parameters. In this context, first generation cellular technologies, called 1G (First Generation), have led the development of 2G, 3G, 4G and 5G technologies over time.

3.1. 1G Cellular Communication System

1G is the first generation wireless telephony technology and uses a cellular network system. 1G systems are designed to provide voice service and circuit-switched low speed data service (9.6 Kbps) (Garg, 2010). The first generation uses only analog modulation techniques. Therefore, since it uses an analog data connection, anyone can listen to the conversations. In analog systems, audio signals are sent over the air without changing their format. No compression or digitization is done. In this model, in which circuit switching technology is used, it is not possible to provide service to a user on the move (Yadav, 2017). This technology has been used since the beginning of radio communication.

3.2. 2G Cellular Communication System

It uses a cellular network system. The greatest advantage of 2G over 1G is that it has switched from analog broadcasting to digital broadcasting. In digital systems, audio is converted into digital form before it is sent. When the digital signal reaches the receiving radio, it is converted back to analog. One of the advantages of converting to digital signals is that the coverage is large and the sound quality is improved. GSM uses dual bands between 890 Mhz-915 Mhz and 935 Mhz-960 Mhz frequencies for mutual communication. 124 channels were fitted into these band gaps (Forouzan, 2008).

This model, in which 2G, TDMA or CDMA multiplexing technologies are used, supports voice and data transmission together (Del Peral-Rosado, 2017). GSM, a 2G standard designed to operate at 850/900MHz frequency, was moved to the 1800MHz band as the number of users increased. In this way, simultaneous communication with multiple users was enabled, but with the increase in frequency, the range of the cell, that is, the base stations, decreased.

When the 2G standard was developed, there was a lot of bandwidth and few processors, so a technology was created that kept the line busy even when not using it. On the other hand, it becomes more and more difficult for operators to avoid the "network busy" message that appears

in many cases due to this choice. In response to this, 3G, a technology where the line is not used when data is not sent, and two devices can detect when they send data at the same time, just like in Ethernet technology, has been created.

3.3. 3G Cellular Communication System

It is the name given to the third generation wireless communication technology. It uses cellular network system like 1G and 2G. UMTS is an outcome of this technology. By using WCDMA technique for modulation and communication, it can reach wider bandwidths (Anttalaınent, 2003). In 3G, digital data is transmitted, not voice. In addition, unlike GSM, when the user is not actively using his phone, it consumes much less capacity than when he is using it, it puts much less load on the cell. In this way, the biggest problem we mentioned in 2G, which is busy when the network is not actively used, has been overcome with 3G. This has allowed service providers to use capacity more efficiently.

The broadcast frequency, which was increased in 2G, was slightly increased in 3G and increased to 2100/2400MHz. This led to further narrowing of the broadcast area of the cells and communication problems in the closed area, since the wave's interference decreases with increasing frequency. One of the missing points of 3G is the decrease in speed when data communication is made on the move. 3G, which can provide 2Mbit data communication at 40km per hour, drops to EDGE speed when reaching 120km, and communication is almost zero at 360km. In order to overcome this speed problem, HSDPA and HSUPA technologies have been developed. This new version network model, which can reach 2Mbps transmission speeds with HSDPA (High-Speed Downlink Packet Access) access technology, is called 3.5G. This new version 3G network, which has achieved transmission speeds of 30Mbps with HSUPA (High-Speed Uplink Packet Access) access technology, is called 3.75G (Mondal at al., 2015).

Since 3G enables high-speed secure data communication, it enables messaging, conversation and internet facilities to be used in a very fast and secure way compared to 2G. In addition, positioning service can be

provided. Thanks to high-speed packet switched services, 3G internet connection, mobile TV, video conferencing, 3D games and video calls and similar technologies have become available (Churı at al., 2012).

3.4. 4G Cellular Communication System

It is the fourth generation of wireless phone technology. It is more commonly known as LTE technology. Due to the financial size of the infrastructure investments it requires, it can actually be used in a geography that can be said to be very rare in the world. The biggest difference of 4G from 3G is again in speed. The standard accepted as 2-28 mbit in 3G has been replaced by a download speed of 100 Mbps for mobile devices and 1Gbps for Wi-Fi in 4G. The upload speed is expressed as 50 Mbps.

The system, which is called Advanced LTE (Long Term Evolution Advanced), which promises 1Gbit / s download and 500 Mbit / Upload speed, works entirely on LTE, that is, 4G platform, and promises higher speeds with some improvements. OFDM / SC-OFDM multiplexing technology is used (Gupta and Jha, 2015). Although there is not a big difference when reading or writing web pages in daily use, this difference will be felt much more especially when using multimedia files and game applications with advanced graphics.

3.5. 5G Cellular Communication System

According to the current technology literature, it is the fifth generation standard and the highest speed capability in wireless phones. The 5G cellular network model has a strong cellular structure equipped with WWWW (World Wide Wireless Web) and IPv6 technologies. The data transmission rate is higher than 1Gbps. With its high-capacity coverage areas, it offers a high usage impact as it can provide service in large geographical areas, regardless of the frequency and extent of user mobility. With the technologies it contains in its infrastructure, 5G networks have a very secure communication infrastructure (Gohil at al., 2013). CDMA and BDMA multiplexing technologies are used in these networks where both circuit switching and packet switching technologies are combined.

The development of smart cities offers high data rates and bandwidth for precision latency and fault-tolerant applications for healthcare and seamless communication of IoT devices.

It promises theoretical speed up to 10 times that of LTE, that is, 4G. The only test that can give an idea of what the situation is in practice was carried out by the world technology giant Samsung. The data obtained in Samsung's test has reached a speed of 7.5 Gbps in a fixed location on a 28 GHz network connection. In the same test, a speed of over 1.2 Gbps was recorded in the measurement made inside a vehicle traveling at 100 kmh. In other words, 940 MB per second for a fixed location means a data rate of 150 MB per second in motion at a speed of 100 kmh. This is even faster than any wired connection in use. In other words, there is exactly 30 times more performance than 5G, not 10 times. In Figure 7, the characteristics and comparison of wireless communication technologies using cellular network technology are given.

Generation	Deployment	Standard	Services	Technology	Switching	Core Network	Bandwidth
1G	1970 - 1980	AMPS	Only Voice	Analog	Circuit switching	PSTN	2kbps
2G	1980 -1990	GSM	Digital voice,	Digital	Circuit switching	PSTN	14-64kbps
		IS-95 JDC	Short messaging				
		iDEN					
2.5G	2000- 2003	GPRS EDGE	Digital voice, Short messaging	GPRS	Packet switching for data transfer	PSTN	14-64kbps
3G	2000	UMTS (WCDMA)	Integrated High quality audio, video and data.	Broad bandwidth/ CDMA/IP Technology	Packet	Packet N/W	2Mbps
3.5G	2006 – 2010	HSDPA/	High speed voice/data/	HSPA	Packet	GSM	14.4 Mbps 1-3 Mbps
		HSUPA	video			TDMA	
4G	2010	LTE-TDD LTE-FDD Mobile WiMAX	Dynamic information access, wearable devices.	WiMAX	All packet	Internet	100mbps
				LTE			
5G	2020	IP broadband LAN/WAN/PAN & WWWW	Dynamic information access, wearable devices with AI capabilities.	WWWW (coming soon)	All packet	Internet	1 to 10 Gbps

Figure 7. Comparison of Different Mobile Technologies (Yadav, 2017)

4. Conclusion

In this study, cellular network technology and cellular communication systems are discussed in general and their working principles are explained. Especially the developments in cellular communication systems, the technologies used and their technical features are presented and a comparison table is presented. The increase in the number of mobile devices and users increases the need for cellular networks, which are the main communication networks of wireless communication technologies. Considering the 6G and 7G technologies that are being developed, it is predicted that the need for cellular network technology will increase and the development in cellular network technology will continue.

In this study, the technical features of the cellular network concept and the evolution of cellular communication technologies from the first generation to the fifth generation were analyzed in this rapidly evolving process of mobile cellular communication technology, and multiple access techniques (FDMA, TDMA, CDMA, WCDMA, OFDMA), UMTS Technology, LTE technology were analyzed. complementary technologies such as When all standards are examined, it is observed that more efficient use of the limited frequency spectrum lies at the basis of technological developments. It is seen that increasing bandwidth values, efficient use of the line and data transfer rates have increased significantly with the developing semiconductor technologies and transmission techniques, new multiple access, multiple antenna and modulation techniques.

References

Anttalaınen, Tarmo. 2003. Introduction to telecommunications network engineering. Artech House, 2003.

Bondyopadhyay PK. 1998. "Sir JC Bose diode detector received Marconi's first transatlantic wirelesssignal of December 1901 (the "Italian Navy Coherer" Scandal Revisited)," in Proceedings of the IEEE, Cilt.86 (1), s.259-285.

Churı, J. R., Surendran T. S., Tigdi, S.A., Yewale, S. 2012. Evolution of networks (2G-5G). In: IJCA Proceedings on International Conference on Advances in Communication and Computing Technologies 2012. Foundation of Computer Science (FCS), p. 8-13.

Cox, C., 2012. An Introduction to LTE. John Wiley & Sons, Ltd,337p, Chichester, UK.

Dahlman, E., Parkvall, S., Sköld, J.,2013. 4G LTE/LTEAdvanced for Mobile Broadband. WILEY, 447, UK.

Del Peral-Rosado, J. A., Raulefs, R., López-Salcedo, J. A., & Seco-Granados, G. (2017). "Survey of cellular mobile radio localization methods: From 1G to 5G." IEEE Communications Surveys & Tutorials, 20(2), 1124-1148.

Ersoy, M. 2017. LTE Teknolojilerinde Tıkanıklık Tahminlerine göre Gerçek Zamanlı ve Yüksek Çözünürlüklü Video Aktarımı. Doktoro Tezi, Süleyman Demirel Üniversitesi, Türkiye.

Forouzan, B.A. 2008. Data Communication and Networking. 3rd/4th Edition, Tata McGraw.

Garg, V. 2010. Wireless communications & networking. Morgan Kaufmann.

Gohil, A., Modi, H., & Patel, S. K. 2013. 5G technology of mobile communication: A survey. In 2013 international conference on intelligent systems and signal processing (ISSP) (pp. 288-292). IEEE.

Gupta, A., & Jha, R. K. 2015. A survey of 5G network: Architecture and emerging technologies. IEEE access, 3, 1206-1232.

Mondal, S., Sinha, A., & Routh, J. (2015). A survey on evolution of wireless generations 0G to 7G. International Journal of Advance Research in Science and Engineering (IJARSE), 1(2), 5-10.

Stefania, S., Issam, T. ve Matthew, B., 2009. LTE, the UMTS long term evolution: from theory to practice. A John Wiley and Sons, Ltd, 6,. ,6136-144,.

Yadav, R. (2017). Challenges and Evolution of Next generation Wireless Communication. In Proceedings of the International MultiConference of Engineers and Computer Scientists (Vol. 2).

CHAPTER III

TRIBOLOGICAL, MECHANICAL, AND THERMO-ELECTRICAL PROPERTIES OF Sn-Bi-Cu HYPEREUTECTIC ALLOY

Fatma MEYDANERİ TEZEL
(Prof. Dr.) Department of Metallurgy and Materials Engineering, Faculty of Engineering, Karabük University, 78050, Karabük, Turkey,
E-mail: fatmameydaneri@karabuk.edu.tr, meydaneri@yahoo.com
ORCID: 0000-0003-1546-875X

1. Introduction

Lead and the compounds containing lead are regarded as toxic substances because of their hazardous influences on the environment and humans (Mahmudi et al, 2008; 2009; 2010). Many countries worldwide have introduced restrictions in development programs and industrial areas where lead is used for environmental protection. Significant efforts are being made to replace conventional Sn-Pb solder alloys with lead-free alternatives. The melting temperature of lead-free solder alloys must be near to the melting point of Sn-Pb alloy (Esfandyarpour and Mahmudi, 2011; Directive, 2003). Nevertheless, new solder alloys should fulfill economic, physical, and chemical properties and some other conditions. The melting points of lead-free solder alloys developed in this respect should be close to the conventional Sn-Pb eutectic alloy, and their strength and stability should be similar or superior (Dong et al., 2008; Lin et al., 2009). Also, in terms of production cost, the costs of new alloys should compete with lead-containing alloys (Lin et al., 2008). For this purpose, many studies focused on Sn-based multicomponent alloys. However, these solder alloys' melting points

are higher than the Sn-Pb eutectic alloy due to production conditions and chemical composition changes. Considering these limitations, Sn-based alternative solder alloys have been chosen to be used in the existing production line without any modification (Rani and Murthy, 2013). Soldering in the electronics sector has focused on the benefits of these alloys, as mechanical integrity is affordable and manufacturability is relatively low (Mei and Morris, 1992; Suganuma, 2001; Tong, 2011; Osorio et al., 2013; Laurila and Vuorinen, 2010; Goh et al., 2013; Shen et al., 2014). It is known that solder joints can damage the electronic device and shorten the device's useful life due to thermal stresses, stresses, and warpage during prolonged work or fluid behavior when overheated (Goh et al., 2013; Vianco et al., 2004; Silva et al., 2015). If the solder alloy' mechanical features are recognized, these merits can be used to anticipate the solder's life and reliability (using mathematical models) (Yoon et al., 2002; Takaku et al., 2004; Lin et al., 2014). It is well understand that heat treatment plays an important role (Das et al., 2009; Li et al., 2006), but the microstructure and rigidity control of solder alloys is complicated in metallurgy and micromechanics (Mokhtari and Nishikawa, 2016; Silva et al., 2017). This work purposes to explore the thermo-electrical, structural, mechanical, corrosion, and wear properties of Sn-30 wt.% Bi-0.5 wt.% Cu hypereutectic alloy obtained by permanent mould casting.

2. Experimental Procedure

In this study, Bi-Sn-Cu hypereutectic alloy was produced in a vacuum induction furnace under a high purity argon atmosphere. Master raw materials were melted at 300 ˚C, and waited at this temperature for 3 hours. The molten alloy was depleted into a permanent/kokil mould preheated up to 350 ˚C. The surface pollutions of the samples obtained after casting processes were cleaned; heat treatment was applied for 15 mins at about 70 ˚C, and it was left for cooling in the furnace. In the first step of this work, the thermal conductivity varia-

tions versus temperature were measured using the laser flash method. In the second step, the electrical conductivity variations depending on the temperature were determined from the Wiedemann-Franz law and Smith-Palmer equation using the thermal conductivity values and Lorenz coefficient. In the third step, the fusion enthalpy (ΔH) and the specific heat capacity change (ΔC_p) were determined. Finally, the alloy's tensile strength, elongation, micro hardness, wear, and corrosion properties were investigated. Metallographic processes (mechanically ground with 240, 400, 600, 800, 1000, 1200, 2000, 2500 grit SiC papers followed by polishing with 6, 3 and 1 μm diamond paste) were conducted for all samples for XRD, FESEM, and EDX. Polished samples were etched with nital solutions.

3. Results and Discussion

3.1. Measurement of the thermal conductivity (TC)

For diverse materials having distinct thermal conductivity and different ranges of temperature, several different measurement methods are applied for the experimental determination of their TC. In this work, the Sn-30 wt.% Bi-0.5 wt.% Cu hypereutectic alloy' TC is measured by the laser flash method. The method measures the temperature rise on the backside of a thin disk sample resulting from a low energy pulse on the forepart. The sample (10 mm in diameter and about 1-5 mm thick) is placed in a vacuum furnace and isothermally heated at a uniform temperature. Then, a short (450 μs) laser pulse of 1.06 μm wavelength irradiates one surface of the sample. The temperature raise on the opposite side is measured by an IR detector (HgCdTe or InSb depending on the temperature). A high-speed recorder collects data representing the temperature rise (see Fig.1).

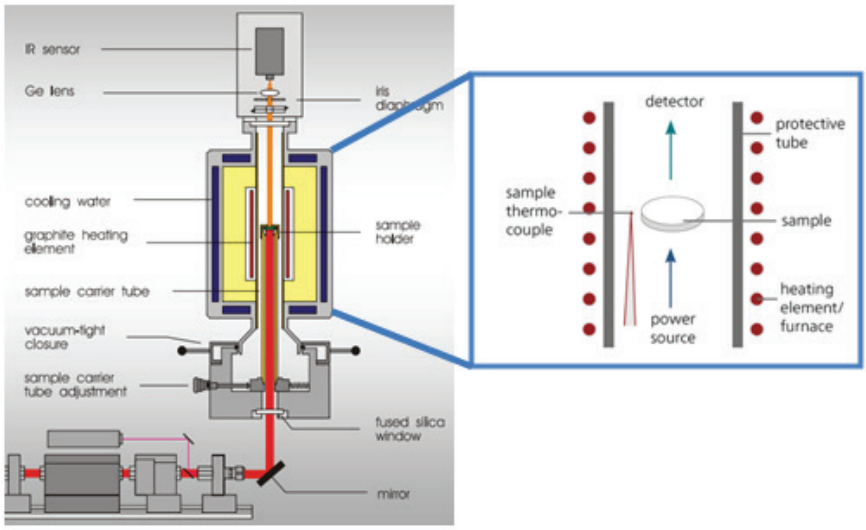

Fig.1: The scheme of the laser flash measurement device.

The diffusivity is determined from the line of the temperature-time plot (thermo gram) and sample thickness (e). This study's TC and diffusion coefficients according to temperature are depicted in Figs. 2 (a) and (b).

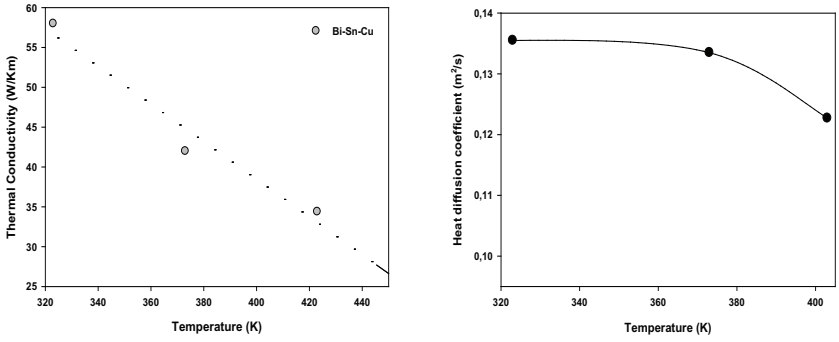

(a) (b)

Fig. 2: a) Thermal conductivity, b) Diffusion coefficient vs. temperature curves of Sn-30 wt.% Bi-0.5 wt.% Cu hypereutectic alloy.

According to the current experimental results, the alloy' both the TC and the thermal diffusion parameters decrease with increasing temperature.

The solid-phase alloy's TC and diffusion coefficient at approximately melting temperature are 28.1 W/Km and 0.122 m^2/s, respectively. For a given alloy, the thermal temperature coefficient of solid-phase according to temperature can be given as (Terada et al., 1999);

$$\kappa_f - \kappa_i = \kappa_i[\alpha_{TTC}(T_f - T_i)] \quad (1)$$

where κ_i *and* κ_f are the TCs at the initial (T_i) and final T_f temperatures, α_{TTC} is the temperature coefficient. In the work, the α_{TTC} was calculated to be $4.05x10^{-3}$ K^{-1}.

3.2. Determination of the electrical conductivity (EC)

EC is affected by substances' chemical composition and the stress state of crystalline structures. The EC and TC of metals and alloys in solid and liquid situations are mainly carried by free electrons. Therefore, the Wiedemann-Franz explains the connection between TC and electrical resistivity as below (Yamasue et al., 2003):

$$\frac{\kappa\rho_e}{T} = \frac{\pi^2 k^2}{3e^2} = L_0 = 2.445x10^{-8}\ W\Omega K^{-2} \quad (2)$$

$$\sigma = \frac{\kappa_S}{LT} \quad (3)$$

where k is the Boltzman constant, e is the electron charge, L_0 is the Lorenz number (constant), T is the temperature (K), σ is electrical conductivity, κ_S is the TC of the solid-phase at temperature *T,* and *L* is the Lorenz number of alloy. This relationship is attributed on the reality that both heat and electrical transport involve the free electrons in the metal. The Wiedemann-Franz-Lorenz relationship can be modified into the following form to associate the thermal conductivity and electrical resistivity of complex alloys:

$$\kappa = A\frac{L_0 T}{\rho_e} + C \quad (4)$$

where A, B, and C are empiric constant. Smith-Palmer (Smith and Palmer, 1935) suggested that the thermal conductivity of many alloys could be expressed by Eq.(4) if A=0.904 and C=5.27.

In the current study, the variation of electrical conductivity ver- sus temperature was determined from the Wiedemann-Franz law and Smith-Palmer equation using κ_S and L. The values of L for pure materials are well-known, but they are unknown for alloys. The values of L and κ_S are required to determine the variations of electrical conductivity versus temperature. The Lorenz numbers for pure Bi, Cu, and Sn are 2.25×10^{-8} (http://www.kayelaby.npl.co.uk/general _physics/2_6/2_6_1. html), 2.23×10^{-8} (Kittel, 1965), and 2.49×10^{-8} $W\Omega/K^2$ (Sergent and Krum1998), respectively.

$$L_{alloy} = \sum_{n=1}^{3} x_n L_n \qquad (5)$$

Lorentz value for Bi-Cu-Sn alloy was calculated from Eq. (5). X_n *is* the weight percentage of the n^{th} component; L_n is the Lorentz value of the n^{th} component. The electrical conductivity versus temperature of the alloy is depicted in Fig. 3.

The dependence of electrical conductivity on temperature can be given as below (Meydaneri and Saatçi, 2014),

$$\alpha_{ETC} = \frac{\sigma - \sigma_0}{\sigma_0 (T - T_0)} \qquad (6)$$

where σ and σ_0 are the electrical conductivities of the solid phase at the final temperature T and initial temperature T_0, respectively, and α_{ETC} is the electrical temperature coefficient.

Metals' electrical resistivity increases with temperature, and electron-phonon coactions can act a significantly role. The dynamic charge carriers' number in a metal depends on the carrier' intensity on Fermi energy. Free electron concentration in metals (finite temperatures like room temperature) does not change with increasing temperature since it is already too high to contribute new electrons. In the study, σ decrease but ρ increase with the temperature increase.

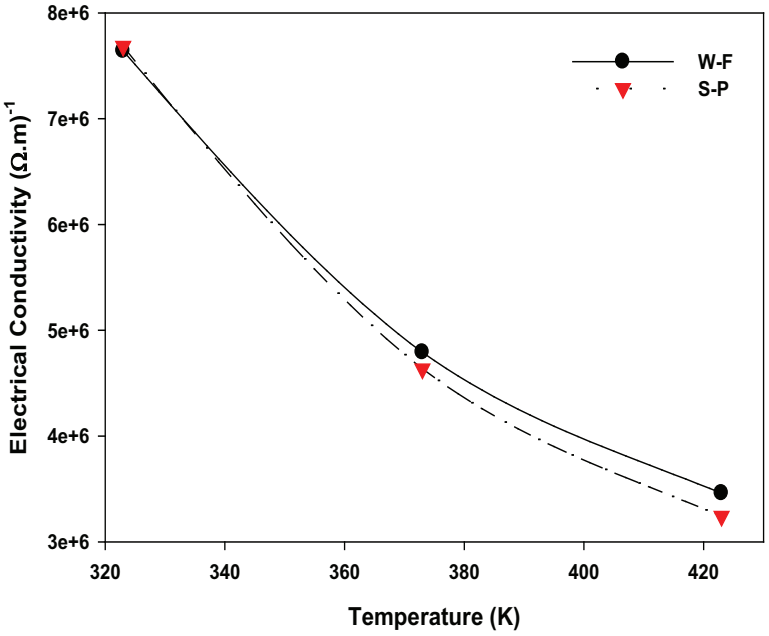

Fig. 3: Electrical conductivity vs. temperature curve of Sn-30 wt.% Bi-0.5 wt.% Cu hypereutectic alloy.

3.3. Change of enthalpy and specific heat capacity

The heat capacity results from the vibrations/phonons within the solid. In metals, free conduction electrons also promote to the heat capacity. In the metals' free electron model, conduction electrons are considered the ideal gas that fits Fermi-Dirac statistics. The interactions of electrons with positively charged atomic ions and other electrons are neglected. It is not as bad a dealing as it might sight at first glance: ions ensure a positively charged frame that partially sweeps electrons from each other. Residual collisions are usually relatively insignificant - the energetically accessible end states are already occupied, forbidding any collision excitation processes prohibited via the Pauli Exclusion Principle. Solely electrons in orbitals within a k_BT range around Fermi energy can be thermally excited. In terms of phase transitions and thermodynamics of materials, the phase alteration' latent heat and the heat capacity of the materials should be known. When heat is given to the system, the tem-

perature does not change/stay constant during the phase transformation. The given heat is used to provide the enthalpy of fusion (the latent heat of fusion) required to transform the solid into a liquid.

$$\Delta C_p = \frac{dH}{dT} = \left(\frac{\Delta H}{T_M} \right)_p \quad (7)$$

T_M is the melting temperature, and ΔC_P is the specific heat change. The DSC (Hitachi DSC7000) thermal quantity was executed in the temperature range of approximately 323-573 K with a heating ratio of 1°C/min and by a constant nitrogen flow at atmospheric pressure. The DSC plot observed for the alloy is depicted in Fig. 4.

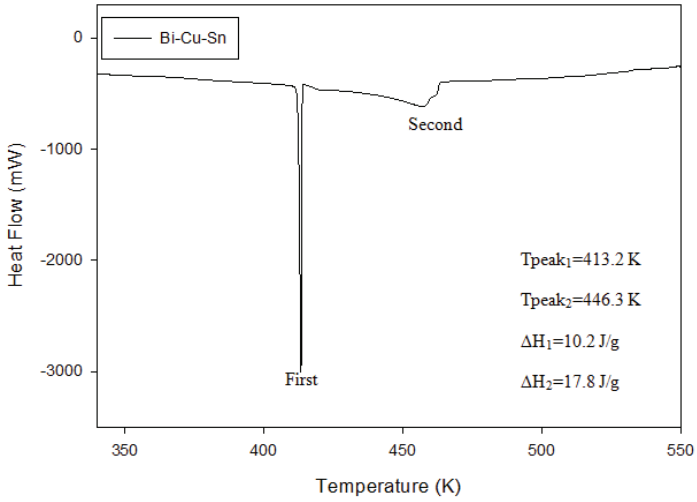

Fig. 4: DSC plot of Sn-30 wt.% Bi-0.5 wt.% Cu hypereutectic alloy.

The alloy's enthalpy of fusion (ΔH) was obtained by getting the area' integral below the peak. The value of specific heat change (ΔC_P) was determined by dividing to the T_M temperature of the fusion enthalpy. As can be conferred from the alloy' DSC plot, the areas' total under the two peaks gives the fusion enthalpy. At melting temperature, the enthalpy of fusion (ΔH_1 *and* ΔH_2) for the two peaks is calculated to be 10.2 and 17.8 J/g, respectively. Also, the change of specific heat (ΔC_P) for the alloy is detected to be 0.065 J/gK.

3.4. Tensile test and micro hardness results

The tensile test of Bi-Cu-Sn hypereutectic alloy was carried out with a Zwick/Roell Z600 Universal test device at a speed of 1 mm/min, and its strength properties were determined. Q10 A+ QNESS Vickers micro hardness device was used to determine micro hardness. A load of 50 kg was implemented to the specimen for 10 seconds. Approximately 7 measurements were made on the grain boundaries and different colored phases; the average micro hardness was obtained as 37.13. The morphology of the broken surfaces after the tensile test and the phases' elemental mapping were examined with FESEM+EDX. This image and composition analysis evaluated the ductility/brittleness of the sample. The tensile diagram of Bi-Cu-Sn hypereutectic alloy is depicted in Fig. 5, and the obtained tensile test outcomes are seen in Table 1. Figures of the broken surfaces are depicted in Fig.6. Fractured surfaces have an indented, opaque surface. These indentations indicate that shear fracture occurs due to the shifting of atomic planes. The formation of dimples in the structure and a fibrous appearance indicate a ductile fracture, which is quite in compatible with the tensile test strength results.

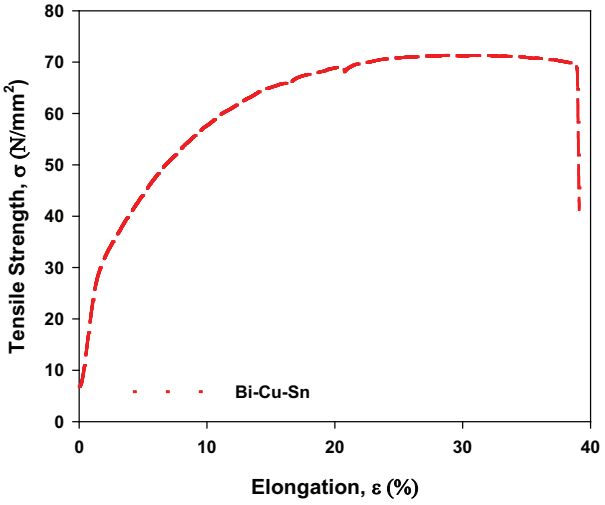

Fig. 5: The σ-ε curve of Sn-30 wt.% Bi-0.5 wt.% Cu hypereutectic alloy.

Table 1: Mechanical properties of Sn-30 wt.% Bi-0.5 wt.% Cu hypereutectic alloy.

Sn-30 wt.% Bi-0.5 wt.% Cu			
Yield Strength (σ_a)	32.78 MPa	Sample Diameter	9.0 mm
Tensile Strength (σ_c)	71.31 MPa	Cross Sectional Area	63.90 mm^2
Breaking Strength (σ_k)	41.25 MPa	Sample Length	54 mm
Total % elongation (ϵ_t)	% 39.50	Average microhardness	37.13

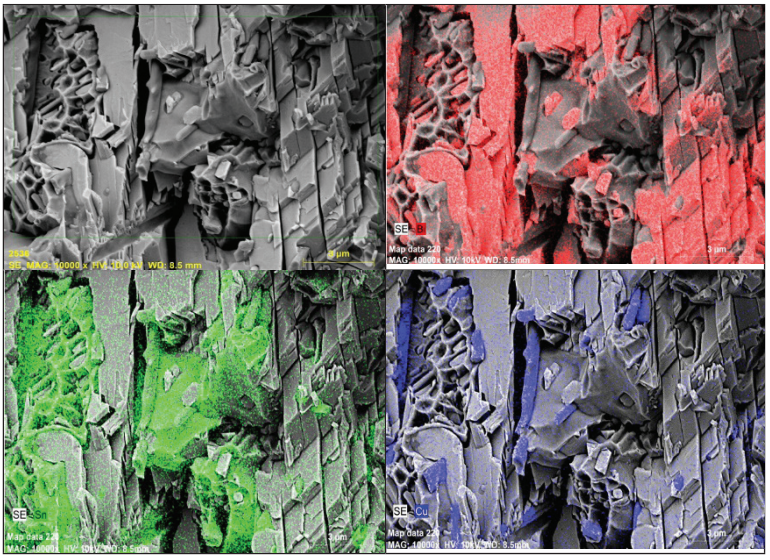

Fig. 6: Composition mappings and the broken surface' FESEM figure of Sn-30 wt.% Bi-0.5 wt.% Cu hypereutectic alloy after tensile test.

3.5. Structural, surface, and composition analysis

The crystallographic parameters and orientations of the phases formed in Sn-30 wt.% Bi-0.5 wt.% Cu hypereutectic alloy were procured via Rigaku-Ultima IV XRD with a 0.02° step at 3°/min speed. The XRD diffraction peaks and phase components obtained at 2θ=20°-90° are given in Fig.7. Regarding binary phase diagrams of Bi-Sn and Cu-Sn, only the Bi element shows a maximum solubility of 21% in the α-Sn

phase at a eutectic temperature of 139 °C. This solubility decreases to 3% as the temperature approaches room temperature. Therefore, the Bi element will disperse in the Sn matrix phase. Otherwise, the Cu-Sn phase diagram indicates that the Cu_6Sn_5 intermetallic phase, albeit very little, is formed when Cu combines with Sn at 186 °C. However, as it goes down to room temperature, the Cu_6Sn_5 intermetallic phase will be seen as precipitation in the Sn matrix phase. According to the XRD diffraction peaks, Sn, Bi, and Cu_6Sn_5 intermetallic phase peaks were observed and indexed in Sn-30 wt.% Bi-0.5 wt.% Cu hypereutectic alloy. The crystal structures, parameters, and Miller indices of the phases formed in this structure are imputed in Table 2. The approximate grain sizes (D) of Bi, Sn, and Cu_6Sn_5 phases were calculated by the X-Powder computer program versus higher intensity peak of XRD patterns using Debye Scherrer's formula (Cullity, 1978; Mott and Davis, 1979):

$$D = \frac{0.9\lambda}{\beta \cos\theta} \tag{8}$$

Grain sizes of Bi, Sn, and Cu_6Sn_5 were calculated as 350, 370, and 330 nm.

Table 2: Crystal structure parameters of Sn-30 wt.% Bi-0.5 wt.% Cu hypereutectic alloy.

	2θ (°)	d (Å)	(h k l)
	32.02	2.792	(1 0 1)
	43.88	2.062	(2 2 0)
	44.91	2.017	(2 1 1)
Sn (Tetragonal)	55.35	1.659	(3 0 1)
a=b=5.830	63.80	1.458	(4 0 0)
c=3.181	64.60	1.442	(3 2 1)
	72.43	1.304	(4 2 0)
	73.18	1.292	(4 1 1)
	79.52	1.204	(3 1 2)
	89.42	1.095	(5 0 1)

	27.24	3.271	(0 1 2)
Bi (Trigonal)	38.09	2.361	(1 0 4)
a=b=4.535	48.83	1.863	(2 0 2)
c=11.814	56.20	1.635	(0 2 4)
	59.57	1.551	(1 0 7)
	63.07	1.473	(2 1 1)
	64.69	1.440	(1 2 2)
	71.01	1.326	(2 1 4)
	85.82	1.131	(1 0 1)
Cu_6Sn_5	30.66	2.914	(-1 1 3)
(Monoclinic)	43.80	2.065	(2 0 4)
a=10.926	47.73	1.904	(3 3 1)
b=7.113 c=9.674	44.00	2.056	(1 3 2)
	61.85	1.499	(-1 3 5)
	65.38	1.426	(0 4 4)
	86.38	1.125	(4 4 5)

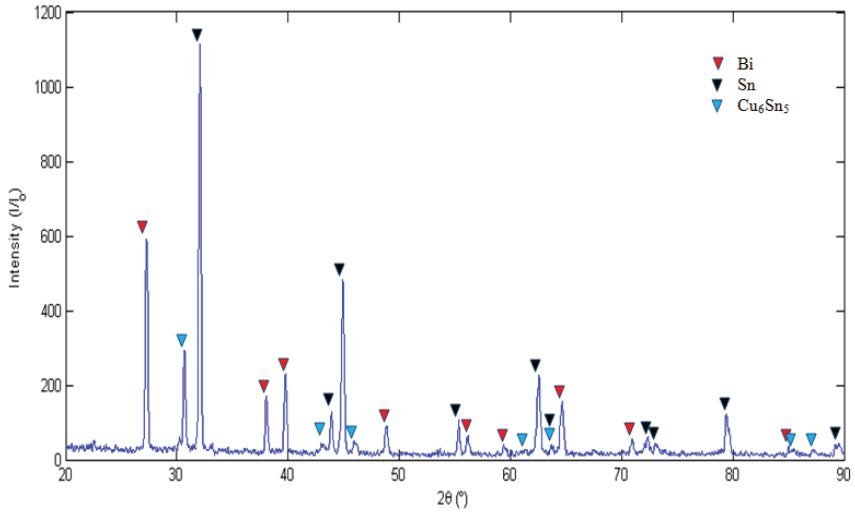

Fig. 7: XRD pattern of Sn-30 wt.% Bi-0.5 wt.% Cu hypereutectic alloy.

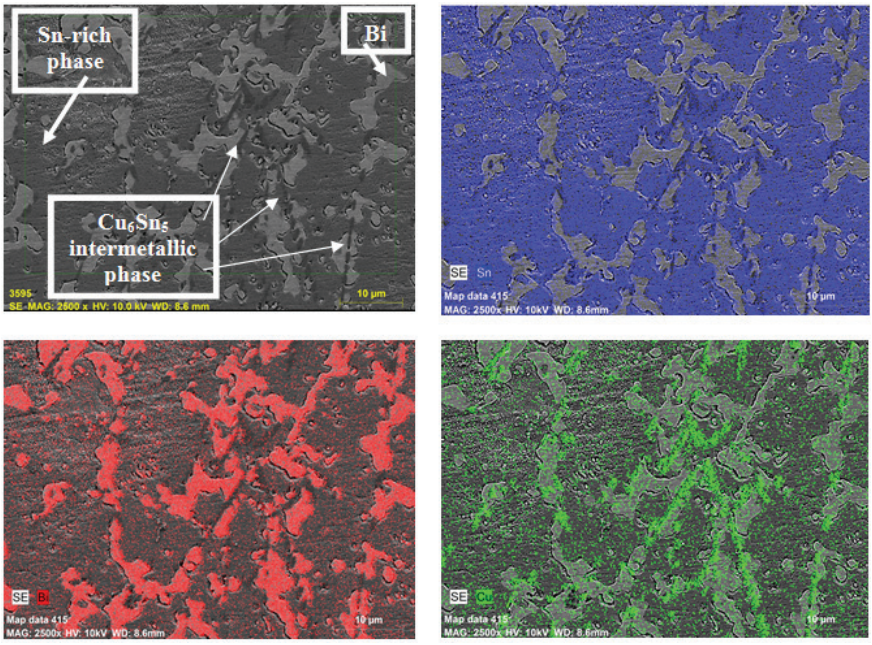

Fig. 8: FESEM and EDX images of Sn-30 wt.% Bi-0.5 wt.% Cu hypereutectic alloy.

Two-dimensional (2D) surface morphology of Sn-30 wt.% Bi-0.5 wt.% Cu hypereutectic alloy was obtained by FESEM and elemental mapping by EDX, and they are depicted in Fig. 8. Thereafter, the red-colored Bi-phase with various sizes is dispersed into the Sn matrix phase, shown in blue. The needle-like long rod-shaped structures shown in green indicate the Cu_6Sn_5 intermetallic phase. Small amounts of Bi and Cu are diffused into the Sn matrix phase.

3.6. Corrosion and wear properties

Electrochemical corrosion tests for Sn-30 wt.% Bi-0.5 wt.% Cu hypereutectic alloy were performed in a 250 ml 3.5% NaCl solution complying with G 102 – 89 (2004) standard with a computer-controlled PARSTAT 4000 (Potentiostat-Galvanostat-EIS Analyzer corrosion tester) using a standard three-electrode cell. The samples were encapsulated

in cold-cured resin, leaving a surface of 0.126 cm^2 open and exposed to the solution. A copper cable placed behind the resin-coated sample was used to establish an electrical connection. A graphite bar was used as the counter electrode, Ag/AgCl as the reference electrode, and the classical three-electrode cell with the sample surface was utilized as the working electrode. The open-circuit potential (OCP) was pursued as time-dependent after immersion. For the polarization curve measurement, polarization scanning was performed in the range of -0.32 V (vs. open circuit potential, E_{oc}) +0.12 V (vs E_{oc}) at a scanning rate of 1 mV/s. The Potentiodynamic Tafel curve is given in Fig. 9.

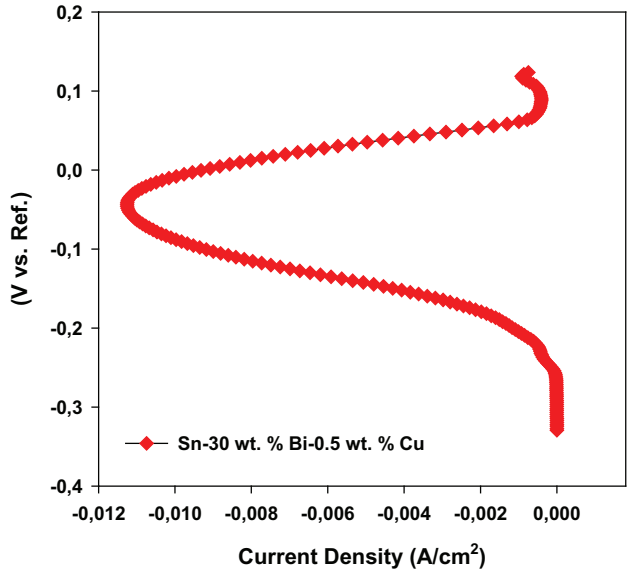

Fig. 9: Tafel curve of Sn-30 wt.% Bi-0.5 wt.% Cu hypereutectic alloy.

According to the outcomes, corrosion potential E_{corr} (V), corrosion current intensity (i_{corr}, μA/cm^2), and corrosion rate C_R (mm/year) were measured as -0.339 Volt, 10.70 μA/cm^2 and 0.48 mm/year, respectively. The sample's post-corrosion FESEM image and the EDX analysis for the oxidation amount are given in Fig. 10.

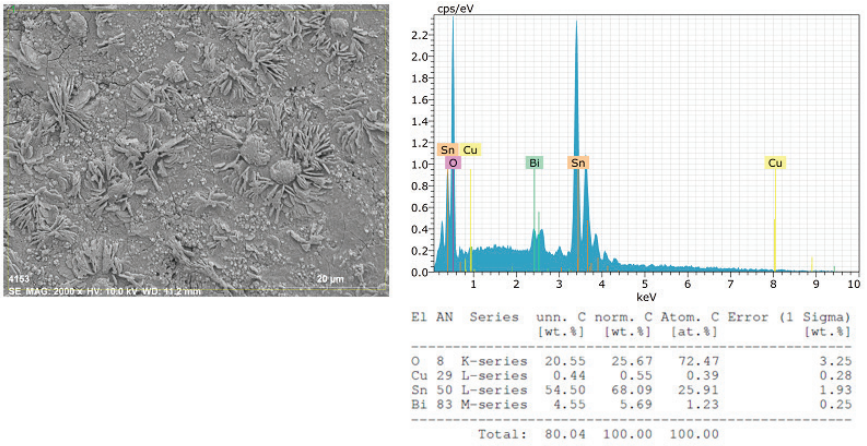

Fig. 10: Post-corrosion FESEM image and EDX analysis of Sn-30 wt.% Bi-0.5 wt.% Cu hypereutectic alloy.

Wear is a complex system, inevitable in all machine elements working with friction. It causes large amounts of material loss and energy wastage. In technical terms, wear is an undesirable change on objects' surfaces due to the breaking of micro particles under mechanical factors. There must be a mechanical effect for the attrition seen in the materials to be considered wear. The friction must cause changes on the material's surface slowly or continuously, and they must occur under coercion. In this work, wear tests were executed according to ASTM G133 standard, using the UTS TRIBOMETER T10/20 device via ball-on-flat method, 50 m forward-backwards under 5 N and 10 N loads. Figure 11 shows the wear trace of the steel ball, FESEM images of the particles broken off after wear, and their composition analysis. In wear rate calculations, the wear volume loss (V_w) is calculated using the wear depth (a), the wear width (b) and the stroke distance (c) from Equation (9).

$$V_W\,(mm^3) = 2 \times a \times b \times c/3 \qquad (9)$$

The wear rate (mm^3/m) was found by dividing wear volume loss by the sliding distance. This study calculated the wear volumes for 5 N and 10 N loads as 0.059 mm^3 and 0.822 mm^3, respectively. Wear rates for 5 N, and

10 N loads were obtained as $1.188x10^{-3}$ mm^3/m and $1.64x10^{-2}$ mm^3/m, respectively. Regarding the wear trace in Fig. 11, the wear lines on the surface in the sliding direction are evidence of typical abrasive wear. The broken parts and oxygen appearance in the structure, according to EDX analysis, also show that there is oxidation wear by friction.

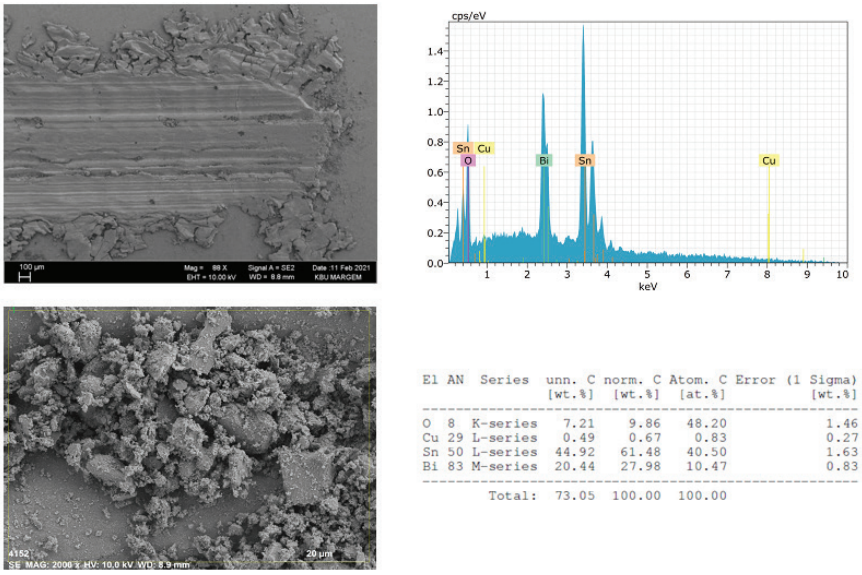

Fig. 11: Wear trace, FESEM image of the particles broken from Sn-30 wt.% Bi-0.5 wt.% Cu hypereutectic alloy and their composition analysis.

3.CONCLUSION

The Sn-30 wt.% Bi-0.5 wt.% Cu hypereutectic alloy was explored for the first time in the letterure; therefore, the outcomes could not be compared. In this study, Sn-30 wt.% Bi-0.5 wt.% Cu hypereutectic alloy cast on a permanent mould was treated at 70 °C for 15 min, and then it was released to cool in the oven. As a result of metallographic processes, the structural properties of the Bi-phase and Cu_6Sn_5 phase dispersed into the Sn matrix phase were determined by XRD, EDX, and FESEM. The grain size was the highest in the Sn phase and the lowest in the Cu_6Sn_5 intermetallic phase. Thermal conductivity and diffusion coeffi-

cient according to temperature were found by the laser flash method, and a decrease was observed with increasing temperature. In order to better comprehend the phase changes and lattice vibrations, the fusion enthalpy change, and the specific heat change were analyzed with the DSC device. Electrical conductivity was calculated from Wiedeman-Franz law and Smith-Palmer equations using thermal conductivity coefficients. With increasing temperature, the electrical conductivity decreases as the electrons' free path decrease due to electron-electron and electron-impurity collisions. The corrosion rate obtained from the potentiodynamic Tafel curve is quite low due to the amount of Sn. Both abrasive and oxidation wear were observed at the wear test.

REFERENCES

Cullity, B.D. (1978) Elements of X-ray Diffraction. 2nd Edition, p. 102, Addison-Wessley, California.

Das, S.K., Sharif, A., Chan, Y.C., Wong, N.B. (2009) Influence of small amount of Al and Cu on the microstructure, microhardness and tensile properties of Sn-9Zn binary eutectic solder alloy. J. Alloys Comp. 481, 167-172.

Directive, E. (2003) 95/CE of the European Parliament and of the Council of the EU, Restriction of Hazardous Substances (RoHS). Off. J. Eur. Union 13, L37.

Dong, W., Shi, Y., Xia, Z., Lei, Y., Guo, F. (2008) Effects of trace amounts of rare earth additions on microstructure and properties of Sn-Bi-based solder alloy. J.Electron.Mater.37, 982-991.

Esfandyarpour, M.J., Mahmudi, R. (2011) Microstructure and tensile behavior of Sn-5Sb lead-free solder alloy containing Bi and Cu. Mater. Sci. Eng. A 530, 402-410.

Goh, Y., Haseeb, A.S.M.A., Sabri, M.F.M. (2013) Effects of hydroquinone and gelatin on the electrodeposition of Sn-Bi low temperature Pb-free solder. Electrochim. Acta 90 265-273.

Kittel, C. (1965) Introduction to solid state physics. 6th ed. John Wiley&Sons, New York.

Laurila, T., Vuorinen, V. (2010) Impurity and alloying effects on interfacial reaction layers in Pb-free soldering. Mater. Sci. Eng., R 68, 1-38.

Li, J.F., Mannan, S.H., Clode, M.P., Whalley, D.C. (2006) Interfacial reactions between molten Sn-Bi-X solders and Cu substrates for liquid solder interconnects. Acta Mater. 54, 2907- 2922.

Lin, S.K., Yang, C.F., Wu, S.H., Chen, S.W. (2008) Liquidus projection and solidification of the Sn-In-Cu ternary alloys. J. Electron. Mater. 37, 498-506.

Lin, S.K., Chung, T.Y., Chen, S.W., Chang, C.H. (2009) 250 °C isothermal section of ternary Sn-In-Cu phase equilibria. J. Mater. Res. 24, 2628-2637.

Lin, S.-K., Nguyen, T. L., Wu, S.-C., Wang, Y.-H. (2014) Effective suppression of interfacial intermetallic compound growth between Sn-58 wt.% Bi solders and Cu substrates by minor Ga addition. J. Alloys Comp. 586, 319-327.

Mahmudi, R., Geranmayeh, A.R., Noori, H., Jahangiri, N., Khanbareh, H. (2008) Effect of cooling rate on the room-temperature impression: creep of lead-free Sn-9Zn and Sn-8Zn-3Bi solders. Mater. Sci. Eng. A 487, 20-25.

Mahmudi, R., Geranmayeh, A.R., Khanbareh, H., Jahangiri, N. (2009) Indentation creep of lead-free Sn-9Zn and Sn-8Zn-3Bi solder alloys. Mater. Des. 30, 574-580.

Mahmudi, R., Geranmayeh, A.R., Salehi, M., Pirayesh, H. J. (2010) Impression creep of the rare-earth doped Sn-2% Bi lead-free solder alloy. Mater. Sci.: Mater. Electron. 21, 262-269.

Mei, Z., Morris, J.W. (1992) Characterization of eutectic Sn-Bi solder joints. J. Electron. Mater. 21, 599-607.

Meydaneri, F., Saatçi, B. (2014) Thermal, Electrical, Microstructure and Microhardness Properties of Eutectic Magnesium-Tin. The Arabian Journal for Science and Engineering. 39, 5815-5824.

Mokhtari, O., Nishikawa, H. (2016) Correlation between microstructure and mechanical properties of Sn-Bi-X solders. Mater. Sci. Eng. A. 651, 831-839.Mott, N.F., Davis, E.A. (1979) Electronic Processes in Non- Crystalline Materials. 2nd Edition, p. 273, Clarendon Press, Oxford.Osorio, W.R., Peixoto, L. C., Garcia, L. R. (2013)

Microstructure and mechanical properties of Sn-Bi, Sn-Ag and Sn-Zn lead-free solder alloys**.** J. Alloys Comp. 572**,** 97-106.

Rani, S.D., Murthy, G.S. (2013) Evaluation of bulk mechanical properties of selected lead-free solders in tension and in shear. J. Mater. Eng. Perform. 22, 2359-2365.

Resistivities of metallic elements,http://www.kayelaby.npl.co.uk/general_physics/2_6/2_6_1.html

Sergent, E.J., Krum, A. (1998) Thermal management handbook: for electronic assemblies. Chapter 7, p. 26, McGraw Hill Professional, New York.

Shen, J., Pu, Y., Yin, H., Luo, D., Chen, J. (2014) Effects of minor Cu and Zn additions on the thermal, microstructure and tensile properties of Sn-Bi-based solder alloys. J. Alloys Comp. 614, 63-70.

Silva, B.L., Garcia, A., Spinelli, J. E. (2017) Complex eutectic growth and Bi precipitation in ternary Sn-Bi-Cu and Sn-Bi-Ag alloys. J. Alloys Comp. 691, 600-605.

Silva, B. L., Reinhart, G., Nguyen-Thi, H., Mangelinck-Noël, N., Garcia, A., Spinelli, J.E. (2015) Microstructural development and mechanical properties of a near-eutectic directionally solidified Sn-Bi solder alloy. Mater. Charact. 107, 43-53.

Smith, C.S., Palmer, E.W. (1935) Thermal and electrical conductivities of copper alloys. Trans. AIME 117, 225-243.

Suganuma, K. (2001) Advances in lead-free electronics soldering. Curr. Opin. Solid State Mater. Sci. 5, 55-64.

Takaku, Y., Liu, X.J., Ohnuma, I., Kainuma, R., Ishida, K. (2004) Interfacial reaction and morphology between molten Sn base solders and Cu substrate. Mater. Trans. 45, 646-651.

Terada, Y., Ohkubo, K., Mohri, T., Suzuki, T. (1999) Thermal conductivity in Pt-based alloys. J. Alloy Compd. 285, 233-237.

Tong, X.C. (2011) Thermal interface materials in electronic packaging, in: Advanced Materials for Thermal Management of Electronic Packaging. Springer Series.

Vianco, P., Rejent, J., Grant, R. (2004) Development of Sn-based, low melting temperature Pb-free solder alloys. Mater. Trans. 45, 765-775.

Yamasue, E., Susa, M., Fukuyama, H., Nagata, K. (2003) Deviation from Wiedemann-Franz law for the thermal conductivity of liquid tin and lead at elevated temperature. Int. J. Thermophys. 24, 713-730.

Yoon, J.W., Lee, C.B., Jung, S.B. (2002) Interfacial reactions between Sn-58 mass% Bi eutectic solder and (Cu, electroless Ni-P/Cu) substrate. Mater. Trans. (Japan) 43, 1821-1826.

CHAPTER IV

ELECTRON PARAMAGNETIC RESONANCE INVESTIGATION OF GAMMA IRRADIATED SULINDAC AND GLYBURIDE WITH SIMULATION METHOD

Kerem SÜTÇÜ[1*]&Yunus Emre OSMANOĞLU[2]
[1]Corresponding Author, (Assoc. Prof.)*
Dicle University, email: ksutcu@dicle.edu.tr
Orcid: 0000-0002-5791-1492
[2](Assoc. Prof.) Dicle University, email: yunus.osmanoglu@dicle.edu.tr
Orcid: 0000-0001-7338-7603

1. Introduction

In the changing and developing world conditions, radiation energy is used for different purposes. Protecting the health of society now and in the future is paramount when aiming to use radiation for human benefit (Coşkun & Coşkun 2003). The sterilization process is the purification of anywhere from microorganisms at any time. (Gopal 1978). This process differs according to the type of material to which it will be applied and its properties such as stability. When choosing a sterilization method, attention should be paid to the type, structure and preparation stage of the material to be sterilized. Because there is no one ideal sterilization method to be applied for all substances. Many methods are used to sterilize drugs and pharmaceutical raw materials. However, these methods used to sterilize drugs have advantages as well as some disadvantages.

Pharmaceutical raw materials can be sterilized by heat sterilization (Varshney & Dodke 2004), but since this method requires high tem-

peratures, it may cause an increase in temperature in the sample to be sterilized. This is not a desirable situation for the sample to be sterilized.

Sterilization with ethylene oxide is one of the methods used to sterilize drug samples. In sterilization with ethylene oxide, carcinogenic gases accumulate on the sample and a very long ventilation period is required (Nishikawa et al., 2018). Again, this is an undesirable situation for the sample to be sterilized.

It is increasingly important to sterilize the material to be sterilized using ionizing radiation rather than exposure to high temperatures or a chemical gas (Basly et al., 1998). Radiosterilization, which is a non-contact process, does not cause any chemical residue and contamination on the sample. Thanks to its high penetrating property, it can be used even in the packaged form of the sample to be sterilized. In addition, in gamma sterilization, no temperature increase is observed in the material to be sterilized and the sample does not gain radioactive properties (Basly 1999). These are among the advantages of radiation sterilization. However, it is possible to count the disadvantages of radiation sterilization. Since ionizing radiation has high energy, it can cause molecular destruction when applied to the sample to be sterilized, and as a result, intermediate products are formed (Basly et al., 1997). For this reason, it is necessary to identify the structures and stability of the intermediate products formed. In addition, a method should be determined to distinguish between irradiated and non-irradiated materials against unapproved and uncontrolled radiation applications, especially for economic gain (Basly et al., 1998). The most important disadvantages of the radiation sterilization method are the formation of free radicals in the sample as a result of the irradiation process and the variation in irradiation regulations from country to country (Basly & Bernard 1997). In this case, the basic logic is to detect the free radicals that will form in the structure after irradiation. These free radicals can be detected by several methods and thermoluminescence, chemiluminescence and electron paramagnetic resonance (EPR) are the most popular of these methods. EPR spectroscopy is most suitable for detecting free radicals due to its high sensitivity (Murieta et al., 1996). There are many EPR studies examining the structures and radiation sensitivities of free radicals formed

in the structure after irradiation (Osmanoğlu et al., 2005; Başkan et al., 2015; Sütçü & Osmanoğlu 2018).

The EPR spectra of Odansetron which is an anti-emetic drug were investigated by Damian (Damian 2003). The investigated radical is of the form R-CH_2 and the measured spectroscopic splitting factor (g) value is calculated as 2.009. Yurus et al. studied the dosimetric investigation of gamma irradiated sulbactam sodium (Yurus et al., 2004). The experimental g value determined for strong resonance peak is 2.0097. In another study, the g values of two drug samples used calculated and the values obtained were attributed to the carbon or nitrogen-centered radicals (Ambroz et al., 2000). To our knowledge sulindac (SUL) and glyburide (GB) have not been studied by EPR technique, yet. In this context, in this study, it was aimed to investigate the characteristic properties of free radicals formed in 15 kGy irradiated SUL and GB drug raw materials using EPR spectrometry at room temperature. Since irradiation at low doses has the advantage of minimizing the radiation damage that may occur in the sample, irradiated samples with a dose intensity of 15 kiloGray (kGy) were used in this study (Gopal 1977). In today's world where we are struggling with the pandemic, the importance of radiation sterilization, which is a non-contact process, has increased even more, as the necessity of presenting non-contact products to the consumer has become very important.

2. Experimental

The drugs used in this study were purchased from commercial companies. The names of drugs used in this work with their chemical formulas are shown in Table 1.

Powder samples were γ-irradiated to a dose of 15 kGy with ^{60}Co γ-ray source at room temperature (295 K) at Turkish Energy Nuclear and Mineral Research Agency (TENMAK) in Ankara. EPR measurements were carried out on samples in standard quartz EPR tubes at room temperature with a bruker EMX model spectrometer. The parameters of the spectrometer are given in Table 2.The EPR spectra of the powder samples are shown in Figures 1a and 2a, respectively. The *g*-factors

were found by preforming a comparison with a dipenhylpicrylhydrazyl (DPPH) sample (g = 2.0036). The simulation spectra obtained using the EPR simulation program which is available through internet are shown in Figures1b and 2b, respectively.

Table 1. Commercial names, chemical formulas, molecular weights (g/mol) and chemical structures of SUL and GB

Sulindac, $C_{20}H_{17}FO_3S$, 356.41	Glyburide, $C_{23}H_{28}ClN_3O_5S$, 494.00
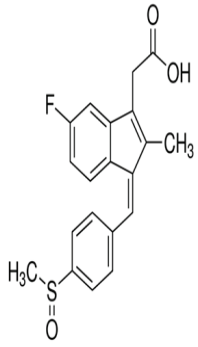	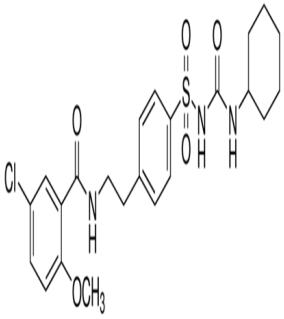

Table 2. Parameter List of EPR Spectrometer

Field	Center Field: 3494.910 G
	Sweep Width: 150.000 G
	Resolution: 512 points
Microwave	Frequency: 9.824 GHz
	Power: 1.577 mW
Receiver	Receiver Gain: 3.17 e+002
	Phase: 1.33 deg
	Harmonic: 1
	Modulation Frequency: 86.00 kHz
	Modulation Amplitude: 2.03 G
Signal Channel	Conversion: 10.240 ms
	Time Constant: 40.960 ms
	Sweep Time: 5.243 s

3. Results and Discussions

SUL is a non-steroidal anti-inflammatory drug of the acetic acid class: it has anti-neoplastic properties against colorectal cancers (Cavallari et al., 2016; Gong et al., 2016). Samples irradiated at room temperature were observed to present a sharp and clear singlet EPR signal centered at g = 2.0082 ± 0.0005. The EPR spectrum of 15 kGy irradiated SUL powder at 295 K is shown in Figure 1a.

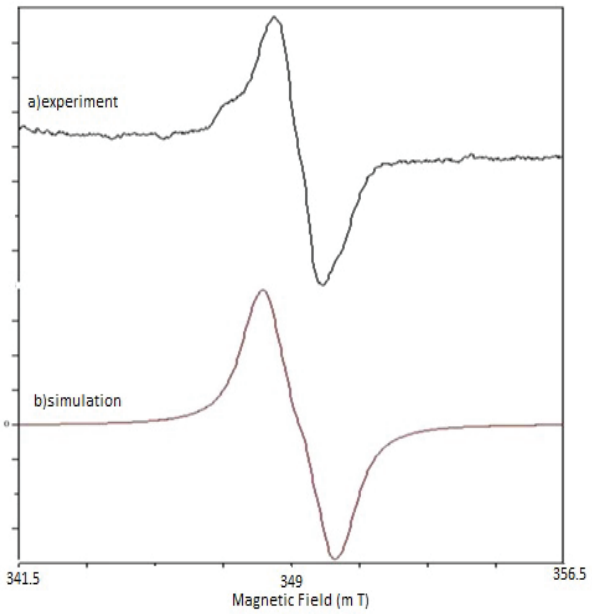

Figure 1. (a) Experimental spectrum of 15 kGy irradiated SUL powder

(b) Simulation of the spectrum

The linewidth is on the order of 0.6 mT. This complex singlet is probably a superposition of many lines superimposed on $\dot{C}HCCCH_3$ radical. We suppose that this spectrum is due to the interaction of free electron with one α-proton and three methyl protons which are magnetically equal. When the spectrum was examined, it was seen that the linewidth value was high and because it was difficult to obtain the hyperfine parameters from the experimental spectrum, the simulation spectrum of

the sample was obtained and these parameters were calculated from the simulation spectrum. That's why these parameters were calculated by simulation program. The calculated hyperfine parameters of the radical is a_{α} = 1 mT, $a^{1}_{CH3} = a^{2}_{CH3} = a^{3}_{CH3}$ = 0.4 mT, respectively. The simulated spectrum obtained using these hyperfine parameters is given in Figure 1b. When the Fig.1b is examined it is seen that the experimental and the simulated spectra are highly compatible. The EPR parameters of SUL were consistent with the literature data (Damian 2003; Yurus et al., 2004).

Among several poorly soluble drugs, GB is a weakly acid derivative belonging to the second generation group of the sulfonylurea antidiabetics, used as oral hypoglycemic agent (Cirri et al., 2016). 15 kGy irradiated GB showed a singlet EPR spectrum at room temperature (Figure 2a).

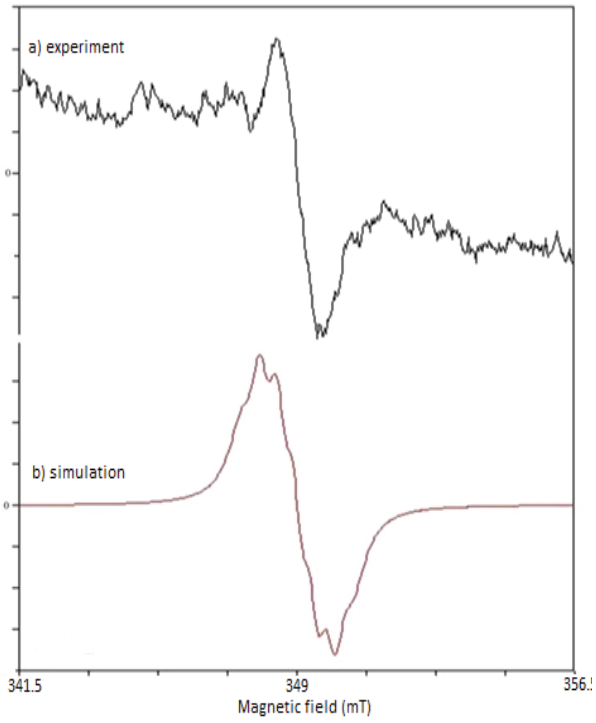

Figure 2. (a) Experimental spectrum of 15 kGy irradiated GB powder

(b) Simulation of the spectrum

When the spectrum obtained from the irradiated GB was examined, it was determined that the radical formed in the structure was formed as a result of the abstraction of the H atom from CH_2 molecule. The measured hyperfine parameters values for the unpaired electron are a_{CH} = 0.8 mT, $a^1_{CH2} = a^2_{CH2}$ = 0.5 mT and a_N = 0.46 mT. As a result of calculations; the g value and the linewidth values of the radical formed in the structure by irradiation were obtained as g = 2.0089 ± 0.0005, ΔH = 0.44 mT, respectively. Since the nitrogen coupling constant value obtained is very small, its effect in the experimental spectrum is not observed. The EPR parameters of GB were consistent with the literature data (Damian 2003; Yurus et al., 2004; Ambroz 2000). The simulation spectrum of GB obtained by using these hyperfine parameters is given in Fig. 2b. The experimental and simulated EPR spectra were observed to be in good conformity with each other. It was concluded that $N\dot{C}HCH_2$ radical was formed in the GB irradiated to 15 kGy at room temperature.

4. Conclusions

After the gamma irradiation of SUL and GB with gamma rays it was concluded that $\dot{C}HCCCH_3$ and $N\dot{C}HCH_2$ radicals were formed, respectively. The hyperfine coupling constants and the g values of both samples were calculated. It was determined that the calculated EPR parameters were compatible with the literature. Although the spectra of the samples were singlet, the EPR parameters could be calculated from the simulation spectra and the radicals could be determined. In conclusion, investigating the magnetic properties of radicals formed in pharmaceutical raw materials may be beneficial for similar radicals formed in biological systems.

References

Ambroz, H. B., Kornacka, E. M., Marciniec, B., Ogrodowczyk, M., & Przybytniak, G. K. (2000). EPR study of free radicals in some drugs γ-irradiated in the solid state, Radiation Physics and Chemistry , 58: 357-366.

Başkan, M. H., Osmanoğlu, Y. E., Sütçü, K., Aydın, M., & Osmanoğlu, Ş. (2015). Radiation Effect Studies in Single Crystal Of Trifluoroacetyl-α-Aminoisobutyric Acid. Radiation Effects and Defects in Solids, 170 (10): 854-861.

Basly, J. P. (1999). Radiation induced effects on cephalosporins: an ESR study. International journal of radiation biology, 75(2), 259-263.

Basly, J. P., & Bernard, M. (1997). Radiosterilization dosimetry by ESR spectroscopy: Ritodrine hydrochloride and comparison with other sympathomimetics. International Journal of Pharmaceutics, 149: 85-91.

Basly, J. P., Longy, I., & Bernard, M. (1997). Influence of radiation treatment on theodrenaline: ESR and HPLC study. International journal of pharmaceutics, 152(2), 201-206.

Basly, J. P., Longy, I., & Bernard, M. (1998). Radiosterilization dosimetry by electron-spin resonance spectroscopy: Cefotetan. Analytica Chimica Acta, 359: 107-113.

Cavallari, C., Tarterini, F., & Fini, A. (2016). Thermal characterization of some polymorph solvates of the anti-inflammatory/anti-cancer sulindac (2016). Thermochimica Acta, 633, 129-139.

Cirri, M., Roghi, A., Valleri, M., & Mura, P. (2016), Development and characterization of fast-dissolving tablet formulations of glyburide based on solid self-microemulsifying systems. European Journal of Pharmaceutics and Biopharmaceutics, 104, 19-29.

Coşkun, M., & Coşkun, M. (2003). Biological dosimeter and related developments. Cerrahpaşa J Med, 34, 207-218.

Gong, E. Y., Shin, Y. J., Hwang, I. Y., Kim, J. H., Kim, S. M., Moon, J. H., & Hong, S. W. (2016). Combined treatment with vitamin C and sulindac synergistically induces p53-and ROS-dependent apoptosis in human colon cancer cells. Toxicology Letters, 258, 126-133 .

Gopal, N. G. S. (1977). Radiation Sterilization of Pharmaceuticals and Polymers. Radiation Physics and Chemistry,12 (1-2): 35-50.

NIH. 2012. Public Electron Paramagnetic Resonance Software Tools, http://www.niehs.nih.gov/research/resources/software/tox-harm/tools/index.cfm

Nishikawa, T., Abe, N., Yonesu A., & Hayashi, N. (2018). Sterilization of Small Vial Using Electron Cyclotron Resonance Plasma. Vacuum, 157: 100-104.

Osmanoğlu, Ş., Aydın, M., & Başkan, M. H., (2005). EPR of Gamma-Irradiated L-Glutamine Hydrochloride and N-Carbamoyl-L-Glutamic Acid. Zeitschrift für Naturforschung A, 60 (7): 549-553.

Sütçü, K., & Osmanoğlu, Y. E. (2018). Electron Spin Resonance Identification of Gamma İrradiated 2, 4′-Dichlorodiphenyl Dichloroethane and 6-Mercaptopurine Monohydrate in the Solid State. Journal of Molecular Structure, 1174: 67-73.

Varshney, L., & Dodke, P. B. (2004). Radiation effect studies on anticancer drugs, cyclophosphamide and doxorubicin for radiation sterilization. Radiation Physics and Chemistry, 71(6), 1103-1111.

CHAPTER V

A REVIEW OF RECENT ADVANCES IN GRAPHENE AND GRAPHENE OXIDE BASED UV PHOTODETECTORS

Satiye KORKMAZ
(Asst. Prof.) Karabük University, satiyekorkmaz@karabuk.edu.tr
ORCID: 0000-0002-7592-3366

1. Introduction

Recently, ultraviolet (UV) photodetectors have attracted a great deal of attention from researchers with their high performance in optical communication, night vision, chemical sensors, industrial quality control, and military and biomedical applications (Lin, Cheng, Yang, Zhou, Lee and Wang, 2014:2811; Liang et al., 2016:25925). The studies on UV photodetectors based on nanostructured materials such as Nb_2O_5, GaN, SiC, AlGaN, ZnO, V_2O_5, and TiO_2 with wide band gaps were increased (Müller et al., 2009:319; (Inamdar and Rajpure, 2014:57). Studies on UV photodetectors based on these metal oxide semiconductors (MOS), which are highly sensitive, easy to produce, and low cost, draw attention. Their absorption coefficient for light detection is also high. The sensing properties of such structures are greatly affected by their surface morphology, chemical composition, and oxygen vacancies (Yu et al., 2021:159508; Liu et al., 2020:5072; Zhou et al., 2020:153416). On the other hand, the performance improvement principles of photodetectors and gas sensors are different. More electrons are released from the oxygen vacancy states to the conduction band in gas sensing, allowing the gas absorption to proceed actively (Wu et al., 2018:1713). Electrons excited by the thermal energy move freely in the conduction band, inducing a large dark current

and reducing the photocurrent/dark current ratio (Wu et al., 2018:1713). Specific oxygen gap states near the mid-band gap act as recombination centres that reduce photocurrent (Huang, Xiao, Chang, Chen, Chen and Li, 2021:095013). For this reason, some researchers have developed strategies to improve the sensing properties of both light and gas molecules. Accordingly, amorphous oxide semiconductors (AOS) are frequently used in electronic devices due to their high mobility and optical transparency. In order to increase the sensitivity of photodetectors, the metal-semiconductor-metal (MSM) structure has gained importance with the development of UV photodetector variations based on nanomaterials such as Schottky photodiodes and organic-based composites.

The increasing interest towards photodetectors in portable electronic equipment has also increased the interest in developing low- or even zero-energy optoelectronic devices to solve the energy problem. Self-powered photodetectors can directly convert optical signals to electrical signals without requiring any external power supply; they have significant advantages with low energy consumption, highly improved sensitivity, fast response time, and continuous operation (Hatch, Briscoe and Dunn, 2013:868; Bai, Liu, Liu and Zhang, 2017:804). On the other hand, the demand for flexible electronic devices integrated into wearable products such as smart clothing, flexible displays, and stretchable circuits has increased researchers' interest in flexible photodetectors. The application characteristics of photodetectors are mainly dependent on the response bands. Most UV in the environment is scanned by the ozone layer, resulting in higher signal quality and less noise generation in UV photodetectors (Chen, Ren, Gu and Ye, 2019:382; Li et al., 2020:2202). It is the reason for the interest in UV photodetectors in optical communication, flame tracking, and missile launching applications.

Graphene is a promising material for new electronic devices due to its high electron mobility, atomic layer thickness, and unique mechanical flexibility. The broadband absorption has made graphene an attractive candidate for solar cells, ultrafast photodetectors, and terahertz modulators. Photoresponse states of graphene and GOs in p–n junction devices have been widely investigated. However, the inherently low absorption coefficient and quantum efficiency of graphene severely limit the

performance of high-performance photonic or optoelectronic devices. Researchers aimed to overcome these limitations with different graphene and GO-based composite structures. The primary purpose of this chapter is to review the development of graphene and GO-based UV photodetectors in recent years. In this context, photodetector structure/properties and parameters, graphene and GO structures will be introduced, and the developments in research on graphene and GO-based photodetectors will be discussed.

2. Photodetectors

2.1. Structure And Properties

As the variety of application areas of photodetectors capable of converting light into electrical signals increases, the need for innovative technologies in which the materials with flexibility, transparency, and higher performance are used, along with higher speed, efficiency, or wavelength ranges, also increases. A good photodetector should have high sensitivity, low noise, fast response time, and low cost. Various studies have been carried out to discover photodetectors with low noise, high sensitivity to light, and good stability. However, the desired performance level has not been reached for these materials.

The UV light region is the electromagnetic radiation between X-ray and visible light, with wavelengths ranging from 100 nm (12.4 eV) to 400 nm (3.1 eV). The UV light with high energy and short wavelengths is absorbed by the ozone layer before reaching the earth. Meanwhile, the UV light with a longer wavelength can reach the ground, posing a danger to human health in long-term exposure. Photodetectors can be divided into vacuum UV photodetectors and Solid-State UV photodetectors. Vacuum UV photodetectors used as UV sensors consist of Photomultiplier Tubes, which is not preferred because of consuming too much power. Therefore, semiconductor UV photodetectors, which attract attention with lower cost, high sensitivity, and low power consumption, are frequently used in medicine, communication, and space. The nanoscale materials inspired by nanoscience and nanoengineering,

such as quantum dots (QDs), nanowires, and nanolayers, have superior photoelectronic properties and their high performance in photodetectors is particularly remarkable. The high precision, fast response, and functionality of these materials have also increased the diversity in practical applications. The studies carried out to improve the performance of wide-bandgap semiconductors, and UV photodetectors showed that nanostructured devices' UV photoresponse properties are greatly affected by different amounts of impurities, crystallographic orientation, and grain size (Adinolfi et al., 2016:7265; Bo, Nasiri, Chen, Caputo, Fu and Tricoli, 2017:2608).

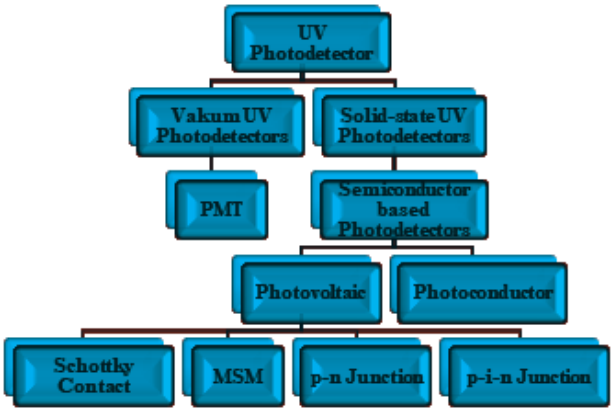

Figure 1. Classification of UV photodetectors.

The photoconductor, a radiation-sensitive resistor, consists of a semiconductor with two ohmic contacts. The schematic structure is shown in Figures 2 a, b. ZnO has the most common UV photoresistance with its superior photodetection performance. Its high performance is attributed to the tendency to adsorb oxygen molecules in the air by capturing free electrons from the n-type semiconductor by surface traps (Figure 3a,b) (Fang, Armin, Meredith and Huang, 2019:2; Kim, Jo, Lee and Choi, 2018:90). It forms an electron-depleted region near the surface and causes a significant decrease in device conductivity with band bending, as seen in Figure 2b. Band bending creates an internal electric field that separates photogenerated electron holes, causing photocarrier recombi-

nation and long carrier lifetime (Scharber et al., 2006:790; Park et al., 2009:297). These effects are more evident in nanocrystalline films where the surface area is large, and the depletion regions extend throughout the film. Electrons in the valence band (VB) are excited to the conduction band (CB) by simultaneous generation of the same number of holes in the VB. There are two options for holes that migrate to the surface with belt bending. First, they discharge negatively charged adsorbed oxygen ions to photodesorb oxygen from surfaces. Second, they effectively adhere to ZnO surfaces (Fig. 3 c,d). When the UV light is turned off, the holes and unpaired electrons are recombined, and the oxygen is slowly absorbed into the surface, causing the current to deteriorate (Soci et al., 2007:1003; Yang et al., 2010:6287).

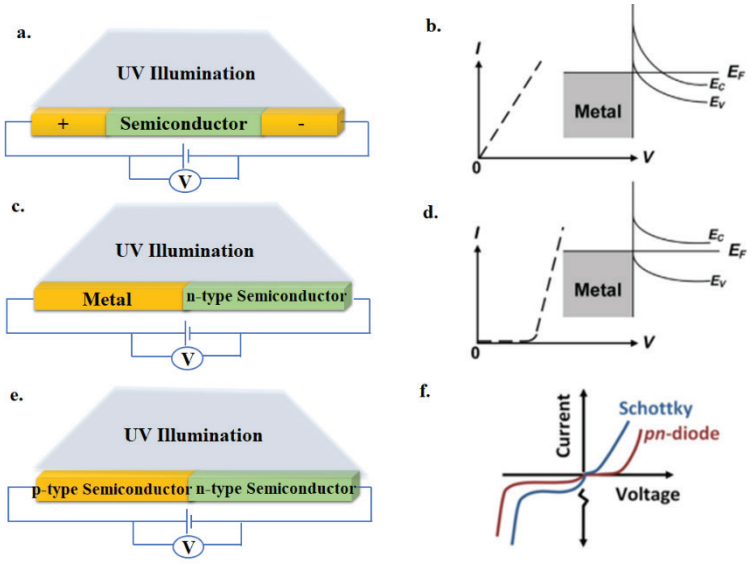

Figure 2. Schematic illustration and current-voltage characteristics of (a,b) Ohmic contact photoresistor (c,d) Schottky contact (e,f) Photodiode.

The schematic structure of Schottky contact photodetectors consisting of a metal layer such as gold, silver, or aluminium in contact with a moderately doped n-type semiconductor is shown in Figure 2 (c,d). It is a unipolar device because it has electrons on both sides of

the junctions as majority carriers (Cooper and Agarwal, 2002:957). Therefore, since there is no depletion layer is near the junction, no significant current will occur with metal-to-semiconductor reverse bias. Schottky contact devices exhibit a rectifying behaviour due to the electrostatic barrier caused by the difference in operating functions between the metal-semiconductor (Schalwing et al., 2002:1223). In these devices, the primary current sustained by optically generated carriers in the depletion region and the secondary current resulting from the reduction of the Schottky barrier caused by light and trapping in the interface states contribute to the photoresponse (Strobel, Seiberlich, Rödlmeier, Lemmer and Hernandez-Sosa, 2018:42735). In Schottky contact devices, the photogenerated electron-hole pairs can be separated by the local electric field in the Schottky barrier region, reducing the recombination rates of the electron-holes, thus extending the carrier lifetime and increasing the free carrier density. Increasing carrier density will change the Fermi energy and the semiconductor's work function, resulting in a decrease in the Schottky barrier height and width between the semiconductor layer and the electrons (Tung, 2001:122). Electron-hole pairs will recombine rapidly in semiconductors when UV light is turned off (Cheng, Wu, Liu, Li, Zhang and Du, 2011:203105; Zhou et al., 2009:191103).

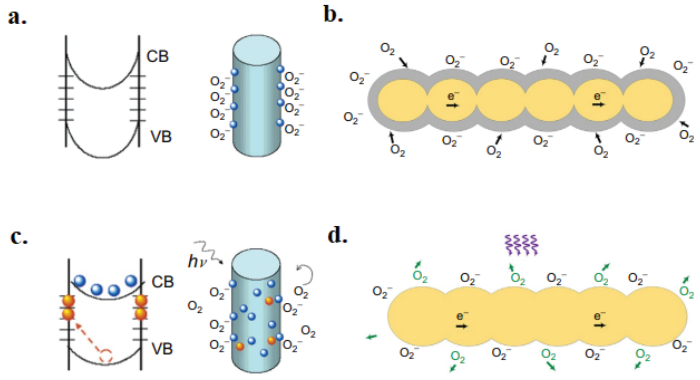

Figure 3. Schematic representation of a nanowire (a,c) and nanoparticle network (b,d) photoconductor in the dark and under UV light.

Photodiodes, consisting of a p-n junction and a p-i-n structure, are widely used in various electronic applications, especially in UV photodetection. The device has a p-i-n structure comprised of a highly doped transparent p-type layer and an n-type high-doped layer with a pure undoped absorbent layer in the middle (Figure 2e). When p- and n-type materials are put in contact, the connection will behave very differently from these two types (Figure 2f). The current will flow easily in one direction but not in the other direction and act as a base diode. There are holes in the p-type region and extra electrons in the n-type region. When the p-n junction is formed, some electrons reach the CB from the n region, diffuse across the junction and combine with the holes. Since filling a hole will create negative ions, it will leave a positive ion on the n side. The depletion region is formed with the hole charge, preventing electron transfer. Under UV light, photogenerated electron-hole pairs will contribute to the photocurrent induced under reverse bias (Brown et al., 1993:326; Moses and Derenzo, 1994:1442)

2.2. Parameters Of A Photodetector

2.2.1. Responsivity (R)

Photoresponse or responsivity (R) is the ratio of the electrical output signal to the optical input as given in equation 2.1.

High photoresponse is a desirable result for a higher output signal. Besides the detector's noise and the camera system, the radiation wavelength to which the detector is sensitive, called the spectral photoresponse, will also significantly affect the output signal.

2.2.2. Quantum Efficiency (η)

The electrical sensitivity of devices to radiation is defined as quantum efficiency. It is given as the percentage of photons forming electron-hole pairs in photodetectors relative to the photons coming to the detector. Accordingly, as the photocurrent of the photodetector increases, the quantum efficiency and sensitivity will also increase; the relationship between photoresponse and quantum efficiency is given by equation 2.2:

Here, q is the electron charge, η is the detector's quantum efficiency, g is the detector gain, λ is the wavelength of the incident radiation, h is the Planck constant, and c is the speed of light in a vacuum. Quantum efficiency is the ratio of optically generated electrons to incident photons, the ratio of the mean free path of the excited carriers to the total active layer thickness of the detector.

2.2.3. Signal-to-Noise Ratio (SNR)

Unwanted signals in the output signal are defined as noise. Noise can be reduced by keeping the Signal/Noise Ratio (SNR) high. The origin of the noise source is usually the structure of the photodetector. These noises, which occur due to fluctuations in the photon arrival rate, lattice vibrations in the semiconductor, or the random movement of electrons, cannot be prevented. However, various noise mechanisms, including 1/f, Johnson, Generation-Recombination (G-R), and Beat Noise, attempt to explain these situations. The spectral power density of 1/f noise is inversely proportional to frequency, and there are many studies on the relationship between this noise and low current mechanisms (Bae, Lee, Kim, Lee and Kim, 2000:878; Ozer and Besikci, 2003:560). The noise caused by thermal fluctuations occurring when the semiconductor temperature is over absolute zero is called Johnson Noise. Generation-Recombination (G-R) Noise, generated by the continuous repetition of production and recombination processes, may be due to either an optical or thermal generation. On the other hand, Beat Noise results from photons arriving at the detector with a random arrival rate, representing the minimum obtainable noise level.

2.2.4. Noise Equivalent Power (NEP)

Noise Equivalent Power (NEP) is the power that can generate a signal equal to the amount of noise on the detector. Although NEP is defined as a detector sensitivity measurement, it is unsuitable for determining detector sensitivity because SNR is not constant and increases with the input power. NEP is obtained by dividing the noise voltage or current by the photoresponse:

2.2.5. Detectivity (D)

The inverse of NEP is defined as detectivity (D). Detector performance can be improved by increasing detectivity. NEP is called specific detectivity (D^*) for detectors and is proportional to the detector area (A_d) and the square root of frequency bandwidth (Δf) (Jones, 1952:28):

Using D^*, the detectors of the same type with different detector areas can be compared.

3. Graphene And Graphene Oxide (GO)

Graphene and GO is an interdisciplinary research topic covering many disciplines, including science, materials science, device production, and nanotechnology. In particular, the 2010 Nobel Prize in Physics was awarded for the groundbreaking experiments of graphene (Geim, 2011:6980). Its high charge carrier mobility, electrical and thermal conductivity, transparency, and mechanical strength make graphene an indispensable material for future cutting-edge technologies. Studies show that graphene-based devices exhibit high performance when used in photodetectors, capacitors, sensors, energy, and biomedical applications, especially in wearable electronics (Wassei and Kaner, 2013:2245; Li and Östling, 2013:172; Kumar et al., 2013:240; Wu, He, Tan, Wang and Zhang, 2013:1165). Scientific and technological research in energy and the environment focus on basic materials' performance, functionality, and durability. Advanced materials such as activated carbon, carbon nanotubes, graphene, and similar carbon-based nanomaterials are starting to play an essential role in science and technology. Therefore, solving the difficulties encountered in the application areas of such materials has become more critical. Graphene, one of these nanomaterials, is an allotrope of carbon in a 2-D and atomic-scale hexagonal lattice. It is also the basic structural unit of all graphite carbons such as fullerenes, CNTs, and graphite. Graphene has received rapidly increasing attention since it was first discovered in 2004. Graphene has numerous remarkable properties such as high surface area, high electrical conductivity, excellent flexibility, and excellent mechanical properties. Despite the superior properties of

graphene, its practical applications are limited due to the difficulties in the large-scale formation of specially organized structures.

Graphene, a 2-D sp^2 hybridized hexagonal crystal material, is a monolayer form of graphite. Graphene sheets are formed when the Van der Waals forces holding the layers together are broken. Graphene is widely used in nanocomposites, detectors, and supercapacitors because of its superior chemical, mechanical and electrical properties. Its proneness to chemical reactions with the carbon atoms in its structure makes it a chemically active material that can be converted into desired forms. Graphene is a light and elastic material with its high tensile strength; it becomes a conductive material thanks to the sp^2 hybridized carbons in its structure.

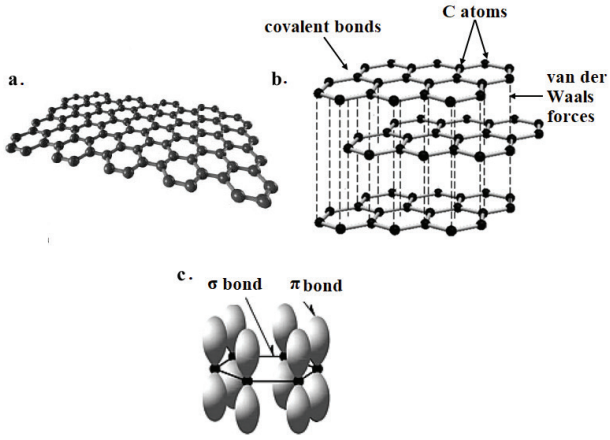

Figure 4. (a) The structure of graphene, (b) stacking of graphene layers, (c) distribution of σ and π bonds on the graphene structure.

As seen in Figure 4a, graphene is a 2-D monolayer of carbon atoms tightly packed in a lattice. The graphite structure with Van der Waals forces holding graphene monolayers together is given in Figure 4b. Graphene layers are formed when these forces break. The π bonds at the top and bottom of each graphene layer (Figure 4c) can overlap with neighbouring carbon atoms. The σ electrons are tightly bound and do not contribute significantly to the electrical conductivity. However, π electrons can move freely in the structure, making graphene a good conductor, so it has

superior electrical properties and high carrier velocity. As is known, the bandgap is the minimum energy that allows an electron to pass from the valence band to the conduction band so that the electron can contribute to conduction (Yildiz, Warberg and Awaja, 2021:65).

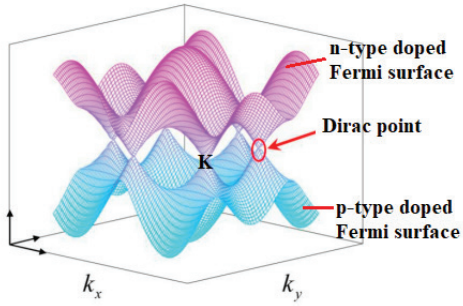

Figure 5. Electron band structure of graphene and Dirac point (Li, Zhang and Xing, 2019:2461)

Since the bandgap is zero in metals, no energy is used in transmission. As a zero-bandgap material, graphene can also be called a zero-gap semiconductor or zero-gap metal. With these properties, graphene can be functionalized with organic and inorganic materials, and its electrical properties can be controlled. These outstanding performances of graphene, including its superior optical and electronic properties, result from its electronics and lattice structure. Figure 5 shows the electron band structure of graphene and Dirac point. The conduction and valence bands touch each other at six different points, called the K points. When these six points are divided into two equivalent sets of three points, the points within each set become equivalent because they can reach each other by reciprocal lattice vectors. This proximity shows that near K points, the dispersion relationship is similar to the energy spectrum of massless Dirac particles. The Fermi energy surface is at the intersection of the full valence band and the empty conduction band, and the middle of the p band containing valence electrons (Cao, Wang, Cao and Yuan, 2015:6590). These valence electrons are massless Dirac fermions at $1/300^{th}$ the speed of light. It is the lowest resistivity material, even lower than copper or silver (Morozov et al, 2008:016602; Gorbachev et al,

2012:898). GO consists of single-layered carbon layers such as graphene, possessing sp^3 and sp^2 hybridized carbon atoms in its structure. GO, which has an irregular structure, has hydrophobic and hydrophilic zones. The usage areas of GO are expanding day by day with its easy solubility in solvents, dielectric properties, transparency, adjustable electronic properties, and superior mechanical properties.

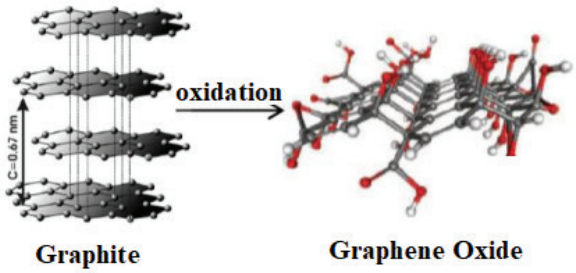

Figure 6. Obtaining GO from Graphite

On the other hand, hydrophilic GO becomes an insulator in terms of electrical conductivity due to the breakdown of sp^2 bonds and its oxygenated groups such as hydroxyl, epoxy, and carboxyl. Graphene can gain electrical, mechanical, and thermal properties by thermal annealing or chemical reducing agents. Although the surface area of GO is smaller than that of graphene, it exhibited high capacitance because of the oxygen-containing functional groups on its surface.

4. Recent Developments

Titanium dioxide (TiO_2), a semiconductor with a wide bandgap, is highly photoactive when exposed to UV light, is economical, non-toxic, and chemically stable; it has demonstrated high performance in solar cells, with these properties (Yu et al., 2016:2762; Timoumi, Alamri and Alamri, 2018:48; Pramanik et al., 2016:144502). TiO_2 has been reported to be effective in reducing surface recombinations with carbon nanotubes, graphene, GO, reduced GO, fullerene, and metal nanoparticles, especially to improve sensitivity in photodetectors (Yang, Zhang and Xu, 2013:1157; Leary and Westwood, 2011:767). Graphene, which draws

attention with its high conductivity and carrier mobility, is widely used in optoelectronic devices such as photodetectors, solar cells, and light-emitting diodes. On the other hand, GO has played a significant role in developing solar cells with its high stability and carrier mobility as a photocatalyst (Wang, Chang, Yeh, Lee and Teng, 2014:20574). It is possible to convert GO to reduced GO (rGO) by removing the functional oxygen groups in its structure via thermal or chemical reduction. Thin-film forms of rGO are synthesized cheaply; they are well-dispersed in organic solvents, are highly compatible with various organic and inorganic semiconductors, and exhibit remarkable properties in the photodetectors and gas sensors, and other fields (Suriani et al., 2018:10735). Recent studies show that p-type rGO is suitable for efficient charge transfer and high photoresponse to be used with inorganic semiconductor materials (Bansode, Harpale, Khare, Walke, More, 2016:115023). The photocatalytic activity of TiO_2/rGO has been reported to be at least several times higher than that of pure TiO_2 (Konatham and Striolo, 2008:4633). The performances of solar cells, lithium-ion batteries, photocatalysts, and especially photodetectors are improved by using TiO_2/rGO nanocomposites (Ding, Zhang, Chen, Hu, Qiu and Zhao, 2015:32). For this purpose, AlShammari et al. produced and characterized metal-semiconductor-metal (MSM) UV photodetector based on TiO_2 and TiO_2/rGO films (AlShammari, Halim, Yam and Kaus, 2020:103630). Photoelectric and photodetection performances of TiO_2/rGO structure grown on glass substrates by spray pyrolysis technique (SPT) were investigated and compared with pure TiO_2.

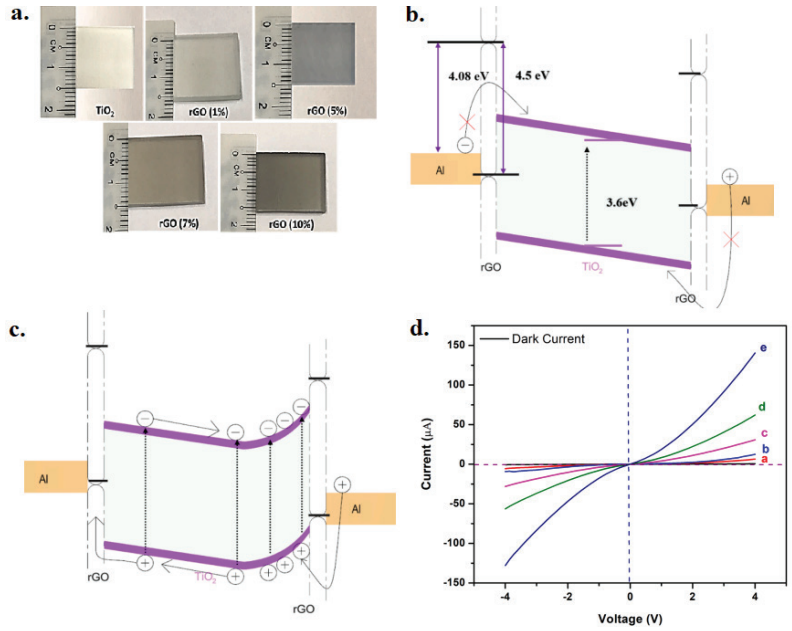

Figure 7. (a) Images of thin films with different rGO concentrations (TiO_2, TiO_2/rGO (1, 5, 7, and 10% wt)), (b) Energy level diagrams of Al/TiO_2-rGO/Al photodetector in the dark, (c) Energy level diagrams of Al/TiO_2-rGO/Al photodetector under UV light, (d) IV graph of MSM photodetector (AlShammari, Halim, Yam and Kaus, 2020:103630)

As seen in Figure 7a, the films contain different concentrations of rGO (1, 5, 7, and 10% wt). The energy bandgaps of thin films decreased from 3.60 to 3.04 eV as the concentration increased. This result demonstrates the effect of rGO concentration on conductivity (Figure 7b,c). FESEM images revealed that the graphene nanolayers became more embedded in the TiO nanoparticle matrix as rGO concentration increased. Al/TiO_2 and Al/TiO_2/rGO MSM photodetectors and I-V characteristics under 375 nm UV light and 3 V bias (Figure 7d) showed that the produced photodetectors exhibit Schottky metal-semiconductor contacts. The optimum values of photosensitivity, current gain, sensitivity rise, and fall times for 10% wt. Al/TiO_2/rGO were 3.064 (A/W), 11.27%, 1027.02%,

0.051 s, and 0.058 s, respectively. The results confirm the effect of GO concentration on TiO_2/rGO UV photodetector performance and show that the structure is a promising candidate for photodetector applications.

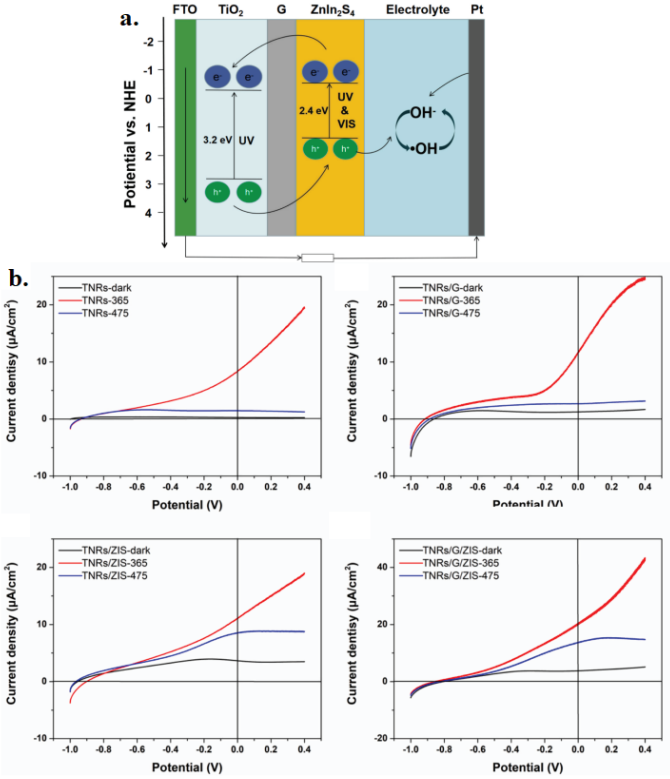

Figure 8. (a) Operational schematic diagram of UV-visible SPPD based on TNRs/G/ZIS, (b) I–V curves of SPPD photodetectors in the dark and under UV light and visible (Wang et al, 2022).

Conventional photodetectors consume large amounts of energy. Therefore, UV-visible self-powered photodetectors (SPPDs), which convert optical signals directly into electrical signals without energy problems, attract researchers' interest. SPPDs have advantages such as high sensitivity, short feedback time, and high stability. They are divided into 3 according to working principle and composition: p-n junction, Schottky junction, and photoelectrochemical (PEC) (Bai et al, 2017:804). PEC type SPPDs

have an inherent electric field, consume extremely low energy, require a simple manufacturing process, and have short feedback times; they work with light without an external voltage (Bianca et al, 2020:48600).

PEC type SPPDs, produced by simple methods with metal oxide semiconductor materials such as TiO_2, SnO_2, WO_3, Fe_2O_3, ZnO, are corrosion resistant. TiO_2, standing out with its chemical stability, light corrosion resistance, and low production costs, absorbs only the UV portion of sunlight due to its wide bandgaps, which limits the applications of SPPDs (Hu et al, 2013:9580). For this reason, researchers have resorted to doping TiO_2 with different elements to expand the absorption spectra of TiO_2-based SPPDs (An, Wang, Huang, Li, Wang and Yin, 2019:1170). Absorption spectra can be extended with heterojunction structures that combine TiO_2 with narrow bandgap semiconductors (Liu et al, 2015:3526).

$ZnIn_2S_4$ (ZIS), a ternary chalcogenide semiconductor, exhibits superior photoelectrochemistry properties with energy band gaps between 2.2-2.8 eV. Displaying a narrower energy range than TiO_2 (3.2 eV), ZIS forms a good heterojunction with TiO_2, helping to separate electron-hole pairs from each other and increase the absorption of visible light. Graphene, which has a high specific surface area and electron transportability, can be used as an electron mediator attached to semiconductor materials to reduce electron-hole pair recombination by promoting electron transfer (Liu et al, 2011:5315). For this reason, Wang et al. predicted that SPPDs based on TiO_2 nanorods (TNRs), graphene, and ZIS would respond well to the UV visible light range. They reported high responses such as 13.79 mA/W for UV and 0.39 mA/W for visible light with TNRs/G/ZIS/electrolyte heterojunction arrays synthesized by the three-step synthesis method (Wang et al, 2022). TNRs/G/ZIS-based UV-visible SPPDs showed high photocurrent densities of 20.25 μA/cm2 and 13.63 μA/cm2 for UV (365 nm, 0.71 mW/cm2) and visible light (475 nm, 7.4 mW/cm2) (Figure 8b). Figure 8a describes the structure composition and working principle of TNRs/G/ZIS-based PEC-type UV-Visible SPPD. When the SPPD receives UV light, many electron-hole pairs in TNRs and ZIS are excited by light. Due to the difference in the bandgap, electrons generated in ZIS are easier to transport to TNRs with higher band values. Thus, TNRs offer an efficient way for electron transport, and the energy band

structure created by ZIS has significantly improved the response of TNRs to UV and visible light. In addition, the charge-gathering capabilities of the graphene interlayers ensured the separation of carriers and accelerated their transfer. Such triple heterojunction structures are a promising development for UV-visible SPPDs.

Another research on PEC-type photodetectors belongs to Huang et al. (Huang, Zhang and Bai, 2019:349), ZnO is one of the wide bandgap semiconductors; it is an essential material for photodetectors with its simple preparation technique, good corrosion resistance, and low cost. Combining ZnO with a narrow bandgap semiconductor may effectively increase the visible light response. Therefore, CdS, a semiconductor with a bandgap of 2.4 eV, can be combined with ZnO to form a band arrangement that facilitates the isolation of electron-hole pairs and widens the spectral absorption range. On the other hand, it is a known fact that graphene can be bonded to semiconductor nanomaterials via functional groups. Therefore, the heterostructure of graphene, CdS, and ZnO is expected to show excellent responsiveness under UV and visible light. From this point of view, researchers designed the ZnO nanowire arrays (NAs)/graphene/CdS/electrolyte heterostructure and used a three-step synthesis method for SPPDs.

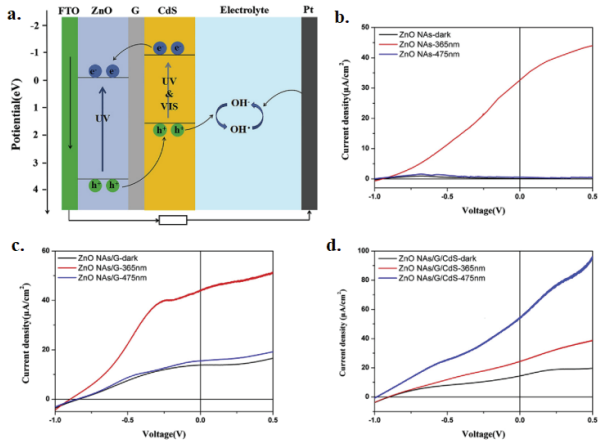

Figure 9. (a) Energy band diagram of UV-visible ZnO NAs/G/CdS-based SPPD. (b-d) Current density-voltage curves of SPPDs based on ZnO NAs, ZnO/G, and ZnO NAs/G/CdS in the dark and under UV light (Huang, Zhang and Bai, 2019:349).

The current density-voltage curves in the dark, under UV, and visible light were examined in Figure 9 to analyze the photoelectric properties of the photodetector. In the dark, all curves show rectification properties similar to those of Schottky diodes; conductivity was observed to increase with the addition of graphene and CdS nanoparticles. Thus, it was found that PEC-type photodetector exhibited high sensitivity under UV and visible light; the photocurrent density under UV light was 26.17 $mAcm^{-2}$.

It is suggested that heterojunction structures based on TiO_2 nanotubes (NT) will perform better than photodetectors based on pure TiO_2 NTs (Khalid, Ahmed, Hong and Ahmaed, 2013:660). As it has been frequently mentioned before, the proven performance of graphene in photoelectricity and photothermoelectricity contributed to the development of optoelectronic and photonic devices. For this reason, using TiO_2 and graphene together, which has become an attractive material class for the development of broad wavelength heterojunction-based photodetectors, will enable the transfer of electrons from TiO_2 to graphene due to the difference in energy levels. Thus, the heterojunction formed at the interface will prevent charge recombination of electron-hole pairs. Among various methods used for producing TiO_2 NTs, electrochemical synthesis (anodization of Ti foil) is the most popular method for producing high-quality NTs. Noothongkaew et al. transferred TiO_2 NTs produced by anodizing Ti foils onto transparent glass substrates and produced a UV photodetector based on TiO_2 NTs on a transparent substrate coated with several layers of graphene (Noothongkaew, Thumthan and An, 2018:277).

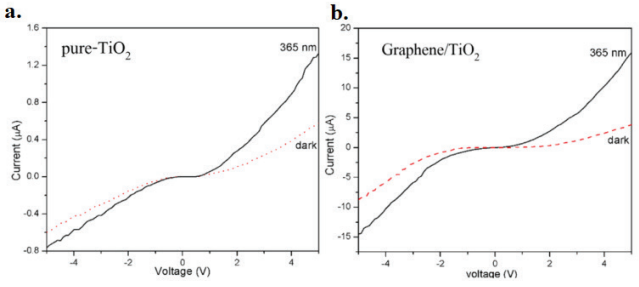

Figure 10. Current-voltage (I-V) curves of (a) pure TiO_2, (b) graphene/TiO_2 NT devices under and in the absence of UV light (Noothongkaew, Thumthan and An, 2018:277).

Figure 10 shows the results of the I-V characteristic of pure TiO_2 and graphene/TiO_2 NT devices under UV light at 365 nm and in the absence of UV light. The results show that the current is less at dark forward and reverse bias than the one under UV light. The produced UV photodetector devices were very sensitive to 365 nm UV light. The sensitivity and photocurrent gain of graphene/TiO_2 NT devices were better than TiO_2 NTs.

On the other hand, ZnO, another wide-bandwidth (3.37 eV) semiconductor, attracts great attention in optoelectronic technology with its high chemical stability, activity, and low cost (Özgür et al, 2005:041301). It is particularly remarkable in UV-sensing with its large surface areas that have emerged by combining with other low-dimensional materials such as 1-D ZnO nanowires (ZNWs), 1-D NTs, 2-D materials, metal, semiconductor nanoparticles. The inclusion of these low-dimensional carbon materials into ZNWs improves the separation efficiency of electron-hole pairs. On the other hand, there are disadvantages such as these structures' production processes, limited connection area, and low photoelectric efficiency. Graphene and CNT are both promising candidates for improving the photosensitivity of ZNW photodetectors. However, the performances of ZNW-based photodetectors, in which these nanomaterials are used, have not been studied in detail. Chen et al. prepared two types of composites using ZNWs combined with graphene and single-wall CNT (SWCNT) (Chen, Zhang, Hu, San, Cheng, and Hofmann, 2019:642). They made a comprehensive analysis of carbothermal ZNWs combined with rGO and SWCNTs, their UV-visible photoresponse properties to improve UV-vis detection. The researchers presented a comprehensive analysis of the photoresponse properties under UV and visible light of carbothermal ZNWs combined with rGO and SWCNTs to improve UV-vis detection. The photoelectric properties of rGO/ZNWs and SWCNT/ZNWs composites were better than pure ZNWs. The physical mechanism for the photoelectric effects of rGO, SWCNT, and ZNWs was presented by interface face transfer due to chemical adsorption and photodesorption of oxygen. Photoforming electrons at rGO/ZNWs and SWCNT/ZNWs interfaces tend to be transferred from ZNWs' conduction band to SWCNT and rGO. As a

larger contact area will occur in the rGO/ZNWs interface, it can collect and transfer carriers more effectively (Figure 11a).

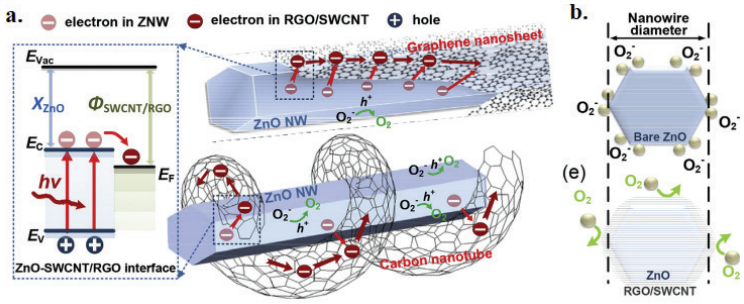

Figure 11. (a) Energy-band diagrams of SWCNT/ZNWs and rGO/ZNWs systems and carrier strategy at their interface (b) Surface chemical adsorption of oxygen molecules in bare ZnO (Chen, Zhang, Hu, San, Cheng, and Hofmann, 2019:642).

On the other hand, oxygen molecules in the air will capture the free electrons in ZnO and quickly adsorb them to the remaining surface of ZnO, which will cause the conductivity of ZnO to decrease, as seen in Figure 11b. With continuous UV radiation, photocurrent increases rapidly in ZNWs, leading to photocurrent degradation. The photosensitivity of the rGO/ZNWs-based photodetector is higher (~16 AW^{-1}) than the SWCNT/ZNWs-based one under low UV radiation (<10μWcm^{-2}). On the other hand, SWCNT/ZNWs have a higher on/off current ratio (8.41 × 104) and a faster response time. Besides, the rGO/ZNWs-based device shows both maximum sensitivity and maximum photoelectric efficiency. Researchers reported that SWCNT/ZNWs prepared with 0.1 wt% SWCNT are more advantageous for practical applications in imaging, photo-sensing, and optical communications, with both more cost-effectiveness and higher sensitivity.

InGaZnO (a-IGZO), which is one of the most common AOS, is an excellent gas detection material that detects low levels of gas molecules such as ozone (O_3), H_2, CO, NO, and NO_2, with a wide bandgap suitable for UV light detection (Huang, Li, Hsiao, Gao and Chen, 2020:115019). Amorphous ZnSnO (ZTO) can be an excellent alternative to a-IGZO,

which is rarely used due to the scarcity and toxicity of gallium (Ga) and indium (In) elements. As they have similar ionic diameters, the structural compatibility of Sn and Zn is critical in producing high-quality films.

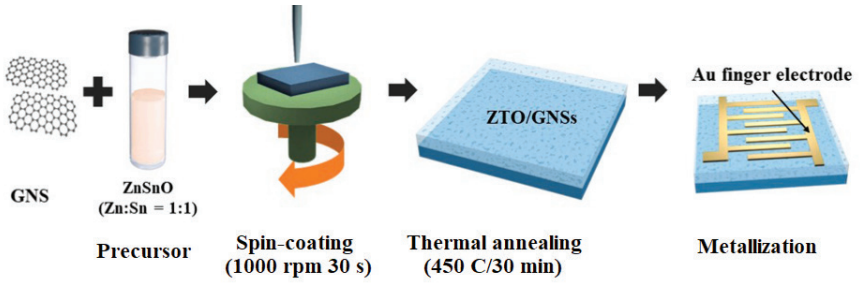

Figure 12. The device production process for a-ZTO/GNS dual-function sensor (Huang, Yan and Lou, 2022:3530).

Thermal treatments applied to AOS (high-temperature annealing) increase the number of oxygen vacancies in the films, increasing the gas response (Wu, Jiang, Chang, Lin and Chen, 2015:355). The lack of studies investigating the material design of AOS that simultaneously improve the sensing properties of both photons and gas molecules makes the research interesting. Graphene nanolayers (GNS) can be used to increase carrier transport with metal oxides. Based on this, Huang et al. developed a model for detecting UV light and O_3 to show that GNSs in a-ZTO improve photons' and gas molecules' sensing properties (Figure 12) (Huang, Yan and Lou, 2022:3530). The dual-functional sensor, consisting of hybrid amorphous a-ZTO/GNS composite films, showed a fast response with a sensitivity of 26.39 AW^{-1} at 350 nm, 0.71 s rise time, 0.95 s decay time. Also, under UV radiation of 10 $mWcm^{-2}$, the dual-function sensor exhibited a gas response of 12.8 against a concentration of 5 ppm ozone gas, indicating that the device acts as a sensitive gas sensor, not just a UV photodetector.

Graphene quantum dots (GQD), defined as parts of a single or several layers of graphene at the nanoscale, have essential properties such as high biocompatibility, fast electron transfer rate, high strength, and large specific surface area. If the particle diameter of GQDs is less than

100 nm, they have a narrow bandgap and respond well to UV and visible light with nuclear structures similar to conductive QDs. Wu et al. used RF magnetron sputtering and hydrothermal reaction methods to prepare a ZnO superstructure/GQD hybrid structure (Wu, Ding, Yang, Li, Shi and Zhou, 2020:17803). The structure exhibited high photocurrent and low dark current. The ZnO superstructure contains a ZnO nanoflower on top of a ZnO nanorod. The nanoflower supports the absorption of weak UV light, while nanorods, which have a large specific surface area, provide a pathway for the transport of carriers. GQDs can also help transfer carriers. The structure was obtained at 365 nm wavelength, with 3V bias and under 50 μWcm^{-2} light (Figure 13). The results show that the device has a low dark current of 40 nA and a photocurrent of 2.1 μA.

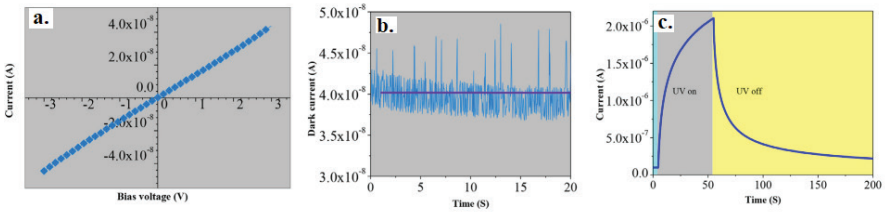

Figure 13. (a) I–V characteristic of the sample, (b) Dark current of the sample, (c) The response of the sample at a bias voltage of 3 V and an irradiance of 50μWcm^{-2} at a wavelength of 365 nm (Wu, Ding, Yang, Li, Shi and Zhou, 2020:17803).

In recent years, sensitive materials such as GaN, Ga_2O_3, diamond, and SiC have been the subject of extensive research involving UV photodetectors (Xie et al, 2019: 1806006). Among these materials, SiC has promising properties for high-temperature and high-power light-operated devices. Wideband gap semiconductors (WBGS), which play an essential role in the formation of heterojunction structures, are one of the most common ways to improve the performance of photodetectors (Zhuo et al, 2019:185).

Inspired by epitaxial graphene grown on SiC, a reliable and straightforward method for preparing graphene/WBGS junctions, the graphene/SiC structure can be obtained by thermal decomposition of SiC at high temperature (Emtsev, Speck, Seyller, Ley and Riley, 2008:155303).

With this method, two materials can be combined to form a heterojunction. Li et al. produced metal-graphene-metal (MGM) UV photodetectors by establishing epitaxial graphene (EG)/SiC coupling on semiconductor 4H-SiC (Li et al, 2021:594). It was found that the geometric parameters of graphene, which determines the number of carriers, affect the performance. Figure 14a, b shows the band diagram of the EG/SiC connection under the light. Electrons transferred from SiC to graphene at the start of radiation due to the built-in electric field in the junction can be seen. Then, graphene is further doped by photogenerated electrons under the light, causing the Fermi energy level to increase and the work function to decrease. By reducing the graphene channel from multilayer to monolayer, the sensitivity of the photodetector increases up to 189.7 mAV^{-1}, and the external quantum efficiency increases up to 66.6%, making the response signal more stable (Figure 14c). The results are important in showing the relationship between the performance of the EG/SiC UV photodetector and the number of carriers in graphene.

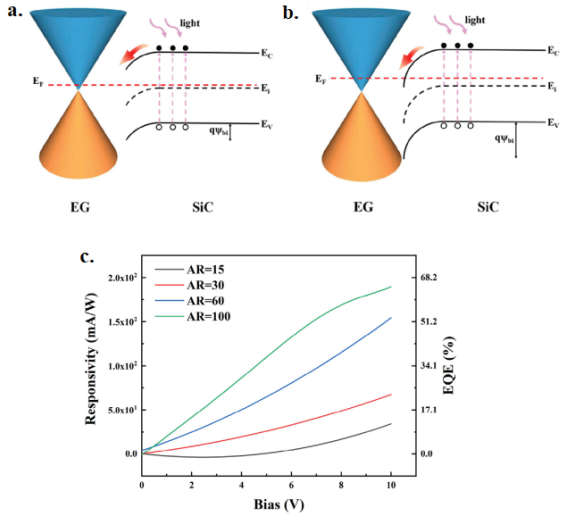

Figure 14. (a) Band diagram of EG/SiC link at the beginning of radiation, (b) Band diagram of EG/SiC link after radiation period, (c) Sensitivity and external quantum efficiency of SL-PDs with graphene channels of different aspect ratio (AR) under radiation (Li et al, 2021:594).

4H-SiC has also attracted the attention of Bencherif et al. with its superior performance in optoelectronic applications resulting from the wide bandgap, high thermal conductivity, and mechanical resistance (Bencherif et al, 2022:107683). Some techniques have been developed to increase the response of optoelectronic photosensing components and increase the devices' absorbance, mainly for practical applications. Commonly used metals, such as Au, Ag, Al, and Pt, are preferred for the interconnected electrodes formalism, which is an essential method. Again, the superior properties of graphene made it an integral part of high-performance photodetectors. Previous studies have shown that the absorption can be changed significantly on the nanoparticles added silicon surface, and better optical and electrical performance can be obtained (Liu et al, 2008:1551). On the other hand, although different approaches mainly focus on nanoparticles, they are concerned with the effect of size on photodetector values (Li et al, 2020:924). For this purpose, Bencherif et al. aimed to improve the sensing capacity of graphene/4H-SiC MSM photodetectors with interconnected graphene electrodes (IGE) by using Au nanoparticles.

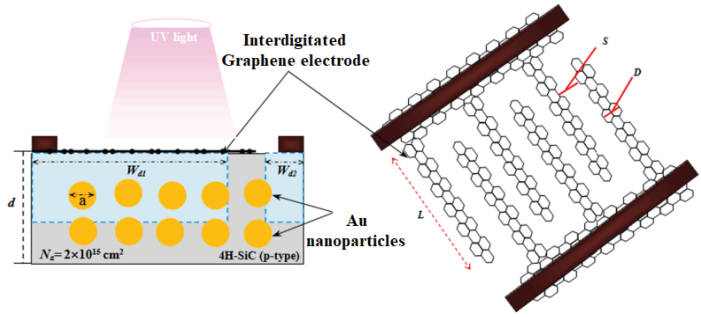

Figure 15. Graphen/Au-4H-SiC/Gr MSM photodetector (Bencherif et al, 2022:107683).

The schematic representation of the suggested Graphene/Au-4H-SiC/Gr MSM photodetector is shown in Figure 15. It is aimed to improve the sensing capacity of the proposed design by using both IGE engineering and Au nanoparticles model through a multi-objective genetic algorithm (MOGA). The obtained results explained the

role of Au nanoparticles in improving the sensing ability of the SiC thin film layer by increasing the absorption of the material. At the same time, this performance also depends on the radius of nanoparticles. The optimization has improved graphene electrodes' and Au nanoparticles' sensitivity and response times by approximately 47.9% and 65%. Its contribution is important in guiding the future development of photodetectors.

Flexible devices generally perform worse than planar devices; therefore, the efforts to improve the interface of optoelectronic devices such as light-emitting diodes and photodetectors have increased. In a study by Liu et al., they designed a method for ZnO/graphene photodetectors (Ju et al, 2019:375701), but the study resulted in poor device performance. To overcome this, interfacial contact can be improved by adding perovskite nanolayers (NS) between ZnO and graphene layers. In addition, $CsPbBr_3$, a p-type inorganic halide perovskite with superior chemical, optical, and semiconductor properties, has limited applications in flexible multilayer devices. Liu et al. used the advantageous properties of Ag nanowires (NW) and graphene, namely high conductivity, stability, and high transmittance. They developed a strategy to integrate PVDF substrate-based $CsPbBr_3$ NSs into ZnO NW/graphene flexible thin-film photodetectors (Liu et al, 2020:110956). Figure 16a shows the schematic illustration of sequentially coated Ag NWs, ZnO NWs, and $CsPbBr_3$ NSs on the PVDF membrane.

The optical microscope image in Figure 16b shows that a uniform and dense packing of Ag/ZnO NWs and $CsPbBr_3$ NSs can be achieved. Compared with the ZnO NWs/graphene structure, ZnO/$CsPbBr_3$ can facilitate the separation and transport of carriers. In addition, the ZnO networks in $CsPbBr_3$ NSs provide a smooth interface, enabling close contact with graphene. With the interface optimization, the carrier efficiency is approximately 10^3, and a high I_{light}/I_{dark} ratio is provided. In addition, this type of PVDF-based photodetectors is an indispensable part of optoelectronic applications with their excellent flexibility.

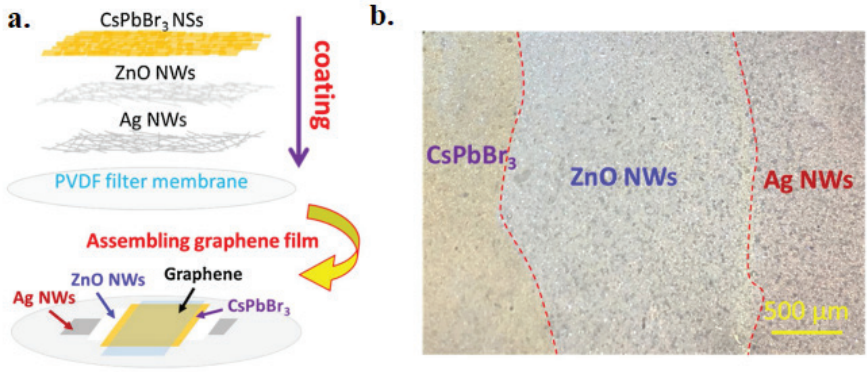

Figure 16. (a) Production procedure of Ag NWs/ZnO NWs/$CsPbBr_3$ NSs, coated on PVDF membrane by pumped filtration method, (b) Top optical microscope view of thin films on PVDF substrate (Liu et al, 2020:110956).

The current developments in nanoelectronics are mainly concerned with optical connections; they aim to develop photodetectors through nanoelectronic-photonic integration (Ferhati and Djeffal, 2017:32). The primary purpose here is to suggest new designs to reduce the output resistance by increasing the interface quality. Although some studies have reported that interconnected electrodes can reduce photodetector response time, this drastically deteriorates device sensitivity (Bencherif, Djeffal and Ferhati, 2016:308). Therefore, research is needed for improving both response time and sensitivity of Si-MSM-based devices. Graphene-based sensors have low sensitivity and high response times compared to gold contacts. Graphene interdigitated electrodes (GrIE) provide a fast response in UV photodetectors and provide new ways to reduce optical losses. For this reason, Ferhati et al. proposed a GrIE-based p-Si-MSM UV photodetector and compared the performance of the proposed model withAu/p-Si (Ferhati and Djeffal, 2019:106166). Figure 17a shows the 3-D schematic illustration of the proposed GrIE/p-Si-MSM-UV structure. Here, s and t represent the spacing and width of the graphene fingers, L represents the receiving aperture of MSM-UV-PD, and d is the active layer thickness of Si. Figure 17b shows the

device sensitivity with I_{on}/I_{off} variation as a function of fingers spacing. Accordingly, in the proposed design, the finger spacing variation does not affect the device performance; the photoresponse of the conventional device with Au electrodes can be significantly impaired with the reduction of the contact spacing. The results show that the optimized GrIE/p-Si structure with low response time (3 μs) and high sensitivity (770 mAW^{-1}) outperformed conventional Au/p-Si photodetectors. As frequently mentioned before, ZnO nanomaterials with a wide bandgap can be prepared easily and provide fast transitions for the transport of photogenerated carriers. However, photodetector applications in dual-spectrum image detection with poor visible light absorption are limited (Hu et al, 2013:9579).

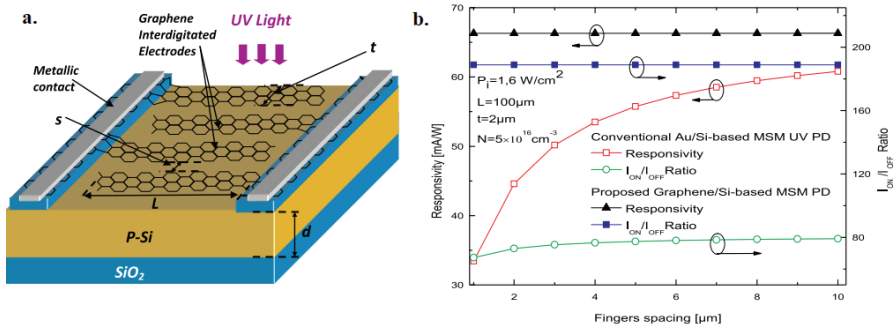

Figure 17. (a) 3-D schematic illustration of the GrIE/p-Si-MSM-UV structure, (b) Device sensitivity with I_{on}/I_{off} variation as a function of Fingers spacing (Ferhati and Djeffal, 2019:106166).

Copper oxide (CuO_2) with a bandgap of 2 eV is particularly attractive for solar energy conversion applications (Dubale et al, 2016:2211). Wide-bandgap metal oxide semiconductors modified with CuO_2 can significantly expand the absorption spectrum (Fan, Yu, Lu, Bai, Zhang and Shi, 2016:11). Especially the ZnO/CuO_2 heterojunction structure shows high performance in photodetection (Wang et al, 2017:220).

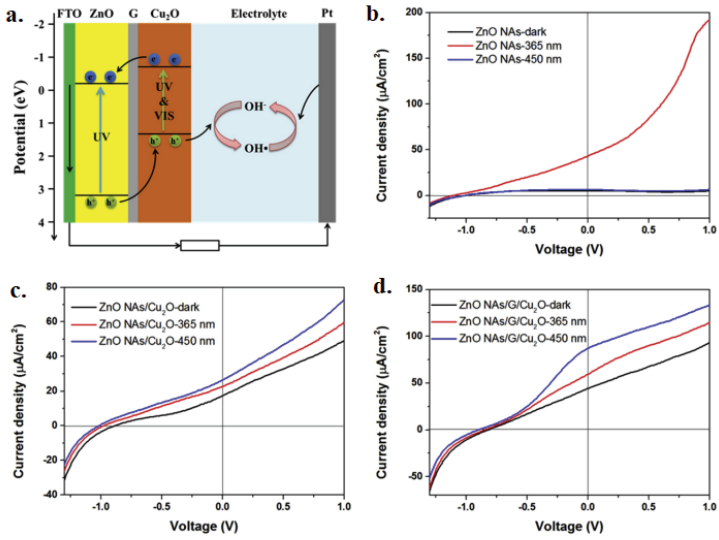

Figure 18. (a) Energy band profile and working principle of PEC-type photodetectors based on ZnO NAs/graphene/CuO_2, (b-d) JV curves of photodetectors based on ZnO NAs, ZnO NAs/Cu_2O, and ZnO NAs/G/Cu_2O in the dark and under UV and visible light (Bai et al, 2017:804).

These heterojunctions provide interface optimization and increase carrier recombination. In addition, the performance of existing structures can be further improved with graphene's ability to bind with semiconductor materials through its functional groups. For this purpose, Bai et al. synthesized ZnO nanowire arrays (NAs)/graphene/CuO_2 composites for PEC type photodetectors by hydrothermal and electrochemical deposition methods. The structure exhibited a sensitivity of 21.2 mAW^{-1} and 17.1 mA W^{-1} for UV and visible light, respectively. Figure 18a shows the energy band profile and working principle of PEC-type photodetectors based on ZnO NAs/graphene/CuO_2. UV light produces numerous photogenerated electron-hole pairs in ZnO NAs, CuO_2 film, and ZnO/CuO_2 interface, separated by an electric field. Photogenerated electrons in the conduction band of CuO_2 can easily pass to ZnO through the graphene interlayer and then be transferred to the Pt counter electrode via the external circuit. Figure 18b shows that ZnO NAs exhibit rectifi-

cation by band bending at the solid/liquid interface of the dark current curve. However, pure ZnO NAs exhibited a negligible response to visible light. ZnO NA/CuO_2 exhibits better electrical conductivity because it has a greater current density in the dark (Figure 18c). With the addition of the graphene interlayer, the charge carrying capability of the device increases, resulting in a greater dark current density, as seen in Figure 18d. Here, CuO_2 improves visible light-sensing ability, and the band alignment between ZnO and CuO_2 ensures the separation of photoexcited carriers. The highly conductive graphene interlayers, on the other hand, contribute to the charge transfer process between ZnO and CuO_2 with their excellent charge collection capacities. These properties make ZnO NAs/graphene/CuO_2 nanostructure a competitive candidate for PEC-type photodetectors.

5. Conclusions

This chapter presents a comprehensive review of the recent and remarkable studies on the production of graphene and GO-based photodetectors. Graphene and its derivatives have become essential in optoelectronic applications in recent years. Graphene is very promising for optoelectronic devices with its high electron mobility, atomic layer thickness, and unique mechanical flexibility. Graphene's outstanding electrical, mechanical, and chemical properties increase the efficiency of photodetectors. In addition, the structure has many more unique properties, which requires further research on the subject. Studies show that heterostructured photodetectors attract more attention. When graphene/GO is combined with semiconductor metal oxides, the energy bandgaps are adjusted, and the desired high performance is obtained. Therefore, graphene/GO-based UV photodetectors have become one of the important research topics of optoelectronics. Apart from the literature, the effects of different material groups on graphene are still unknown. In addition, the lack of studies on the flexibility of graphene that makes it usable in wearable electronics shows that research on the subject should be increased. Forming a heterostructure with clean interfaces for charge transfer between graphene and graphene-based photodetectors with different materials and explaining

and investigating the theoretical background of charge transfer dynamics and working mechanisms are important in developing heterostructured UV photodetectors and guiding future studies.

References

Adinolfi, V., Ouellette, O., Saidaminov, M. I., Walters, G., Abdelhady, A. L., Bakr, O. M., Sargent, E. H. (2016). Fast and Sensitive Solution-Processed Visible-Blind Perovskite UV Photodetectors. Adv. Mater. 28, 7264–7268. https://doi.org/10.1002/adma.201601196

AlShammari, A. S., Halim, M. M., Yam, F. K., Kaus, N. H. M. (2020). Effect of precursor concentration on the performance of UV photodetector using TiO2/reduced graphene oxide (rGO) nanocomposite. Results in Physics, 19, 103630. https://doi.org/10.1016/j.rinp.2020.103630

An, H., Wang, H., Huang, J., Li, M., Wang, W., Yin, Z. (2019). TiO2 nanosheets with exposed {001} facets co-modified by AgxAu1-x NPs and 3D ZnIn2S4 microsphere for enhanced visible light absorption and photocatalytic H2 production, Appl. Surf. Sci., 484, 1168–1175. https://doi.org/10.1016/j.apsusc.2019.04.180

Bae, S. H., Lee, S. J., Kim, Y. H., Lee, H. C., Kim, C. K. (2000). Analysis of 1/f Noise in LWIR HgCdTe Photodiodes. Journal of Electronic Materials, 120 (29), 877- 882. https://doi.org/10.1007/S11664-000-0242-X.

Bai, Z., Liu, J., Liu, F., Zhang, Y. (2017). Enhanced photoresponse performance of self powered UV-visible photodetectors based on ZnO/Cu2O/electrolyte heterojunctions via graphene incorporation. J. Alloys Compd., 726, 803-809. https://doi.org/10.1016/j.jallcom.2017.08.035

Bansode, S. R., Harpale, K., Khare, R. T., Walke, P. S., More. M. A. (2016). Morphological, structural and field emission characterization of hydrothermally synthesized MoS2-RGO nanocomposite. Mater. Res. Express,3 (11), 115023. https://doi.org/10.1088/2053-1591/3/11/115023

Bencherif, H., Djeffal, F., Ferhati, H. (2016). Performance enhancement of Pt/TiO2/Si UV-photodetector by optimizing light trapping

capability and interdigitated electrodes geometry, Superlattice. Microst. 97, 303–312. https://doi.org/10.1016/j.spmi.2016.06.028

Bencherif, H., Meddour, F., Dehimi, L., Faggio, G., Messina, G., …Della Corte, F. G. (2022). Improving graphene/4H-SiC/graphene MSM UV photodetector sensitivity using interdigitated electrodes formalism and embedded gold plasmonic nanoparticles. Optics and laser technology, 148, 107683. https://doi.org/10.1016/j.optlastec.2021.107683

Bianca, G., Zappia, M. I., Bellani, S., Sofer, Z., Serri, M.,… ,Bonaccorso, F. (2020) Liquid-phase exfoliated GeSe nanoflakes for photoelectrochemical-type photodetectors and photoelectrochemical water splitting. ACS Appl. Mater. Interfaces, 12, 48598–48613. https://doi.org/10.1021/acsami.0c14201

Bo, R., Nasiri, N., Chen, H., Caputo, D., Fu, L., Tricoli, A. (2017). Low-Voltage High-Performance UV Photodetectors: An Interplay between Grain Boundaries and Debye Length, ACS Appl. Mater. Interfaces, 9, 2606–2615.

Brown, D. M., Downey, E. T., Ghezzo, M., Kretchmer, J.W., Saia, R.J… Schneider, W.E. (1993) Silicon Carbide UV Photodiodes, IEEE Trans. Electron Dev., 40, 325–333. https://doi.org/10.1109/16.182509

Cao, M. S., Wang, X. X., Cao, W. Q., Yuan, J. (2015). Ultrathin graphene: Electrical properties and highly efficient electromagnetic interference shielding. J. Mater. Chem. C, 3, 6589–6599. https://doi.org/10.1039/C5TC01354B

Chen, C., Zhang, S., Hu, B., San, H., Cheng, Z., Hofmann, W. (2019). Non-aligned ZnO nanowires composited with reduced graphene oxide and single-walled carbon nanotubes for highly responsive UV–visible photodetectors, Composites Part B: Engineering, 164, 640-647. https://doi.org/10.1016/j.compositesb.2019.01.087

Chen, X. H., Ren, F. F., Gu, S. L., Ye, J. D. (2019). Review of gallium-oxide-based solar-blind ultraviolet photodetectors, Photon. Res., 7 (4), 381-415. https://doi.org/10.1364/PRJ.7.000381

Cheng, G., Wu, X., Liu, B., Li, B., Zhang, X., Du, Z. (2011). ZnO nanowire Schottky barrier ultraviolet photodetector with high sensitivity and fast recovery speed. Appl. Phys. Lett., 99, 203105. https://doi.org/10.1063/1.3660580

Cooper, J. A., Agarwal, A. (2002). SiC power-switching devices - The second electronics revolution?. Proc. IEEE, 90, 956–968. https://doi.org/10.1109/JPROC.2002.1021561

Ding, H., Zhang, S., Chen, J.T., Hu, X.P., Qiu, Y.X., Zhao, D.L. (2015). Reduction of graphene oxide at room temperature with vitamin C for RGO–TiO2 photoanodes in dye-sensitized solar cell. Thin Solid Films, 584: 29–36. https://doi.org/10.1016/j.tsf.2015.02.038

Dubale, A. A., Tamirat, A. G., Chen, H. M., Berhe, T. A., Pan, C. J., …Hwang, B. J. (2016). A highly stable CuS and CuS-Pt modified Cu2O/CuO heterostructure as an efficient photocathode for the hydrogen evolution reaction. J. Mater. Chem. A, 4, 2205–2216. https://doi.org/10.1039/c5ta09464j.

Emtsev, K. V., Speck, F., Seyller, T., Ley, L., Riley, J. D. (2008). Interaction, growth, and ordering of epitaxial graphene on SiC{0001} surfaces: a comparative photo electron spectroscopy study. Phys. Rev. B. 77 (15), 155303. https://doi.org/10.1103/PhysRevB.77.155303

Fan, W., Yu, X., Lu, H. C., Bai, H., Zhang, C., Shi, W. (2016). Fabrication of TiO2/RGO/Cu2O heterostructure for photoelectrochemical hydrogen production, Appl. Catal. B-Environ. 181, 7-15. https://doi.org/10.1016/j.apcatb.2015.07.032

Fang, Y., Armin, A., Meredith, P., Huang, J. (2019). Accurate characterization of next-generation thin-film photodetectors. Nat. Photonics, 13, 1-4. https://doi.org/10.1038/s41566-018-0288-z

Ferhati, H., Djeffal, F. (2017). Planar Junctionless Phototransistor: A Potential High-Performance and Low-Cost Device for Optical-Communications, Optics & Laser Technology, 97, 29–35. https://doi.org/10.1016/j.optlastec.2017.06.002

Ferhati, H., Djeffal, F. (2019). Performance assessment of Gr/Si/Gr UV-photodetector: Design and optimization of graphene interdigitated electrodes. Superlattices and Microstructures,, 132, 106166. https://doi.org/10.1016/j.spmi.2019.106166

Geim, A. K. (2011). Random Walk to Graphene (Nobel Lecture), Angew. Chem. Int. Ed., 50, 6966-6985. https://doi.org/10.1002/anie.201101174

Gorbachev, R., Geim, A., Katsnelson, M., Novoselov, K., Tudorovskiy, T.,…,Taniguchi, T. (2012) Strong coulomb drag and broken symmetry in double-layer graphene. Nat. Phys., 8, 896-901. https://doi.org/10.1038/nphys2441

Hatch, S. M., Briscoe, J., Dunn, S. (2013). A self-powered ZnO-nanorod/CuSCN UV photodetector exhibiting rapid response, Adv. Mater., 25, 867-871. https://doi.org/10.1002/adma.201204488

Hu, L., Zhu, L., He, H., Guo, Y., Pan, G., …Ye, Z. (2013). Colloidal chemically fabricated ZnO:Cu-basedphotodetector with extended UV-visibledetection waveband, Nanoscale, 5, 9577–9581. https://doi.org/10.1039/C3NR01979A

Huang, C. Y., Li, W. Y., Hsiao, Y. H., Gao, W. N., Chen, C. J. (2020). Trap-assisted photomultiplication in a-IGZO/p-Si heterojunction ultraviolet photodiodes, Smart Mater. Struct. 29, 115019. https://doi.org/10.1088/1361-665X/aba81a

Huang, C. Y., Xiao, L. K., Chang, Y. H., Chen, L. Y., Chen, G. T., Li, M. H. (2021) High performance solution-processed ZnSnO metal–semiconductor–metal ultraviolet photodetectors via ultraviolet/ozone photo-annealing. Semicond. Sci. Technol. 36, 095013. https://doi.org/10.1088/1361-6641/ac1565.

Huang, G., Zhang, P., Bai, Z. (2019). Self-powered UVevisible photodetectors based on ZnO/graphene/ CdS/electrolyte heterojunctions. Journal of Alloys and Compounds, 776, 346-352. https://doi.org/10.1016/j.jallcom.2018.10.225

Inamdar S. I. and Rajpure K. Y. (2014). High-performance metal–semiconductor–metal UV photodetector based on spray deposited ZnO thin films. J. Alloy Compd., 595:55–59. https://doi.org/10.1016/j.jallcom.2014.01.147.

Jones, R. C. (1952). Performance of Detectors for Visible and Infrared Radiation, Advances in Electronics, New York: Academic Press.

Ju, D., Liu, X. H., Zhu, Z., Wang, S., Liu, S.,… Zou, Y. (2019). Solution processed membrane-based wearable ZnO/graphene Schottky UV photodetectors with imaging application, Nanotechnology, 30 (37), 375701. https://orcid.org/0000-0001-5834-5579

Khalid, N. R., Ahmed, E., Hong, Z., Ahmaed, M. (2013). Enhanced photocatalytic activity of graphene TiO2 composite under visible light irradiation, Curr. Appl. Phys., 13, 659–663. https://doi.org/10.1016/j.cap.2012.11.003

Kim, I. K., Jo, J. H., Lee, B. J., Choi, Y. J. (2018) Detectivity analysis for organic photodetectors, Org. Electron., 57, 89-92. https://doi.org/10.1016/j.orgel.2018.02.036

Konatham, D., Striolo, A. (2008). Molecular design of stable graphene nanosheets dispersions. Nano Lett. 8(12), 4630–4641. https://doi.org/10.1021/nl802262p

Kumar, P., Singh, A. K., Hussain, S., Hui, K. N., Hui, K. S., … Singh, J. (2013). Graphene: Synthesis, properties and application in transparent electronic devices. Rev. Adv. Sci. Eng., 2, 238-258. https://doi.org/10.1166/rase.2013.1043

Leary, R., Westwood, A. (2011). Carbonaceous nanomaterials for the enhancement of TiO2 photocatalysis. Carbon, 49(3), 741–772. https://doi.org/10.1016/j.carbon.2010.10.010

Li, C. Y., Duan, S., Wen, B. Y., Li, S. B., Kathiresan, M.,…Tian, Z. Q. (2020). Observation of inhomogeneous plasmonic field distribution in a nanocavity, Nat. Nanotechnol. 15, 922–926. https://doi.org/10.1038/s41565-020-0753-y

Li, C., Huang, W., Gao, L., Wang, H., Hu, L., … Zhang, H. (2020). Recent advances in solution-processed photodetectors based on inorganic and hybrid photo active materials. Nanoscale, 12(4), 2201-2227. https://doi.org/10.1039/C9NR07799E

Li, J., Östling, M. (2013). Prevention of Graphene Restacking for Performance Boost of Supercapacitors-A Review. Crystals, 3, 163-190. https://doi.org/10.3390/cryst3010163

Li, Z., Zhang, W., Xing, F. (2019). Graphene Optical Biosensors. Int. J. Mol. Sci., 20, 2461, doi:10.3390/ijms20102461

Li, X., Wang, R., Zuo, Z., Ge, L., Chen, X.,…Hu, X., (2021). Correlation between the response performance of epitaxial graphene/SiC UV-photodetectors and the number of carriers in graphene. Carbon, 183, 590-599. https://doi.org/10.1016/j.carbon.2021.07.052

Liang, F. X., Zhang, D. Y., Wang, J. Z., Kong, W. Y., Zhang, Z. X., … Luo, L. B. (2016). Highly sensitive UVA and violet photodetector based on single layer graphene-TiO2 heterojunction. Opt. Express, 24(23), 25922–25932. https://doi.org/10.1364/OE.24.025922.

Lin, Z. H, Cheng, G., Yang, Y., Zhou, Y. S., Lee, S., Wang, Z. L., (2014).Triboelectric Nanogenerator as an Active UV Photodetector. Adv. Funct. Mater., 24(19), 2810–2816. https://doi.org/10.1002/adfm.201302838.

Liu, C., Teng, Y., Liu, R., Luo, S., Tang, Y., …Cai, Q. (2011). Fabrication of graphene films on TiO2 nanotube arrays for photocatalytic application, Carbon, 49, 5312–5320. https://doi.org/10.1016/j.carbon.2011.07.051

Liu, H., Mcintosh, D., Bai, X., Pan, H., Liu, M., … Cha, H. Y. (2008). 4H-SiC PIN recessed-window avalanche photodiode with high quantum efficiency, IEEE Photonics Technol. Lett. 20 (18), 1551–1553. https://doi.org/10.1109/LPT.2008.928823

Liu, Q., Wu, F., Cao, F., Chen, L., Xie, X., … Li, L. (2015). A multijunction of ZnIn2S4 nanosheet/TiO2 film/Si nanowire for significant performance enhancement of water splitting, Nano Res., 8, 3524–3534. https://doi.org/10.1007/s12274-015-0852-5

Liu, S., Liu, X., Zhu, Z., Wang, S., Gu, Y.,…Zou, Y. (2020). Improved flexible ZnO/CsPbBr3/Graphene UV photodetectors with interface optimization by solution process. Mater. Res. Bull., 130, 110956. https://doi.org/10.1016/j.materresbull.2020.110956

Liu, Z., Li, S., Yan, Z., Liu, Y., Zhi, Y.,…Tang, W. (2020). Construction of a β-Ga2O3-based metal–oxide–semiconductor-structured photodiode for high performance dual-mode solar-blind detector applications. J. Mater. Chem. C., 8, 5071–5081. https://doi.org/10.1039/D0TC00100G.

Morozov, S., Novoselov, K., Katsnelson, M., Schedin, F., Elias, D.,… Geim, A. (2008). Giant intrinsic carrier mobilities in graphene and its bilayer. Phys. Rev. Lett., 100, 016602. https://doi.org/10.1103/PhysRevLett.100.016602

Moses, W., Derenzo, S. (1994). Design Studies For A Pet Detector Module Using A Pin Photodiode To Measure Depth Of Interaction, IEEE Trans. Nucl. Sci,. 41, 1441-1445. https://doi.org/10.1109/23.322929

Müller, A., Konstantinidis, G., Dragoman, M., Neculoiu, D., Dinescu, A., …Dascalua D. (2009). GaN membrane-supported UV photodetectors manufactured using nanolithographic processes. Microelectron J., 40(2), 319–321. https://doi.org/10.1016/j.mejo.2008.07.021.

Noothongkaew, S., Thumthan, O., An, K. S. (2018). Minimal layer graphene/TiO2 nanotube membranes used for enhancement of UV photodetectors, Materials Letters, 218, 274–279. https://doi.org/10.1016/j.matlet.2018.02.033

Ozer, S., Besikci, C., Assesment of InSb photodetectors on Si substrates (2003). Journal of Physics D: Applied Physics. 36, 559-563. https://doi.org/10.1088/0022-3727/36/5/321

Özgür, Ü., Alivov, Y. I., Liu, C., Teke, A., Reshchikov, M. A., ..., Morkoç, H. (2005). A comprehensive review of ZnO materials and devices. J. Appl. Phys. 98(4), 041301. https://doi.org/10.1063/1.1992666

Park, S. H., Roy, A., Beaupre´, S., Cho, S., Coates, N.,…Moon, J.S. (2009) Bulk heterojunction solar cells with internal quantum efficiency approaching 100%, Nat. Photon, 3, 297-303. https://doi.org/10.1038/nphoton.2009.69

Pramanik, P., Sen, S., Singha, C., Roy, A. S., Das, A., …Bhattacharyya, A. (2016). Compositional inhomogeneities in AlGaN thin films grown by molecular beam epitaxy: Effect on MSM UV photodetectors. J. Appl. Phys.,120 (14), 144502. https://doi.org/10.1063/1.4964420

Schalwig, J., Müller, G., Karrer, U., Eickhoff, M., Ambacher, O., ... Dollinger, G. (2002) Hydrogen response mechanism of Pt–GaN Schottky diodes, Appl. Phys. Lett., 80, 1222–1224. https://doi.org/10.1063/1.1450044

Scharber, M. C., Muhlbacher, D., Koppe, M., Denk, P., Waldauf,… C., Heeger, A.J. (2006) Design rules for donors in bulk-heterojunction solar cells towards 10% energy conversion efficiency, Adv. Mater., 18, 789-794. https://doi.org/10.1002/adma.200501717

Strobel, N., Seiberlich, M., Rödlmeier, T., Lemmer, U., Hernandez-Sosa, G. (2018). Non-fullerene-based printed organic photodiodes

with high responsivity and megahertz detection speed. ACS, Appl. Mater. Interfaces, 10, 42733-42739. https://doi.org/10.1021/acsami.8b16018

Suriani, A. B., Muqoyyanah, Mohamed, A., Othman, M. H. D., Mamat, M. H.,… Abdul Khalil, H. P. S. (2018). Reduced graphene oxide-multiwalled carbon nanotubes hybrid film with low Pt loading as counter electrode for improved photovoltaic performance of dye-sensitised solar cells. J. Mater. Sci: Mater. Electron, 29(13), 10723–10743. https://doi.org/10.1007/s10854-018-9139-4

Timoumi, A., Alamri, S. N., Alamri, H. (2018). The development of TiO2-graphene oxide nano composite thin films for solar cells. Results Phys.,11, 46–51. https://doi.org/10.1016/j.rinp.2018.06.017

Tung, R.T., (2001). Recent advances in Schottky barrier concepts, Mater. Sci. Eng. R. Rep., 35, 1–138. https://doi.org/10.1016/S0927-796X(01)00037-7

Wang, C., Xu, J., Shi, S., Zhang, Y., Gao, Y.,…Li, L. (2017). Optimizing performance of Cu2O/ZnO nanorods heterojunction based self-powered photodetector with ZnO seed layer. J. Phys. Chem. Solids. 103, 218-223. https://doi.org/10.1016/j.jpcs.2016.12.026

Wang, X., Bai, Z., Zhang, Y., Zhang, Z., Liu, J., …Zhang, Q. (2022). High performance self-powered UV–visible photodetectors based on TiO2/ graphene/ZnIn2S4/electrolyte heterojunctions, Ceramic International, Pre-press,. https://doi.org/10.1016/j.ceramint.2022.01.185

Wang, Y. C., Chang, C. Y., Yeh, T. F., Lee, Y. L., Teng, H. (2014). Formation of internal p–n junctions in Ta3N5 photoanodes for water splitting. J. Mater. Chem. A, 2(48), 20570–20577. https://doi.org/10.1039/C4TA04501G

Wassei, J. K., Kaner, R. B. (2013). Oh, the Places You'll Go with Graphene. Acc. Chem. Res., 46, 2244-2253. https://doi.org/10.1021/ar300184v

Wu, C. H., Chang, K. W., Li, Y. N., Deng, Z. Y., Chen, … Chen, J. H. (2018). Improving the sensitive and selective of trace amount ozone sensor on indium gallium-zinc oxide thin film by ultraviolet irradiation, Sens. Actuators B Chem., 273:1713–1718. https://doi.org/10.1016/j.snb.2018.07.075.

Wu, C. H., Jiang, G. J., Chang, K. W., Lin, C. W., Chen, K. L. (2015). Highly sensitive amorphous In–Ga–Zn–O films for ppb-level ozone sensing: effects of deposition temperature, Sens. Actuators B Chem. 211, 354–358. https://doi.org/10.1016/j.snb.2015.01.048

Wu, H., Ding, J., Yang, D., Li, J., Shi, Y., Zhou, Y. (2020) Graphene quantum dots doped ZnO superstructure (ZnO superstructure/GQDs) for weak UV intensity photodetector application. Ceramics International, 46, 17800-17808. https://doi.org/10.1016/j.ceramint.2020.04.086

Wu, S., He, Q., Tan, C., Wang, Y., Zhang, H. (2013). Graphene-Based Electrochemical Sensors Small, 9, 1160-1172. https://doi.org/10.1002/smll.201202896

Xie, C., Lu, X. T., Tong, X. W., Zhang, Z. X., Liang, F. X., … Wu, Y. C. (2019). Recent progress in solar-blind deep-ultraviolet photodetectors based on inorganic ultrawide bandgap semiconductors. Adv. Funct. Mater., 29 (9), 1806006. https://doi.org/10.1002/adfm.201806006

Yang, M. Q., Zhang, N., Xu, Y. J. (2013). Synthesis of Fullerene–, Carbon Nanotube–, and Graphene–TiO 2 Nanocomposite Photocatalysts for Selective Oxidation: A Comparative Study. ACS Appl. Mater. Interfaces, 5(3), 1156–1164. https://doi.org/10.1021/am3029798

Yildiz, G., Warberg, M. B., Awaja, F. (2021). Graphene and graphene oxide for bio-sensing: General properties and the effects of graphene ripples. Acta Biomaterialia, 131, 62-79. https://doi.org/10.1016/j.actbio.2021.06.047

Yu, J., Lou, J., Wang, Z., Ji, S., Chen, J., … Zhang, Y. (2021). Surface modification of β-Ga2O3 layer using pt nanoparticles for improved deep UV photodetector performance. J. Alloys Compd., 872:159508. https://doi.org/10.1016/j.jallcom.2021.159508.

Yu, X., Zhao, Z., Zhang, J., Guo, W., Qiu, J.,.., Liu, H. (2016). Rutile Nanorod/Anatase Nanowire Junction Array as Both Sensor and Power Supplier for High-Performance, Self-Powered, Wireless UV Photodetector. Small, 12(20), 2759–2767. https://doi.org/10.1002/smll.201503388

Zhou, J., Gu, Y., Hu, Y., Mai, W., Yeh, P. H., …, Wang, Z. L. (2009). Gigantic enhancement in response and reset time of ZnO UV nanosensor by

utilizing Schottky contact and surface functionalization, Appl. Phys. Lett., 94, 191103. https://doi.org/10.1063/1.3133358

Zhou, X., Jiang, D., Zhao, M., Wang, N., Duan, Y., …, Sun, J. (2020). Polarization induced two-dimensional electron gas in ZnO/ZnMgO heterointerface for high-performance enhanced UV photodetector, J. Alloys Compd. 820:153416. https://doi.org/10.1016/j.jallcom.2019.153416.

Zhuo, R. R., Zeng, L. H., Yuan, H.Y., Wu, D., Wang, Y. G., … Tsang, Y. H. (2019). In-situ fabrication of PtSe2/GaN heterojunction for self powered deep ultraviolet photodetector with ultrahigh current on/off ratio and detectivity, Nano Res., 12 (1), 183-189. https://doi.org/10.1007/s12274-018-2200-z

CHAPTER VI

THE DETECTION OF IMPURITIES IN NANOSCALE AND PHYSICO-CHEMICAL CHANGES OCCURING IN REFINED STAGES OF SUNFLOWER OIL

Tuğba KARAYIGIT[1] & Erman DUMAN[2]
[1] (MSc), Afyon Kocatepe University, Institute of Science, Nanoscience and Nanotechnology, Afyonkarahisar, Turkey
e-mail: t_krygt1453@hotmail.com.tr
ORCID: 0000-0002-5705-7687
[2] (Assist. Prof. Dr.), Afyon Kocatepe University, Faculty of Engineering, Department of Food Engineering, Afyonkarahisar, Turkey e-mail: eduman@aku.edu.tr
ORCID: 0000-0003-3405-9572

1. Introduction

Sunflower (*Helianthus annuus L.*) is an annual plant that loves temperate climates. It is one of the four most important oilseed crops in the world, which can be grown even in regions with different climate types such as North America (Vilvert 2018). sunflower seeds; It consists of two parts, the shell and the inner part. Approximately 40% oil is obtained from these seeds. The oil obtained from sunflower seeds contains saturated fatty acids (palmitic, stearic), monounsaturated fatty acid (oleic), polyunsaturated fatty acid and mostly linoleic acid and traces of linolenic acid (Lacombe and Berville 2001). In order to use crude sunflower oil, a refining process is required. The purpose of chemical or physical refining required to obtain vegetable oils suitable for consumption is to remove unwanted substances from oil and to remove impurities with the least possible oil loss during these processes (Ferrari et al., 1996). Refining processes are divided into two

as physical and chemical, and generally, degumming consists of neutralization, bleaching, winterization and deodorization processes. In addition to physical and chemical refining, nanorefining studies are also starting with advancing technology (Yemişçioğlu et.al., 2013). Nano-food technologies are gaining more and more importance in the world, and today, the food sector is the field where most of the nanotechnology researches are carried out. Food and agriculture applications are in search of new methods and solutions with nanotechnology studies in the process from production to consumer, such as increasing the yield of cultivated products, protecting them against plant pests, ensuring the best absorption of the fertilizer by the plant, increasing their quality during processing. In this direction, this research has two important aims; The first aim was to determine the changes in the physico-chemical characterization of sunflower oil during the refining stages, and the second purpose was to determine the nano-sized impurities during the refining stages. In addition, it is aimed to provide information for nano refining in future research.

2. Material and methods

2.1. Materials

2.1.1 Supply of research material

Sunflower oil refining samples, which were subjected to chemical refining used in the research, were produced by a vegatable oil production factory in Turkey company, neutralization, bleaching, winterization and deodorization stages of the same crude oils. Samples; It was filled in 500 ml glass jars, wrapped with aluminum foil, and stored in a cool, moisture-free environment for the following analyzes.

2.2. Methods

2.2.1. Proximate analyses

The sunflower oils in refining all stages, the analyses of free fatty acidity, peroxide number, iodine number, color, saponification number, unsa-

ponifiable matter number were carried out according to the methods of AOCS Ca-5a-40, Cd 8-53, Cd1-21, Cc 13c-50, Cd3-25, Ca6a-40, respectively (AOCS, 1990).

2.2.2. Fatty acids composition

In line with the method specified in AOCS, the fatty acid compositions of the sunflower oils in refining all stages were made by using Shımadzu GC-2025 brand gas chromatography. The fatty acid methyl esters prepared by treating the fats by n-Heptane and potassium hydroxide were determined by gas chromatography (AOCS, 1990).

The column used is at the length of 60 m, at the diameter of 0.25 mm and at the film thickness of 0.20 μm and is of RTX-2330 brand. The operating conditions of GC are given below.

Temperatures
Column : 180˚C
Injection : 200˚C
Detector : 200˚C
Flow rates
Carrying gas (N_2) : 30 ml/min.
Combustible gas (H_2) : 28 ml/min.
Dry air : 220 ml/min.
Injection amount : 1 μl

2.2.3. Mineral matter analysis

0.5 gram oil was put into the combustion container and 15 gml pure HNO_3 was added onto it. It was burned in MARS 5 microwave oven at 200 °C. The solution was diluted to 100 g/ml with ultra-pure water and filtered through ashless filter paper (Macherey-Nagel MN 640w, black-tape, 110 mm diameter). The concentrations of the mineral matters were determined by reading the prepared samples in ICP-AES (Inductively Coupled Plasma Atomic Emission Spectrometer) device (Skujins, 1998).

2.2.4. Sterol compositions

1.5-gram oil sample was weighed and cholesterol standard (0.1 %) dissolved in 2 ml chloroform was added. Then, chloroform was evaporated in rotating evaporator. 10 ml ethanol and 6 ml 6 M KOH were added and held in oil bath 90 °C for 1.5 hours for saponification. The unsaponifiable part was extracted with hexane. After evaporating hexane, 0.25 ml pyridine and 0.3 ml BSTFA were added and derivatized in the drying oven at 80 °C for 30 minutes. 1 ml GC vialine was taken from the derivatized extract (Tanacı, 2013).

Device	: GC-2010
Detector	: FID
Column	: TRB-Sterol (30 m x 0.22 mm x 0.22 um)
Injection Block Temperature	: 280 °C
Injection Mode	: Split
Flow Control Mode	: Pressure
Pressure	: 180 kPa
Split Ratio	: 50
Column Temperature Program	: 280 °C 40 min. (Isothermal)
FID Temperature	: 300°C

2.2.5. Imaging analyzes at nanoscale of impurities

For this analysis, sunflower oils obtained from every stage of refining, from crude sunflower oil to refined sunflower oil, were treated directly and with ethanol, passed through Wattman No: 22 diameter filter paper, and the impurities remaining on the surface of the filter paper were analyzed by LEO 1430VP secondary electron microscope (SEM) and elements analysis with EDX.

2.2.6. Statistical analysis

The data obtained in the research were analyzed using the SPSS (Statistical Package for Social Sciences) for Windows 22.0 program. The

mean standard deviation was used as descriptive statistical methods in the evaluation of the data.

3. Results and Discussion

In Table 1, the physico-chemical characterization of oils obtained from each stage of refining, from crude sunflower oil to refined sunflower oil, is given.

Table 1. As Refined Stages of Sunflower Oils Proximate Analysis Results

Refining Stages	Free fatty acidity (%)	Peroxide number (meqO_2/kg)	Refractive index (nD)	Saponification number (mgKOH/g)	Unsaponifiable matter (g/kg)
Crude Oil	2.400 ±0.300	3.57 ±0.300	1.4758 ±0.000	205.710 ±0.030	0.020 ±0.003
Neutralization	0.070 ±0.002	1.38 ±0.002	1.4760 ±0.000	208.550 ±0.040	0.010 ±0.004
Bleaching	0.060 ±0.001	1.56 ±0.001	1.4761 ±0.000	206.740 ±0.020	0.220 ±0.030
Winterization	0.220 ±0.004	0.85 ±0.004	1.4763 ±0.000	208.630 ±0.030	0.140 ±0.020
Deodorization	0.050 ±0.003	0.00 ±0.00	1.4762 ±0.000	204.740 ±0.030	0.790 ±0.030

±: Standard deviation

According to this, while the amount of free fatty acidity was found at the highest value (2.40) in crude sunflower oil, it gradually decreased during the refining stages and took the lowest value (0.05) in deodorized oil. Gomes et al. (2003) worked with two different sunflower oils and determined the free acidity value in crude oil, which is one of the refin-

ing stages, 1.16%-2.13% in neutralized oil, 0.05-0.21% in bleaching oil, 0.11-0.23% in deodorized oil, and 0.06-0.09% in deodorized oil.

While the peroxide number had the highest value (3.57 meq O_2/kg) in crude sunflower oil, it was determined at a low rate after neutralization (1.38 meq O_2/kg). However, the peroxide ratio, which increased again in the bleaching process (1.56 meq O_2/kg), was determined to be the lowest after the deodorization (0 meq O_2/kg), which is the last part of the refining stage, and in the amount suitable for the use of oil as edible oil (Pestana et al. 2008). Kreps et al. (2014) determined the peroxide values of the oils in crude oil and physical refining stages in their study with rapeseed oil and sunflower oil. According to this; for sunflower oil with high oleic fatty acid content, this value is 3.12±0.20 meq O_2/kg for crude oil, 1.18±0.06 meq O_2/kg for degumming oil, 1.67±0.07 meq O_2/kg for bleached oil, 1.25±0.06 meq O_2/kg for winterized oil, and 0.32±0.04 meq O_2/kg in deodorized oil.

Sunflower oil refractive index ratios did not vary in all refining stages from crude oil to deodorized oil (1.476 n_D) and remained statistically constant. Refractive index values (at 25°C) are 1.472-1.474 n_D for sunflower oil, 1.470-1.474 n_D for corn oil, 1.470-1.474 n_D for both rapeseed oil with low and high erucic acid, groundnut 1.462-1.460, 1.470-1.476 n_D for soybean oil , 1.4636-1.4698 n_D for cottonseed oil, and 1.457-1.459 n_D for palm oil measured at 40°C. (Aluyor et.al., 2009). Unsaponifiable matter values of crude sunflower oil were 0.020 g/kg (±0.003) before refining, 0.010 g/kg (±0.004) after neutralization, 0.22 g/kg (±0.03) during bleaching, 1.40 during winterization g/kg (±0.02) and 0.79 g/kg (±0.03) at the deodorization stage. In addition, while the saponification number value of crude sunflower oil was 205.71 (±0.03) mg KOH/g before refining, it was 208.55 (±0.04) mgKOH/g in the neutralization step, 206.74 (±0.02) mgKOH/g in the bleaching step, 208.63 (±0.03) mgKOH/ in the winterization phase. g and at the end of the deodorization stage, it was determined as 204.74 (±0.03) mgKOH/g. Saponification number of sunflower oil 188-194, Saponification number of corn oil 187-193 mgKOH/g, High erucic acid of rapeseed oil 170-180 mgKOH/g, Low erucic acid 188-193 mgKOH/g, Soya oil Saponification number 185-195 mgKOH/ g, Saponification number of cotton oil is given as 189-198

mgKOH/g, Saponification number of groundnut oil is given as 188-192 mgKOH/g (Aluyor et.al., 2009). It was determined that the saponification number separete ration of corn oil was close to the previous one. (Haşlak and Duman, 2021)

Table 2. As Refined Stages of Sunflower Oils Colors Results

Refining Stages	Color
Crude Oil (1[II])	7.5R-70.0Y-0.0B-0.0D
Neutralization (5.25 [II])	2.6R-70.0Y-0.0B-0.0D
Bleaching (5.25 [II])	1.2R-14.0Y-0.0B-0.0D
Winterization (5.25 [II])	1.5R-27.0Y-0.0B-0.0D
Deodorization (5.25 [II])	1.0R-8.4Y-0.0B-0.0D

[II]:inç; R:red; Y: yellow; B:blue ; D:dark

Table 3. As Refined Stages of Sunflower Oils Fatty Acids Compositions Results

Fatty acids (%)	Crude Oil	Neutralize	Bleaching	Winterized	Deodorize
Myristic acid	0.061±0.001	0.063±0.003	0.061±0.001	0.064±0.003	0.067±0.002
Palmitic acid	6.193±0.003	6.225±0.005	6.266±0.060	6.162±0.005	6.376±0.003
Stearic acid	3.486±0.002	3.467±0.001	3.372±0.003	3.272±0.020	3.081±0.012
Araşidic acid	0.243±0.002	0.242±0.001	0.237±0.002	0.229±0.002	0.222±0.002
Lignoseric acid	0.226±0.002	0.234±0.002	0.219±0.001	0.202±0.001	0.233±0.012
Heptadecanoic acid	0.028±0.001	0.028±0.002	0.029±0.002	0.027±0.002	0.027±0.002
Palmitoleic acid	0.035±0.001	0.034±0.001	0.033±0.003	0.031±0.001	0.027±0.002
Oleic acid	25.225±1.500	25.565±1.500	25.294±1.250	25.176±1.002	25.086±0.060
Nervonic acid	0.003±0.001	0.004±0.001	0.004±0.004	0.004±0.001	0.005±0.001
Linoleic acid	63.788±1.750	63.419±1.080	63.758±1.750	64.111±1.020	64.15±1.02
Linolenic acid	0.007±0.001	0.013±0.001	0.012±0.002	0.006±0.001	0.009±0.002
cis-11.14 Eicosadienoic acid	0.658±0.001	0.661±0.006	0.669±0.005	0.671±0.001	0.676±0.001
Arachidonic acid	0.046±0.020	0.045±0.002	0.045±0.030	0.045±0.020	0.042±0.002

Σ Saturated Fatty acids	10.237±0.050	10.259±0.060	10.184±0.021	9.956±0.020	10.006±0.080
Σ Unsaturated fatty acids	89.762±0.090	89.741±0.075	89.815±0.060	90.044±0.120	89.995±0.085

±: Standard deviation

As can be seen in Table 2, while the color of sunflower oil is darker in crude oil depending on the refining stages, it is seen that the color of sunflower oil becomes lighter towards the last stage. Ertürk (1999), in study with crude sunflower oil, determined 0.3 red, 2 yellow and 0.2 red colors after bleaching in the color determination of the oil before bleaching. Wiedermann (1981), in study with soybean oil, determined the red color values of 7-8, 2.0-2.5, 0.4-0.8 in the color determination (for neutralization, bleaching, deodorization, respectively) in the chemical refining step.

As seen in Table 3, in the refining stage, myristic acid (crude oil 0.06%, deodorized oil 0.07%), palmitic acid (crude oil 6.19%, deodorized oil 6.38%), linoleic acid (crude oil 63.79 %, deodorized oil 64.15%), eicosadienoic acid (crude oil 0.66%, deodorized oil 0.68%), lignoceric acid (crude oil 0.22%, deodorized oil 0.23%) values crude It is seen that it rises from oil to deodorized oil stage. In the refining stage, heptadecanoic acid (crude oil 0.03%, deodorized oil 0.03%), palmitoleic acid (crude oil 0.04%, deodorized oil 0.03%), stearic acid (crude oil 3.49%, deodorized oil 3.08%), oleic acid (crude oil 25.23%, deodorized oil 25.09%), arachidic acid (crude oil 0.24%, deodorized oil 0.22%), arachidonic acid (crude oil 0.05 %, deodorized oil 0.04) decreased from crude oil to deodorized oil stage. In addition, the total saturated fatty acidity value was determined as 10.24% in crude oil, which is the first stage of refining. It is seen that the value increased to 10.26% in neutralized oil and decreased to 10.01% in deodorized oil, which is the last stage of refining. Total monounsaturated fatty acidity values (%) reached the highest value of 25.60 in the neutralization stage, while the lowest value was 25.12 in deodorized oil. However, it decreased during the refining stages. In his study with canola oil, Güler (2009) determined the amount of Σ saturated fatty acids in cold pressed oil to be 7.585 on average (as %), while the amount of unsaturated fatty acids was found to be 7.685% in refined oil on average,

and 92.415% in cold pressed oil, on average 92.315% in refined oil. Σ The amount of monounsaturated fatty acids was found to be 64.625% on average in cold pressed canola oil and 64.815% on average in refined canola oil, Σ The amount of polyunsaturated fatty acids was determined as 27.790% in cold pressed oil and 27.500% in refined oil. In a study conducted with hazelnut oil, the amount of saturated fatty acids (%) in the fatty acid composition of crude hazelnut oil and refined hazelnut oil was 8.36% in crude oil and 8.38% in refined oil, while the amount of monounsaturated fat in crude hazelnut oil was 77.53 refined hazelnuts. oil, on the other hand, a value of 71.2 was obtained. In terms of polyunsaturated fatty acids, the values obtained in the examinations made in crude and refined hazelnut oil are 14.11% and 20.42%, respectively. (Kesen et.al., 2016; Özcan et.al., 2021).

Table 4. As Refined Stages of Sunflower Oils Sterol Compositions Results

Sterol analysis (%)	Crude Oil	Neutralize	Bleaching	Winterized	Deodorize
Cholesterol	nd	nd	nd	nd	nd
Brassicasterol	nd	nd	nd	nd	nd
Campasterol	8.413±0.750	9.235±0.080	9.019±0.080	9.048±0.060	8.818±0.075
Stigmasterol	10.493±1.250	12.066±0.750	11.909±0.090	12.641±0.060	12.445±0.058
Δ5,23-Stigmastadienol	0.821±0.090	1.278±0.005	0.807±0.002	0.759±0.005	0.767±0.002
Clerostenol	0.879±0.060	1.04±0.02	0.965±0.005	0.945±0.003	0.969±0.001
β -sitosterol	62.053±2.025	63.214±1.25	66.276±1.02	72.733±0.70	72.41±0.60
Δ5-Avenasterol	4.811±0.070	6.289±0.005	4.055±0.002	nd	nd
Δ5,24-Stigmastadienol	0.766±0.009	0.76±0.02	0.496±0.001	nd	nd
Δ7-Stigmasterol	11.059±0.006	4.875±0.050	5.786±0.750	3.876±0.003	4.248±0.012
Δ7-Avenasterol	0.707±0.005	1.244±0.010	0.690±0.002	nd	0.344±0.003

nd: not detected; ±: Standard deviation

As seen in Table 4, when the sterol composition of sunflower oil is examined; cholesterol and brassicasterol could not be detected at any stage of the

refiningThe lowest value of campasterol detected at each stage of refining was in crude sunflower oil (8.41%), while its highest value was in neutralized sunflower oil (9.23%). The lowest value of stigmasterol (10.49%) was determined in crude oil. The refining stage with the highest value (12.64%) is the winterization stage and it was found at each stage. Δ5,23-Stigmastadienol was detected at each step of refining, with the highest value (1.28%) in neutralized oil. It decreased gradually after the neutralization stage, but the lowest value (0.76%) was determined during the winterization stage. The lowest value (0.88%) of this type of sterol, which is present at every stage of the clerostenol refining and has very close values, was determined in crude oil and the highest value (1.04%) in neutralized oil. β-Sitosterol was detected at all stages of refining and at increasing values. Δ5-Avenasterol was detected only in the first three steps of refining, with the lowest value (4.06%) in the bleaching step and the highest value (6.29%) in neutralization. Δ5,24-Stigmastadienol was diluted in decreasing values starting from the crude oil stage and could not be detected in the last three stages of refining. Δ7-Stigmasterol was detected at every stage of refining and had a very high (11.06%) value in the crude oil stage, while it was detected at approximately half its value in other stages and had the lowest value (3.88%) in the winterization stage. Δ7-Avenasterol was detected in four of the refining steps and was not detected in winterized oil. It decreased compared to the initial value and the lowest value (0.34%) was detected in deodorized oil. In other studies, it has been stated that there are changes in the sterol composition of canola and hazelnut oils depending on the refining stages (Duman and Özcan, 2020).

Table 5. As Refined Stages of Sunflower Oils Mineral Matter Results (ppm)

Mineral Matter (ppm)	Crude Oil	Neutralization	Bleaching	Winterization	Deodorization
Li	0.02±0.01	0.07±0.02	0.46±0.02	0	0.005±0.002
Na	271.61±1.25	174.85±1.10	0	0	0
Mg	1.63±0.30	0.88±0.40	0.14±0.02	6.39±0.90	3.52±0.90
Al	4.46±0.20	2.29±0.60	0	0	0

Si	29.53±1.00	26.58±1.02	23.37±1.01	22.154±1.26	24.53±1.03
P	967.39±1.56	756.68±1.75	157.66±2.25	162.92±2.30	217.69±2.25
K	1.55±0.02	0	0	0	0
Ca	2.73±0.01	0.87±0.05	0	1.74±0.05	0
V	0.002±0.001	0	0.001±0.001	0.004±0.002	0
Cr	0.16±0.02	0.09±0.04	0	0.30±0.03	0
Mn	0.10±0.01	0.01±0.01	0.01±0.01	0.90±0.03	0.04±0.01
Fe	25.65±0.45	0	0	97.26±0.80	0
Co	0.007±0.002	0.001±0.001	0	0.006±0.002	0
Ni	0.17±0.02	0.44±0.02	0	0.12±0.01	0
Cu	0.01±0.01	0.09±0.03	0.13±0.01	0.26±0.02	0.25±0.02
Ga	0.0006±0.0002	0.001±0.001	0.001±0.001	0.002±0.001	0.0009±0.0002
As	0.006±0.001	0	0.004±0.002	0.015±0.002	0.006±0.002
Se	0	0	0.006±0.003	0.002±0.001	0.002±0.001
Ru	0.005±001	0.002±0.001	0	0	0
Pd	0.005±0.002	0.002±0.001	0	0	0
Ag	0.003±0.001	0.001±0.001	0.004±0.002	0.0009±0.0002	0.002±0.001
Cd	0	0	0.01±0.01	0.04±0.01	0.05±0.02
In	0.15±0.01	0.10±0.02	0	0	0
Sn	46.97±0.30	36.74±0.60	0	0	0
Sb	0.006±0.002	0.006±0.002	0	0	0.001±0.001
Ba	0.04±0.01	0.01±0.01	0	0.03±0.01	0.03±0.01
Pt	0.00001±0.00001	0	0	0	0
Pb	0.04±0.01	0.008±0.001	0	0	0

±: Standard deviation

As can be seen in Table 5, the P amount of crude sunflower oil was determined well above the amount of P in crude soybean and canola oil. The Fe content of the crude oil sample in our study is higher than the Fe content of canola crude oil. The amount of Cu was determined in low amount. It was observed that the P, Fe and Na amounts of our crude sunflower oil samples were higher than those found in rice bran crude oil, while the Ca, K and Mg amounts were lower than the rice bran crude oil rates. Increases and decreases in the amount of certain mineral substances during the refining showed that it could also be caused by the degree of corrosion of the equipment used. Mounts et al. (1979) detected

600ppm phosphorus in crude soybean oil in their study with soybean oil. Ostri et al. (1980) reported the amounts of iron and copper in ppm in continuous refining stages in their study with sunflower oil, between 0.75-0.062 ppm in post-neutralization oils, between 0.63-0.0055 ppm in bleaching, and 0.70-0050 ppm in deodorized oil, respectively.

During the refining of sunflower oil, SEM analysis and EDX elemental chemical detector were used to determine the nano-sized impurities at each stage. SEM images of the control filter and each refining step are given in Figures 1-6.

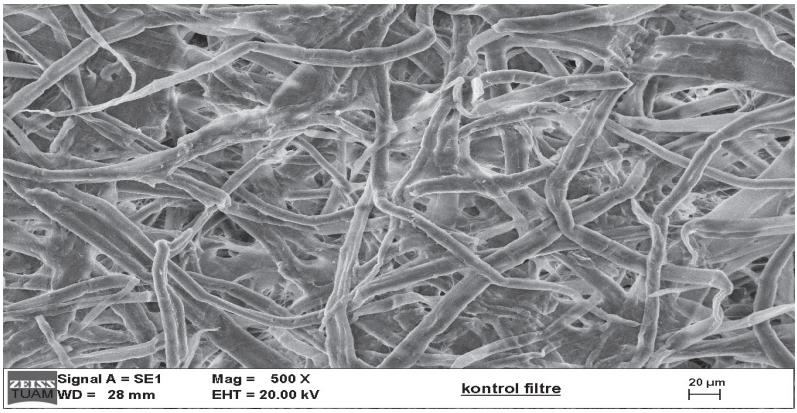

Figure 1. Control filter, topographic 500 times magnified topographic view in SEM

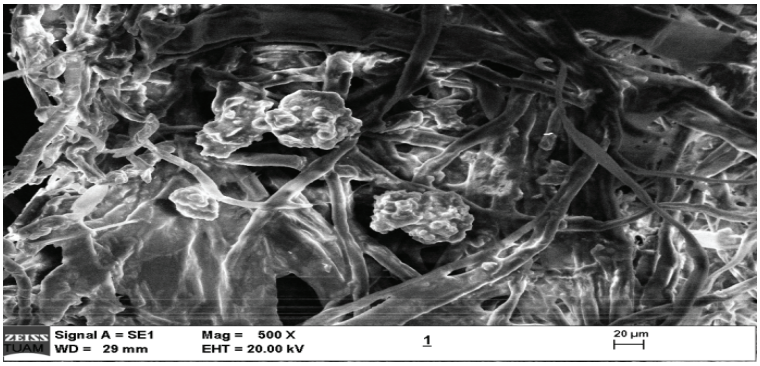

Figure 2. Crude sunflower oil, 500 times magnified topographic view in SEM.

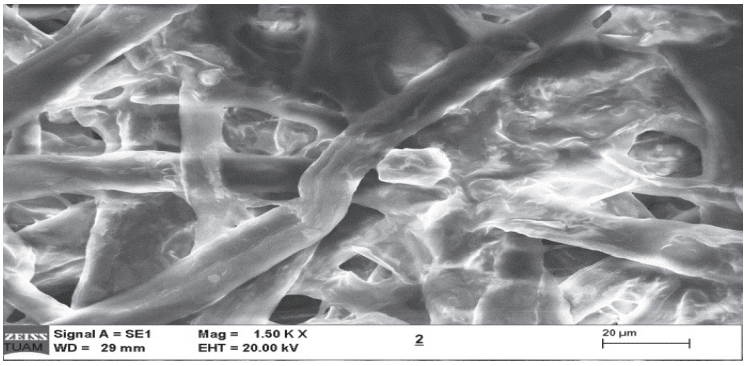

Figure 3. Neutralized sunflower oil, 1500 times magnified topographic view in SEM oil

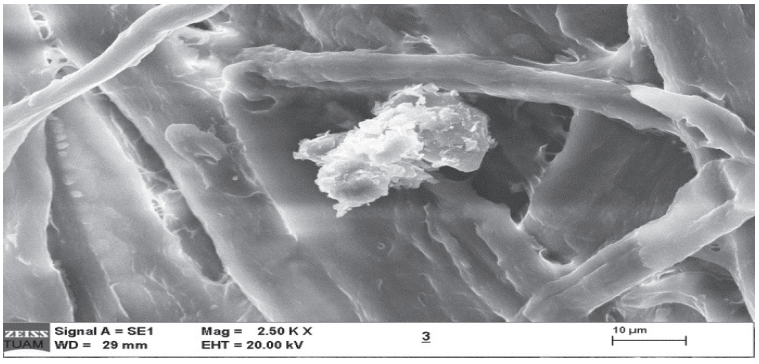

Figure 4. Bleached sunflower oil, 2500 times magnified topographic view of in SEM

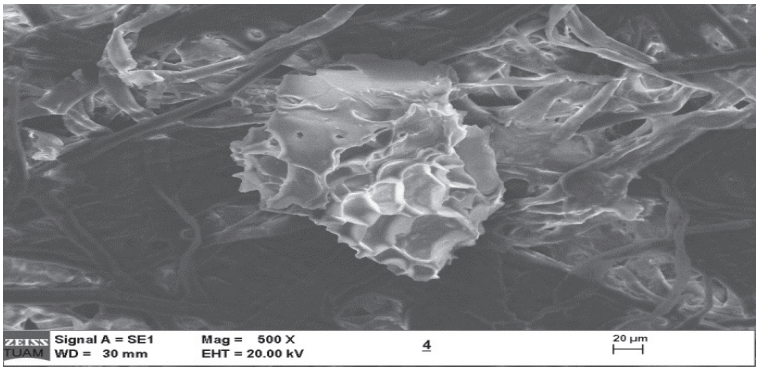

Figure 5. Winterized sunflower oil, 500 times magnified topographic view in SEM

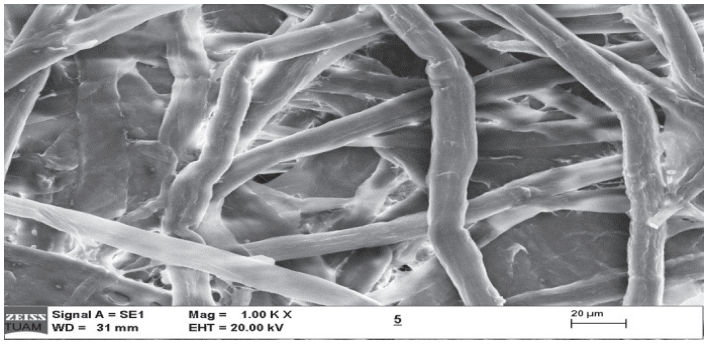

Figure 6. Deodorized sunflower oil, 1000 times magnified topographic view of in SEM

As seen in the SEM images, it was determined that no nano-sized impurities were detected in the deodorization stage, which is the last stage of refining. In addition, the elemental analysis of the impurities seen in the Sem images were given in Table 6.

Table 6. As Refined Stages of Sunflower in EDX analysis detected elements (%)

Refining Stages	Crude oil	Neutralization	Bleaching	Winterization	Deodorization
C	53.80	57.13	54.72	72.37	66.85
O_2	44.38	42.86	45.28	27.63	33.01
Na	1.01	nd	nd	nd	nd
Silicon	0.33	nd	nd	nd	0.15
P	1.28	nd	nd	nd	nd
Ca	0.27	nd	nd	nd	0.27

* nd: not determined

Accordingly, while C and O elements were detected at every stage of refining, Na and P elements were determined only in crude oil sample, while Silicon and Ca elements were detected in crude oil and deodorized sunflower oil impurities. Although there is no visible impurity in the deodorization stage in the SEM images, the removal of silicon and

calcium in the elemental analysis shows that it may be caused by the contamination of the refining process from machinery and equipment. Since there is no comparable source for the SEM analysis and elemental results obtained as a result of our study, the data obtained are the first data in the literature.

4. Conclusions

As a result; It was determined that the physico-chemical properties of sunflower oil (except for the refractive index) changed in neutralization, bleaching, winterization and deodorization stages until refined oil production. On the other hand, it has been determined that nano-sized impurities can occur at every stage during refining. The results obtained show that SEM and EDX analyzes can be used to detect the corrosion of machinery and equipment used at every stage, especially in vegetable oil technology. In addition, certain issues related to sunflower oil have been investigated in line with the literature reviews, but it is understood that there are few studies related to this research that we have done for the detection of nano-sized impurities. For this reason, examining the physicochemical properties of sunflower oil by detecting the changes in the refining stage and its nano-sized impurities is also important in terms of future nano-refining in the field of vegetable oil technology, and it is recommended to carry out these studies on other oils at nanoscale.

Acknowledgements

This study is a part of master science thesis of Tuğba Karayiğit and was financially supported by Afyon Kocatepe University Office of Scientific Research Projects (Project ID: AKU-BAP-17.Fen.Bil.03).

References

AOCS, (1990). American Oil Chemists' Society Champaign, 4th ed vol.1. American Oil Chemists' Society, Champaign, IL.

Aluyor EO, Aluyor P, Ozigagu CE, (2009). Effect of refining on the quality and composition of groundnut oil. Afr J Food Sci 3(8):201–205

Duman E, Özcan MM., (2020). The influence of industrial refining stages on the physico-chemical properties, fatty acid composition and sterol contents in hazelnut oil. J Food Sci Technol 57, 2501–2506. https://doi.org/10.1007/s13197-020-04285-w

Ersungur, S, (2008). Investigation of the Effect of Production Method on the Properties of Rapeseed Oil, Master Thesis, Istanbul Technical University, Institute of Science and Technology, İstanbul.

Ferrari, R., A., Schulte, E., Esteves, W., Brühl, L., Mukherjee, K., D., (1996). Am. Oil Chem. Soc. 73: 587-592.

Gomes, T., Caponıo, F., and Delcuratolo, D., (2003). Fate of Oxidized Triglycerides During Refining of Seed Oils, *Journal Agriculture Food Chemistry*, 51: 4647–465. Bari, Italy.

Güler, G., (2009). Comparison of Some Physical and Chemical Properties of Canola (Rape) Oils Produced by Cold Press and Chemical Refining Methods, Master Thesis, Namık Kemal University, Institute of Science and Technology, Tekirdağ. Gürkan, H. Bayraktar, N. B.

Haslak, M., Duman, E., (2021). Effects of Industrıal Refınıng Stages on Corn Oıl's Qualıty And Bıoactıve Components Determıned Usıng Gas Chromatography And Inductıvely Coupled Plasma Atomıc Emıssıon Spectroscopy, Current Engineering Sciences Research. Editör: Dilek Kavak, Livre de Lyon. France.

Kesen, S., Sönmezdağ, A. S. , Kelebek, H. & Selli, S. (2016). Fatty Acids Composition of Crude and Refined Hazelnut Oils. Çukurova J. Agric. Food Sci., 31 (1) , 79-84 .

Kreps, F., Vrbikova, L., and Schmidt, S., (2014). Influence of Industrial Physical Refining On Tocopherol, Chlorophyll and Beta-Carotene Content in Sunflower and Rapeseed Oil, Eur. *J. Lipid Sci. Technol.*,116: 1572–1582.

Lacombe, S., and Berville, A., (2001). A Dominant Mutation For High Oleic Acid Content Ġn Sunflower (Helianthus Annuus L.) Seed Oil Ġs Genetically Linked To A Single Oleate-Desaturase RFLP Locus, Molecular Breeding 8: 129–137, Netherlands

Özcan, MM, Duman, E, Duman, S., (2021). Influence of refining stages on the physicochemical properties and phytochemicals of canola oil. J Food Process Preserv. 45:e15164. https://doi.org/10.1111/jfpp.15164

Pestana, V. R., Zambiazi, R. C., Mendonça, C. R. B., Bruscatto, M. H., Lerma-Garcia, M. J., and Ramis-Ramos, G., (2008). Quality Changes and Tocopherols and c-Orizanol Concentrations in Rice Bran Oil During the Refining Process, J Am Oil Chem Soc,85: 1013–1019, Doi: 10.1007/s11746-008-1300-4.

Skujins, J., (1998). A short Guide to Vista Series ICP-AES Operation. Switzerland.

SPSS for Windows, version 22. https://ibm-spss-statistics base. en.uptodown.com/windows Accessed at: 20.08.2018.

Tanacı H, (2013). Sterol Analysis in Vegetable Oils with GC-FID, GC Application Note, Istanbul.

Vilvert, E., Lana, M., Zander, P., and Sieber, S., (2018). Multi-Model Approach For Assessing The Sunflower Food Value Chain In Tanzania, Agricultural Systems, 159: 103-110.

Yemişçioğlu, F., Özdikicierler, O., (2013). Saygın Gümüşkesen, A., Sönmez, A.E., 2013. Bitkisel yağ rafinasyon artıklarının değerlendirilmesi. Gıda 38 (6): 367-374.

CHAPTER VII

IN THE DEFENSE INDUSTRY, COVID-19 Risk Assessment USING THE FINE-KINNEY METHOD

Zehra Gülten YALÇIN[1] & Sakine KIRATLI[2] & Mustafa DAĞ[3]
[1](Asst. Prof. Dr.) , Çankırı Karatekin University, Faculty of Engineering
Department of Chemical Engineering, zaltin@karatekin.edu.tr
ORCID:0000-0001-5460-289X
[2](Asst. Prof. Dr.), Çankırı Karatekin University, Faculty of Engineering
Department of Mechanical Engineering, skiratli@karatekin.edu.tr
ORCID: 0000-0001-6292-5605
[3](Dr.), Çankırı Karatekin University, Faculty of Engineering
Department of Chemical Engineering, mudag@karatekin.edu.tr
ORCID:0000-0001-9540-3475

1. Introduction

The area where the production of all kinds of military vehicles, equipment, machinery, weapons, equipment and materials needed in manufacturing is known as the defense industry (Tang, 2006). In this industry which has such a wide range, the features sought in materials stand out as product variety and functionality.

The countries have to keep strong the defense industry to ensure security. The United States is one of the world's countries with a developed defense industry. Turkey is a candidate for a significant role due to its forward-thinking investments and developments in the defense industry (Saraçöz, 2018). The defense industry is one of our country's most important strategic sectors. The development of this sector depends on the continuity of domestic defense projects (Performance Report, 2020).

The COVID-19 pandemic, which began in late 2019, has also had an impact on the defense and aerospace industries. The effects of the pandemic on Turkey's defense and aerospace industries have been studied. The effects of the current pandemic period on the defense and aviation industries were evaluated by Projects, Supply, Finance, Logistics, Labor (health-working environment, etc.) and Legal Legislation (incentive, exemption, force majeure, customs duties, etc.) in a study performed by analyzing the ideas and feedbacks of SASAD (Defense and Aviation Industry Manufacturers Association) (Performance Report, 2020). According to this report, the pandemic process has created a risk for the defense and aviation industries in these areas.

A facility within the scope of a hazardous workplace where equipment production supporting the Turkish defense industry is made has been investigated in this study. The studies were carried out inside the scope of the present Covid-19 process in the examined facility in order to minimize or completely eliminate biological risks. The Fine-Kinney method was used in the risk analysis study.

2. Historical process of Turkish Defense Industry

The current defense and aviation power of the state should always be sufficient. In any attack, it is important to have an industry that meets all the strategic requirements and keeps up with the technological development. For this reason, it is imperative to go head-to-head with other industrial sectors. The Turkish defense industry has its roots in the increase of the Ottoman Empire. It is possible to argue that the cannons poured in Istanbul, particularly during land wars with large sieges, constituted the most developed fighting capabilities of the time. Our weapon technology, which had a strong position in land wars until the 17th century, has remained outside of European technological advances since the 18th century. Industrialization was adopted as a state policy in the early years of the Republic, and the defense industry was accepted as a component of total industrialization and development. The constraints that Turkey was exposed to as a result of the Cyprus crisis have reaffirmed the importance and urgency of a national defense industry. This period can be viewed as

a duration where the state made efforts to establish a national defense industry (Şahbaz, 2007).

A development is not possible for the defense industry of the country which has an underdeveloped industry. The economic importance of the defense industry is an inevitable fact (Gülsoy, 2020).

Industrialization was implemented as a state policy in the beginning of the Republic. It is expected that the defense industry will grow alongside other industrial sectors (Gümüşdaş, 2010).

3. Law No. 6331 on Occupational Health and Safety

The Occupational Health & Safety Law No. 6331 went into effect on June 30, 2012, after becoming reported in the Official Gazette No. 28339. Previously, regulations on the concept of Occupational Health & Safety were included in the 5th part of the Work Law No. 4857 in items 77-89, the Social Security and General Medical Insurance Law No. 5510, and the appropriate parts of the Law of Obligations No. 818, as well as secondary legislation derived from these laws. Prior to this, Law No. 6331 went into effect due to deficiencies in some regulations that protect employees in a way of occupational health and safety inside the scope of Labor Law No. 4857. Occupational Health & Safety Law No. 6331, which was accepted by the Parliament and entered into force on 03.04.2012, is the first and only impartial law made in order to address the principle of "protection of health and safety" of all workers, with certain exceptions (Eravcı, 2019).

3.1. Benefits of Law No. 6331

Occupational Health & Safety Law No. 6331 had been planned in accordance with national and international legislation. Accordingly, the general obligations of the employer are mentioned in item 4. Employer;

a) It works for the prevention of occupational risks, taking all kinds of precautions including training and information, organizing the organization, providing the necessary tools and equipment, adapting health

and safety measures to changing conditions and improving the current situation.

b) It monitors and inspects the workplace to ensure that occupational health and safety measures are followed and that nonconformities are eliminated.

c) It makes a risk assessment or has someone else do it.

d) When assigning a task to the employee, it considers the employee's suitability for the job in relation to health & safety.

e) It takes necessary measures to prevent from entering life-threatening places employees other than those who have been given sufficient information and instructions.

Within the scope of this law, the employer is required to provide a healthy and safe working environment for its employees. If it is not an Occupational Safety Specialist and there is no employee with a specialist certificate in the workplace, it can purchase outsourcing services. In all cases, the employer is responsible for this law and its consequences.

In addition, the employer does not charge employees for Occupational Health and Safety services (Eravcı, 2019).

3.2. Risk assessment

The concept of risk assessment was implemented during the first period in Turkey with the Labor Law No. 4857 and the requirements imposed in response to it. Although the proactive approach of the European Union in the field of Occupational Health and Safety was transferred to the law numbered 4857, it was not successful. This shortcoming in the workplace has been brought about in accordance with the Occupational Health & Safety Law No. 6331 and the applicable requirements, the 89/391/EEC Framework Directive and the contract items of the ILO No. 161 on Health Services. In the 3rd element of the Occupational Health & Safety Law No. 6331, the definition of risk assessment has been made. According to this item, it is defined as "the work that needs to be done in order to identify the dangers that exist in the workplace or that may come from outside, the reasons that influence these dangers to become risks, as well as the analysis and rating of the risks

posed by the hazards, and the selection of control measures" (Eravcı, 2019).

There are things that the employer is obliged to do to ensure that its employees work in an environment that is both healthy and safe., regardless of the hazard class. These are briefly;

a) Avoiding risks,
b) Analyzing the risks that are unavoidable,
c) To combat with risks at their source,
d) Paying attention to workplace design and the selection of work equipment, work habits, and manufacturing processes in making the work appropriate for people, to avoid any negative effects of uniform working and production tempo on health and safety, and to reduce them if they cannot be avoided,
e) To adapt to technical developments,
f) Replacing the dangerous with the non-hazardous or less dangerous,
g) Creating a unified and comprehensive prevention strategy that addresses the effects of factors such as technology, organization of work, conditions of employment, social connections, and the workplace culture.
h) Giving priority to collective protection measures over personal protection measures,
i) Giving appropriate instructions to employees, must carry out protective/preventive activities in accordance with such principles (Eravcı, 2019).

3.2.1. Definitions used in the risk assessment study

Hazard: It refers to the potential for harm or damage that exists in the workplace or may come from outside, which may affect the employee or the workplace.

Risk: The probability of loss, injury, or other harmful outcome resulting from the hazard (combination of probability and severity).

Accident: It is an event that occurs upon contact with danger and causes physical and mental malfunctions to employees or those directly or indirectly related to the enterprise.

Near miss incident: The occurring in the workplace, it refers to an event that does not cause harm although it has the potential to damage the employee, workplace or work equipment.

Incident: The work-related events with the potential to cause injury, deterioration of health or death. "Non-Damage Incident - Near Miss" refers to activities that happen without causing damage, worsening of wellness or dying.

Risk assessment: It refers to the analyses that must be conducted in order to determine the hazards that exist in the workplace or that may come from outside, the factors that lead these dangers to become risks, and the analysis and grading of the risks resulting from the dangers, as well as the decision on control measures (Occupational Health &Safety Regulation, 2012).

Acceptable risk: It is the level of risk that will not cause loss or injury, in accordance with legal obligations and the workplace's prevention policy.

Prevention: It encompasses all actions involved or affected to remove or minimize occupational health & safety risks at all stages of work performed in the workplace.

Risk Management: It is all of the initiatives carried out to provide, enhance and sustain the health and safety conditions of an organization (Serin & Çuhadar, 2015, p.44-59).

3.2.2. Risk assessment team and those responsible

The risk evaluation is performed by an employer-formed team. The team performing the risk assessment consists, as a minimum, of the following:

- Employer or employer's representative,
- Occupational safety experts and occupational doctors who provide workplace health and safety services,
- Employee representatives at work,
- Support staff in the workplace.

The employer meets all the necessary needs such as tools, equipment, space and time for the persons assigned in risk assessment studies to fulfill their duties. They cannot restrict their rights and powers due to the execution of their duties.

• Employees who are decided to show all parts in the workplace and are knowledgeable about the work performed in the workplace, as well as current or potential sources of danger and risk.

Employer/Employer's Attorney: It conducts an occupational health and safety risk assessment with the goal of ensuring, maintaining, and improving the health and safety of the working environment and employees.

Occupational Safety Specialist: Engineers, architects or technical personnel who have been approved by the Ministry to work in the area of occupational health and safety and have occupational safety expertise and who participate in risk analysis studies.

Occupational Physician: They have a workplace doctor certificate and are approved by the Ministry to work in the area of occupational health and safety. They also take part in risk analysis studies.

Employee representative: An employee elected unanimously or by appointment among the employees authorized to participate in the work in relation to occupational health & safety, to monitor the work, to request measures, to make proposals and to represent the employees. These people participate in risk analysis studies.

All Managers: Ensures that the control measures proposed resulting from the risk evaluation are implemented according to the activity plan and provides for the purchase of new products, projects, processes, machinery, etc. In cases and when it deems necessary, the employer requests the risk assessment process to be carried out or repeated.

Support staff: It refers to the person who, additionally his primary duty, has been specially assigned in the fields of prevention, defense, evacuation, fire fighting, first help, and related issues related to occupational health and safety. It participates in risk analysis studies (Serin & Çuhadar, 2015, pp. 44-59).

3.2.2.1. Fine-Kinney risk analysis method

The Fine-Kinney risk analysis method is a frequently used risk method. This method shows that each part of the workplace should be given importance when classifying risks. Three parameters are used in this risk assessment method. These three parameters are multiplied to

obtain the risk level, and the risks are graded. Corrective and preventive actions are recommended according to the degree of risk (Özkılıç, 2005). Risk scores are calculated by scoring and multiplying the probability of harm or damage, the frequency of exposure to the danger, and the impact it will create even if the danger occurs. Table 1 shows the values that should be assigned to these variables. The risk score is calculated using the values in Table 2 and the results calculated are the results of the risk evaluation based on the risk values in Table 3. Table 4 contains the data in which the numerical value of the risk is interpreted.

Table 1. Fine Kinney Method Intensity Values (Şimşek, 2020).

Intensity Value	Meaning
1	To be considered (insignificant, harmless or mild)
3	Important (minor damage, low loss of business, first aid may be required)
7	Serious (Lack of work, external treatment, significant damage)
15	Very serious (environmental impact, loss of limb, disability)
40	Very bad (severe environmental impact, total disability, death)
100	Disaster (Significant environmental disaster, multiple deaths)

Risk value= İ x F x D
İ: Possibility (0.2-10)
F: Frequency (0.5-10)
D: Severity

Table 2. Fine Kinney Method Frequency Values (Yalçın et al., 2018).

Intensity Value	Meaning
0,5	Very uncommon (less than once a year)
1	Extremely uncommon (once or a few times a year)
2	Unusual (once or several times a month)
3	Infrequently (once or several times a week)
6	Regularly (once or several times a day)
10	Continuous (continuous or multiple times per hour)

Table 3. Fine Kinney Method Probability Values (Yalçın et al., 2018).

Probability Value	Meaning
0,2	Practically meaningless
0,5	Weak probability
1	Pretty low probability
3	Rare but can happen
6	Strongly probable
10	Very strong probability
0,2	Practically meaningless

Table 4. Fine Kinney Method Risk Assessment Result (Yalçın et al., 2018).

Risk Value Meaning	Meaning
R<20	Acceptable risk (may not require immediate action)
20<R<70	Definite risk (must be included in action plan)
70<R<200	Significant risk (should be included and noted in the plan of action for the year)
200<R<400	High danger (It should be part of the short-term plan of action)
R>400	Extremely high (precautions should be taken by interrupting work immediately)

3.2.2.2. The Covid-19 pandemic and its consequences for the defense industry

Covid-19 (coronavirus pandemic), which has distributed rapidly throughout the world, first appeared in Wuhan, China. Although the reason is not known exactly, it has affected all life in China. Later it was seen in Thailand, South Korea, Iran and all over Europe. In Turkey, it emerged as of March 2020 and has caused problems in the health sector around the world, as well as in our own country.

The high number of cases and deaths, which emerged rapidly as a result of the spread speed and power of the COVID-19 virus (the ability to live for an extended period of time without being attached to a living organism), first caused partial limitations in economic and social life; Then came the limitations that have never been seen in human history. At this stage of the epidemic, all workplaces with the risk of not maintaining physical contact and social distance between people had to pause or stop their activities (Balcı et al., 2020).

The Covid-19 pandemic has had a negative impact on both the global and Turkish economies. In this process, it is seen that restrictions on tourism, food, entertainment and education sectors have emerged. The impact on exports of the Covid-19 process in Turkey was not seen at first and it was felt quite a lot in the later period. In our country, exports fell in July and August of the third period comparison to the prior year, but they began to rise in the fourth period. In our country, exports were 18 billion dollars in April 2021 and 16 billion dollars in May (İzgi, 2021).

The primary sectors affected by the Covid-19 process in the world are agriculture, petroleum products, the secondary sectors are the production industry and the tertiary sectors are education, finance, hotel management, health, medicine, food, aviation, real estate, housing, sports industry, information technology, media and research and development (Nicola et al., 2020:185-190).

Approximately 30% of upper respiratory tract infections experienced by people are caused by coronavirus (Budak & Korkmaz, 2020, p. 65). The coronavirus is known to be transferred from animals to humans and via contact. Human-to-human transmission occurs through coughing, sneezing, and close contact while speaking. In addition, the transmission accelerates by touching the surfaces that the sick person comes into contact or by shaking hands, hugging and touching the mouth, nose and eyes of the hands. The complaints seen in people who have caught the coronavirus are given below.

- Fever
- Tremble
- Cough, sore throat
- Respiratory failure, shortness of breath
- Muscle pain
- Diarrhea
- Nausea, vomiting (Görür, 2021).

It is clear from the review of literature that the pandemic did not have a devastating effect in the defense and aviation sector, on the contrary, it gained momentum after May (İzgi, 2021).

In this study, a company that produces machinery and equipment for the defense and aerospace industry, which is considered a dangerous workplace according to the Nace code, is discussed. During the Covid-19 pandemic process, a study was conducted for this company to minimize or remove biological risk factors in the workplace with the Fine-Kinney risk assessment method.

In the risk assessment, first of all, the hazard that creates a risk is determined, and the risks that these hazards will cause are created. In the risk analysis study, it is determined which of the current risks will be given priority. Control measures are taken in order of risk priority.

Fine Kinney risk analysis method was used in this study. The method was first used in 1971 and it is a method widely used in Europe in the field of Occupational Health and Safety. It has been used in Turkey as of 2012, with the law no. 6331. This method is frequently used especially in cement, construction and heavy industry (Birgören, 2017).

3.3 Literature Review

As a result of the literature research, it is seen that the Fine-Kinney method is used in studies because it is more preferred among other risk analysis methods. It is known that studies show a more careful approach in the determination of possible risk due to the separate evaluation of probability, severity and frequency parameters.

(Yiğit, 2015) determined that a wide-scale evaluation can be made in the risk study he conducted using the Fine-Kinney method.

(Erzurumluoğlu et al., 2015), on the other hand, conducted a risk analysis study using the Fine-Kinney method in the construction sector, which is classified as a dangerous workplace, and minimized the risks.

(Okumuş et al., 2016) examined the occupational accidents in the shipbuilding industry and compared the risk analysis with two methods. These risk methods are the 5x5 Matrix and Fine-Kinney method, and they emphasized that the Fine-Kinney method creates a sensitive and deeper examination in the study.

Based on these studies, it was seen that the Fine-Kinney method would be effective in in-depth risk determination and was preferred in this study.

4. Conclusion

In the company where the risk analysis was made, the workplace was evaluated in sections and the situations that would pose a risk were determined by photographing. Existing risks and hazards within the legal framework were determined by responsible persons who would conduct risk analysis, and efforts were made to eliminate these hazards.

The measures to be taken are handled according to the size of the existing risk values. Coloring was done on the risk analysis evaluation table in order of importance in order to eliminate the risks. Considering the current situation, the risks are listed in order of importance from the biggest to the tiniest. The risks that were determined above the acceptable risk level were reduced to the acceptable risk level after the employer took precautions.

Appendix 1 shows the Covid-19 influenza risk assessment study conducted in the company. In the company, in the general workplace area, in the scope of activity, in the work areas and social facilities, the current biological risk, Covid-19, is considered as a hazard. Damage and death caused by the danger of Covid-19 are seen as risks. First of all, employee screening, which poses a risk among employees, was made every now and then. In order to avoid this situation, an emergency plan regarding biological risks has been prepared. In addition, the work of special risk groups allowed by the state during the pandemic process has been stopped until a second decision. There are personnel with first aid certificates in the workplace. Necessary trainings were given to the cleaning staff in charge of cleaning the working environment periodically. Fourteen rule booklets were prepared and given to the employees and the necessary warnings were posted on the boards. Information meetings were held by the workplace doctor about what the symptoms of Coronavirus are. Disinfectants in the workplace are placed in visible places in the working environment of the employees.

Soap and disinfectant use was ensured in the research and development laboratories at the workplace. In addition, masks were distributed to the employees. Employees were warned that masks should only be purchased from pharmacies. It has been stated that people who have

caught the coronavirus should inform the workplace, avoid close contact, and comply with social distance rules.

As a result of the Fine-Kinney risk assessment, it was stated in the decision deadline plan with a risk level of R> 400 that the measures to be taken within 15-30 days, which included high risk, were stated. These measures are intended to measure the temperature at the workplace's inlets and outlets. It can be seen that the employees' use of gloves and masks has been tightened. Frequent use of disinfectants was reminded. Furthermore, social distance rules are enforced in places such as the cafeteria and dressing room. With these measures, the current risk value has been reduced to between 70 < R < 2.

Another precaution taken is that those with chronic diseases, pregnant workers and employees over the age of sixty-five were asked to work from home, if possible.

As a precaution, routine cleaning of surfaces and machinery is provided. Employees were asked to comply with personal hygiene rules. By reducing the crowded working environment as much as possible, the current risk value has been reduced.

With these measures, the current high risk value has been reduced below 100. In this case, the work still continues with the current measures.

References

Balcı, Y. & *Çetin*, G. (2020). COVID-19 The effects of the pandemic process on employment in Turkey and the measures that should be taken from the point of view of the public, *Istanbul Trade University Journal of Social Sciences, 19* (37), 40-58.

Birgören, B. (2017). Calculation challenges and solution suggestions for risk factors in the risk analysis method in the Fine Kinney risk analysis method, *International Journal of Engineering Research and Development*, *9* (1), 19-25. doi.org/10.29137/umagd.346168

Boz-Eravcı, D. (2019). Obligations of the employer within the framework of the Occupational Health and Safety Law No. 6331 and related regulations. *HAK-IŞ International Journal of Labor and Society*, *8* (22), 330-355.

Budak, F. & Korkmaz, Ş. (2020). A general assessment of the COVID-19 pandemic process: the case of Turkey, *Journal of Social Research and Management,* 1, 62-79. doi.org/10.35375/sayod.738657

Erzurumluoğlu, K., Köksal, K., & Gereki, İH. (2015). Conducting a risk analysis in the construction industry using the Fine-Kinney method. 5. Occupational Health and Safety Symposium, İzmir.

Görür, N. (2021). Coronavirus (COVID-19) pandemic, the University of the eating habits of the impact of food safety knowledge and practices with students and academics, Master Thesis, Hacettepe University Institute of Sciences, Department of Food Safety, Mus.

Gul, M., Guven, Busra. & Guneri, AF. (2018). A new Fine-Kinney-based risk assessment framework using FVIKOR incorporation, *Journal of Loss Prevention in the Process Industries*, 53, 3-16.

Gul, M., Mete, S., Serin, F. & Celik, E. (2021). Fine-Kinney-based fuzzy multi-criteria occupational risk assessment: Approaches, case studies and python applications. Springer, New York.

Gümüşdaş, E. (2010). The place of defense industry and defense expenditures in the economy in Turkey, Master's Thesis, Niğde University Institute of Social Sciences, Department of Economics, Niğde.

İzgi, F. (2021). The effect of COVID-19 process on Konya exports, *Journal of Science-Technology-Innovation Ecosystem*, 2 (1), 31-43.

Occupational Health and Safety Regulation, Official Gazette Date: 29.12.2012, Resmî Gazete Sayısı: 28512.

Okumuş, D. & Barlas, B. (2016). An applied comparison of the 5x5 analysis matrix and Fine-Kinney methods in the shipbuilding industry, *GMO*, 204-205, 95-106.

Özkılıç, Ö. (2005). Occupational Health and Safety Management Systems and Risk Assessment Methodologies, Ankara, *Tisk Publications,* 7-14.

Performance Report, Defense and Aerospace Industry Manufacturers Association, 2020, www.sasad.org.tr

Şahbaz, F. (2007). The impact of the defense industry on foreign policy and the example of Turkey, Master's Thesis, Gazi University Institute of Social Sciences Department of International Relations, Ankara. Tang, CS. (2006). Perspectives in supply chain risk management,

International Journal of Production Economics, *103* (2), 451-488. doi. org/10.1016/j.ijpe.2005.12.006

Şimşek, S. (2020). An evaluation of the Fine-Kinney Method, one of the risk assessment methods in the scope of Occupational Health and Safety, with an example, *İSG Academic-OHS Academic,* 2 (2), 91-99.

Yalçın, ZG., Dağ, M. & Aydoğmuş, E. (2018). Risk anaysis by Fine Kinney method in a laboratory, *Journal of Physical Chemistry and Functional Materials (JPCFM)*, 1(1), 54-58.

Yiğit, Ö. (2015). Application of three different risk assessment methods in feed production processes and comparison of methods. (Published Occupational Health and Safety Specialization Thesis). General Directorate of Occupational Health and Safety, Ankara.

Appendix 1. Covid-19 Influenza Risk Analysis Study Using Fine-Kinney Method

Revision date: 02.03.2020			Unit and/or Persons to Take the Measures (Responsible)		Employer / employer's representative / Administrative affairs / Occupational doctor
			Fine-Kinney Method: Decision Plan by Risk Level	Decision	Significant Risk
				Risk Level	70<R<200
			Rating of Risk After Taking Precautions	Risk Value	100
				Effect	100
				Frequency	1
				Possibility	1
PANDEMIC INFLUENZA RISK ASSESSMENT			Measures Taken		Temperature is taken at the entrance and exit of the workplace. Employees are provided with masks and gloves. There are disinfectants in the workplace and they are provided for employees to use. Social distance rules are followed in social facilities such as cafeteria, service, dressing room.
			Precautions to take		Group 4 biological factors: Biological factors that cause severe human diseases, pose a serious danger to workers, have a high risk of spreading to the community, but do not have effective prevention and treatment methods. The employer is obliged to take collective and personal precautions against the dangers that the employees may encounter in the workplace.
			Fine-Kinney Method: Decision and Deadline Plan by Risk Level	Deadline	15-30 days
				Decision	Very High Risk
				Risk Level	R>400
			Grading of risk	Risk Value	10000
				Effect	100
				Frequency	10
				Possibility	10
Company Name/Address: **Publication date:** **Validity date: 02.03.2024**			Current State		There is no GROUP 4 biological risk personnel in the workplace.
			Risk		Illness, Death
			Hazards		GRUP 4 Biological risks
			Activity		WORK AREAS, SOCIAL FACILITIES, TOOLS
			Unit Name		GENERAL WORKPLACE
			Hazard No		1

Employer / employer's representative / Administrative affairs / Occupational doctor	Employer / employer's representative / Administrative affairs / Occupational doctor	Employer / employer's representative / Administrative affairs / Occupational doctor	Employer / employer's representative / Administrative affairs / Occupational doctor
Significant Risk	Significant Risk	Significant Risk	Significant Risk
70<R<200	70<R<200	70<R<200	70<R<200
100	100	100	100
100	100	100	100
1	1	1	1
1	1	1	1
An emergency plan for biological risks has been prepared.	Unit evaluation report has been prepared.	The employment of special risk groups has been stopped until a second decision taken by the state.	The number of employees in areas where intensive work is carried out has been reduced.
1. Covid 19 An emergency plan regarding biological risks should be prepared and emergency teams should be updated. 2. It should be ensured that employee representatives and/or employees are informed about the updated emergency plan and are aware of what they should or should not do within the scope of the plan.	Workplace-specific hazards related to COVID-19 should be identified, risk assessment should be carried out and necessary precautions should be taken.	Those with chronic diseases, pregnant workers, employees over 65 should be allowed to work from home if possible, and if it is not possible, they should not be allowed to work. Employees should be informed.	1. Necessary arrangements should be made in the working areas, taking into account the health conditions first, and giving importance to the conditions of the work, 2. It should be ensured that the number of workers who are or may be exposed to is kept as low as possible.
15-30 days	15-30 days	15-30 days	15-30 days
Very High Risk	Very High Risk	Very High Risk	Very High Risk
R>400	R>400	R>400	R>400
10000	10000	10000	10000
100	100	100	100
10	10	10	10
10	10	10	10
An emergency plan for biological risks has been prepared.	Unit evaluation report has been prepared.	The employment of special risk groups has been stopped until a second decision taken by the state.	The number of employees has been reduced in areas with intensive work.
Illness, Death	Illness, Death	Illness, Death	Illness, Death
Lack of contingency plan regarding biological risks	Lack of risk assessment report on biological risks	Continuation of special risk groups	Not reducing the number of employees in areas with intensive work
WORK AREAS, SOCIAL FACILITIES, TOOLS	WORK AREAS, SOCIAL FACILITIES, TOOLS	WORK AREAS, SOCIAL FACILITIES, TOOLS	WORK AREAS, SOCIAL FACILITIES, TOOLS
GENERAL WORKPLACE	GENERAL WORKPLACE	GENERAL WORKPLACE	GENERAL WORKPLACE
2	3	4	5

Employer / employer's representative / Administrative affairs / Occupational doctor	Employer / employer's representative / Administrative affairs / Occupational doctor	Employer / employer's representative / Administrative affairs / Occupational doctor
Significant Risk	Significant Risk	Significant Risk
70<R<200	70<R<200	70<R<200
100	100	100
100	100	100
1	1	1
1	1	1
There are personnel with first aid certificates in the workplace.	Working environments are cleaned periodically. Employees are warned about this.	Employees were informed about 14 rule booklets. It was informed that disinfectants in the workplace should be used. Employees comply with personal hygiene rules.
First aid personnel; there should be 1 person for every 10 people in the very dangerous class, every 15 people in the dangerous class, and every 20 people in the less dangerous class, and the first aid training should be updated every 3 years.	1. Regular cleaning practices should be maintained, including routine cleaning and disinfection of surfaces, equipment, and other elements of the work environment. 2. Hygiene conditions should be followed in common areas such as work areas, sinks, toilets, bathrooms, stair rails, faucets and dining halls, rest areas, dressing rooms, doors, turnstiles, and keyboards and other devices should be cleaned regularly. As far as possible, workers should be prevented from using other employees' phones, desks, offices or other work tools and equipment, and controls and inspections should be ensured.	1. Employees should be informed about personal hygiene rules, hands should be washed with soap and water for at least 20 seconds after contact and at regular intervals. should be washed. 2. Employees should pay attention to the hygiene of work clothes. Clothes should be washed at least 60 degrees every day, work clothes and protective equipment should be removed before leaving the work area, and they should be informed about ventilation. 3. Effective hand washing training should be given to the employees by the authorized person in the workplaces and their awareness on hygiene should be increased. 4. Within the possibility of keeping the virus on the beard and mustache, it should be ensured that the employees shave frequently, if possible, and the necessary warning should be made regarding the issue. 5. Employees should be warned to pay attention to nail cleaning and to do nail care regularly.
15-30 days	15-30 days	15-30 days
Very High Risk	Very High Risk	Very High Risk
R>400	R>400	R>400
10000	10000	10000
100	100	100
10	10	10
10	10	10
There are personnel with first aid certificates in the workplace.	Working environments are cleaned periodically. Employees are warned about this.	Employees were informed about 14 rule booklets. It was informed that disinfectants in the workplace should be used. Employees comply with personal hygiene rules.
Illness, Death	Illness, Death	Illness, Death
Lack of personnel with first aid certificate in the workplace	Lack of hygiene in the working environment	Lack of personal hygiene in employees
WORK AREAS, SOCIAL FACILITIES, TOOLS	WORK AREAS, SOCIAL FACILITIES, TOOLS	WORK AREAS, SOCIAL FACILITIES, TOOLS
GENERAL WORKPLACE	GENERAL WORKPLACE	GENERAL WORKPLACE
6	7	8

Employer / employer's representative / Administrative affairs / Occupational doctor	
Significant Risk	Significant Risk
70<R<200	70<R<200
100	100
100	100
1	1
1	1
Occupational doctor is interested in the subject.	All employees were informed about the symptoms of the coronavirus.
Employees should be informed about hygiene, banners/posters/instructions containing etiquette in case of coughing and sneezing and explaining the importance of hand hygiene should be hung at the entrance of the workplace and other areas where everyone can see it.	Information should be given about the symptoms caused by the coronavirus, posters/posters etc. should be hung in other areas where everyone can see it.
15-30 days	15-30 days
Very High Risk	Very High Risk
R>400	R>400
10000	10000
100	100
10	10
10	10
Occupational physician is interested in the subject.	All employees were informed about the symptoms of the coronavirus.
Illness, Death	Illness, Death
Lack of basic hygiene knowledge	Lack of knowledge about the symptoms caused by the coronavirus
WORK AREAS, SOCIAL FACILITIES, TOOLS	WORK AREAS, SOCIAL FACILITIES, TOOLS
GENERAL WORKPLACE	GENERAL WORKPLACE
9	10

CHAPTER VIII

ENDOCRINE DISRUPTOR POLLUTION IN AQUATIC ENVIRONMENT

Ayşe Kurt
(Inst. Dr.) Bursa Uludag University, Science and Technology Application and Research Center (BİTUAM), Bursa, Turkey;
E-posta: kurtayse1987@gmail.com
ORCID:

1. Introduction

Industry, population and agricultural sectors are in a great competition in terms of water use in worldwide. While industrial investments need water, they also seriously threaten the water quality in regions with rich groundwater potential. Considering that Turkey and most of the countries suffers from water scarcity, water use and management are of great importance (Turan, 2018; Yannopoulos, Giannopoulou, & Kaiafa-Saropoulou, 2019). Increasing global warming and drought threats in recent years lead to a significant decrease in potable water resources, which are limited, as well as a decrease in the quality of existing surface/groundwater resources (Lipczynska-Kochany, 2018; Trnka et al., 2019).

The source, transport pathway and type of pollution discharged into the aquatic system are needed to be known for identifying preventive and mitigation strategies (Schmaltz et al., 2020). After passing of domestic wastewaters through the sewer catchment, the emerging wastes are collected and categorized as human waste, kitchen waste, large-sized plastics, etc. and recycled by treatment plants (Sreelakhmi & Chitra, 2021). Manufacturing industries, that emit heavy pollution emissions are also located in/or near the urban areas thus, dangerous pollutants are easily transported in

water and some of them contaminate even our drinking water sources with urban runoff, storm water overflows and failure of authorities to control wastewater discharges well, etc. (Abdalla & Khalil, 2018). Pollution load, location and type can be traced against human and industrial behaviours, it is realistic and proposed to collect and analyse the water samples from different points (source of pollution, various environmental water matrices etc.) at regular periods by the authorities and researchers.

However, endocrine disruptor compounds (EDCs) are the matters of concern in aquatic ecosystems (Wee, Aris, Yusoff, & Praveena, 2020). Mostly detected endocrine disruptor types in aquatic environment are hormones, surfactants, microplastics, disinfectants, pesticides and heavy metals (Pironti et al., 2021). There are various ways of distribution of endocrine disruptors in receiving environment through urban water systems (Bedoya-Ríos et al., 2018). Medical drugs, hormones and personal care products which are used in homes and hospitals reach to the sewage systems by the excretion of them with the feces and urinary tract in unchanged forms or metabolites after taken into the body. Then, they are discharged into the wastewater treatment facilities through sewage systems. In addition, they could also be disposed of directly into the garbage without ever using. These medicines which were disposed of into the garbage may be mixed with leachate and dispersed into the aquatic system. Another endocrine disruptor sources are pesticides which are used for agricultural purposes commonly. These products can seep into the soil and contaminate groundwater (Chaturvedi et al., 2021). Also, endocrine disruptor micro-contaminants originating from industries are discharged into the sewage systems and reach to the wastewater treatment plants. These endocrine disruptor pollutants, which cannot be completely removed/destroyed in wastewater treatment plants are discharged to the receiving environment and reach to rivers, lakes, and seas and thus, they cause to pollution in water resources even in groundwaters and drinking waters (Kim & Zoh, 2016).

2. Endocrine Disruptors

Endocrine disruptor chemicals are the substances that disrupt the natural functioning of endocrine systems by changing/mimicking the effects

of hormones and preventing their movements, when they enter the body of living organisms (Rodgers-Gray et al., 2000; Varjani & Sudha, 2020). Endocrine disrupting chemicals are mainly consist of birth control pills, steroids, industrial chemicals, pesticides (dichlorodiphenyl trichloroethane, dieldrin, lindane, atrazine), surfactants, phthalate acid esters, polyaromatic hydrocarbons (PAHs), polychlorinated dioxins (solid waste storage incineration systems) that consists of substances such as biphenyls. It has been stated that estrogenic endocrine disruptors cause to hermaphroditism highly and thus, they are the most important species of endocrine disrupting chemicals (Tran et al., 2019). When the studies were examined, researchers have found that endocrine disrupting chemicals may cause eye diseases, respiratory system diseases, gastrointestinal system diseases, liver and kidney damages as well as central nervous system diseases by affecting the nervous system. One of the negative effects of EDCs is that they act as estrogen (Mueller & Korach, 2001; Shanle & Xu, 2011). For example, Diethylstilbestrol (DES), which is one of the most important synthetic estrogen endocrine disrupting compounds was widely used during the 20th century, until it was banned worldwide due to the complications of it in female genitals, especially cervix, vagina and uterus (Bibbo et al., 1977; Herbst, Ulfelder, & Poskanzer, 1971; Zamora-León, 2021).

2.1. Legislations On Endocrine Disruptor Compounds

Unfortunately, there are no discharge standards in legislations for these endocrine disruptor micro-pollutants in wastewater treatment plants. Because that, the majority of currently operated wastewater treatment plants are operated up to tertiary treatment and this treatment systems can not be able to remove micro-contaminants fully. In addition, since the treatment of micro-pollutants varies according to their types, all of the treatment systems cannot achieve the same efficiency. Although, there is no globally accepted legislations, Switzerland has prepared a regulation as example for micropollutant removal and has decided to make a quaternary treatment step for 100 wastewater treatment plants in accordance

with their own laws. At a meeting held by the European Commission for the removal of micropollutants from wastewaters at IFAT (2018), the commission stated that it is necessary to make an additional treatment - a quaternary step - for wastewater treatment plants, but financially it is impossible to build and operate such a system in all facilities (IFAT, 2018). The European Union legislation includes the quality criteria that must be fulfilled for the receiving environment within the scope of the Water Framework Directive (2000/60/EC) and Environmental Quality Standards (2008/105/EC) (Directives, 2008; EC, 2000; Jurado, Walther, & Díaz-Cruz, 2019). The water framework directive aims to publish the standards for eceiving environment for priority substances and specific pollutants. In this context, the EU Watch has prepared a list (2015/495/EU) for specific pollutants and priority substances (EU, 2015). The last added endocrine disruptor micropollutants to the EU Watch List are non-steroidal anti-inflammatory drugs (diclofenac), macrolide antibiotics (azithromycin, clarithromycin and erythromycin), synthetic hormones (17α-ethinylestradiol (EE2)) and natural hormones (estrone (E1) and 17ß-estradiol). Furthermore, some pesticides (methiocarb, oxadiazon, imidacloprid, thiacloprid, thiamethoxam, clothianidin, acetamiprid, and triallate), 2-ethylhexyl-4-methoxycinnamate, and an antioxidant commonly used as a food additive; 2,6-di-tert-butyl-4-methylphenol were included into the list (Souza et al., 2017). The World Health Organization (WHO) published a guideline on pharmaceuticals found in drinking water (WHO/HSE/WSH/11.05) (WHO, 2011). In Turkey, the Surface Water Quality Regulation (RG:28483,30.11.12) and the Regulation on the Monitoring of Surface and Groundwater (RG:28910,11.02.2014) with the water quality and classification parts of the EU legislation are largely transferred into the legislations within the scope of the Water Framework Directive.

2.2. Hormones

Hormone residues can be found to a large extent in wastewaters, groundwaters and drinking water sources like many other micropollutants (Baronti et al., 2000; Luo et al., 2014) and are well-known endocrine

disrupting chemicals (EDCs) (Jarošová, Bláha, Giesy, & Hilscherová, 2014). Various treatment strategies such as adsorption, enhanced oxidation, photo-catalytic degradation, biodegradation and membrane separation such as nanofiltration or reverse osmosis have been adopted to remove these micro-contaminants (Hatt, Germain, & Judd, 2013; Nghiem, Schäfer, & Elimelech, 2004; Ohko et al., 2002; Onesios, Jim, & Bouwer, 2009).

In aquatic environments, estrogen E2 (B.-H. Zhao et al., 2020) and estrone predominate in estrogenic activity (Vélez et al., 2019). Estrone and E2 hormones have been detected in surface waters in many countries such as Austria, the United States, Brazil and China (Benotti et al., 2009; Hohenblum, Gans, Moche, Scharf, & Lorbeer, 2004; Torres et al., 2017). Liz et al. (2017), detected E2, estrone and E3 hormones in water samples in Paraná, Brazil, which are the increasing concentrations of metabolites such as precursor molecules (EE2, mestranol and diethylstilbestrol) caused by inadequate disposal of expired drugs from pharmaceutical industries, households and hospital wastes (Liz, Amaral, Stets, Nagata, & Peralta-Zamora, 2017). A very few studies in literature reported detectable concentrations of hormone/natural estrogen, or EE2, in treated waters from drinking water treatment plants (DWTP), unlike spring/surface waters. Metcalfe et al. (2014) reported concentrations of E1 (1.5 ng L^{-1}) in treated water samples from Ontario DWTP (Metcalfe et al., 2014). Kuch and Ballschmiter (2001) also reported detections of E1 with E2 and EE2 in German tap water, from groundwater wells unlike DWTP's, where these samples were taken from (Kuch & Ballschmiter, 2001).

2.3. Antibiotics

Antibiotic compounds are found among the endocrine disrupting compounds, which are considered to be one of the most dangerous types of pollutants in terms of microorganism resistance create in environment and have a widespread use in Turkey and worldwide. Antibiotics are widely used for the protection and treatment of human and animal health and improvement of agricultural processes at high rates without

control (Oberlé, Capdeville, Berthe, Budzinski, & Petit, 2012). According to IMS (International Medical Statistics) (2014) data, it was obtained that cephalosporins, penicillins and quinolones are the antibiotic groups that are at the top of list for their consumption in Turkey (IMS, 2014).

Antibiotics are the drugs which are most used all over the world. Approximately, 35% of the health budgets of developing countries are spent on antibiotics. In some countries, antibiotics can be sold in pharmacies or even in markets without a prescription (Topal, Şenel, Topal, & Erdal, 2015). After the antibiotics are taken into the human body, some of them are used by the metabolism, while the unused part is excreted through the urine (Kolpin et al., 2002; Kümmerer, 2001). In this way, they can reach to the sewage system and to the wastewater treatment plants from there. However, they can reach even to the drinking waters, if they are not biodegradable or can not be removed well in wastewater treatment plants. In addition to the hospitals and homes, where antibiotics are used in and then, they are thrown directly into the sewage systems from there, garbages are also the main sources of antibiotic pollution in receiving environment (Holm, Ruegge, Bjerg, & Christensen, 1995). Thus, it is important to detect and remove antibiotics from water. Today, unfortunately, conventional wastewater treatment plants are inadequate in terms of removal of antibiotics, which are widely used in Turkey and Northern European countries (Heberer, 2002; Kümmerer, 2001; Ternes, 1998).

Due to the limited treatment rates of wastewater treatment plants, large amounts of antibiotics are transferred from wastewater to surface waters, groundwater and even drinking water (Jurado et al., 2019; Sharma et al., 2019). However, the presence of antibiotics in groundwater has recently attracted great attention around the world. A US national expedition of pharmaceuticals and other organic pollutants in water supplies reported the presence of antibiotics in a sampling network of 47 groundwater sites with a detection frequency of more than 30% (Barnes et al., 2008). Fick et al. (2009) investigated surface water, groundwater, and drinking water thought to be contaminated with antibiotics and other drugs in an area where the mass-pharmaceutical industry has developed, and found high levels of antibiotics, including ciprofloxacin, enfloxacin, ofloxacin, and trimethoprim, in well water samples (Fick et al., 2009).

2.4. Pesticides

The circulation of pesticides in the environment has a versatile and complex structure. The circulation of pesticides in the environment is a versatile and complex situation. The atmosphere, soil and water environment are the three most important factors in transportation mechanisms of them and this is an exact reason that, why pesticides are the most important contaminants for the environment (Teonian Meriç, 2004). International Environmental Protection Agency (EPA) (2002) stated that, pesticides could be used to prevent formation of insects, pests, rodents, weeds, fungi, bacteria and viruses and thus, to develop agricultural processes and they defined pesticides as any substance or mixture of substances used to prevent, mitigate, destroy or keep the negative effects of living organisms under control (DSİ, 2018; EPA, 2007). The long-term activity of pesticides in the environment, their tendencies to bioaccumulation and their effects on non-target species pose a great danger to health and ecosystem. Pesticide pollution occurs in groundwater and surface water sources, with drainage from the soil and transport from agricultural lands. Pesticide contamination into surface waters occurs through mixing of rain and irrigation waters in surface waters by washing of terrestrial surface and the lower layers of soil. Pesticide particles in the atmosphere descend into the surface waters with gravitation and/or rain, and direct application to water in order to eliminate some unwanted plant species in aquatic environment. Pesticide contamination to the groundwater may occur as a result of vertical downward movement of pesticide on the soil surface with the effect of rain or irrigation water (Özkan et al., 2007).

Hintze et al. (2020) investigated the effect of surface water-groundwater interactions on the spatial distribution of pesticide metabolites in groundwater, and found that in areas affected by a river from a mountainous region, metabolite concentrations were low (median values ≤ 0.50 μg L^{-1} for desphenyl-chloridazone - DPC, ≤0.19 μg L^{-1} for methyl-desphenyl-chloridazone - MDPC). Conversely, high concentrations have been observed in areas dominated by farmland recharge and/or affected by a stream from a intensively farmed watershed (median values up to 1.9 μg L^{-1} for DPC and 0.75 μg L^{-1} for MDPC). An end-member analy-

sis using hydrochemical data showed that, approximately 20% of the mass of DPC in a pumping well originates from the neighboring basin, resulting in a concentration of over 0.1 μg L^{-1} for DPC. The findings highlight that, mobile metabolites can be imported from heavily farmed areas outside the exploited aquifer through surface-water groundwater interactions that affect the metabolite concentration level and long-term dynamics in the aquifer (Hintze, Glauser, & Hunkeler, 2020).

2.5. Polychlorinated Aromatic Hydrocarbons

Polychlorinated biphenyls (PCBs) and polychlorinated aromatic hydrocarbons (PAHs), which are the other semi-volatile members of endocrine disruptors, are highly toxic chemicals. With the effect of long-range atmospheric transport, these pollutants are released from emission sources that can reach distant areas due to their semi-volatility, and thus reach a threatening level for aquatic ecosystem and drinking water sources.

PAHs are organic compounds consisting of two or more aromatic rings with semi-volatile properties such as PCBs and pesticides (Zohair, Salim, Soyibo, & Beck, 2006). PAHs are mostly formed as a result of incomplete combustion and pyrolysis of fossil fuels (Cetin, Yurdakul, Gungormus, Ozturk, & Sofuoglu, 2018). Vehicle emissions, heating and industrial combustion processes can be listed as the main sources of PAHs. (Fatma, Yucel, & Siddik, 2010). They are listed as priority pollutants by the United States Environmental Protection Agency (EPA) due to the toxic, endocrine disrupting, carcinogenic and mutagenic effects of human exposure to PAHs through ingestion or inhalation. (Stewart et al., 2021). In addition, these compounds accumulate in food chain and adversely affect living organisms (Vardar, Tasdemir, Odabasi, & Noll, 2004).

In studies investigating PAHs in drinking water in literature, a total of 16 types of PAHs, ranging from 703 to1238 ng/L were obtained in the effluent of different treatment plants in Egypt (Badawy & Embaby, 2010). The concentrations of 16 species of PAH measured in two different studies conducted in China were in the range of 3.89-231.39 ng/L and 7.5-73.3. (Kanno et al., 2010). When the studies made in aquatic

environment in Turkey are evaluated, 13 types of PAH concentrations varying between 1800-24900 ng/L have been obtained in Menderes River (Ardag, Ozel, & Sen, 2011). The 13 types of PAH levels measured in sea water in Aliağa are in the range of 5.11-294.62 ng/L (Odabasi, Cetin, Demircioglu, & Sofuoglu, 2008).

2.6. Polychlorinated Biphenyls

Organochlorine pesticides, which are also found in Polychlorinated Biphenyls group (PCBs) are of great importance as they are found in 12 most dangerous Persistent Organic Pollutants (POPs) stated in Stockholm Convention (2001), besides their disruptive effects on endocrine systems (Baqar et al., 2017; Lallas, 2001). Since the PCBs are stable compounds with low vapor pressures and solubilities and high dielectric constant values, they have been widely used for industrial purposes (Cindoruk & Tasdemir, 2007). Although PCBs are mostly used as insulating liquid and coolant in transformers and condensers, paints, hydraulic fluids, carbonless paper manufacturing, etc. they have been used frequently in industrial products (Odabasi et al., 2009). As a result of being detection in high amounts in fishes and different environmental matrices, their production and use were prohibited. Their persistence in the environment and their constant tendency to transition between different environments, their stability, their ability to move long distances in the atmosphere and their bioaccumulation properties in living organisms have made these compounds much more important (Barber, Thomas, Kerstiens, & Jones, 2004; Ozcan & Aydin, 2009).

It can be thought that semi-volatile organic compounds (S-VOCs) (Baqar et al., 2017), which have low solubility in water, will generally prefer to be in particulate phase in water and can be treated with conventional treatment processes. However, it has been reported that the rates of S-VOCs in dissolved phase in spring water could reach to 73% of the total (particle + dissolved phase). Reported levels of S-VOCs in drinking water, in different parts of the world indicated that, conventional treatment methods may not be sufficient for the emoval of these pollutants from water. For example, Li et al. (2018), observed measurable levels of

PCB at each focal point they studied, in China (Li et al., 2018). In the same country, while Zhao et al. (2011) have been reported PCB levels ranging from 31.58 to 344.9 ng/L, Hong et al. (2009) measured 0.3 ng/L total 8 types of PCB pollution (Hong, Chunhong, & Xiaoxiong, 2009; Q. Zhao et al., 2011). In a study made in USA, the concentrations ranging from <9.3 to 186.6 ng/L were reported for a total of 147 species of PCBs in samples collected from 7 different regions (Palmer, Wilson, Casey, & Wagner, 2011). When the studies made in Turkey were evaluated (Gedik & Imamoğlu, 2010), it was obtained that, while PCB measurements were made in wastewater collection systems and sea waters in urban coastal areas (Aydin, Wichmann, & Bahadir, 2004; Tor et al., 2003) also, it was reported PCB contamination in tap water (Kurt & Ozkoc, 2004; Odabasi et al., 2008; Telli-Karakoç et al., 2002).

2.7. Microplastics

Microplastics (MP) are the second category of urban aquatic system pollution as endocrine disruptors. Identifying, monitoring, preventing and eliminating of MP pollution in aquatic ecosystems is currently known as one of the most important problems in worldwide. MP contamination in waters may be caused by direct transition to the water or the degradation of plastics that are turn into micro-contaminants later. It is projected that 4 to 12 million tons of plastic waste is dumped into the urban sewage system, rivers, and oceans annually, and as a result, it is estimated that by 2050 it will outweigh the amount of fish. Based on the current studies, characterization of microplastics in water is still one of the challenges, as they can be easily interfere with organic or other types of substances. Thus, there is an urgent requirement to establish alternative ways for describing the nature of MP chemically. For this reason, the latest techniques and instrumentation for MP characterization (Raman and fourier-transform infrared spectroscopy and microscopes, pyrolysis and thermal desorption gas chromatography, imaging techniques, etc.) must be considered with the versatility of the problem (Picó & Barceló, 2019).

Although, neither official definition or full agreement within the authors, MPs are generally defined as plastic fragments smaller than 5

mm in any dimension with an indeterminate lower limit. Recently, the launch of the term "nanoplastics" establish a lower limit (commonly <100 nm) for these particles. However, latest studies showed certain discrepancies on the range of MP sizes besides, evolution of the terminology according to MP's impact (Picó & Barceló, 2019).

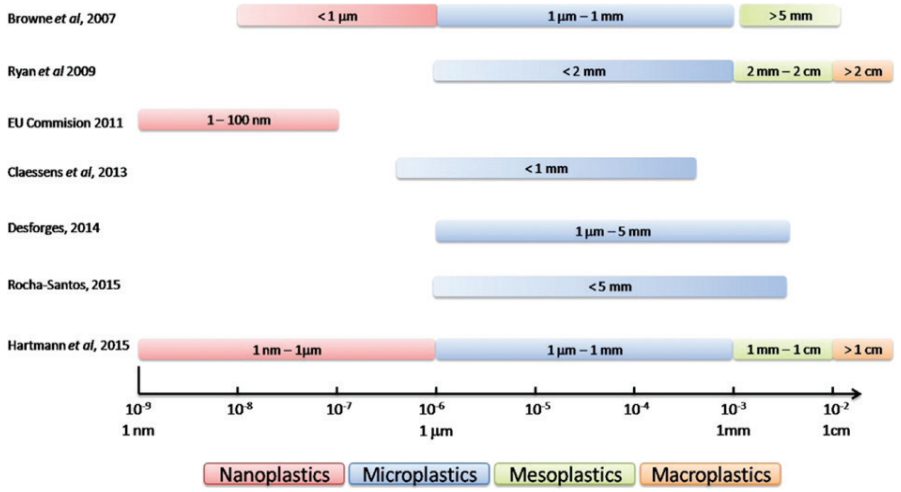

Figure 1. Size-based definition of plastics (Reprinted from ref Copyright (2016) with permission from Elsevier) (da Costa, Santos, Duarte, & Rocha-Santos, 2016)

Although neither exact definition or agreement fully within the researchers, microplastics are generally defined as plastic fragments smaller than 5 mm in any dimension with an indefinite lower limit. In Figure 1 it was stated the size-based definition of plastics (Browne, Galloway, & Thompson, 2007; Claessens, Van Cauwenberghe, Vandegehuchte, & Janssen, 2013; Desforges, Galbraith, Dangerfield, & Ross, 2014; Hartmann, Nolte, Sørensen, Jensen, & Baun; Ryan, Moore, Van Franeker, & Moloney, 2009).

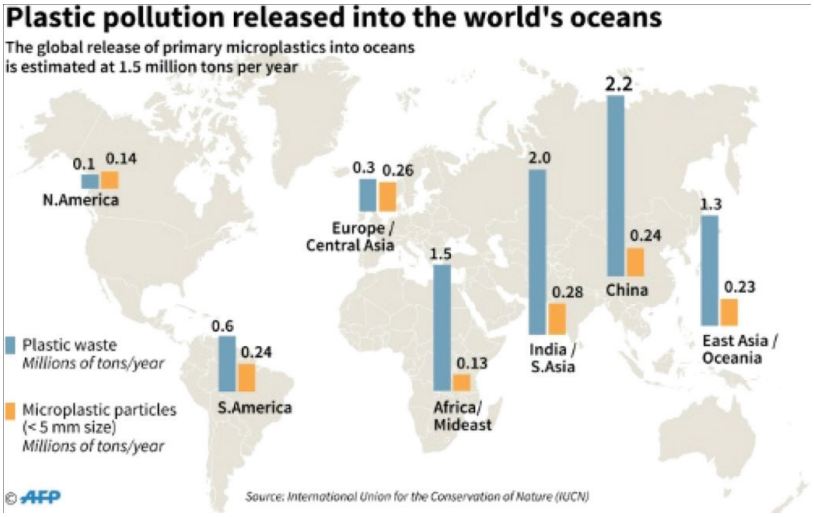

Figure 2. Global release of microplastics into the oceans and comparison of them with plastics originated from mismanagement of wastes. Reprinted from ref Copyright (2017) with permission from International Union for Conservation of Nature and Natural Resources (IUCN) (Boucher & Friot, 2017).

In Figure 2, the release of microplastics into the oceans worldwide and comparison of them with the other plastics which are originated from wastes were showed (Picó & Barceló, 2019). Microplastics are classified mainly into two categories: primary and secondary MPs (Ter Halle et al., 2017). Primary MPs are already manufactured with a microsize, including microspheres (<500 μm) which are used in some cosmetic products, mixtures used for sandblasting/shotblasting, and are employed as pharmaceutical vectors and 3D printing material (Rowenczyk et al., 2020). Secondary MPs are the products of degradation of macro-plastic materials by mechanical or photo-oxidative pathways. It is estimated that 1.5 million tonnes of primary MPs are released into water environment annually. The plastics entcountering into the aquatic environment sourced from mismanagement of wastes, which may form secondary MPs, are higher in almost all of the countries worldwide than the European countries and USA (United States of America) (Figure 2) (Caldwell et al., 2021).

3. Conclusions

Endocrine disruptor compounds are the matters of concern in aquatic ecosystems. Mostly detected endocrine disruptor types in aquatic environment are hormones, antibiotics, microplastics, polychlorinated biphenyls, polychlorinated aromatic hydrocarbons and pesticides. There are various ways of distribution of endocrine disruptors in receiving environment through urban water systems. Medical drugs, hormones and personal care products which are used in homes and hospitals reach to the sewage systems by the excretion of them with the feces and urinary tract in unchanged forms or metabolites after taken into the human body. Then, they are discharged into the wastewater treatment facilities through sewage systems. In addition, they could also be disposed of directly into the garbage without ever using. These medicines which were disposed of into the garbage may be mixed with leachate and dispersed into the aquatic system. Another endocrine disruptor sources are agricultural prosses, where pesticides are used widely. These products can seep into the soil and contaminate groundwater. Also, endocrine disruptor micro-contaminants originating from industries are discharged into the sewage systems and reach to the wastewater treatment plants. These pollutants, which cannot be completely removed/destroyed in wastewater treatment plants are discharged into the receiving environment and reach to the rivers, lakes, and seas and thus, they cause to pollution in water sources even in groundwaters and drinking waters.

- When the studies were considered, it has been reported that hormone residues are largely detected in wastewaters, underground waters and drinking water sources. Estrone and E2 hormones, which are the dominant species in aquatic environments (in estrogenic activity), have been detected in surface waters in many countries such as Austria, the United States, Brazil and China. However, only at a few studies it has been reported natural concentrations of estrogen or EE2 in drinking water.

- However, in recent years the presence of antibiotics in groundwater has received great attention around the world. In a US national expedition made for detection of pharmaceuticals and other organic pollutants in water supplies it was seen that, high levels of antibiotics, including ciprofloxacin, enfloxacin, ofloxacin, and trimethoprim were found in groundwater samples.
- When the studies are considered made on pesticides, metabolite concentrations have been found to be low in the areas which are affected by rivers in mountainous regions, but on the contrary, high concentrations (desphenyl-chloridazone and methyl-desphenyl-chloridazone) were detected in areas affected by streams from watersheds, where intensive agricultural processes are made.
- A total of 16 types of PAHs, varying in different concentration ranges, were detected in the wastewater of different treatment plants in Egypt and China. When the studies conducted in the aquatic environment in Turkey are evaluated, 13 species of PAHs with different concentrations have been observed the Menderes River and in the sea water of Aliağa.
- For the detection of polychlorinated biphenyls in the aquatic environment carried out in different countries, measurable levels of 8 types of PCBs have been observed in many different water matrices in China. In a study conducted in USA, high concentrations were reported for a total of 147 PCB species in the samples from different regions. When the studies made in Turkey are evaluated, PCB concentrations were found in wastewater collection systems and sea waters in urban coastal areas, even in tap water.
- It is estimated that between 4 and 12 million tons of plastic waste is dumped into the urban sewage systems, rivers and oceans annually, as a result of that, it is estimated that, the amount of microplastics will exceed the amount of fishes by 2050. The characterization of microplastics in water still has great technological challenges, as they can easily interact with

organic or other types of substances. Thus, there is an urgent need to establish alternative ways to chemically describe the structure of MPs.

However, unfortunately, there is no discharge standard in the legislation for endocrine disrupting pollutants in wastewater treatment plants. Thus, most of the currently operated wastewater treatment plants are operated up to tertiary treatment and these treatment plants cannot completely remove micropollutants. There is no legislation accepted by worldwide, but in some countries such as Switzerland, governments have prepared some regulations for the removal of micropollutants and decided to make a quaternary treatment step for different wastewater treatment plants in accordance with their own laws.

References

Abdalla, F., & Khalil, R. (2018). Potential effects of groundwater and surface water contamination in an urban area, Qus City, Upper Egypt. *Journal of African Earth Sciences, 141*, 164-178.

Ardag, H., Ozel, M. Z., & Sen, A. (2011). Polycyclic aromatic hydrocarbons in water from the Menderes River, Turkey. *Bulletin of environmental contamination and toxicology, 86*(2), 221-225.

Aydin, M., Wichmann, H., & Bahadir, M. (2004). Priority organic pollutants in fresh and waste waters of Konya-Turkey. *Fresenius Environmental Bulletin, 13*(2), 118-123.

Badawy, M. I., & Embaby, M. A. (2010). Distribution of polycyclic aromatic hydrocarbons in drinking water in Egypt. *Desalination, 251*(1-3), 34-40.

Baqar, M., Sadef, Y., Ahmad, S. R., Mahmood, A., Qadir, A., Aslam, I., ... Zhang, G. (2017). Occurrence, ecological risk assessment, and spatio-temporal variation of polychlorinated biphenyls (PCBs) in water and sediments along River Ravi and its northern tributaries, Pakistan. *Environmental Science and Pollution Research, 24*(36), 27913-27930.

Barber, J. L., Thomas, G. O., Kerstiens, G., & Jones, K. C. (2004). Current issues and uncertainties in the measurement and modelling

of air–vegetation exchange and within-plant processing of POPs. *Environmental pollution, 128*(1-2), 99-138.

Barnes, K. K., Kolpin, D. W., Furlong, E. T., Zaugg, S. D., Meyer, M. T., & Barber, L. B. (2008). A national reconnaissance of pharmaceuticals and other organic wastewater contaminants in the United States—I) Groundwater. *Science of the total environment, 402*(2-3), 192-200.

Baronti, C., Curini, R., D'Ascenzo, G., Di Corcia, A., Gentili, A., & Samperi, R. (2000). Monitoring natural and synthetic estrogens at activated sludge sewage treatment plants and in a receiving river water. *Environmental Science & Technology, 34*(24), 5059-5066.

Bedoya-Ríos, D. F., Lara-Borrero, J. A., Duque-Pardo, V., Madera-Parra, C. A., Jimenez, E. M., & Toro, A. F. (2018). Study of the occurrence and ecosystem danger of selected endocrine disruptors in the urban water cycle of the city of Bogotá, Colombia. *Journal of Environmental Science and Health, Part A, 53*(4), 317-325.

Benotti, M. J., Trenholm, R. A., Vanderford, B. J., Holady, J. C., Stanford, B. D., & Snyder, S. A. (2009). Pharmaceuticals and endocrine disrupting compounds in US drinking water. *Environmental science & technology, 43*(3), 597-603.

Bibbo, M., Gill, W. B., Azizi, F., Blough, R., Fang, V. S., Rosenfield, R. L., . . . Wied, G. L. (1977). Follow-up study of male and female offspring of DES-exposed mothers. *Obstetrics and gynecology, 49*(1), 1-8.

Boucher, J., & Friot, D. (2017). *Primary microplastics in the oceans: a global evaluation of sources*: Iucn Gland, Switzerland.

Browne, M. A., Galloway, T., & Thompson, R. (2007). Microplastic—an emerging contaminant of potential concern? *Integrated Environmental Assessment and Management: An International Journal, 3*(4), 559-561.

Caldwell, J., Lehner, R., Balog, S., Rhême, C., Gao, X., Septiadi, D., . . . Rothen-Rutishauser, B. (2021). Fluorescent plastic nanoparticles to track their interaction and fate in physiological environments. *Environmental Science: Nano, 8*(2), 502-513.

Cetin, B., Yurdakul, S., Gungormus, E., Ozturk, F., & Sofuoglu, S. C. (2018). Source apportionment and carcinogenic risk assessment of passive air sampler-derived PAHs and PCBs in a heavily industrialized region. *Science of the Total Environment, 633*, 30-41.

Chaturvedi, P., Shukla, P., Giri, B. S., Chowdhary, P., Chandra, R., Gupta, P., & Pandey, A. (2021). Prevalence and hazardous impact of pharmaceutical and personal care products and antibiotics in environment: A review on emerging contaminants. *Environmental Research, 194*, 110664-110664. doi: 10.1016/j.envres.2020.110664

Cindoruk, S. S., & Tasdemir, Y. (2007). Deposition of atmospheric particulate PCBs in suburban site of Turkey. *Atmospheric Research, 85*(3-4), 300-309.

Claessens, M., Van Cauwenberghe, L., Vandegehuchte, M. B., & Janssen, C. R. (2013). New techniques for the detection of microplastics in sediments and field collected organisms. *Marine pollution bulletin, 70*(1-2), 227-233.

da Costa, J. P., Santos, P. S. M., Duarte, A. C., & Rocha-Santos, T. (2016). (Nano) plastics in the environment–sources, fates and effects. *Science of the Total Environment, 566*, 15-26.

Desforges, J.-P. W., Galbraith, M., Dangerfield, N., & Ross, P. S. (2014). Widespread distribution of microplastics in subsurface seawater in the NE Pacific Ocean. *Marine pollution bulletin, 79*(1-2), 94-99.

Directives, E. (2008). Directive 2008/105/EC of the European Parliament and of the Council. *Official Journal of the European Union*.

DSİ. (2018). *Toprak ve Su Kaynakları*. Bursa.

EC. (2000). Directive 2000/60/EC of the European Parliament and of the Council establishing a framework for Community action in the field of water policy *OJ L327*.

EPA. (2007). Method 1699: Pesticides in Water, Soil, Sediment, Biosolids, and Tissue by HRGC/HRMS. In U. S. E. P. A. O. o. W. O. o. S. a. Technology (Ed.), *Engineering and Analysis Division (4303T)*. 1200 Pennsylvania Avenue, NW Washington, DC 20460

EU. (2015). Commission Implementing Decision (EU) 2015/495 *Official Journal of the European Union*.

Fatma, E., Yucel, T., & Siddik, C. S. (2010). Determination of mass transfer rates and deposition levels of polycyclic aromatic hydrocarbons (PAHs) using a modified water surface sampler. *Atmospheric Pollution Research, 1*(3), 177-183.

Fick, J., Söderström, H., Lindberg, R. H., Phan, C., Tysklind, M., & Larsson, D. J. (2009). Contamination of surface, ground, and drinking water from pharmaceutical production. *Environmental Toxicology and Chemistry, 28*(12), 2522-2527.

Gedik, K., & Imamoğlu, I. (2010). An assessment of the spatial distribution of polychlorinated biphenyl contamination in Turkey. *CLEAN–Soil, Air, Water, 38*(2), 117-128.

Hartmann, N. B., Nolte, T., Sørensen, M. A., Jensen, P. R., & Baun, A. (2015). *Aquatic ecotoxicity testing of nanoplastics: lessons learned from nanoecotoxicology*.

Hatt, J., Germain, E., & Judd, S. (2013). Powdered activated carbon-microfiltration for waste-water reuse. *Separation Science and Technology, 48*(5), 690-698.

Heberer, T. (2002). Occurrence, fate, and removal of pharmaceutical residues in the aquatic environment: a review of recent research data. *Toxicology letters, 131*(1-2), 5-17.

Herbst, A. L., Ulfelder, H., & Poskanzer, D. C. (1971). Adenocarcinoma of the vagina: association of maternal stilbestrol therapy with tumor appearance in young women. *New England journal of medicine, 284*(16), 878-881.

Hintze, S., Glauser, G., & Hunkeler, D. (2020). Influence of surface water–groundwater interactions on the spatial distribution of pesticide metabolites in groundwater. *Science of The Total Environment, 733*, 139109.

Hohenblum, P., Gans, O., Moche, W., Scharf, S., & Lorbeer, G. (2004). Monitoring of selected estrogenic hormones and industrial chemicals in groundwaters and surface waters in Austria. *Science of the Total Environment, 333*(1-3), 185-193.

Holm, J. V., Ruegge, K., Bjerg, P. L., & Christensen, T. H. (1995). Occurrence and distribution of pharmaceutical organic compounds in the groundwater downgradient of a landfill (Grindsted, Denmark). *Environmental science & technology, 29*(5), 1415-1420.

Hong, Y., Chunhong, Z., & Xiaoxiong, Z. (2009). Investigation of pollution characteristics of polychlorinated biphenyls in the typical

drinking water sources in Jiangsu Province, China. *Environmental monitoring and assessment, 158*(1), 573-579.

IFAT. (2018). Call on EU to develop standards for micropollutants in waste water.

IMS. (2014). Intercontinental Medical Statistics.

Jarošová, B., Bláha, L., Giesy, J. P., & Hilscherová, K. (2014). What level of estrogenic activity determined by in vitro assays in municipal waste waters can be considered as safe? *Environment international, 64*, 98-109.

Jurado, A., Walther, M., & Díaz-Cruz, M. S. (2019). Occurrence, fate and environmental risk assessment of the organic microcontaminants included in the Watch Lists set by EU Decisions 2015/495 and 2018/840 in the groundwater of Spain. *Science of the Total Environment, 663*, 285-296.

Kanno, A., Nishi, I., Kishi, T., Kawakami, T., Takahashi, Y., & Onodera, S. (2010). Mutagenic potentials of Amberlite XAD-2-resin extracts obtained from river and drinking waters in the Northwest district of Chiba, Japan. *The Journal of toxicological sciences, 35*(6), 817-826.

Kolpin, D. W., Furlong, E. T., Meyer, M. T., Thurman, E. M., Zaugg, S. D., Barber, L. B., & Buxton, H. T. (2002). Pharmaceuticals, hormones, and other organic wastewater contaminants in US streams, 1999–2000: A national reconnaissance. *Environmental science & technology, 36*(6), 1202-1211.

Kuch, H. M., & Ballschmiter, K. (2001). Determination of endocrine-disrupting phenolic compounds and estrogens in surface and drinking water by HRGC-(NCI)- MS in the picogram per liter range. *Environmental science & technology, 35*(15), 3201-3206.

Kurt, P. B., & Ozkoc, H. B. (2004). A survey to determine levels of chlorinated pesticides and PCBs in mussels and seawater from the Mid-Black Sea Coast of Turkey. *Marine Pollution Bulletin, 48*(11-12), 1076-1083.

Kümmerer, K. (2001). Drugs in the environment: emission of drugs, diagnostic aids and disinfectants into wastewater by hospitals in relation to other sources–a review. *Chemosphere, 45*(6-7), 957-969.

Lallas, P. L. (2001). The Stockholm Convention on persistent organic pollutants. *American Journal of International Law, 95*(3), 692-708.

Li, Z., Chang, F., Shi, P., Chen, X., Yang, F., Zhou, Q., . . . Li, A. (2018). Occurrence and potential human health risks of semi-volatile organic compounds in drinking water from cities along the Chinese coastland of the Yellow Sea. *Chemosphere, 206*, 655-662.

Lipczynska-Kochany, E. (2018). Effect of climate change on humic substances and associated impacts on the quality of surface water and groundwater: A review. *Science of the total environment, 640*, 1548-1565.

Liz, M. V. d., Amaral, B. d., Stets, S., Nagata, N., & Peralta-Zamora, P. (2017). Sensitive estrogens determination in wastewater samples by HPLC and fluorescence detection. *Journal of the Brazilian Chemical Society, 28*(8), 1453-1460.

Luo, Y., Guo, W., Ngo, H. H., Nghiem, L. D., Hai, F. I., Zhang, J., . . . Wang, X. C. (2014). A review on the occurrence of micropollutants in the aquatic environment and their fate and removal during wastewater treatment. *Science of the total environment, 473*, 619-641.

Metcalfe, C., Hoque, M. E., Sultana, T., Murray, C., Helm, P., & Kleywegt, S. (2014). Monitoring for contaminants of emerging concern in drinking water using POCIS passive samplers. *Environmental Science: Processes & Impacts, 16*(3), 473-481.

Mueller, S. O., & Korach, K. S. (2001). Estrogen receptors and endocrine diseases: lessons from estrogen receptor knockout mice. *Current opinion in pharmacology, 1*(6), 613-619.

Nghiem, L. D., Schäfer, A. I., & Elimelech, M. (2004). Removal of natural hormones by nanofiltration membranes: measurement, modeling, and mechanisms. *Environmental science & technology, 38*(6), 1888-1896.

Oberlé, K., Capdeville, M.-J., Berthe, T., Budzinski, H. l. n., & Petit, F. (2012). Evidence for a complex relationship between antibiotics and antibiotic-resistant Escherichia coli: from medical center patients to a receiving environment. *Environmental science & technology, 46*(3), 1859-1868.

Odabasi, M., Bayram, A., Elbir, T., Seyfioglu, R., Dumanoglu, Y., Bozlaker, A., . . . Cetin, B. (2009). Electric arc furnaces for steel-making: hot spots for persistent organic pollutants. *Environmental science & technology, 43*(14), 5205-5211.

Odabasi, M., Cetin, B., Demircioglu, E., & Sofuoglu, A. (2008). Air–water exchange of polychlorinated biphenyls (PCBs) and organochlorine pesticides (OCPs) at a coastal site in Izmir Bay, Turkey. *Marine Chemistry, 109*(1-2), 115-129.

Ohko, Y., Iuchi, K.-i., Niwa, C., Tatsuma, T., Nakashima, T., Iguchi, T., . . . Fujishima, A. (2002). 17α-Estradiol degradation by TiO2 photocatalysis as a means of reducing estrogenic activity. *Environmental science & technology, 36*(19), 4175-4181.

Onesios, K. M., Jim, T. Y., & Bouwer, E. J. (2009). Biodegradation and removal of pharmaceuticals and personal care products in treatment systems: a review. *Biodegradation, 20*(4), 441-466.

Ozcan, S., & Aydin, M. E. (2009). Polycyclic aromatic hydrocarbons, polychlorinated biphenyls and organochlorine pesticides in urban air of Konya, Turkey. *Atmospheric Research, 93*(4), 715-722.

Özkan, S., Tüzün, H., Görer Tamer, N., Ceyhan, M., Aycan, S., Albayrak, S., & Bumin, A. (2007). Su kesintilerinin ve su tüketim alışkanlıklarının diyare oluşumu üzerine etkileri: Gölbaşı örneği.

Palmer, P. M., Wilson, L. R., Casey, A. C., & Wagner, R. E. (2011). Occurrence of PCBs in raw and finished drinking water at seven public water systems along the Hudson River. *Environmental monitoring and assessment, 175*(1), 487-499.

Picó, Y., & Barceló, D. (2019). Analysis and prevention of microplastics pollution in water: current perspectives and future directions. *ACS omega, 4*(4), 6709-6719.

Pironti, C., Ricciardi, M., Proto, A., Bianco, P. M., Montano, L., & Motta, O. (2021). Endocrine-disrupting compounds: An overview on their occurrence in the aquatic environment and human exposure. *Water, 13*(10), 1347.

Rodgers-Gray, T. P., Jobling, S., Morris, S., Kelly, C., Kirby, S., Janbakhsh, A., . . . Tyler, C. R. (2000). Long-term temporal changes in the

estrogenic composition of treated sewage effluent and its biological effects on fish. *Environmental Science & Technology, 34*(8), 1521-1528.

Rowenczyk, L., Dazzi, A., Deniset-Besseau, A., Beltran, V., Goudounèche, D., Wong-Wah-Chung, P., . . . Roux, C. (2020). Microstructure characterization of oceanic polyethylene debris. *Environmental science & technology, 54*(7), 4102-4109.

Ryan, P. G., Moore, C. J., Van Franeker, J. A., & Moloney, C. L. (2009). Monitoring the abundance of plastic debris in the marine environment. *Philosophical Transactions of the Royal Society B: Biological Sciences, 364*(1526), 1999-2012.

Schmaltz, E., Melvin, E. C., Diana, Z., Gunady, E. F., Rittschof, D., Somarelli, J. A., . . . Dunphy-Daly, M. M. (2020). Plastic pollution solutions: emerging technologies to prevent and collect marine plastic pollution. *Environment international, 144*, 106067.

Shanle, E. K., & Xu, W. (2011). Endocrine disrupting chemicals targeting estrogen receptor signaling: identification and mechanisms of action. *Chemical research in toxicology, 24*(1), 6-19.

Sharma, B. M., Bečanová, J., Scheringer, M., Sharma, A., Bharat, G. K., Whitehead, P. G., . . . Nizzetto, L. (2019). Health and ecological risk assessment of emerging contaminants (pharmaceuticals, personal care products, and artificial sweeteners) in surface and groundwater (drinking water) in the Ganges River Basin, India. *Science of the Total Environment, 646*, 1459-1467.

Souza, F., Quijorna, S., Lanza, M., Sáez, C., Cañizares, P., & Rodrigo, M. (2017). Applicability of electrochemical oxidation using diamond anodes to the treatment of a sulfonylurea herbicide. *Catalysis Today, 280*, 192-198.

Sreelakhmi, T., & Chitra, K. (2021). Microplastics contamination in the environment: An ecotoxicological concern. *Intern J Zool Invest, 7*(1), 230-258.

Stewart, G. J., Nelson, B. S., Acton, W. J. F., Vaughan, A. R., Farren, N. J., Hopkins, J. R., . . . Mondal, A. (2021). Emissions of intermediate-volatility and semi-volatile organic compounds from domestic fuels used in Delhi, India. *Atmospheric Chemistry and Physics*, 2407-2426.

Telli-Karakoç, F., Tolun, L., Henkelmann, B., Klimm, C., Okay, O., & Schramm, K.-W. (2002). Polycyclic aromatic hydrocarbons (PAHs) and polychlorinated biphenyls (PCBs) distributions in the Bay of Marmara sea: Izmit Bay. *Environmental Pollution, 119*(3), 383-397.

Teonian Meriç, B. (2004). Su kaynakları yönetimi ve Türkiye. *Jeoloji Mühendisliği Dergisi, 28*(1), 27-38.

Ter Halle, A., Jeanneau, L., Martignac, M., Jardé, E., Pedrono, B., Brach, L., & Gigault, J. (2017). Nanoplastic in the North Atlantic subtropical gyre. *Environmental science & technology, 51*(23), 13689-13697.

Ternes, T. A. (1998). Occurrence of drugs in German sewage treatment plants and rivers. *Water research, 32*(11), 3245-3260.

Topal, M., Şenel, G. U., Topal, E. I. A., & Erdal, Ö. (2015). Antibiyotikler ve kullanım alanları. *Erciyes Üniversitesi Fen Bilimleri Enstitüsü Fen Bilimleri Dergisi, 31*(3), 121-127.

Tor, A., Cengeloglu, Y., Aydin, M., Ersoz, M., Wichmann, H., & Bahadir, M. (2003). Polychlorinated biphenyls(PCB) and polycyclic aromatic hydrocarbons(PAH) in wastewater samples from the sewage system of Konya-Turkey. *Fresenius Environmental Bulletin, 12*(7), 732-735.

Torres, N. H., de Salles Pupo, M. M., Ferreira, L. F. R., Maranho, L. A., Américo-Pinheiro, J. H. P., Vilca, F. Z., . . . Tornisielo, V. L. (2017). Spatial and seasonal analysis of antimicrobials and toxicity tests with Daphnia magna, on the sub-basin of Piracicaba river, SP, Brazil. *Journal of environmental chemical engineering, 5*(6), 6070-6076.

Tran, T. K. A., Yu, R. M. K., Islam, R., Nguyen, T. H. T., Bui, T. L. H., Kong, R. Y. C., . . . MacFarlane, G. R. (2019). The utility of vitellogenin as a biomarker of estrogenic endocrine disrupting chemicals in molluscs. *Environmental Pollution, 248*, 1067-1078.

Trnka, M., Feng, S., Semenov, M. A., Olesen, J. E., Kersebaum, K. C., Rötter, R. P., . . . Ruiz-Ramos, M. (2019). Mitigation efforts will not fully alleviate the increase in water scarcity occurrence probability in wheat-producing areas. *Science Advances, 5*(9), eaau2406.

Turan, E. S. (2018). Türkiye'nin iklim değişikliğine bağlı kuraklık durumu. *Doğal Afetler ve Çevre Dergisi, 4*(1), 63-69.

Vardar, N., Tasdemir, Y., Odabasi, M., & Noll, K. E. (2004). Characterization of atmospheric concentrations and partitioning of

PAHs in the Chicago atmosphere. *Science of the Total Environment, 327*(1-3), 163-174.

Varjani, S., & Sudha, M. C. (2020). Occurrence and human health risk of micro-pollutants—A special focus on endocrine disruptor chemicals *Current Developments in Biotechnology and Bioengineering* (pp. 23-39): Elsevier.

Vélez, V. P. P., Esquivel-Hernández, G., Cipriani-Avila, I., Mora-Abril, E., Cisneros, J. F., Alvarado, A., & Abril-Ulloa, V. (2019). Emerging contaminants in trans-American waters. *Revista Ambiente & Água, 14*(6).

Wee, S. Y., Aris, A. Z., Yusoff, F. M., & Praveena, S. M. (2020). Occurrence of multiclass endocrine disrupting compounds in a drinking water supply system and associated risks. *Scientific reports, 10*(1), 1-12.

WHO. (2011). *Guidelines for Drinking-water Quality*. Geneva 27, Switzerland: WHO Press, World Health Organization.

Yannopoulos, S., Giannopoulou, I., & Kaiafa-Saropoulou, M. (2019). Investigation of the current situation and prospects for the development of rainwater harvesting as a tool to confront water scarcity worldwide. *Water, 11*(10), 2168.

Zamora-León, P. (2021). Are the Effects of DES Over? A Tragic Lesson from the Past. *International Journal of Environmental Research and Public Health, 18*(19), 10309.

Zhao, B.-H., Sun, Q., Chen, J., Zhang, J., Zhang, X.-Y., Liu, B.-J., & Li, J. (2020). 17 beta-estradiol biodegradation by anaerobic granular sludge: Effect of iron sources. *Scientific reports, 10*(1), 1-10.

Zhao, Q., Ren, Q., Chen, J. A., Qiu, Z. Q., Cao, J., & Shu, W. Q. (2011). Reproductive toxicity in male mice caused by organic extracts in tap water from the Jialing River in Chongqing, China. *Birth Defects Research Part B: Developmental and Reproductive Toxicology, 92*(1), 1-9.

Zohair, A., Salim, A.-B., Soyibo, A. A., & Beck, A. J. (2006). Residues of polycyclic aromatic hydrocarbons (PAHs), polychlorinated biphenyls (PCBs) and organochlorine pesticides in organically-farmed vegetables. *Chemosphere, 63*(4), 541-553.

CHAPTER IX

USE OF PLANT MATERIAL IN CHILDREN'S PLAYGROUNDS: THE CASE OF TEKIRDAG

Assoc. Prof. Dr. Burçin EKİCİ & Prof. Dr. Elif Ebru ŞİŞMAN
Tekirdag Namık Kemal University,bekici@nku.edu.tr
ORCID: 0000-0002-2553-5656
Tekirdag Namık Kemal University, esisman@nku.edu.tr
ORCID: 0000-0002-5114-7480

1. Introduction

Today, as a result of unplanned urbanization, the ecology of cities is deteriorating and the presence of green areas is decreasing day by day. Children's playgrounds, which are very important for urban green space systems, are also affected by these deteriorations and are designed unplanned and disconnected from nature. Playgrounds are important for children living in cities to spend the limited time they spend outside more qualified, to develop them educationally, physically and spiritually and to satisfy their longing for nature (Küçükyağcı et al., 2015; Aklıbaşında et al., 2018). Because play is an important survival activity for children and is one of the most effective tools that helps them express themselves and prepares them for social life (Timur et al., 2018). For this reason, the design of children's playgrounds in urban ecosystems is important in terms of raising healthy generations and creating sustainable and healthy environments.

Studies show that indoor games affect children's mental, physical and social development negatively. Natural areas, on the other hand, have a very active role in the development of their creativity by supporting their development (Özgen and Aytuğ, 1992; Uslu and Shakouri, 2012). There

is strong evidence that the motor skills of children playing in playgrounds designed with natural elements develop at a high level, and that nature increases intelligence by stimulating children with its ever- changing and developing structure (Fjørtoft and Sageie, 2000; Fjørtoft, 2004; Turgut and Yılmaz, 2010; Aksu and Demirel, 2011; Coe et al., 2014; Veitch et al., 2015; Pouya et al., 2016; Timur et al., 2018). At the same time, considering the fact that nature conservation awareness is gained in childhood, bringing nature and natural processes to the forefront in the design works of spaces used by children in urban areas is important in terms of raising individuals who are sensitive to their environment and nature and who protect and ensure its continuity (Çukur and Özgüner, 2008; Özgüner and Şahin, 2009; Turgut and Yılmaz, 2010).

Plants are one of the most important tools for the physical and psychological development of children in playgrounds and for them to develop behavioral patterns such as recognizing and protecting nature. For this reason, it is necessary to take advantage of the aesthetic and functional effects of plants and their morphological features such as size, form, texture, color and similar morphological features by attaching importance to plant material in designs (Pouya et al., 2016). In addition to their effects such as control against light (shading- benefiting from the sun), shielding (wind- noise- image), providing privacy and creating space in children's playgrounds, plants also offer children different opportunities for their plays. While it is a play element with leaves, flowers, fruits, seeds and stems, it stimulates the senses with its color and scent effects, creates comfortable areas by providing shade, helps to perceive seasonal transitions and to recognize the natural ecosystem (Moore, 2014; White and Stoecklin, 2015). In order to make a correct herbal design, the perception of children should be considered and the garden design should enable the children to perceive with their senses; sight, hearing, touch and smell (Çelik et al., 2015). While doing this, plants that are thorny, poisonous, allergenic, that can attract bees and various insects and can create a slippery surface because of their deciduous parts, should be avoided and everlasting species with suitable sizes for children should be selected (Erdönmez, 2007; Çelik, 2012).

In this research, the situation of plant material in children's playgrounds located in urban green areas was examined. The plant potential

of the children's playgrounds in the city of Tekirdag, which was chosen as a sample area, was determined and evaluated in terms of its adequacy and contribution to the playground. In this context, suggestions were presented to eliminate the deficiencies identified in children's playgrounds in urban spaces that are under intense pressure and to contribute to future design and planning studies.

2. Material and Methods

The material of the research consists of 9 children's playgrounds in the Tekirdag city center (Figure 1). Tekirdag is located in the northwest of Turkey, in the north of the Marmara Sea. Its surface area is 6 313 km^2 and its altitude is between 0- 200 m. It is surrounded by Istanbul in the east, Kırklareli in the north, the Marmara Sea and Çanakkale in the south. It is located between 40° 36' and 41° 31' north latitudes and 26° 43' and 28° 08' east longitudes (URL 1). The average rainfall in the area is 598.3 mm, the average minimum temperature is 1.8°C, the average highest temperature is 28.1°C, and a cool and less rainy Mediterranean climate prevails.

Figure 1: The Location of The Playgrounds Examined Within The Scope of The Research (URL 2)

Literature research, field study, analysis, and evaluation methods were used in the study. In this context, after literature research and the principles of children's playground planning and design were revealed, children's playgrounds in Tekirdag city center were examined. The vegetation of the children's playground was determined by on- site inspections and an observation form was filled for each area. According to the observation form created, the plants in the playgrounds were evaluated in terms of their design features and the contributions of the plants to the children's playground were revealed. In terms of plant design, considering the functional contributions of plants, the benefits of limitation, orientation, shading, shielding and highlighting were evaluated. While determining the contribution to the game, the use of the plants in the playgrounds was evaluated according to 8 criteria, considering the effect of the dendrological properties of the plants on the children (Table 1). In addition, using the studies of Özgen (1987), Seçmen and Leblebici (1987), Baytop (1997), Yılmaz et al. (2006), Yücel (2008), Bıçakçı et al. (2009), Çeter (2011), Gemici (2011), Altay et al. (2015), the poisonous, allergenic and thorny plant taxa were investigated. As a result of the research, suggestions were presented to eliminate the deficiencies identified and to shed light on the children's playgrounds to be created in the future.

Table 1: The Effects of Plant Material in Children's Playgrounds in Terms of Playing

No	Features	Effect on playing
1	Color	Has an interesting color
2	Texture	Hard, soft, pricking etc.
3	Smell	Aromatic plants with fragrant leaves or flowers
4	Space creation	Create tunnels, walls, fences, rooms and similar spaces
5	Plant parts that make the area eligible for playing	Has interesting leaves, fruits, flowers, seeds and shoots

6	Dynamism	Waves in the wind
7	Seasonal change	Has an attractive appearance throughout the year
8	Edibility	Has interesting flavors

3. Results

In this research, 28 plant taxa were identified in the playgrounds. Of these taxa, most of which are exotic plants (75%), 1 is genus, 21 are species, 1 is subspecies, 1 is variety, and 4 is cultivar. The dominant species in the area are *Platanus orientalis* and *Rosa* sp. Other common plants are *Nerium oleander*, *Pyracantha coccinea*, *Robinia pseudoacacia* and *Robinia pseudoacacia* cv. "Umbraculifera". In these areas, where the composition and density of species is quite low, the plants are predominantly woody. Some of the children's playgrounds do not have any trees, while others mostly contain similar species (Table 2).

It has been observed that, in terms of design principles, the functional contributions of plants are the most considered ones. In this context, it has been observed that the most benefited effect of the plants in the area are limitation and shading. In green areas, borders are emphasized mostly with bush- shaped plants (*Buxus sempervirens* cv. "Suffruticosa", *Cotoneaster horizontalis*, *Euonymus japoncius*, *Euonymus latifolius* cv. "Aurea", *Juniperus horizontalis*, *Nerium oleander*, *Photinia serrulata*, *Pittosporum tobira* cv. "Nana" *Pyracantha coccinea*, *Rosa* sp. and *Yucca gloriosa*) and shaded places are created locally with deciduous species (*Acer negundo*, *Morus alba*, *Platanus orientalis*, *Pyrus communis*, *Robinia pseudoacacia* and *Ulmus minor*) species (Table 2).

Although the contribution of natural areas to the development of children is known, it is seen that the existing areas do not show a potential to support children's communication with nature. In Table 2, the contribution of plants to the game was determined by making use of the different features of the plants and it was aimed to contribute to the children's learning about nature and gaining different experiences.

Table 2: Ornamental Plants and Plant Design Features and Their ontribution to The Game in The Children's Playgrounds of The Province of Tekirdag

Latin Name	Design Features	Contributions to the Playground	Research Areas								
			RCP	ABP	SP	KSSP	MEP	FSMP	GOP	BMP	MP
											
Abelia x grandiflora	Limitation	3, 7	✓								
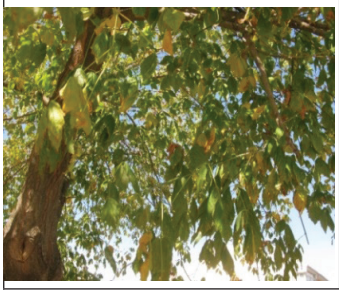											
Acer negundo	Shading	5, 6, 7									✓
											

Buxus sempervirens cv. "Suffruticosa" 	Limitation	4	✓								
Cotoneaster horizontalis 	Limitation	1, 2, 4, 7	✓								
Cotoneaster lacteus 	Shielding	1, 2, 4, 7		✓							
Eriobotrya japonica 	Orientation	5, 8		✓							

Euonymus japoncius 	Limitation	2				✓					
Euonymus latifolius cv. "Aurea" 	Limitation	1, 2, 4	✓								
Hibiscus syriacus 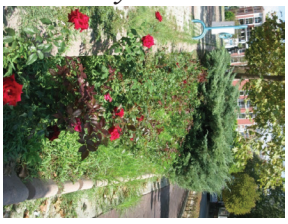	Limitation	7			✓						
Juniperus horizontalis 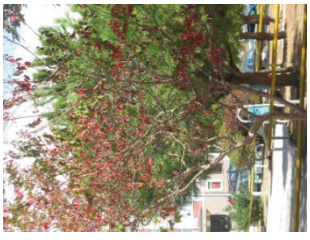	Limitation	2, 4			✓						

Lagerstroemia indica 	Highlighting	1, 5, 7								✓	
Magnolia grandiflora 	Highlighting	4		✓							
Morus alba 	Shading	4, 7, 8			✓						
Nerium oleander 	Limitation	-	✓			✓					

Photinia serrulata 	Limitation	1, 3, 4, 7	✓								
Picea pungens 	Shielding	2	✓								
Pinus brutia 	Shading	2					✓				
Pinus nigra ssp. *pallasiana* 	Shielding	2				✓					

Pittosporum tobira cv. "Nana" 	Limitation	2, 4		✓							
Platanus orientalis 	Shading	4, 5, 6, 7			✓				✓	✓	
Pseudotsuga menziesii var. *viridis* 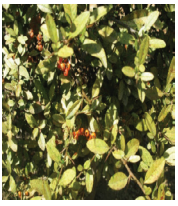	Shielding	2	✓								
Pyracantha coccinea 	Limitation	-				✓				✓	

Pyrus communis 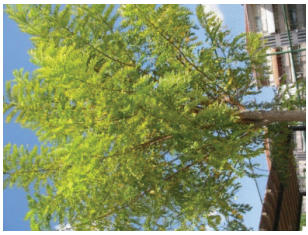	Shading	5, 7, 8	✓								
Robinia pseudoacacia 	Shading	-						✓			✓
Robinia pseudoacacia cv. "Umbraculifera" 	Shading	7						✓			✓
Rosa sp. 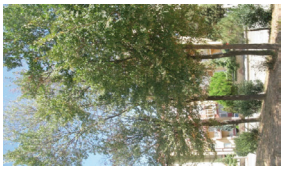	Limitation	-	✓		✓	✓					

Ulmus minor 	Limitation	4, 6, 7				✓					

4. Conclusion and Recommendations

Children's playgrounds, which form an important part of urban green areas, contribute to both the physical and spiritual development of children and the ecology of cities. One of the most important issues in children's playground designs is the plant arrangement. In today's current practices, it is striking that the necessary care is not given to children's playgrounds and the regulations are insufficient. In the children's playgrounds of the province of Tekirdag, which is the subject of the research, the plant material is quite insufficient in terms of both quality and quantity.

Children's playgrounds should be designed to appeal to the five senses and increase the perceptual awareness of children (Uslu and Shakouri, 2012; Çelik et al., 2015). Plants with warm color leaves, flowers and fruit, such as *Malus* sp. and *Viburnum* sp. are perceived more quickly and allow the garden to be perceived with the sense of sight. Plants that make noise with the wind movement, such as *Bambusa* sp., *Pinus* sp. and *Populus* sp., allow the garden to be perceived with the sense of hearing. Aromatic plants, such as *Jasminum* sp., *Syringa* sp., *Laurus* sp., *Lavandula* sp., *Lonicera* sp. and *Rosmarinus* sp., activate the sense of smell; plants with edible fruits, such as *Cornus* sp., *Malus* sp. and *Prunus* sp., activate the sense of taste; and plants with hairy, fleshy or different textured leaves, activate the sense of touch while perceiving the area. The use of these plants in the design of the research area will increase children's awareness of the environment they live in.

In landscape arrangements, designs suitable for the aesthetic and functional characteristics of plants increase the success of the applications. In the study area, it is seen that plant design principles are not considered at all, and in the bordering and shading uses, there are thorny shrubs such as *Pyracantha coccinea*, *Rosa* sp. and *Yucca gloriosa* and poisonous shrubs such as *Nerium oleander* as well as bee hosting plants such as *Robinia pseudoacacia*. When designing plants in playgrounds, using plants that may negatively affect the safety of children should be avoided. Having *Abelia* sp., *Artemisia* sp., *Buddleia* sp., *Cistus* sp., *Philadelphus* sp., *Pittosporum* sp., *Symphoricarpus* sp., shrubs and trees providing a source of life and food for birds such as *Acer* sp., *Betula* sp., *Carpinus* sp., *Celtis* sp., *Eriobotrya* sp., *Fagus* sp., *Fraxinus* sp., *Malus* sp., *Prunus* sp., *Tamarix* sp. and *Tilia* sp. will support wildlife in these areas and teach children the natural life. The plants to be used should create spaces which allow children benefit from sunlight sufficiently beside providing environmental control against wind, reflection, light, and temperature.

As a result of the observations made in the research area, it has been revealed that the green space potential of the spaces is quite low and that they lack arrangements that will contribute to physical and spiritual development of children. It will contribute to the development of children if local governments and planners establish existing playgrounds and newly designed spaces as nature- related playgrounds.

References

Aklıbaşında, M., Tırnakçı, A. and Özhancı, E. (2018). Çocuk oyun alanlarının önemi ve tasarım kriterlerinin Nevşehir kenti örneğinde irdelenmesi. *İnönü Üniversitesi Sanat ve Tasarım Dergisi*, 8(*17*), 59-71.

Altay, V., Keskin, M. and Karahan, F. (2015). An assessment of the plant biodiversity of Mustafa Kemal University Tayfur Sokmen campus (Hatay- Turkey) for the view of human health. International Journal of Scientific and Technological Research, 1(*2*), 83-103.

Baytop, T. (1997). Türkçe bitki adları sözlüğü. Ankara: Türk Dil Kurumu Yayınları.

Bıçakcı, A., Altunoğlu, M. K., Bilişik, A., Celenk, S., Canıtez, Y., Malyer, H. and Sapan, N. (2009). Türkiye'nin atmosferik polenleri. Asthma Allergy Immunology, *7*, 11-17.

Coe, D. P., Flynn, J. I., Wolff, D. L., Scott, S. N. and Durham, S. (2014). Children's physical activity levels and utilization of a traditional versus natural playground. Children Youth and Environments, 24(*3*), 1-15.

Çelik, A. (2012). Okul öncesi eğitim kurumlarında açık alan kullanımı: Kocaeli örneği. Atatürk Üniversitesi Ziraat Fakültesi Dergisi, 43(*1*), 79-88.

Çelik, A., Ender, E. and Akdeniz, N. S. (2015). Engelsiz parklarda peyzaj tasarımı. International Journal of Agricultural and Natural Sciences, 8(*2*), 5-11.

Çeter, T. (2011). Uzun mesafeli polen taşınması ve küresel ısınmanın polen allerjenitesi ve dağılımına etkisi. Journal of Allergy, 4 (*1*), 25-30.

Çukur, D. and Özgüner, H. (2008). Kentsel alanda çocuklara doğa bilinci kazandırmada oyun mekanı tasarımının rolü. Türkiye Ormancılık Dergisi, 9(2), 177-187.

Erdönmez, İ. M. Ö. (2007). İlköğretim okul bahçelerinde peyzaj tasarım normları. Journal of the Faculty of Forestry Istanbul University, 57(*1*), 107-122.

Fjørtoft, I. and Sageie, J. (2000). The natural environment as a playground for children: Landscape description and analyses of a natural playscape. Landscape and urban planning, 48(*1-2*), 83-97.

Fjørtoft, I. (2004). Landscape as playscape: The effects of natural environments on children's play and motor development. Children Youth and Environments, 14(*2*), 21-44.

Gemici, Y. (2011). Atmosferik koşullarının polen dağılımına etkisi. Journal of Allergy, (*1*), 31-37.

Küçükyağcı, P. Ö., Atasayan, Ö. and Oktay, S. Ö. (2015.28-30.05). Çocuk oyun alanı tasarımlarında sürdürülebilirlik. 2nd International Sustainable Buildings Symposium, 572-576, Ankara.

Moore, R. (2014). Nature play & learning places. Greating and managing places where children engage with nature. Raleigh, NC: Natural Learning Initiative and Reston, VA: National Wildlife Federation Version 1.2. ISBN 978-0-9907713-0-2.

Özgen, Y. (1987). Peyzaj düzenlemelerinde kullanılan insan sağlığına zararlı bitkiler. İstanbul Üniversitesi Orman Fakültesi Dergisi, Seri: A, 37 (*1*), 89-97.

Özgen, Y. and Aytuğ, A. (1992). Kullanıcı eğilimleri açısından çocuk oyun alanları ve araçları üzerine bir inceleme. *İstanbul Üniversitesi Orman Fakültesi Dergisi*, 42(*2*).

Özgüner, H. and Şahin, C. (2009). Isparta kent merkezindeki çocuk oyun alanlarının mevcut durumu ve çocukların bu alanlara karşı davranış biçimleri. Türkiye Ormancılık Dergisi, 10(*1*), 129-143.

Pouya, S., Bayramoğlu, E. and Demirel, Ö. (2016). Doğa ile uyumlu fiziksel engelli çocuk oyun alanları. Mimarlık Bilimleri ve Uygulamaları Dergisi, 1(*1*), 51-60.

Seçmen, O. and Leblebici, E. (1987). Yurdumuzun zehirli bitkileri. İzmir: Ege Üniversitesi Fen Fakültesi Kitaplar Serisi No: 103.

Timur, U. P., Erzin, P. E., Aytaş, İ. and Timur, Ö. B. (2018, 28-30.06) Çocuk oyun alanlarında çocuk- oyun- doğa bütünleşmesi için tasarım önerileri. Uluslararası Kentleşme ve Çevre Sorunları Sempozyumu, Eskişehir.

Turgut, H. and Yılmaz, S. (2010, 20-22.05). Ekolojik temelli çocuk oyun alanlarının oluşturulması. III. Ulusal Karadeniz Ormancılık Kongresi, Cilt: IV, 1618-1630

URL 1 http://www.tekirdag.gov.tr/cografi-durumu, date of access: 08.12.2021.

URL 2 https://earth.google.com/web/search/tekirdag, date of access: 13.12.2021.

Uslu, A. and Shakouri, N. (2012). Horticulture therapy for the mental and physical disabled. Kastamonu Üniversitesi Orman Fakültesi Dergisi, 12(*1*), 134-143.

Veitch, J., Ball, K., Crawford, D., Abbott, G. R. and Salmon, J. (2012). Park improvements and park activity: a natural experiment. American Journal of Preventive Medicine, 42(*6*), 616-619.

White, R., & Stoecklin, V. (1998). Children's outdoor play & learning environments: Returning to nature. Early Childhood News, 10(*2*), 24-30.

Yılmaz, H., Akpınar, E. & Yılmaz, H. (2006). Peyzaj Mimarlığı Çalışmalarında Kullanılan Bazı Süs Bitkilerinin Toksikolojik Özellikleri. Süleyman Demirel Üniversitesi Orman Fakültesi Dergisi, *1*, 82-95.

Yücel E (2008) Tıbbi Bitkiler 1 (A- L). Çetemenler Yayınevi, ISBN: 978- 975- 93746- 3- 1, Eskişehir.

CHAPTER X

REFUNCTIONING OF AN INDUSTRIAL HERITAGE BUILDING: A PROPOSAL FOR İZMİT SEKA GRINDING MILL BUILDING AS AN ART MUSEUM

Asst. Prof. Dr. Cahit Arsal ARISAL
İstanbul Gedik Üniversitesi, İstanbul, Turkey,
e-mail: arsal.arisal@gedik.edu.tr
Orcid No: 0000-0003-1386-7730

1. Introduction

The foundation of the first factory that produces paper dates back to the 1930s after the establishment of the Republic. Mehmet Ali Kağıtçı, who was a paper engineer, was in charge of the establishment of the factory. The foundation of the first factory was laid in 1934, and, in the 1940s it became a larger building complex with the newly added facilities. (Kocabaşoğlu et al., 1996).

SEKA Cellulose and Paper Factories founded by Mehmet Ali Kağıtçı in 1936 with the name of Sumerbank Paper and Board Factory in İzmit, Kocaeli, was the first paper production facility of Turkey (Kocabaşoğlu et al., 1996). The factory was not only a production facility but also an important symbol of the modernization of Turkey with the residential buildings, sport facilities, movie theatre, apprentice school, kindergarten, the newspaper - SEKA Post, etc. (Sarıoğlu, 2013). With all these features, SEKA was going to be not only a factory, but also an important element which was going to serve as "dough of the civilization" for Turkey (Kocabaşoğlu et al., 1996). The factory had maintained this mission until it was made over to Kocaeli Metropolitan Municipality (URL-1).

The Factories were designed and constructed by a German Company named *Gutcoffnungshütte (G.H.H.)* according to the plans designed by also a German company named *Voith* in 1934 and kept operating from 1936 to 2005 (Kocabaşoğlu et al., 1996). The facility, which became the property of Kocaeli Metropolitan Municipality after 2005, was registered with the decision of Bursa Cultural and Natural Heritage Conservation Board, dated 11.02.2005 and numbered 412.

Along with the decrease in the production or end of the production, new spatial developments start in the cities where industrial areas are located. The reuse of non-functional heavy industry and port areas has been adopted to meet the new urban space needs emerging with growth as an extremely economical and environmental policy, both for the trade of historical images, which is now important for cities, and for the more balanced use of diminishing environmental resources (Tolga, 2006). Seka area as a non-functional industry area and a registered site by the conservation board is still in need of transformation.

In this study, the Grinding Mill Building, - property of Kocaeli Metropolitan Municipality - which is designed by Restart Architecture and Restoration is covered (Figure 1). The main aim of the project is to include the building which has been left unusable since 2005 to the city life again as a production facility but this time with a different program as an art museum.

Besides the traces of the existing building and the period photographs; the measured drawings, reconstitution and restoration projects were used with the permission of the designer. Measured drawings were approved by Kocaeli Cultural and Natural Heritage Conservation Board with the decision dated 27.04.2018 and numbered 3467. The reconstitution and restoration projects were approved by the board with the decision, dated 26.10. 2018 and numbered 3495. The consultancy of the projects is also provided by the author of this article.

Figure 1- *Aerial Photo Of The Site (Google Earth, 2018).*

2. Current Situation

Grinding Mill Building of the SEKA Paper Factory, which is located in İzmit, Kocaeli on the city block 3317 and parcel 1, has a location that is embracing the city center from the east of the factory. The building is located at a central point and it is convenient for pedestrian and public transport and private car access as there is a tram stop in the south and a parking lot in the east. The Science and Paper Museums are just to the west of the building. The Grinding Mill Building has been left idle since 2005 when the factory ended its production (Figure 2).

Figure 2-The Grinding Mill Building

The building, which is located on a flat area, consists of two separate construction systems and two parts. There is a two -storied building which has a reinforced concrete structure on the South and the mill building has steel construction with a semi basement floor. In the reinforced concrete structured part, there is a mezzanine floor just above the first floor with steel construction. The building is detached from all directions and has entrances from the east, south and west facades. The structure is made of brick wall between reinforced concrete and steel construction. The roof is coated with slaty membrane over steel construction and has a slope to the east and west.

While the reconstitution projects were being prepared, the addition of this two-storied part (Figure 3) was accepted as the second period and reconstitution projects were prepared for two periods.

Figure 3- *Concrete addition on the left*

The room in the north was created by a wall which was built afterwards, and an inauthentic steel staircase can be seen descending from the south of the wall. The staircase that goes down to the basement from the middle part on the western wall is the authentic staircase of the building (Figure 4, Figure 5).

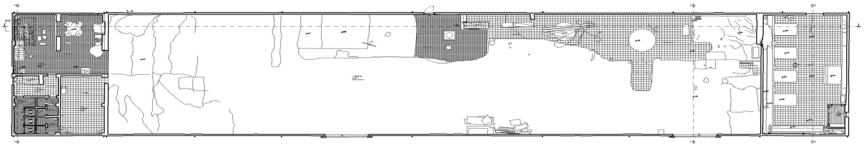

Figure 4-*Measured drawing of the ground floor of the building*

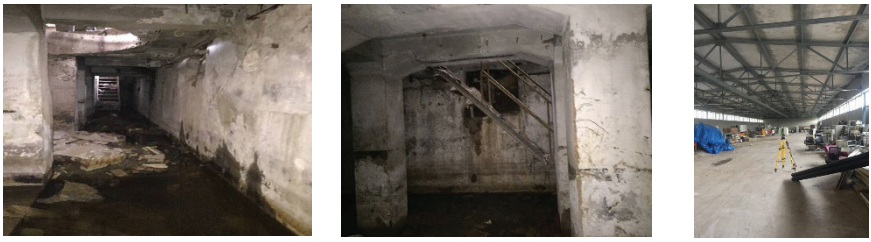

(a) (b) (c)

Figure 5- *Ground Floor Interior (a). Staircase descending to basement floor level (b), (c)*

The semi- basement floor of the building was flooded due to the underground waters and because of the areaways subsequently closed. Although the water was drawn by pumps many times, the next day it was observed that the water on the floor was same as the previous day (Çelik Arısal, 2018 [a]).

The entire building was scanned with a laser scanner and aerial shots were taken with a drone (Figure 6). Measured drawings were started based on the data obtained by these methods and traditional measurement methods were also used for the details (Çelik Arısal, 2018 [a]).

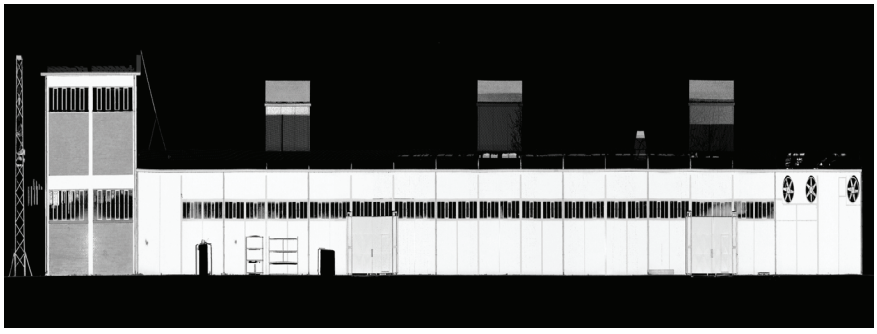

Figure 6- *Laser Scanner Data Of The East Elevation*

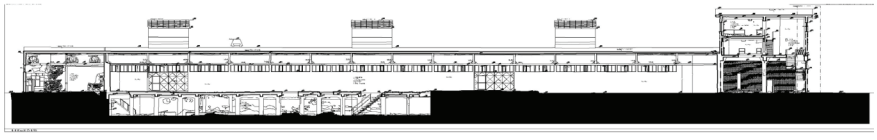

Figure 7- *Longitudinal Section*

3. Reconstitution Phase

The construction process of the building consists of two separate periods. The first period has a single storied steel building which has a partial basement floor. The second period has an addition of a two storied rein-forced concrete building. Walls of the both buildings are made of bricks between the structural elements (Çelik Arısal,2018 [b]).

***Figure 8**- Photo showing the first reconstitution period (Mehmet Ali Kağıtçı Library Archive).*

***Figure 9**- Photo showing the second reconstitution period (Mehmet Ali Kağıtçı Library Archive).*

The interventions that the building has undergone until today, have partially affected the plan scheme and facade identity. In the reconstitution projects for both periods, all the inauthentic additions were removed and also material losses on windows and doors, fall off of the plasters due to atmospheric conditions and negligence are detected on the basis of both measured drawings and old photographs. As a result, the recon-stitution projects were designed in accordance with its original form and design (Çelik Arısal, 2018 [b]).

3.1. Facade Identity

On the south facade, where the two-storied reinforced concrete addition (second period) is located today, it can be seen in the old photographs that there were strip windows at +2.90 level in the first period of the building. So, in the drawings of the first reconstitution period, the concrete building was removed and south facade of the building was reconstituted protecting the original facade identity of the first period also based on the old photographs (Figure 8). With the addition of the two-storied building, the strip windows on the south were blocked off (Figure 9). This facade represents the second period of the building which is still in the same condition today and it has an identity consisting of brick walls with two storeys which have iron-jointed strip windows. It has been determined that the windows are locally made shorter in the Y direction in order to pass the beam of the halfpace staircase which ascends to the first floor from the ground floor on the western part. It is thought that the two single iron doors which are nearly in the middle of the south facade were opened later within the scope of the second period (Çelik Arısal, 2018 [b]).

The eastern facade is the main entrance facade of the building. Today, there are two iron sliding doors. However, it has been seen that there are eight iron bolt doors in the old photographs (Figure 8). All of the doors in the original facade identity of the first period were reconstituted as it was in its original form. While the three ventilation shafts, seen from this facade, look original, another small one which could not be seen in the photographs was removed from the reconstitution projects. It was seen that the three ventilation flaps were built later, and they were removed from the reconstitution project as they did not have a place in the original facade identity. It is seen that the iron doors were reduced to two in the second period and all of the doors in the facade identity of the second period have been reconstituted as in its period (Figure 3, Figure 9, Çelik Arısal, 2018 [b]).

On the north facade; a single winged window (second period), known to have been added later, can be seen today. While this window was removed for the first period reconstitution project, an iron bolt door and on the upper side of the door, the strip windows are added to reach the original facade identity (Figure 10).

In order to ensure the identity of the original western facade, old photographs and the traces of the building itself were examined (Çelik Arısal, 2018 [b]). For the first period, the door in the middle, the windows on the northern part of the western façade were removed. Also, an iron staircase which was made for access to the roof was added to the northern part of the wall same as on the southern part of the wall to reach the original facade identity of the first period of reconstitution. In the second period of the reconstitution, the strip windows on both levels of the con-crete building were reconstituted (Çelik Arısal, 2018[b]).

Figure 10 *– Photograph taken from the North – East of the building (Mehmet Ali Kağıtçı Library Archive).*

Restoration Phase

While preparing the restoration project for the building, the data obtained from the survey works of the building, the restitution projects and the criteria needed for its new function were taken into consideration.

3.2. Removed Interventions

The partial basement of the building, which is located under the single-storied steel building, is preserved with its original plan scheme. In the basement floor, which was left as a single space, two stairs were identified in the survey studies. Since the stairs on the northern part of the building were not included in the restitution projects, they

were also removed in the restoration phase. And the original staircase of the building, which was attached to the western facade, was included in the restoration project (Figure 11). Since the current state of the staircase has lost its structural properties and does not provide sufficient security for the users, it has been suggested to re-project it from steel construction keeping its original position.

Figure 11 *– The staircases that are re-projected in the restoration phase*

It is known that the concrete part of the building was added in the second reconstitution period, but within the scope of the requirements of the building which is aimed to be opened to public use with the function of an art museum, the spaces of this part were used out of necessity and the restoration projects were carried out in this direction (Çelik Arısal, 2018 [b]).

In this space; it has been determined that access to the first floor is provided by two stairs (Figure 12). The stairs on the south wall of the building affect the dimensions of the windows of the south façade. The second staircase, which corresponds to the middle of the north-south axis of the building, affects the functional use of the space and

Figure 12 – *The two staircases ascending to the first floor of the reinforced concrete part*

is not functional due to its inappropriate height. For these reasons, it was decided to remove both stairs and design a new staircase with the original railing detail which serves the current function of the building (Çelik Arısal, 2018 [b]).

A steel mezzanine floor can be seen over the first floor in the two-storied reinforced concrete part which was found to have been built later. While the restoration projects were being prepared, the steel mezzanine floor was removed based on the reconstitution projects of the building (Çelik Arısal, 2018 b).

Figure13– *Mezzanine floor which is removed in the restoration projects*

There are two iron doors on the south façade of the building (Figure 14). These doors were moved to the east facade for the security issues due to the new function of the building.

Figure 14– *South Facade Of The Building*

In the restoration projects, the toilet and shower units located in the east of the two-storied reinforced concrete part were also removed because of the new function of the building (Çelik Arısal, 2018 [b]).

On the north side of the single-storied steel part of the building, there is a second space created with a divider wall (Figure 15). According to the reconstitution projects, this dividing wall and the connecting western door were removed and the building has been brought back to the original plan scheme and facade identity.

Figure 15*- The additional wall creating a separate space*

4.2- Refunctioning The Building As An Art Museum

Restoration projects have been prepared for the building, which is the property of Kocaeli Metropolitan Municipality to be used as an 'art museum'. In this context, the original form was preserved on the floor plans and facades, and restoration decisions were taken on the basis of the reconstitution projects of the building.

4.2.1- Partial Basement Floor

In order to eliminate the water intake problem in the basement floor plan, a drainage line was created and insulating the building for the foundation was proposed. The basement floor is planned to serve as a storage for the exhibition hall on the ground floor. Also the technical spaces will be located here. The additional staircase in the north direction seen in the measured drawings was removed, and the original staircase on the western wall was redesigned with a steel construction (Çelik Arısal, 2018[c]).

4.2.2. Ground Floor

Since the Seka Art Museum is designed to exist in one of the first production facilities of the republic, it was designed with reference to the production of the past, with production-oriented spatial decisions (Figure 16).

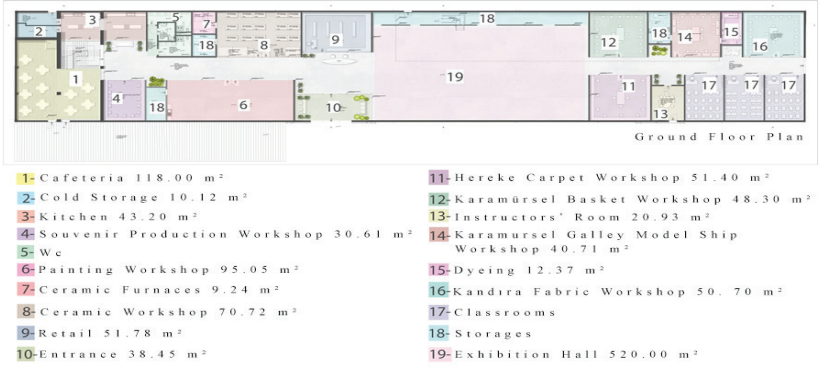

Figure 16 *– Ground Floor Plan*

The information desk is located just across the glass section where the main entrance of the building is located. The entrance located with the aim of being able to dominate the corridors opening to both the exhibi-tion space and the workshops is the only spot where the building accepts guests for security reasons. The other doors will serve as a controlled entry-exit (Figure 16 (10), Figure 17).

Figure 17 *– Perspective looking at the entrance*

The exhibition area is flexibly designed for a multifunctional exhibition layout. The rail panel system designed in the exhibition area and the exhibition elements obtained from the cubes serve the functional use of the space. It helps with the aesthetic appeal of the space which is intended to be able to serve several exhibitions simultaneously and by hiding the rails inside the floors, the roof construction was exposed in its original form (Figure 156 (19), Figure 18).

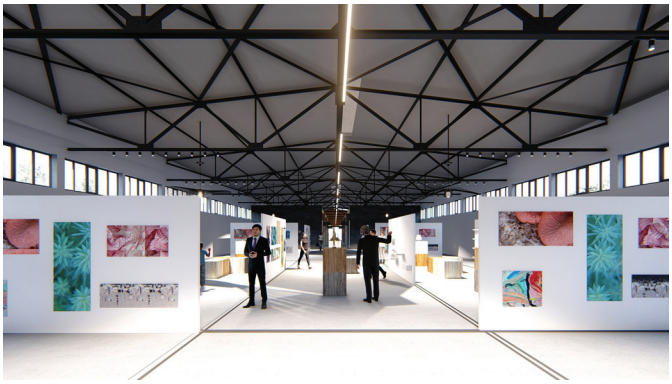

Figure 18*– Exhibition Area*

There are workshops located on the right and left on the corridor extending from the exhibition space to the north and south. Lighting elements in the same direction emphasizing the corridor axis provide artificial light, while the skylights of the roof placed on the corridors provide natural lighting. In order for the rows of windows on the east and west facades to illuminate the corridors as well, the corridor facades of the workshops were completely processed with glass partitions walls. iron. The names of the workshops will be written on these plates (Figure 16, Figure 19).

Figure 19*- Workshops seen from the corridor*

The kitchen workshop located in the cafeteria overflows into the steel structure from the north part of the space. This overflowing part creates a viewing space with the glass partition placed in front of it. So, the kitchen workshops carried out inside or the use of the kitchen in daily routine can be watched by the guests (Figure 16(3), Figure 20).

Figure 20 *– Kitchen Workshop Area*

The classrooms are designed to serve as three separate spaces or they can be combined to form a single larger classroom. Although the walls of the workshops facing the corridors are planned to be completely transparent, there is occasional use of opaque glass, which is determined according to the needs inside the space. The opaque glasses used for the classrooms are placed on the axis where the teachers' desks are located (Figure 16, Figure 21).

***Figure 21** – Classrooms*

The cafeteria, which is designed on the ground floor of the two-storied reinforced concrete part of the building, is also planned in accordance with interactive service with a kitchen where the local delicacies of Kocaeli will be exhibited. The terrace area in the east was also functioned to serve the cafeteria (Figure 16, Figure 22).

***Figure 22** – View from the cafeteria*

4.2.3. Upper Floor

On the upper floor of the reinforced concrete part of the building, there is Mustafa Kandıralı Music Workshop and the units belonging to the workshop. While arranging the spaces on this floor, the design is created by considering the relationship of the music workshop units with each other in a technical sense. Transparent dividers have been placed between the rehearsal room and the recording room, and a musical instrument warehouse that can be easily accessed from the classroom has been planned (Figure3)2

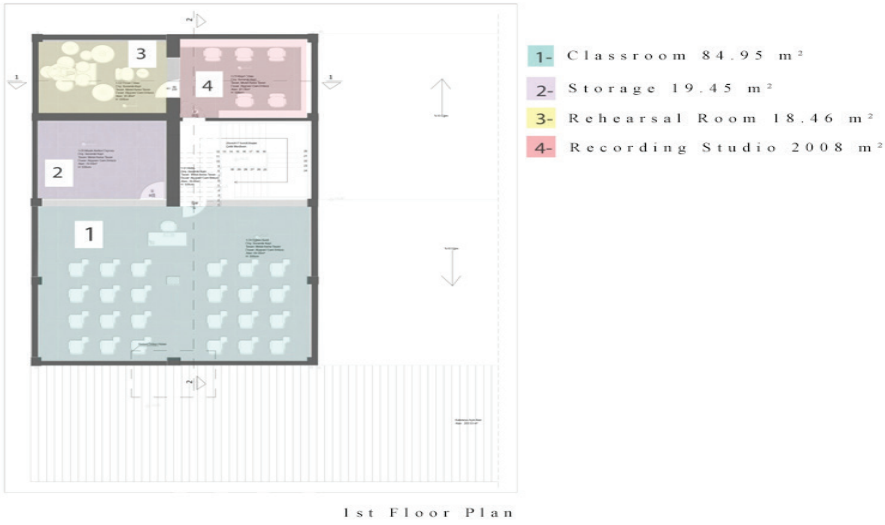

Figure 23 – *First Floor Plan*

4.2.4. Landscape and Environmental Design Of The Building

The fact that the Seka Grinding Mill Building is a registered industrial heritage has guided the design to preserve its rational identity on the facade and not to ruin its original design. In order to emphasize the main entrance of the building, orientation axes were designed with the land-scape and an arch which is designed disconnected from the building. The cubes formed in the north and south of the arch create social reinforce-ment spaces, and the green areas that are attached provide orientation and landscape integrity (Figure 24).

Figure 24 *– Landscape and the entrance of the building*

4. Conclusion

After Seka was closed in 2005 and transferred to Kocaeli Metropolitan Municipality, an industrial facility in the city fell into an inactive and unproductive state. The transformation of the area as a public space started with an arrangement of a recreational area under the name of Seka Park in 2008. Then in 2016, one of the most important production-oriented struc-tures of Seka was transformed into Paper and Science Museums (URL-2, 2022). The traces of paper production in Seka have been symbolic and to a limited extent then.

limited extent since then. The contribution of the area to the city life and culture is provided in a limited way through only a recreational area, cafeterias, two museums and such spaces. Due to the problems brought about by the transportation plans of the city, the site is no different from a social reinforcement area in the periphery of the city. This is because transportation by vehicle is almost compulsory although it is located in the city.

Seka Grinding Mill Building has a privileged location as it is located in the eastern part of the Seka complex, facing the city center. The wish for a production-oriented design by Kocaeli Metropolitan Municipality was the most important starting point for the restoration projects. With Kandıra Fabric, Hereke Carpet, Karamürsel Basket Workshop, Karamürsel Galley Model Ship, painting, ceramic, music workshops and classrooms, a restoration project in which production plays a leading role was designed. It was hoped that the production-oriented setup provided by the design would be a new way to reach new factories; new living spaces and cultures from these factories with production branches that were aimed to be born from the ashes of an area that was once the 'dough of the civilization' and to be passed on to future generations, just like the master-apprentice relationship as we had in the past.

Acknowledgements

Unless stated otherwise, all the visuals of the projects were produced from the measured drawings approved by Kocaeli Cultural and Natural Heritage Conservation Board with the decision dated 27.04.2018 - numbered 3467, and the reconstitution - restoration projects with the decision dated 26.10.2018 - numbered 3495. Elif Çelik Arısal is the designer of the architectural projects and Arsal Arısal is the project consultant of the design office. Unless stated otherwise, all the photographs belong to Elif Çelik Arısal – Arsal Arısal archive and period photographs belong to Mehmet Ali Kağıtçı Library Archive. The sources of Elif Çelik Arısal mentioned in the text and in the references section, refer not to a publication but to the projects mentioned above.

References

Çelik Arısal, E. (2018 [a]), *Measured Drawings - Surveys, Restart* Architecture and Restoration, Kocaeli *(Projects are approved by Kocaeli Cultural and Natural Heritage Conservation Board with the decision dated 27.04.2018 and numbered 3467).*

Çelik Arısal, E. (2018 [b]), *Reconstitution Projects,* Restart Architecture and Restoration, Kocaeli *(Projects are approved by Kocaeli Cultural and Natural Heritage Conservation Board with the decision, dated 26.10. 2018 and numbered 3495).*

Çelik Arısal, E. (2018 [c]), *Restoration Projects*, Restart Architecture and Restoration, Kocaeli *(Projects are approved by Kocaeli Cultural and Natural Heritage Conservation Board with the decision, dated 26.10. 2018 and numbered 3495).*

Google Earth (2018), Seka Aerial Photograph.

Kocabaşoğlu, U., Bulutgil, A., Çiloğlu, F., Binbaş, İ.E., and Şeker, N. (1996), *Seka Tarihi, Türkiye Selüloz ve Kağıt Fabrikalarının Tarihsel Gelişimi*, Ankara: Seka Genel Müdürlüğü Yayınları.

Sarıoğlu, M. (2013), *Seka Postası'nın Işığında İzmit'te Kültürel Yaşam*, Kocaeli: Kocaeli Büyükşehir Belediyesi Kültür Yayınları

Tolga, H.B., (2006), *Endüstriyel Alanların Dönüşümü, Kentsel Mekâna Etkileri: Beykoz Kundura ve Deri Fabrikası İçin Bir Dönüşüm Senaryosu,* İstanbul: Yıldız Teknik Üniversitesi, Fen Bilimleri Enstitüsü, Mimarlık Anabilim Dalı, Yüksek Lisans Tezi.

URL-1 https://www.hurriyet.com.tr/ekonomi/seka-izmit-isletmesi-belediyeye-devrediliyor-293296 (Date of Access 10.02.2022).

URL-2 http://sekakagitmuzesi.com/#anasayfa (Date Of Access10.02.2022).

CHAPTER XI

THE EFFECT OF URBAN TRANSFORMATION ON LANDSCAPE; THE EXAMPLE OF NİĞDE EFENDİBEY NEİGHBORHOOD

Assoc. Prof. Dr. Gülden SANDAL ERZURUMLU
Niğde Ömer Halisdemir University, Faculty of Architecture, Department of Landscape Architecture, e-mail: gpeyzaj@gmail.com
ORCID: 0000-0001-9664-2902

Introduction

The city is a physical, spatial and social environment that is formed as a result of the accumulation of physical, social and cultural processes belonging to different periods during its existence (Birol, 2007). Urban transformation includes the risky soil structure of a part or a significant part of the city, systematically determining the risk values of the existing building stocks against possible earthquakes, demolition in a possible earthquake and damaging other structures in the vicinity while being demolished. It is expressed as one of the public works carried out in order to take the ground and risky structures out of use and replace them with foundations suitable for the structure of the soil ground, thus minimizing the loss of life and property that may occur in possible earthquakes (Anonim, 2022).

In Niğde, after the First World War and the Second World War, there were periods when urban transformation came to the fore. The construction of the cities destroyed in the wars was planned as an urban transformation, and preserving the cultural and historical values of the cities was a priority (Anonim, 2022a).

The concept of "Urban Transformation" came to our agenda with the Law No. 6306 on the "Transformation of Areas Under Disaster Risk"

prepared in 2012. In this law, there are two definitions called 'Risky Structure' and 'Risky Area'. As a result of the fact that the public began to express the process of making risky buildings resistant to earthquakes with the concept of "Urban Transformation", the law numbered 6306 has been expressed as the Urban Transformation Law (Anonim, 2022a).

Within the scope of urban transformation, the selection of the residences to be proposed to the property owners from regions and places other than the existing properties of the property owners has led to criticism. The weakening of the environment and neighborhood relations in sociological terms in public living areas, and the proposal of places that will not correspond to the full value of the left space, as the real estate value of the buildings will increase more quickly with urban planning, has brought up another problem. Thus, the urban distribution began to progress to areas far from the city center. The buildings close to the city center appear either as commercial areas or as high-cost living areas.

The high demand in the city center caused the construction of multi-storey and successive buildings, and the decrease in green areas. In areas suitable for zoning areas that are far from the center, importance is given to the number and size of green areas. Due to both increasing population and migration, a lot of buildings are needed. Planned and multi-storey new residential areas are being created.

Urban parks are organized in order to serve more people in places where buildings are concentrated. Urban parks have also shaped the changing states of the landscape and the forms of relationship it establishes with the city, in the process spanning from the creation of nature within the city to the debates in which the city is interpreted as a landscape today. However, landscape-oriented urbanism approaches (such as landscape urbanism, ecological urbanism and infrastructural urbanism), which have undoubtedly been on the agenda for the last 20-30 years, have expanded the theory and practice of landscape; Many cities have adopted the necessity of addressing urban development and landscape in an integrated framework (Bütüner ve Sert, 2021).

Ensuring the sustainability of cities with new approaches is not only limited to big cities, but also reflected to developing cities. The city of Niğde does not have enough green space due to its location. Evaluations

have been made about whether the recreational areas built within the scope of urban transformation and to be built in the future are sufficient in number..

Efendibey neighborhood, which was chosen as the research area, was home to unplanned detached houses, animal breeding areas and small agricultural areas before the urban transformation. With the urban transformation, more planned and organized spaces have been created.

Material and Method

Efendibey Mahallesi is located at latitude 37.975948 and longitude 34.681824. As a district/neighborhood, it is connected to Efendibey District and Merkez district. Efendibey Mahallesi GPS coordinates are 37° 58´ 33.4128" and 34° 40´ 54.5664" (Figure 1). (Anonymous, 2022b).

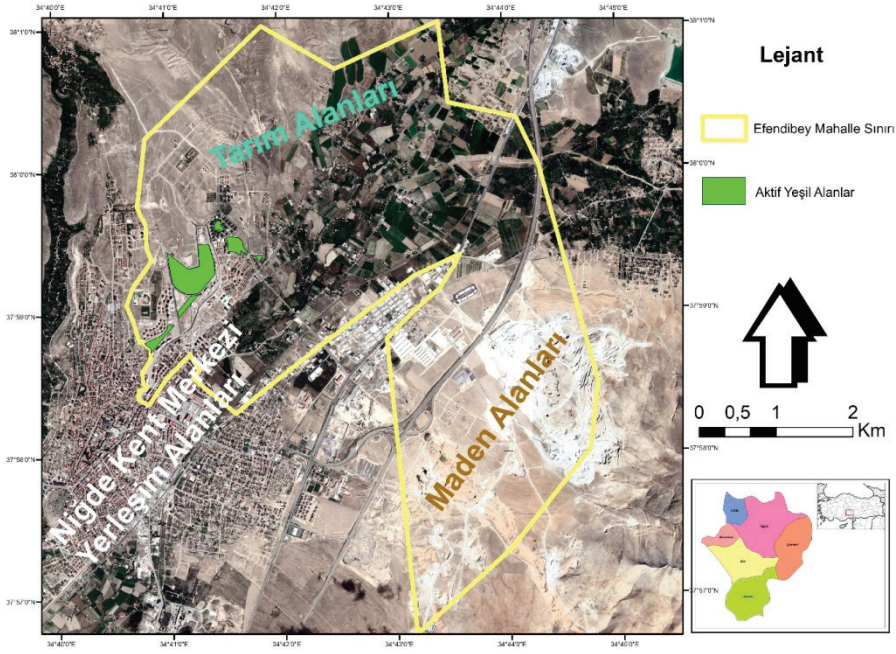

Figure 1. Research Area

Active green area (national garden, residential gardens and neighborhood parks) was determined in Efendibey neighborhood, which is the

research area, and the amount of green area per capita was calculated by proportioning to the population.

The total size of the active green areas (national garden, site gardens and neighborhood parks) in Efendibey District was calculated and evaluated as 330336,42 m^2.

Research Findings

The change of Efendibey neighborhood between 2009 and 2021 has been examined, and it has recently turned into a planned and regular neighborhood with urban transformation (Figure 2).

Figure 2. Images of 2009 and 2021

As seen in Figure 2, while the unplanned and agricultural area is dominant in the image of 2009, it is seen that the planned and active green area is included in the image of 2021. When the population increases in the researched area, the amount of green space will be insufficient.

Looking at the Niğde city data, there are 69 neighborhoods in the city center (Table 1). The most densely populated place is Aşağı Kay-

abaşı, while Efendibey takes the second place. When we look at the borders of Efendibey district, some of them are in the city center and some of them cover the more rural area of the city where the mines are located.

Table 1. Niğde City Central Neighborhoods 2021 population information (TUIK, 2021)

	Neighborhood Name	**Total Population**	**Male Population**	**Female Population**
1	AşağıKayabaşı	36.761	18.484	18.277
2	Efendibey	**23.989**	**11.906**	**12.083**
3	Selçuk	21.837	11.305	10.532
4	İlhanlı	21.675	11.392	10.283
5	Fertek	8.871	2.925	5.946
6	Şahinali	7.456	3.694	3.762
7	İnönü	6.863	3.393	3.470
8	Dere	6.818	3.377	3.441
9	Yenice	5.680	2.742	2.938
10	Yukarı Kayabaşı	5.045	2.506	2.539
11	Şahsüleyman	4.090	2.049	2.041
12	Hürriyet	3.424	1.805	1.619
13	Şehitler	3.284	1.672	1.612
14	Nar	3.167	1.632	1.535
15	Eskisaray	2.515	1.237	1.278
16	Cumhuriyet	2.010	1.059	951
17	Yeni	1.827	910	917
18	Kumluca	1.778	868	910
19	Yeni	1.610	802	808
20	Aşağı	1.575	846	729
21	Burhan	1.487	757	730
22	Yeni Gümüş	1.486	724	762
23	Zafer	1.476	740	736

24	Cumhuriyet	1.431	721	710
25	Hürriyet	1.419	694	725
26	Hürriyet	1.383	722	661
27	Fatih	1.373	722	651
28	Çayır	1.313	659	654
29	Yeni	1.273	672	601
30	Cumhuriyet	1.270	657	613
31	Eski Gümüş	1.266	621	645
32	Cumhuriyet	1.243	619	624
33	Zafer	1.141	560	581
34	Yavuz	1.136	600	536
35	Hürriyet	1.133	604	529
36	Yeni	1.084	563	521
37	Cumhuriyet	1.073	572	501
38	Bahçelievler	1.060	513	547
39	Cumhuriyet	1.036	539	497
40	Milliyet	942	504	438
41	Yeni	938	486	452
42	Esenbey	930	470	460
43	Yukarı	928	463	465
44	Saruhan	920	445	475
45	Hürriyet	912	456	456
46	Aşağı	908	461	447
47	Fatih	867	447	420
48	Yukarı	850	437	413
49	Aşağı	842	434	408
50	Dumlupınar	833	415	418
51	Fevzipaşa	760	368	392
52	Hürriyet	744	364	380
53	Sırali	736	402	334
54	Yeni	726	384	342

55	Devlet	689	349	340
56	Cumhuriyet	681	345	336
57	Yenice	633	317	316
58	Yukarı	502	275	227
59	Songur	420	210	210
60	Hüyük	352	190	162
61	Cumhuriyet	343	170	173
62	Orta	336	163	173
63	Ahipaşa	255	138	117
64	Fatih	253	117	136
65	Balhasan	237	123	114
66	Boğaziçi	230	121	109
67	Hamamlı	191	98	93
68	Kale	142	84	58
69	Alaaddin	51	32	19

Since the boundaries of Efendibey District, which has an area of 26,194,141,40 m^2, are located between the city center settlements and rural settlements, a very small part of the study area; The area of 4,280,747.73 m2 is located within the urban settlement pattern. The total size of the active green areas (national garden, residential gardens and neighborhood parks) in Efendibey District was calculated and evaluated as 330,336.42 m2. The urban settlement structure and therefore active green areas are located close to the city center, as seen on the map, within the housing pattern and serve the individuals there.

Efendibey District, chosen as the study area, is the second largest district among Niğde Merkez districts in terms of population. Urban transformation in Efendibey neighborhood took place approximately in 2015. After 2018, the settlements were completed. When the population change table is evaluated by years, the highest jump occurred in 2019 (Table 2). As the reason for this growth; Urban transformation projects of Efendibey Neighborhood and housing development in residential areas can be shown. In Efendibey neighborhood, the population increased by

only 4953 people from 2019 to 2021. The amount of active green area in the research area was determined as 330,336.42 m^2.

While the amount of green space per capita in 2019 was 17.33 m^2, it was determined as 15.49 m^2 in 2020 and 13.75 m^2 in 2021. It has decreased by 3.68 m^2 in 3 years. If the increase continues in the following years, there will be no green areas after 10-15 years. Within the scope of urban transformation, new settlement areas will not be included in the city center in the research area. With the urban transformation and increasing population, the amount of green space per capita decreases. The population that will increase due to migration or other reasons will also decrease the amount of green space per capita.

Table 2. Efendibey Neighborhood Population Change by Years (TUIK,2021)

Year	**Total Population**
2021	23.989
2020	21.293
2019	**19.036**
2018	15.736
2017	14.634
2016	14.377
2015	14.833
2014	14.697
2013	14.234
2012	14.108
2011	13.721
2010	12.410
2009	11.378
2008	11.001
2007	10.838

However, it may be possible to prefer vacant lands as residential areas in the surrounding area. The fact that Efendibey neighborhood covers the

rural area and there are lands that are not suitable for agriculture will enable this area to be considered as a residential area.

Results

With the decrease in the products and profits obtained from the agricultural activities of the villages around the city of Niğde, migration to the city center started due to unemployment and education. In addition, the population in the city center has increased recently with the arrival of Syrian immigrants and Afghans. The observation and examination studies carried out in the study show that the number of buildings is increasing day by day in the areas open to development and where unplanned urbanization is dominant in the city. Active and passive green areas are given importance while transitioning to planned settlement in areas where zoning has increased.

These approaches have led to the creation of new solutions that provide many benefits to the city. With these approaches, of which we can see design examples in many world cities today, new opportunities are created by offering sustainable solutions to current problems. In providing these opportunities, especially local administrations have a duty to direct the designers and the demands of the users. Sustainable urban development can be achieved by integrating these different and innovative approaches of urban landscape designs into the decisions taken by local governments regarding the future of the cities within the framework of sustainability, the goals they set and their targets in this direction. Urban areas, where innovative urban landscape approaches can be applied most easily and quickly, are newly developing areas in cities (Tezgör, 2021).

It has been proven by many studies that green areas have a positive effect on people. The importance of nature has become even better understood all over the world. The protection of nature and ensuring its continuity are important criteria for the life of all living things. Our country is trying to contribute to nature with planned urbanization. It will be possible to associate nature-oriented landscape works, green areas in small parts that have lost their context in the city today, and green areas increasing with urban transformation with new and large connec-

tions. With the designed active and passive green areas, it will be possible to ensure the integrity of the above-ground assets and create effective areas that the city needs.

REFERENCES

Anonymous, 2022. https://tr.wikipedia.org/wiki/Kentsel_d%C3%B6n%C3%BC%C5%9F%C3%BCm (Date of access: 21.02.2022)

Anonymous, 2022a. Dünya'da ve Türkiye'de Kentsel Dönüşüm". Alıntı tarihi (20.02.2022)

Anonymous, 2022b. https://www.haritamap.com/yer/efendibey-mahallesi-merkez. Date of access. 22.02.2022

Birol, G. (2007). "Bir Kentin Kimliği ve Kervansaray Oteli Üzerine Bir Değerlendirme", Arkitekt Dergisi, Kasım-Aralık 2007, sayı: 514, s. 46-54.

Bütüner, F.B., Sert, S.Ç., 2021. Kentsel Peyzajın Değişen Kavramsal Çerçevesi: Ankara Üzerine Değerlendirmeler. Ankara Araştırmaları Dergisi. 9(1), 89-107, Haziran/ June 2021.

Tezgör, DGE. 2021. Sürdürülebilir Kentsel Gelişmede Yenilikçi Kentsel Peyzaj Yaklaşımları: Edirne Örneği. T.C. Trakya Üniversitesi Fen Bilimleri Enstitüsü.Doktora Tezi. 288s.

Kalaycı Önaç, A., Birişçi T., Karcı Demirkol A. (2020).Kentsel Kimlik ve İmge Olarak İzmir Basmane-Kadifekale Aksının Dünü Bugünü Yarını, Kent Akademisi, Volume, 13, Issue 3, Pages, 404-416.

TUİK, 2021. Türkiye İstatistik Kurumu, Konularına Göre İstatistikler, Adrese Dayalı Nüfus Kayıt Sistemi Sonuçları, https://biruni.tuik.gov.tr/medas/?kn=95&locale=tr, Date of access: 16.02.2022

CHAPTER XII

A THEORETICAL OUTLINE OF STRATEGIC SPATIAL PLANNING AND AN OVERVIEW OF TURKEY[1]

Pelin KEÇECİOĞLU DAĞLI[1] & Canan CENGİZ[2]

[1](Res. Asst. Dr.) Bartın University, Faculty of Engineering, Architecture and Design, Department of Landscape Architecture, Bartın, Turkey,
pkececioglu@bartin.edu.tr
ORCID: 0000-0003-2419-0147

[2](Assoc. Prof. Dr.) Bartın University, Faculty of Engineering, Archi-tecture and Design, Department of Landscape Architecture, Bartın, Turkey,
canancengiz@bartin.edu.tr
ORCID: 0000-0003-1492-1081

1. Spatial Planning

Spatial planning, in general, is a process that involves making assumptions about the environment and the future lives of people who will utilize it in specific and restricted stages based on their requirements and then making environmental decisions based on these assumptions. Each step's outputs serve as inputs for the subsequent stage. The organizational structure is hierarchical. As a result, the outputs' correctness is critical. It is vital to contemplate the unpredictability of the future, be receptive, strike a balance between requirements and opportunities, and make optimal use of available resources during this process (İlgar, 2016). In other words, "spatial planning," which defines which activities will take place where and at what scale, is characterized as a dynamic process within the sustainable development framework by describing the development of regional and metropolitan infrastructure and its management based on these decisions. While it aims to

---

* This study was produced from the Ph.D. thesis titled "Evaluation of The Change in Urban Land Use within the Context of Strategic Spatial Planning: Istanbul Riva Case" completed at Bartın University Graduate School Department of Landscape Architecture in 2021.

improve individuals' living standards by regulating the distribution of social and economic activities within space, it also necessitates cooperation between the economic and social sectors regarding space-related applications (Gürbüz, 2012).

As a more passive, pragmatic, and localized kind of planning, spatial planning aims to regulate how space is used through a zoning system. The comprehensive nature of land use planning stands in stark contrast to the ever-dwindling availability of resources. A more adaptable system was required to react more rapidly and effectively to changing social and economic situations (Kreukels, 2000; Albrechts, 2004). Spatial planning and regional planning are distinct ideas in terms of scale and scope and should not be confused. Spatial planning is more upper scale than regional planning since it depicts the distribution of built and natural environment elements. The distribution of these elements as defined by the spatial development strategies developed in this environment needs physical and social interventions that offer new chances for achieving goals. Local, regional, and international spatial plans are utilized to impact spatial development dynamics (Gürbüz, 2012).

2. Reflections of Changes in the Globalization Process on Urban Planning

Globalization's social, political, economic, and technical changes affects urban systems as well, and the traditional planning approach could not produce answers to the problems of the new urban systems. Acceleration of information flow with technology, rapid increase in population, the emergence of spatial problems with increasing population, changes in socioeconomic living conditions, loss of importance of national borders and global world understanding gaining importance, the transition from the management approach to the governance approach and the prominence of communicative rationality had an impact on planning theory and practices (Tekeli, 2004; Tekeli, 2009; Kotan, 2008; Bülbül, 2014).

The change experienced in planning with postmodern ideas has occurred in the form of a transition from rational comprehensive planning based on instrumental reason (result-oriented planning approach) to participatory planning based on communicative rationality (process-oriented planning approach). The process-oriented planning approach was chosen to foster an interactive planning process in which all essential stakeholders collaborate and find consensus at each level of the planning process. This transition to participatory planning might be defined as this approach (Tekeli, 2009; Kulözü, 2011; Bülbül, 2014).

The Traditional Spatial Planning approach is unable to adequately provide a relationship system between spatial development and socioeconomic development; it fails to connect urban, regional, and local planning frameworks and scales; it lacks integration between short, medium, and long term projects; and it encounters significant problems such as not ensuring the participation of all stakeholders in the process (Göksu, 2006; Özalp, 2006). For all of these reasons, additional research into planning techniques has been done. Especially in 1980 and later with the dominance of postmodern thought, a planning approach that emphasizes communication, negotiation, interaction, and participation has been adopted instead of the traditional planning approach (Göksu, 2006; Özalp, 2006; Bülbül, 2014). The 1990s saw an increase in a strategic approach to space organization at various scale levels. Strategic planning, which has the ability to combine solutions of complex problems and strategic visions with short-term actions, involves designing shared futures and developing common assets (Albrechts, 2004). It took time and effort to apply this approach throughout cities which is defined as Strategic Planning. It started to be implemented first in some European and American cities and then in Asian cities (Özalp, 2006; Şimşek Deniz, 2014). Table 1 summarizes the features of Traditional Planning and Strategic Planning.

Table 1: Traditional Planning and Strategic Planning Features (Özalp, 2006; Şimşek Deniz, 2014).

Traditional Planning	Strategic planning
Short-term	Long-term
Single topic	Multiple topics
Organizational issues	Social issues
Hierarchical order	Not hierarchical
Low interest	High interest
Directive based	Agreement based
Employee-based	Citizen-based
Management based	Policy-based
Employee awareness	Public awareness
Operational focus	Political focus

SSP (Strategic Spatial Planning) is fundamentally different from traditional planning methodologies. Traditional planning is a planning method in which there is legally binding in a hierarchical structure; plan decisions remain constant, and the planning boundary is defined inside the management boundary. SSP, which is the adaptation of the strategic planning method to cities, is defined as a method that prioritizes networking and participation, is not legally binding, is based on possibility and flexibility (Sınacı, 2009).

Traditional planning tools have proven useless in recent years in contemporary cities and urban regions, as states of stability reflect certainty and are intended to offer a single clarity to the problems to be handled. In most traditional spatial planning initiatives, the emphasis is obviously on producing a plan, with public participation producing as a means to an end, but in SSP, the plan is a means of producing change, among other things. Since traditional spatial planning has almost no potential to incorporate strategies, strategic spatial planning entails significant contributions, procedural competencies, and key actors contributing to the acceptance, essential support, and legitimacy (Albrechts and Balducci, 2013).

SSP is a form of planning that adopts a long-term approach, is more adaptable and comprehensive than traditional planning, and adopts

competition and democratic thinking. It is not only a matter of land arrangement, as with traditional planning. Unlike traditional planning, it is a collaborative process involving several stakeholders, not only local governments. In traditional planning, the planner works as a technical staff member, but in strategic spatial planning facilitating communication amongst stakeholders. SSP develops short, medium, and long-term decisions; the plan is implemented through monitoring, feedback, and revision (Özalp, 2006; Şimşek Deniz, 2014). The general distinctions between the plans are summarized in Table 2.

Table 2: Differences Between Traditional Planning and SSP (Sınacı, 2009).

	Traditional Planning	**Strategic Spatial Planning**
Responsible Institution	It is made and outsourced by public institutions with areas of responsibility within a particular hierarchy. Often, the actors and actions necessary to reach the final state are not questioned.	It is produced with the cooperation of a networked organization coordinated by a public or private institution but works horizontally and under identical conditions at all stages. All components of the current situation participate in the process in line with their internal-external environment and interaction with each other and the selection of different decision-making mechanisms. It puts more emphasis on actors and actions. Outvariables are a constantly changing range of probabilities rather than a standardized list of estimates.

Table 2: Differences Between Traditional Planning and SSP (Sınacı, 2009) (continues)

	Traditional Planning	**Strategic Spatial Planning**
Legal Status	It is included in national laws on spatial planning; it is legally binding.	It does not have to be legally binding; it can also be done as a voluntary action.
Plan Form	It consists of maps and its annexes, in which the forms, sizes, population densities of the land uses are determined precisely.	Consists of a written document containing multisectoral strategies and objectives that do not necessarily have to be spatial but directly or indirectly impact spatial development and a general physical diagram showing the main strategies.
Plan Boundaries	It is done within administrative boundaries.	Administrative borders can be crossed. Because the relations in the space (institutional, sectoral) can go beyond administrative boundaries.
Contents	Current trends are assumed to continue. It is based on physical development; it may indirectly include other sectors. It is about setting goals and targets and adapting them to the current budget and working conditions. The most probable future conditions are tried to be arranged.	It is assumed that there may be new trends, discontinuities, and surprises. Physical, social, economic, environmental, cultural, and organizational development issues are handled in a complementary manner. It is more concerned with identifying and resolving problems in the research area. Represents plans that include qualitative change-transformation and forecasting. An attitude is followed in which possible futures are constantly monitored. The knowledge and skill experience of the person in the leadership or managerial position is of great importance.

Table 2: Differences Between Traditional Planning and SSP (Sınacı, 2009) (continues)

	Traditional Planning	**Strategic Spatial Planning**
Time Limit	There is a long-term planning approach to implement strictly defined land-use decisions.	The vision is long-term. However, a continuous project proposal can be developed regarding this vision; the time limit is mentioned according to the project's content.
Main Purpose	It is aimed to regulate and control physical development.	It aims to provide communication, informatics, and transportation infrastructures, increase urban competitiveness with strategies for encouraging domestic and foreign capital, and increase the quality of urban and environmental life by protecting local values following the sustainability principle.

3. Strategic planning

Strategic planning possesses the characteristics of being adaptable, transparent, long-term, and participation in nature, as it is the process of ensuring the development of a business, institution, or city by utilizing available resources most effectively, within the confines of a predetermined vision that serves as a general guide. The contribution and collaboration of interested parties, appropriate authorities, administrators, and individuals at all levels during the planning process enables a future based on common values to be included in planning. Strategic planning is outcome-oriented, adaptable, dynamic, and a foundation for accountability. Due to these characteristics, it is necessary to frequently assess and change the plan to changing situations and demands. Rather than the result, the planning

process is critical in strategic planning because it establishes ownership of the plan and its implementation (Özalp, 2006; Levend, 2008).

The most critical step of the strategic plan development process is the decision to create the plan, the management's commitment to making the plan decision, their confidence in managing the plan, and the formation of the planning team and beginning work. Within the established vision, objectives are defined, and methods for achieving them are produced (Özalp, 2006). Strategic planning includes determining "where we are, where we want to reach, how we can reach there, and how we will follow and evaluate our progress." The strategic planning management process comprises the responses to these questions (DPT, 2006). Table 3 summarizes the strategic planning management process.

Table 3: Management Process Of Strategic Planning (DPT, 2006).

Plans and Programs SWOT (Strengths-Weaknesses-Opportunities-Threats) Analysis Stakeholder Analysis	SITUATION ANALYSIS	WHERE ARE WE?
The reason for the existence of the organization Basic principles	MISSION AND PRINCIPLES	WHERE DO WE WANT TO REACH?
Desired future	VISION	
Aims to be achieved in the medium term Specific, concrete, and measurable objectives	AIMS AND OBJECTIVES	
Methods of achieving aims and objectives	STRATEGIES	
Detailed business plans Costing Performance program Budgeting	ACTIVITIES AND PROJECTS	HOW CAN WE REACH?
Reporting Comparison	TRACING	HOW DO WE FOLLOW AND EVALUATE OUR SUCCESS?
Feedback Determination of measurement methods Performance indicators Evaluation of implementation progress and results	PERFORMANCE MEASUREMENT AND EVALUATION	

4. Strategic Spatial Planning

Mazza (2000) defines SSP as a spatial strategy for the society that encompasses spatial development strategies for physical, sociocultural, economic, and managerial-institutional sustainability. It also adopts a communicative and collaborative planning process (Bülbül 2014). According to Healey et al. (1999), "by emphasizing how this planning approach fosters the process of creating local institutional capacity for shaping the future, they demonstrate how strategic planning is an active social process that transforms inter-institutional interactions and policy agendas" (Kotan, 2008). According to Mastop (1999), "it underlines that interaction (networking, variety of solutions, stakeholders) is just as essential as content (problems, goals, and tools)" in strategic spatial planning. (Bülbül, 2014). According to Konuk (2003), "within the framework of modern planning principles, it is an integrated collection of actions founded on an entrepreneurial basis that generates resources with the goals of economic, cultural, and social development and restructuring in the whole city or in different regions. It is the understanding of integrating the projects, transformations and dynamics envisioned for the city in a coordinated manner. It is a tool that assumes all the responsibilities associated with the change process, as well as ensuring the reproduction of the space through public participation, and includes participation and openness in this direction" (Kotan, 2008).

SSP is the application of strategic planning method and management for urban areas. Within this framework SSP prioritizes programs, budget and action plans that incorporate long- and medium-term visions and goals for the city's spatial problems. Additionally, it is a complex, new and holistic approach that places a premium on participation aims to produce and develop locally specific outcomes at the economic, physical, social, cultural, and organizational levels of cities/regions and employs a systematical perception of spatial problems (METREX, 2003; Özalp, 2006; Ersoy, 2007; Kotan, 2008; Bülbül, 2014). In general, cities/urban areas undertake the SSP process with the goal of "thinking about the future," "integrating the decision-making process", and "developing coordinating mechanisms" (Albrechts and Balducci, 2013).

Given the critical role of cities and urban areas in ensuring a sustainable future, several cities, and urban districts are utilizing SSP, a transformational and integrative public sector initiative, to achieve sustainable development and construct a coherent spatial development strategy (Hersperger et.al., 2020). Since the 1990s, SSP has become more prevalent at the urban-regional level in Europe to solve economic, social, and environmental challenges. The overarching objective of the transition to SSP has been to produce a coherent spatial development strategy that would guide the medium- and long-term development of urban districts, frequently in combination with specific strategic urban development projects (Hersperger et.al., 2019).

SSP, a social process in which diverse stakeholders from diverse institutional contexts collaborate to produce strategies and projects for managing spatial changes (Healey, 2009; Kunzmann, 2013), is increasingly being used globally to build a collective vision to guide urban district development (Hersperger et.al., 2019).

SSP entails both planning and executing the plan. The phase of plannig strategic spatial planning includes the development of visions and decision-making frameworks for representing, managing, and influencing urban developments. This phase's preliminary result is often a plan that includes strategic urban projects and an overall development strategy for the urban region. Plans are the order of a selection of selected topics (settlement, transportation, green infrastructure, etc.) in which they establish a long-term vision and short-term activities to be genuinely strategic (Albrechts and Balducci, 2013). Along with visual features such as plan, diagram, map etc, it includes a textual portion that explains the socio-economic and ecological environment, sets forth and justifies spatial planning goals and strategies, and gives implementation and monitoring instructions (Hersperger et al., 2019). At the planning stage, a complete examination of the current state and surrounding environment is made, revealing all relevant conditions. The objective and, consequently, the vision are presented realistically according to the outcomes and conditions. Then, within the defined vision, goals and strategies for achieving these goals are determined. Alternative constructs are determined using the most effective participative approach possible to

accomplish goals and objectives and build action strategies for associated challenges. Detailed business plans and budgeting studies are carried out to implement the preferred plan (Şentürk, 2005).

The implementation phase of a strategic spatial planning, on the other hand, refers to the process of translating plans into urban changes, as it promotes expected to change while avoiding unwanted activities and developments (Hersperger et al., 2019). The process and task are followed, appropriate adjustments are made if deemed, and evaluation and performance measurements are supplied (Şentürk, 2005).

In the strategic programming stage, strategic goals and action plans are developed. The tactics to be implemented to achieve these goals and plans are determined, every scenario created in line with the scenario using the 5W-1H (What, Why, When, Where, Who, How) technique to guide the decision-making and implementation process, is determined by what the project is, by whom, for what purpose, at what time or stage within the overall target, in what setting, and in which area within the study area (Mert et.al., 2011). Figure 1 depicts the SSP process.

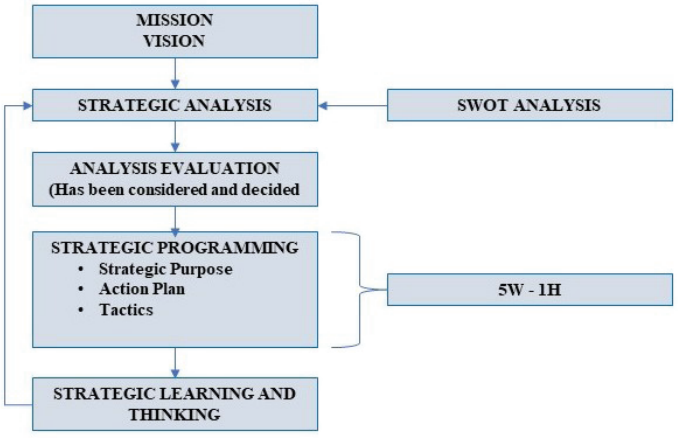

Figure 1: Strategic Spatial Planning Process (Mert et.al., 2011).

With the SSP approach (Mert et.al., 2011):

- Developing a sustainable planning process that takes into account the social benefits, not the individual,

- Developing the potentials of the selected area,
- Establishing city-policy-urbanization-economy-culture relations,
- It is in question to create a planning process and application suitable for the selected area locality.

Strategic Spatial Plan is the plan that is (Yıldız, 2006):

- Providing the spatial organization of country development policies, regional development strategies, and regional plan decisions,
- Transferring policies and decisions at the country and regional level to lower level plans,
- Determining spatial strategies for the protection and development of natural, historical, and cultural values,
- Integrating and harmonizing sectoral decisions with their spatial dimensions at the country level,
- Determining spatial strategies for urban and rural settlements, transportation system and orientation of social and technical infrastructure,
- Guiding the determination of investment locations,
- Prepared in schematic and graphic language at the country and regional level, which is a whole with the sectoral and thematic maps and reports.

5. The Role of Landscape Architecture in Strategic Spatial Planning

Landscape architecture plays an essential role in the process of integrative spatial planning. Because landscape architecture contributes to inform planning and resource management, one may argue that it improves the overall quality of city planning and substantially contributes to strategic planning. As such, landscape architecture is an essential science to bridge scientific disciplines and enhance collaboration across planning stakeholders (Wu, 2013; Wang et.al., 2014; Hersperger et.al., 2020).

When evaluating landscape architecture's role in contemporary SSP, a framework should be used that focuses on how plans leverage the integrative power of landscape, how plans are informed by knowledge of the workings of landscape systems, and how plans demonstrate landscapes' contribution to human well-being. The method of incorporating ecological sustainability in SSP has varying degrees of impact in urban and urban regions. According to the researches, incorporating elements such as green infrastructure, ecosystem services etc. within the plan boosts the impact of SSP (Bjarstig et.al., 2018; Grădinaru and Hersperger, 2019; Hersperger et.al., 2020).

It is essential to establish study-specific criteria for evaluating strategic spatial plans and for improving the integration of landscape architecture as a professional discipline into strategic spatial plans. The landscape is a holistic concept that is expected to be mentioned in context with a variety of environmental and social issues, including agriculture, water management, forestry, nature conservation, biodiversity, green infrastructure, resilience, sustainability/sustainable development, environmental aesthetics, branding, tourism, and recreation. The landscape's inclusivity includes the biophysical, socio-cultural, and aesthetic dimensions of a holistic view of the landscape (Herperger et.al., 2020). The plans make use of the landscape's integrative capacity. As a result, several discourses and approaches have given tools for harnessing the landscape's integrative potential and have been formed by various geographic, thematic, and administrative settings (Sayer et.al., 2013; Pătru-Stuparu et.al., 2016; Mann et.al., 2018). The common purpose is to engage diverse stakeholders in collaborative efforts to build integrated policies and plans for achieving sustainable landscapes. Additionally, because the frequent adaptation of plans to a dynamically developing landscape aims to minimize future uncertainty over time, it is essential to prioritize adaptive management as a suitable process for addressing this uncertainty (Sayer et.al., 2013; Hersperger et.al., 2020).

In SSP, landscape plans significantly contribute to the quality and importance of the place, providing active and passive recreation opportunities, natural and cultural heritage sites etc. For this reason, landscape management is a critical component of the strategic plan that should be

addressed. Additionally, projects, platforms, initiatives, or various activities that support landscape values enable community-based landscape initiatives in terms of landscape management and strategic spatial plans. Additionally, the structural elements of the plans demonstrate an awareness of the landscape. In urban settings, it is critical to actively and correctly manage the landscape to make recommendations for enhancing the environment's role in SSP (Hersperger et.al., 2020). The similarities in the way the landscape is managed in cities and urban regions within the context of strategic spatial planning include establishing goals and strategies in the protection-use context of natural and cultural characters. Hersberger et.al. (2020) also demonstrates that, while strategic spatial plans are often focused on economic development, regions are developed for housing, economic activity, and transportation, and all plans include explicit reference to the landscape. Each city has developed strategies based on a holistic, sociocultural, biophysical, or aesthetic point of view in terms of their unique landscape value. As stated in Şahin et.al. (2014)'s study, landscape protection and development strategies reveal the protection and use value of a landscape. Therefore, management strategies should be included in the production of landscape strategies from a holistic perspective. It is critical to design strategies and policies for the restoration, enhancement, development, and protection of the landscape in this context.

Landscape architecture helps to spatial planning, particularly SSP, by providing an inclusive approach that takes a landscape's natural-ecological character and its socio-cultural identity, and sense of the place. To discuss landscape quality in cities or urban regions, it is critical to substitute landscape architecture in the SSP and plan hierarchy (Hersperger et.al., 2020).

While the city did not previously require SSP, strategic spatial plans of each city have started to be legally prepared and implemented increasingly in recent years (Özalp, 2006; Şimşek Deniz, 2014).

6. Strategic Spatial Planning Studies in Turkey

According to the Ministry of Environment, Urbanization, and Climate Change's official website, "strategic spatial planning is a plan that is pre-

pared throughout the country and in the regions deemed necessary, and that guides physical development and sectoral decisions by associating economic, social, and environmental policies and strategies with space, and that is a plan that is complete with its report." Strategic spatial plans have this characteristic in that they are plans that control spatial development, employ an abstract, visual expressive language and schematic representation approach, and incorporate spatial development strategies." (URL-1, 2022).

A Strategic Spatial Plan was needed to establish a more effective national spatial planning system that aligns economic, social, and environmental policy and strategy with each other in achieving Turkey's development and growth goals and realizing its future vision (URL-2, 2022). In line with this need (URL-2, 2022), "Country Spatial Strategy Plan" studies were initiated with all stakeholders to;

- Turn the spatial potentials of our country into an advantage have been initiated,
- To achieve the vision and goals of our country for 2023 and beyond, studies that ensure the harmonization of the spatial strategies of the economic, social, and environmental policies have been initiated,
- Reflect global and regional sectoral decisions holistically to the space have been initiated,
- Guide spatial development and conservation strategies at the highest level for sustainable development have been initiated,
- Human-oriented, identity, livable, and productive settlements that integrate environmental policies with land-use decisions.

As defined on the official website of the Ministry of Environment, Urbanization and Climate Change, the targets of the Turkey Spatial Strategy Plan (URL-3, 2022) in line with the vision and goals of our country are:

- Creation of human-oriented, sustainable, durable, intelligent, and high socio-economic development cities,

- To ensure the balanced distribution of infrastructure and services following development policies, covering urban and rural areas, in order to ensure economic and social development,
- Supporting the necessary spatial arrangements and infrastructure for the provision of competitive settlements,
- In order to ensure a sustainable environment, it is the integration of sectoral priorities, spatial development, and environmental policies by considering adaptation to climate change.

Turkey's Spatial Strategy Plan studies started in 2012 and "Project for Determining the Methods and Principles for the Spatial Strategy Planning Preparation, Implementation, and Monitoring Process." was completed in 2013. As a result of the project, the basic documents related to the preparation of the Spatial Strategy Plan were obtained and the project's outcomes were defined as the procedures and principles for preparing these plans in the Spatial Plans Production Regulation (URL-4, 2022; Turkey Spatial Strategy Plan, 2021).

Working Group Meetings and High-Level Steering Meetings were held with the participation of relevant public institutions, local works, universities, non-governmental organizations, and the private sector, as preparation of the participatory process for developing the Spatial Strategy Plan. Associating the economic, social, and environmental policies and strategies with space in process to achieve the country's development and growth goals and realize the country's future vision; ensuring a balanced distribution of infrastructure and services for competitive cities following development policies; preparing Turkey's Spatial Strategy Plan, which will guide spatial planning toward creating human-centered, disaster-resistant, climate change-ready, livable and productive cities (URL-4, 2022).

7. Features of Turkey's Spatial Strategy Plan

The process for the preparation of the Turkey's Spatial Strategy Plan (SSP) was formed during the previous decade, under the scope of the 2009 Urbanization Council decision to "create the country's spatial

strategy plan and update the existing planning hierarchy accordingly" (Turkey Spatial Strategy Plan, 2021). In this process, the spatial strategy plan was incorporated into planning legislation for the first time in 2011, and the Ministry of Environment and Urbanization was given the authority to prepare and approve spatial strategy plans in process with institutions and organizations related to the defunct Decree-Law No. 644 on the Organization and Duties of the Ministry of Environment and Urbanization of the Republic of Turkey, which came into force the same year. SSP, described in detail in the Spatial Plans Construction Regulation, which took force in 2014, is identified and defined in Articles 4 and 6 of the regulation as the highest level of spatial plans (Spatial Plans Construction Regulation, Article 6 (h)) (Turkey Spatial Strategy Plan, 2020; Turkey Spatial Strategy Plan, 2021). Accordingly, Turkey's Spatial Strategy Plan is defined as a plan that evaluates regional plans that connect country development policies and regional development strategies at the spatial level, and taking into account economic and social potential, goals and strategies, transportation connections, and physical thresholds of regional plans. Additionally, it is a plan that establishes spatial strategies for utilizing subsurface and surface resources, safeguarding and developing natural, historical, and cultural resources, and guiding settlements, transportation systems, and urban, social, and technological infrastructure. Moreover, it is defined as a plan being made throughout the country that defines the link between spatial policies and strategies related to the sectors through schematic and visual language on 1/250,000, 1/500,000, or upper scale maps (Turkey Spatial Strategy Plan, 2020).

"Turkey's Spatial Strategy Plan-Turkey SSP," defined in the Zoning Law as the highest-scale plan that would guide spatial development, has started to be prepared as of the last quarter of 2018. A participatory method was used throughout this process, and the perspectives of relevant stakeholders were gathered and şntegrated into the report. Additionally, process of Strategic Environmental Assessment of Turkey's Spatial Strategy Plan has started (URL-4, 2022).

With the 2018 amendment to Zoning Law No. 3194, the Spatial Strategy Plan was defined as a plan that is prepared throughout

the country and in the regions deemed necessary, that guides physical development and sectoral decisions by associating economic, social, and environmental policies and strategies with space, and that is complete with its report. The Spatial Plans Construction Regulation, which took force in 2014, defines spatial strategy plans, planning principles, their relationship to planning stratification, and research themes. On the other hand, the part explaining spatial planning level defines spatial plans as "Environmental Plans" and "Zoning Plans" per the Spatial Strategy Plans in terms of the area they cover and their purposes (Turkey Spatial Strategy Plan, 2020; Turkey Spatial Strategy Plan, 2021).

These plans have a progressive integration (Spatial Plans Construction Regulation, Article 6 (2)). In this situation, the spatial plans are prepared in accordance with the plan stratification. Each plan directs the lower-level plan of the current upper-level plans by the idea of progressive plan integration. The Spatial Plans Production Regulation states that when preparing Spatial Strategy Plans and Environmental Plans, the targets established by the Development Plan, Regional Plans, Regional Development Strategies, and other Strategy Documents will be taken into account (Spatial Plans Construction Regulation, Article 6 (5)) (Turkey Spatial Strategy Plan, 2020; Turkey Spatial Strategy Plan, 2021).

8. Interaction of Turkey Spatial Strategy Plan with Other Related Plans and Programs

"Turkey Spatial Strategy Plan 5.3.3. Strategic Environmental Assessment Scoping Report-2020" expresses the following relationship between the Turkey Spatial Strategy Plan and other associated plans and programs.

The relationship between the Turkey Spatial Strategy Plan and the relevant plans/programs have been examined within the context of the plan/program relationships that affect and are impacted by the Turkey Spatial Strategy Plan. The mentioned impact may refer to the (legal) links included in the plan stratification and within the scope of the rel-

evant laws and regulations, and the links that are thematically/sectorally affected and affected.

The Development Plan, which has an effect on the Turkey Spatial Strategy Plan at the national level and is not included in the scope of spatial plans but is characterized as the top-level plan, and the Annual Programs prepared per the development plans are unquestionably considered to be legal and strategic ties affecting the Turkey Spatial Strategy Plan. In this context, the 11th Development Plan covering the years 2019-2023, prepared by the Presidency of the Republic of Turkey, Strategy and Budget Department, and the Presidential Annual Programs prepared for the years 2019, 2020 and 2021 stand out as the programs that affect the Turkey Spatial Strategy Plan. In addition to the Development Plan and related Annual Programs, the following strategies, which are not included in the spatial plans but which guide the plans, have strategic links with the Turkey Spatial Strategy Plan, policy and strategy documents;

- EU Integrated Environmental Harmonization Strategy 2007-2023,
- Integrated Urban Development Strategy and Action Plan 2010 – 2023,
- Republic of Turkey Climate Change Action Plan 2011-2023,
- Regional Development National Strategy 2014 – 2023,
- National Rural Development Strategy 2014 – 2020,
- Urban Planning Council Commission Reports and Concluding Statement.

These plans, policies, and strategy documents with varying objectives and focus areas were seen to have a variety of different bases, such as the 9th Development Plan or the United Nations Framework Convention on Climate Change, and thus were included in the study as they serve as a guide for Turkey Spatial Strategy Plan studies.

As previously stated, Environmental Plans and Zoning Plans are prepared "by the Spatial Strategy Plans in terms of the area they cover and their purpose" under Zoning Law No. 3194. (Zoning Law No. 3194,

Article 6). As of this situation, Turkey's Spatial Strategy Plan affects the Environmental Plans, Master Zoning Plans, and Implementation Development Plans to be prepared. Additionally, Turkey's Spatial Strategy Plan can influence future studies of Regional Plans prepared by Development Agencies on the NUTS Level 2 scale which was prepared with 2023 visions.

Along with regional plans, Integrated Coastal Area Plans (ICAP) (Spatial Plans Construction Regulation, Article 6 (6)) and River Basin Management Plans prepared at the regional level might be regarded plans that will be impacted by the Turkey Spatial Strategy Plan's actions. Although the Turkey Spatial Strategy Plan is not yet capable of taking direct action on the regions covered by the plans on a large scale, the actions taken by the Turkey Spatial Strategy Plan must not have a detrimental effect on the environmental characteristics stated in the relevant plans.

9. Conclusion

When traditional planning tools are insufficient, strategic spatial planning should be used throughout the regional development stage. In this context, it is vital to attempt to establish strategies that can assist in shaping planning processes and the actions associated with these strategies (Keçecioğlu Dağlı and Cengiz, 2019).

Strategic spatial planning considers urban development not only within the scope of physical development, but also within the scope of strategies related to social, cultural and economic development in the city (Anonymous, 2009). Strategic spatial planning, which is intrinsically linked to urban development, significantly impacts urban transitions (Hersperger et.al., 2019). The objective of strategic spatial planning (Hersperger et.al., 2019), which is increasingly being used globally to produce a collective vision for the medium and long-term development of urban regions, is to provide content, images, and decision frameworks to impact and manage spatial change (Albrechts and Balducci, 2013). In this context, urban development strategies are created for cities.

Strategic spatial planning encompasses all of the strategies essential for establishing goals and objectives and achieving them while consid-

ering long- and short-term internal and external environmental issues affecting both the commercial and public sectors. Strategic spatial planning, which ensures harmony between resources, targets and environmental conditions, and creates a strong vision, becomes a requirement. Local governments that engage in strategic spatial planning are more future-ready. As the global trend toward localization gains momentum, the responsibilities of local governments as providers of regional public services grow (Yalçınkaya, 2010). The spatial development framework, which impacts the city's long-term development and change of city and is a critical tool for investors' monitoring and management of investments, collects spatial decisions in line with the common vision, common theme, common direction and common goal of the city. Over the years, cities have evolved, reshaping, transforming, and spreading across vast swaths of land. Spatial development strategy frameworks must be defined to rein in urban growth and expansion. For this reason, it is important that the programs and projects produced are concrete and applicable. In line with the region's present dynamics, it is necessary to maximize the use of existing assets, infrastructure, resources and capacities (URL-5, 2019).

Spatial strategic planning evolved due to the traditional comprehensive planning technique's inadequacies in the face of new phenomena and problems, particularly in large cities, and the necessity for a more flexible approach to generate solutions in the face of sudden and significant changes. Spatial, strategic planning, which is an action-oriented, flexible and participatory approach that covers the identification and solution of problems at the country level, has the following features; putting forward the functional long-term vision, goal, and perspective, creating strategies at different levels, designing platforms where plan decisions can be made to achieve the vision, developing content, images and decision frameworks that will affect and manage spatial change, and handling physical development and economic, social, cultural and institutional development interactively.

The plan is being evaluated to cover the whole country, territorial waters and exclusive economic zones. Turkey Spatial Strategy Plan is located at the top of the planning stages, above the Environmental Plan and the Zoning Plan. In this framework, Turkey Spatial Strategy Plan

is the plan that sets targets, guides and sets principles for the plans in its lower level, and it guides the plans to be prepared at the regional level (Turkey Spatial Strategy Plan, 2020).

In sum, SSP is a process. In this context, participants in the SSP process are recognized as political, economic, and social leaders, representatives (non-governmental organizations-NGOs, associations, social organizations, etc.), and citizens with the ability to make decisions and generate ideas. Therefore, the SSP process benefits all stakeholders, including city residents, local and state government officials, and capital owners etc. Additionally, cities change throughout time due to their dynamic qualities, and their visions harmonize with the global system. In this context, ensuring that limited resources are managed in the most effective way makes it possible to create new management and organization models (Özalp, 2006; Şimşek Deniz, 2014).

Making planning choices in accordance with the unique situation and dynamics of each country increases productivity and efficiency. The strategic spatial planning processes that will emerge as a result of the road maps and spatial development strategy frameworks created as a result of the strategic planning studies conducted by our country's unique values and dynamics will be critical in achieving spatial, social, and economic goals. It will also contribute to the sustainability of the natural and cultural landscape on a regional and local scale (Keçecioğlu Dağlı and Cengiz, 2019).

Acknowledgements

The study has been made within the scope of the Bartın University Scientific Research Project (BAP) coded 2019-FEN-CD-001, which is entitled "Determination and Evaluation of Land Use within the Context of Strategic Spatial Planning: Riva (Istanbul) Example." We hereby acknowledge our university for the support provided.

Notes

The name of the Ministry was updated, thus the date of access to the internet addresses where the Ministry's studies were conducted and the

information included in the addresses were updated, and the appropriate reports were added to the study.

References

Albrechts, L. (2004). Strategic (Spatial) planning reexamined. *Environment and Planning B: Planning and Design*, 31: 743-758.

Albrechts, L., Balducci, A. (2013) Practicing strategic planning: In search of critical features to explain the strategic character of plans. *disP – The Planning Review*, 49(3): 16-27.

Anonymous (2009). Mekansal Planlama Sistemi ve Kurumsal Yapılanma Komisyon Raporu. Kentleşme Şurası 2009. https://webdosya.csb.gov.tr/db/kentges/editordosya/kitap1(1).pdf

Bjarstig, T., Thellbro, C., Stjernstrom, O., Svensson, J., Sandstrom, C., Sandstrom, P., Zachrisson, A. (2018). Between protocol and reality – Swedish municipal comprehensive planning. *European Planning Studies*, 26(1): 35–54.

Bülbül, Ş. (2014). Stratejik Mekansal Planlamada Stratejik Seçim Yaklaşımı ile Karar Verme. Doktora Tezi (yayımlanmamış), Karadeniz Teknik Üniversitesi, Fen Bilimleri Enstitüsü, Mimarlık Anabilim Dalı, Trabzon, 165 s.

DPT (2006). Devlet Planlama Teşkilatı. *Kamu İdareleri İçin Stratejik Planlama Kılavuzu*. 2. Sürüm, Ankara.

Ersoy, M., (2007). *Kapsamlı Planlama Kavramının Tarihsel Gelişimi ve Bugünü, Kentsel Planlama Kuramları*. İmge Kitabevi, Ankara, 440 s.

Göksu, A.F. (2006). Planlamada Stratejik Yaklaşımlar; Klasik Planlama Anlayışı Temelli Askıya mı Çıkıyor? http://www.kentselyenileme.org/dosyalar/Planlamada-Stratejik-Yaklasimlar-son-hali.doc (09.06.2016).

Grădinaru, S.R., Hersperger, A.M. (2019). Green infrastructure in strategic spatial plans: Evidence from European urban regions. *Urban Forestry & Urban Greening*, 40: 17–28.

Gürbüz M. (2012). Analitik Araştırma Süreçlerinin Mekânsal Planlamada Kullanımı ve CBS Uygulamaları; İller Bankası Özelinde Bir İnceleme. Yüksek Lisans Tezi (yayımlanmamış), Süleyman

Demirel Üniversitesi, Fen Bilimleri Enstitüsü, Şehir ve Bölge Planlama Anabilim Dalı, Isparta, 97 s.

Healey, P. (2009). In search of the "strategic" in spatial strategy making. *Planning Theory & Practice*, 10(4): 439–457.

Hersperger, A.M., Bürgi, M., Wende, W., Bacău, S., Grădinaru, S.R. (2020). Does landscape play a role in strategic spatial planning of European urban regions? *Landscape and Urban Planning*, 194:1-12.

Hersperger, A.M., Grădinaru, S., Oliveiraa, E., Pagliarina, S. ve Palkaa, G. (2019). Understanding strategic spatial planning to effectively guide development of urban regions. *Cities*, 94: 96–105.

İlgar, Y. (2016). Kentsel Çevrede Fiziksel Aktivite ve Mekansal Planlama: Denizli Örneği. Doktora Tezi (yayımlanmamış), Süleyman Demirel Üniversitesi, Sosyal Bilimleri Enstitüsü, Siyaset Bilimi ve Kamu Yönetimi Anabilim Dalı, Isparta, 333 s.

Keçecioğlu Dağlı, P., Cengiz, C. (2019). "Spatial Development Strategies within the Scope of Urban Development". International Euroasia Congress on Scientific Researches and Recent Trends V, 16-19 December, Book of Proceedings, Vol III, pp 279-295, Baku, Azerbaijan.

Kotan, A. (2008). Stratejik Mekânsal Planlama'da Kentsel Projeler 'Proje Süreç Yönetimi'. Yüksek Lisans Tezi (yayımlanmamış), Mimar Sinan Güzel Sanatlar Üniversitesi, Fen Bilimleri Enstitüsü, Şehir ve Bölge Planlama Anabilim Dalı, Kentsel Planlama Programı, İstanbul, 171 s.

Kreukels, A, (2000). An institutional analysis of strategic spatial planning: the case of federal urban policies in Germany. In *the Revival of Strategic Spatial Planning*, Eds; W Salet, A Faludi, Royal Netherlands Academy of Arts and Sciences, Amsterdam, pp 53-65.

Kulözü, N. (2011). Planlamaya katılım: araç mı, amaç mı?, *KBAM 2. Kentsel ve Bölgesel Araştırmalar Sempozyumu, Planlamanın Dünü, Bugünü, Yarını: Planlamada Yeni Söylem Arayışları,* Ankara, s 159.

Kunzmann, K. (2013). Strategic planning: A chance for spatial ınnovation and creativity. *disP - The Planning Review*, 49(3): 28–31.

Konuk, G. (2003). Kentsel rönesans uyanış kentsel gelişmeyi yönlendirmede/planlama ilişkisi içinde /kentsel tasarım bakış

açısından/kentsel regenasyonun yeri. *Uluslararası 14. Kentsel Tasarım ve Uygulamalar Sempozyumu*, MSGSÜ, İstanbul.

Levend, S. (2008). Stratejik Mekânsal Planlama Yaklaşımı Üzerine Bir Araştırma: İstanbul Örneği. Yüksek Lisans Tezi (yayımlanmamış), Selçuk Üniversitesi, Fen Bilimleri Enstitüsü, Şehir ve Bölge Planlama Anabilim Dalı, Konya, 153 s

Mazza, L., (2000). *Strategie E Strategie Spaziali, Territorio*, No:13, FrancoAngeli, Milan.

Mann, C., Garcia-Martin, M., Raymond, C.M., Shaw, B.J., Plieninger, T. (2018). The potential for integrated landscape management to fulfil Europe's commitments to the sustainable development goals. *Landscape and Urban Planning,* 177: 75–82.

Mert, Z. G., Kutluca, A. K., Türkeri, İ. (2011). Gölcük İlçesi Mekansal Geliştirme Stratejilerinin Belirlenmesi, www.slideshare.net/GolcukBld/mekansal-gelitirme-stratejilerinin-belirlenmesi (09.06.2016).

METREX, Meeting Spring (2003). International Conference on Metropolitan Governance in Cooperation with: Network of German Metropolitan Regions, https://www.eurometrex.org/events/stuttgart-2/ (21.04.2020)

Özalp, S. (2006). Sosyo-Mekansal Dinamiklerle Değişen Planlama Yaklaşımı Mekansal Stratejik Planlama ve İstanbul Örneği. Yüksek Lisans Tezi (yayımlanmamış), İstanbul Teknik Üniversitesi, Fen Bilimleri Enstitüsü, Şehir ve Bölge Planlama Anabilim Dalı, Şehir Planlama Programı, İstanbul, 121 s.

Pătru-Stupariu, I., Tudor, C.A., Stupariu, M.S., Buttler, A., Peringer, A. (2016). Landscape persistence and stakeholder perspectives: The case of Romania's Carpathians. *Applied Geography*, 69: 87–98.

Sayer, J., Sunderland, T., Ghazoul, J., Pfund, J.-L., Sheil, D., Meijaard, E., Buck, L. E. (2013). Ten principles for a landscape approach to reconciling agriculture, conservation, and other competing land uses. *Proceedings of the National Academy of Sciences,* 110(21): 8349–8356.

Sınacı, F. (2009). Stratejik Mekansal Planlamanın Yasal Boyut Açısından Değerlendirilmesi: Türkiye-AB Karşılaştırması. Yüksek Lisans Tezi

(yayımlanmamış), Gazi Üniversitesi, Fen Bilimleri Enstitüsü, Şehir ve Bölge Planlama Anabilim Dalı, Ankara, 217 s.

Şahin, Ş., Perçin, H., Kurum, E., Uzun, O. ve Bilgili, B. C. (2014). Bölge-Alt Bölge (İl) Ölçeğinde Peyzaj Karakter Analizi ve Değerlendirmesi Ulusal Teknik Klavuzu. PEYZAJ-44 Projesi Çıktısı. TÜBİTAK KAMAG 1007 109G074, Ankara, 148 s.

Şentürk, H. (2005). *Belediyelerde Stratejik Planlama*. İlke Yayıncılık, İstanbul, 151 s.

Şimşek Deniz, S. (2014). Stratejik Mekansal Planlama ve Düzenleyici Geleneksel Planlamanın Katılım, Eylem Projeleri ve Esneklik Boyutlarında İncelenmesi - Bursa İli Örneği. Yüksek Lisans Tezi (yayımlanmamış), İstanbul Teknik Üniversitesi, Fen Bilimleri Enstitüsü, Şehir ve Bölge Planlama Anabilim Dalı, Şehir Planlama Programı, İstanbul, 91 s.

Tekeli, İ. (2004). Tek ve çok kademeli kuramlarının ontolojik kabulleri üzerine. *Doğu Batı Düşünce Dergisi,* 28: 195-225.

Tekeli, İ. (2009). *Bir Demokrasi Projesi Olarak Kent Planlama*. 1. Baskı, Tarih Vakfı Yurt Yayınları, İstanbul, s. 311-327.

Turkey Spatial Strategy Plan (2020). Türkiye Mekansal Strateji Planı 5.3.3. Stratejik Çevresel Değerlendirme Kapsam Belirleme Raporu-2020. https://mekansalstrateji.csb.gov.tr/turkiye-mekansal-strateji-plani-kapsam-belirleme-raporu-yayinlandi.-haber-257280 (12.01.2022).

Turkey Spatial Strategy Plan (2021). Türkiye Mekansal Strateji Planı 9.1. Taslak Türkiye MSP SÇD Raporu-2021. https://mekansalstrateji.csb.gov.tr/turkiye-mek-nsal-strateji-plani-taslak-stratejik-cevresel-degerlendirme-raporu-yayinlandi.-haber-263504 (12.01.2022).

URL-1 (2022). https://mekansalstrateji.csb.gov.tr/mek-nsal-strateji-plani-nedir-i-89080, Türkiye Cumhuriyeti Çevre ve Şehircilik Bakanlığı, Mekansal Strateji Planı Nedir? (12.01.2022).

URL-2 (2022). https://mekansalstrateji.csb.gov.tr/mek-nsal-strateji-planina-neden-ihtiyac-duyuldu-i-89081, Türkiye Cumhuriyeti Çevre ve Şehircilik Bakanlığı, Mekansal Strateji Planı, Mekansal Strateji Planına Neden İhtiyaç Duyuldu? (12.01.2022).

URL-3 (2022). https://mekansalstrateji.csb.gov.tr/hedefleri-i-89086, Türkiye Cumhuriyeti Çevre ve Şehircilik Bakanlığı, Mekansal Strateji Planı, Türkiye Mekansal Strateji Planının Hedefleri (12.01.2022).

URL-4 (2022). https://mekansalstrateji.csb.gov.tr/yapilan-calismalar-i-89083, Türkiye Cumhuriyeti Çevre ve Şehircilik Bakanlığı, Mekansal Strateji Planı, Yapılan Çalışmalar (12.01.2022).

URL-5 (2019). https://www.kentselstrateji.com/wp-content/uploads/YolHaritasiRehberi-1.pdf, Kentlerin Geleceği Yol Haritası Vizyon Planı Rehberi (11.05.2019).

Wang, Z., Tan, P.Y., Zhang, T., Nassauer, J.I. (2014). Perspectives on narrowing the action gap between landscape science and metropolitan governance: Practice in the US and China. *Landscape and Urban Planning*, 125: 329–334.

Wu, J. (2013). Key concepts and research topics in landscape ecology revisited: 30 Years after the allerton park workshop. *Landscape Ecology*, 28(1): 1–11.

Yalçınkaya, Ş. (2010). Yerel Yönetimlerde Stratejik Planlama ve Stratejik Yönetim Üzerine Beykoz Belediyesi Örneği. Yüksek Lisans Tezi (yayımlanmamış), Beykent Üniversitesi, Sosyal Bilimler Enstitüsü, İşletme Yönetimi Anabilim Dalı, İstanbul, 166 s.

Yıldız, R. (2006). Türkiye'de Metropoliten Bölge Ölçeğinde Stratejik Mekânsal Planlama Sürecinin Kurumsal Kapasitenin Geliştirilmesi Bakış Açısından Değerlendirilmesi. Doktora Tezi (yayımlanmamış), İstanbul Teknik Üniversitesi, Fen Bilimleri Enstitüsü, Şehir ve Bölge Planlama Anabilim Dalı, Şehir Planlama Programı, İstanbul, 150 s.